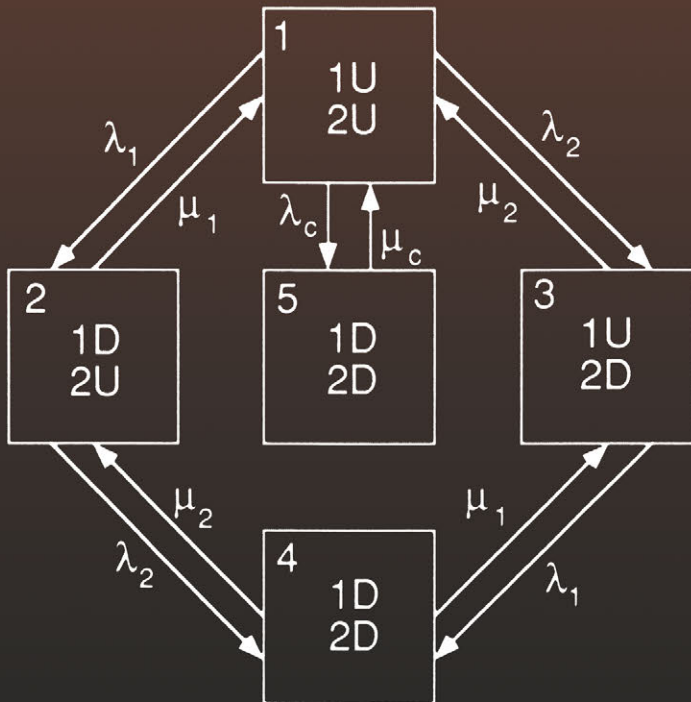


# Reliability Assessment of Electric Power Systems Using Monte Carlo Methods



Roy Billinton  
Wenyuan Li

# **Reliability Assessment of Electric Power Systems Using Monte Carlo Methods**

# **Reliability Assessment of Electric Power Systems Using Monte Carlo Methods**

**Roy Billinton**

*University of Saskatchewan  
Saskatoon, Saskatchewan, Canada*

**Wenyuan Li**

*BC Hydro  
Vancouver, British Columbia, Canada*

**Springer Science+Business Media, LLC**

**Library of Congress Cataloging-in-Publication Data**

---

**Billinton, Roy.**

**Reliability assessment of electric power systems using Monte Carlo methods / Roy Billinton, Wenyuan Li.**

**p. cm.**

**Includes bibliographical references and index.**

**1. Electric power systems--Reliability--Mathematics. 2. Monte Carlo method. I. Li, Wenyuan. II. Title.**

**TK1010.B55 1994**

**621.319'1--dc20**

**94-39034**

**CIP**

---

**ISBN 978-1-4899-1348-7**

**ISBN 978-1-4899-1346-3 (eBook)**

**DOI 10.1007/978-1-4899-1346-3**

**© Springer Science+Business Media New York 1994  
Originally published by Plenum Press, New York in 1994  
Softcover reprint of the hardcover 1st edition 1994**

**All rights reserved**

**No part of this book may be reproduced, stored in a retrieval system, or transmitted in any form or by any means, electronic, mechanical, photocopying, microfilming, recording, or otherwise, without written permission from the Publisher**

To Joyce and Jun  
with thanks for constant  
encouragement and support

# Preface

The application of quantitative reliability evaluation in electric power systems has now evolved to the point at which most utilities use these techniques in one or more areas of their planning, design, and operation. Most of the techniques in use are based on analytical models and resulting analytical evaluation procedures. Improvements in and availability of high-speed digital computers have created the opportunity to analyze many of these problems using stochastic simulation methods and over the last decade there has been increased interest in and use made of Monte Carlo simulation in quantitative power system reliability assessment. Monte Carlo simulation is not a new concept and recorded applications have existed for at least 50 yr. However, localized high-speed computers with large-capacity storage have made Monte Carlo simulation an available and sometimes preferable option for many power system reliability applications.

Monte Carlo simulation is also an integral part of a modern undergraduate or graduate course on reliability evaluation of general engineering systems or specialized areas such as electric power systems. It is hoped that this textbook will help formalize the many existing applications of Monte Carlo simulation and assist in their integration in teaching programs. This book presents the basic concepts associated with Monte Carlo simulation. Its primary focus, however, is on the practical application of these techniques in reliability evaluation of electric power generation, transmission, and distribution systems. The book has arisen from the reliability teaching and research program conducted at the University of Saskatchewan and applications at BC Hydro. The authors would like to thank the many graduate students who have participated in this program and, in particular, Raymond Ghajar, Ligong Gan, Lalit Goel, Easin Khan, and Guangbin Lian, whose work is specifically referenced. Particular thanks are due to Raymond Ghajar for coordinating and completing the work of many graduate students in preparing the figures in the book. The cheerful assistance of Brenda Bergen in a wide range of tasks is also gratefully acknowledged. Wenyuan Li would

also like to thank Yakout Mansour and Fred Turner of BC Hydro, and Jiaqi Zhou and Yihong Qin of Chongqing University, for their constant support and encouragement.

Roy Billinton  
Wenyuan Li

# Contents

## Chapter 1

### Introduction

1.1. Probabilistic Analysis of Power Systems.....	1
1.2. Reliability Evaluation Techniques .....	3
1.3. Outline of the Book .....	4
1.4. References .....	6

## Chapter 2

### Basic Concepts of Power System Reliability

#### Evaluation

2.1. Adequacy and Security .....	9
2.2. Functional Zones and Hierarchical Levels .....	10
2.3. Requirements for Power System Adequacy Assessment .....	12
2.3.1. Generation System (HL1) Studies .....	12
2.3.2. Composite System (HL2) Studies .....	14
2.3.3. Distribution System Studies .....	15
2.4. Reliability Cost/Worth .....	16
2.5. Reliability Data .....	17
2.5.1. General Concepts .....	17
2.5.2. Equipment Reliability Information System .....	18
2.5.3. System Performance Data Collection Systems .....	20
2.6. Adequacy Indices .....	22
2.6.1. Adequacy Indices in HL1 Studies.....	23
2.6.2. Adequacy Indices in HL2 Studies.....	24
2.6.3. Adequacy Indices in Distribution System Evaluation	27
2.6.4. Reliability Worth Indices .....	29
2.7. Conclusions .....	29
2.8. References .....	30

## Chapter 3

### Elements Of Monte Carlo Methods

3.1. Introduction .....	33
3.2. General Concepts .....	34
3.2.1. Two Simple Examples .....	34
3.2.2. Features of Monte Carlo Methods in Reliability Evaluation .....	35
3.2.3. Efficiency of Monte Carlo Methods .....	37
3.2.4. Convergence Characteristics of Monte Carlo Methods .....	37
3.3. Random Number Generation .....	39
3.3.1. Introduction .....	39
3.3.2. Multiplicative Congruential Generator .....	39
3.3.3. Mixed Congruential Generator .....	41
3.4. Random Variate Generation .....	42
3.4.1. Introduction .....	42
3.4.2. Inverse Transform Method .....	43
3.4.3. Tabulating Technique for Generating Random Variates .....	45
3.4.4. Generating Exponentially Distributed Random Variates .....	47
3.4.5. Generating Normally Distributed Random Variates .....	48
3.4.6. Generating Other Distribution Random Variates .....	50
3.5. Variance Reduction Techniques .....	52
3.5.1. Introduction .....	52
3.5.2. Control Variates .....	53
3.5.3. Importance Sampling .....	53
3.5.4. Stratified Sampling .....	56
3.5.5. Antithetic Variates .....	58
3.5.6. Dagger Sampling .....	58
3.6. Three Simulation Approaches in Reliability Evaluation .....	60
3.6.1. State Sampling Approach .....	60
3.6.2. State Duration Sampling Approach .....	62
3.6.3. System State Transition Sampling Approach .....	64
3.7. Evaluating System Reliability by Monte Carlo Simulation .....	66
3.7.1. Example 1 .....	66
3.7.2. Example 2 .....	69
3.8. Conclusions .....	71
3.9. References .....	72

**Chapter 4****Generating System Adequacy Assessment**

4.1. Introduction .....	75
4.2. Single-Area Generating System Adequacy	
Assessment—State Duration Sampling Method .....	76
4.2.1. General Steps .....	76
4.2.2. Generating Unit Modeling .....	78
4.2.3. Stopping Rules .....	83
4.2.4. IEEE RTS Studies .....	84
4.3. Single-Area Generating System Adequacy	
Assessment—State Sampling Method .....	91
4.3.1. Single Load Level Case .....	91
4.3.2. Modeling an Annual Load Curve .....	93
4.3.3. Cluster Technique for a Multistep Load Model.....	95
4.3.4. Stopping Rules .....	96
4.3.5. IEEE RTS Studies .....	96
4.4. Multi-Area Generating System Adequacy	
Assessment—Maximum Flow Algorithm .....	100
4.4.1. Basic Procedure .....	100
4.4.2. Modifying the Area Available Margin Model	
Using the Maximum Flow Algorithm .....	101
4.4.3. Case Studies .....	103
4.5. Multi-Area Generating System Adequacy	
Assessment—Linear Programming Model .....	106
4.5.1. Basic Procedure .....	106
4.5.2. Load Model of a Multi-Area System .....	109
4.5.3. Linear Programming Model for Multi-Area Reliability	
Evaluation .....	112
4.5.4. Case Studies .....	115
4.6. Different Supporting Policies in Multi-Area Generating	
System Adequacy Assessment .....	120
4.6.1. Incorporation of Different Supporting Policies .....	120
4.6.2. Case Studies .....	124
4.7. Conclusions .....	128
4.8. References .....	129

**Chapter 5****Composite System Adequacy Assessment**

5.1. Introduction .....	131
5.2. System State Sampling Method and System Analysis	
Techniques .....	132

5.2.1. Basic Methodology .....	133
5.2.2. Contingency Analysis for Composite Systems .....	134
5.2.3. Linear Programming Optimization Model .....	137
5.2.4. Basic Case Studies .....	139
5.3. Incorporation of the Annual Load Curve .....	142
5.3.1. Multistep Model of the Annual Load Curve .....	142
5.3.2. Ratios of Generation–Transmission Adequacy Indices .....	143
5.3.3. Effect of the Number of Steps in a Load Model .....	145
5.3.4. Effect of a Nonuniform Load Increment Step Model .....	149
5.4. Generating Unit Derated States .....	150
5.4.1. Sampling Multiderated States .....	150
5.4.2. Case Studies .....	151
5.5. Regional Weather Effects .....	153
5.5.1. General Concepts .....	153
5.5.2. Basic Transmission Line Model Recognizing Weather Conditions .....	155
5.5.3. Sampling Regional Weather States .....	156
5.5.4. Determination of Transmission Line Forced Unavailability and Repair Time with Regional Weather Effects .....	157
5.5.5. Test System and Data .....	158
5.5.6. Case Studies .....	160
5.6. Transmission Line Common Cause Outages .....	164
5.6.1. General Concepts .....	164
5.6.2. Case Studies .....	166
5.7. Bus Load Uncertainty and Correlation .....	169
5.7.1. Tabulating Technique for Bus Load Normal Distribution Sampling .....	169
5.7.2. Bus Load Correlation Sampling Technique .....	171
5.7.3. Case Studies .....	172
5.8. Frequency Index and System State Transition Sampling Technique .....	179
5.8.1. Discussion on the Frequency Index .....	179
5.8.2. System State Transition Sampling Technique .....	182
5.8.3. Case Studies .....	185
5.9. Security Considerations in Composite System Adequacy Evaluation .....	187
5.9.1. System Model Including Security Considerations .....	187
5.9.2. System Analysis Techniques .....	189
5.9.3. Hybrid Methodology .....	191

5.9.4. Case Studies .....	193
5.9.5. Application of Variance Reduction Techniques .....	196
5.10. Noncoherence in Composite System Adequacy	
Assessment .....	199
5.10.1. Definitions and Measures of Noncoherence .....	199
5.10.2. A Simple Example .....	202
5.11. Conclusions .....	205
5.12. References .....	206

## Chapter 6

### Distribution System and Station Adequacy

#### Assessment

6.1. Introduction .....	209
6.2. Basic Concepts and Analytical Techniques for Distribution	
System Adequacy Assessment .....	210
6.2.1. General Concepts .....	210
6.2.2. Basic Distribution Systems .....	212
6.2.3. Analytical Techniques .....	213
6.3. Monte Carlo Simulation Approach to Distribution	
System Adequacy Assessment .....	218
6.3.1. Probability Distribution Considerations .....	218
6.3.2. Component State Duration Sampling Method .....	219
6.3.3. Load Point Index Distributions .....	221
6.3.4. System Performance Index Distributions .....	230
6.4. Station Reliability Assessment .....	232
6.4.1. General Concepts .....	232
6.4.2. Station Component Modeling .....	233
6.4.3. Component State Duration Sampling Procedure .....	236
6.4.4. Numerical Example 1 .....	240
6.4.5. Numerical Example 2 .....	244
6.5. Conclusions .....	251
6.6. References .....	253

## Chapter 7

### Reliability Cost/Worth Assessment

7.1. Introduction .....	255
7.2. Customer Surveys and Customer Damage Functions .....	256
7.2.1. Basic Customer Survey Methods .....	256
7.2.2. Questionnaire Content and Data Treatment .....	258
7.2.3. Customer Damage Functions .....	258

7.3.	Generating System Reliability Worth Assessment . . . . .	262
7.3.1.	Assessment Techniques . . . . .	262
7.3.2.	Numerical Example . . . . .	264
7.3.3.	Application of Reliability Worth Assessment in Generation Planning . . . . .	265
7.4.	Composite System Reliability Worth Assessment . . . . .	268
7.4.1.	Assessment Method . . . . .	268
7.4.2.	Modified IEEE Reliability Test System and Additional Data . . . . .	272
7.4.3.	Numerical Results . . . . .	273
7.4.4.	Application of Reliability Worth Assessment in Composite System Planning . . . . .	277
7.5.	Distribution System Reliability Worth Assessment . . . . .	279
7.5.1.	Assessment Techniques . . . . .	279
7.5.2.	Numerical Example . . . . .	281
7.6.	Minimum Cost Assessment in Composite System Expansion Planning . . . . .	282
7.6.1.	Basic Concepts . . . . .	282
7.6.2.	Minimum Cost Assessment Method . . . . .	284
7.6.3.	Case Studies . . . . .	288
7.7.	Conclusions . . . . .	294
7.8.	References . . . . .	296

## Appendix A

### Reliability Test Systems

A.1.	IEEE Reliability Test System (IEEE RTS) . . . . .	299
A.1.1.	Load Model . . . . .	299
A.1.2.	Generating System . . . . .	300
A.1.3.	Transmission System . . . . .	302
A.1.4.	Additional Data . . . . .	305
A.2.	Roy Billinton Test System (RBTS) . . . . .	306
A.2.1.	Brief Description of the RBTS . . . . .	309
A.2.2.	Load Model . . . . .	309
A.2.3.	Generating System . . . . .	309
A.2.4.	Transmission System . . . . .	312
A.2.5.	Station Data . . . . .	313
A.2.6.	Reliability Worth Assessment Data . . . . .	315
A.3.	References . . . . .	316

**Appendix B****Elements of Probability and Statistics**

B.1.	Probability Concept and Calculation Rules .....	317
B.1.1.	Probability Concept .....	317
B.1.2.	Probability Calculation Rules .....	317
B.2.	Probability Distributions of Random Variables .....	318
B.2.1.	Probability Distribution Function and Density Function .....	318
B.2.2.	Important Distributions in Reliability Evaluation .....	320
B.3.	Numerical Characteristics of Random Variables .....	321
B.3.1.	Expectation and Variance.....	322
B.3.2.	Covariance and Correlation Function .....	322
B.4.	Limit Theorems .....	323
B.4.1.	Law of Large Numbers.....	323
B.4.2.	Central Limit Theorem .....	324
B.5.	Parameter Estimation .....	324
B.5.1.	Basic Definitions .....	324
B.5.2.	Sample Mean and Sample Variance .....	325
B.6.	References .....	326

**Appendix C****Power System Analysis Techniques**

C.1.	AC Load Flow Models .....	327
C.1.1.	Load Flow Equations .....	327
C.1.2.	Newton-Raphson Model .....	328
C.1.3.	Fast Decoupled Model .....	328
C.2.	DC Load Flow Models .....	329
C.2.1.	Basic Equations .....	329
C.2.2.	Relationship between Power Injections and Line Flows .....	331
C.3.	Optimal Power Flow.....	331
C.4.	Contingency Analysis .....	332
C.5.	References .....	336

**Appendix D****Optimization Techniques**

D.1.	Linear Programming .....	337
D.1.1.	Basic Concepts .....	337
D.1.2.	Generalized Simplex Method .....	338

D.1.3. Duality Principle .....	340
D.1.4. Dual Simplex Method .....	341
D.1.5. Linear Programming Relaxation Technique.....	342
<b>D.2. Maximum Flow Method .....</b>	<b>344</b>
D.2.1. Basic Concepts .....	345
D.2.2. Maximum Flow Problem .....	346
D.3. References .....	347
<b>Index .....</b>	<b>349</b>

# Introduction

## 1.1. PROBABILISTIC ANALYSIS OF POWER SYSTEMS

The primary function of an electric power system is to provide electrical energy to its customers as economically as possible and with an acceptable degree of continuity and quality. Modern society has come to expect that the supply of electrical energy will be continuously available on demand. This is not possible due to random failures of equipment and the system, which are generally outside the control of power system personnel. Electricity supply generally involves a very complex and highly integrated system. Failures in any part of it can cause interruptions which range from inconveniencing a small number of local residents, to major and widespread catastrophic disruptions of supply. The economic impact of these outages is not restricted to loss of revenue by the utility or loss of energy utilization by the customer but include indirect costs imposed on society and the environment due to the outage. In the case of the 1977 New York blackout, the total costs of the blackouts were suggested to be as high as \$350 million, which 84% was attributed to indirect costs.<sup>(1)</sup>

In order to reduce the probability, frequency and duration of these events and to ameliorate their effect, it is necessary to increase investment in the planning, design and operating phases. A whole series of questions arise from this concept, including:

- How much should be spent?
- Is it worth spending any money?
- Should the reliability be increased, maintained at existing levels, or allowed to degrade?
- Who should decide—the utility, a regulator, the customer?
- On what basis should the decision be made?

It is evident that the economic and reliability constraints can conflict and lead to difficult managerial decisions.

These problems have been long recognized by power system managers, designers, planners, and operators. Design, planning, and operating criteria and techniques have been developed over many years in an attempt to resolve and satisfy the dilemma created by the economic, reliability, and operational constraints. The criteria and techniques first used in practical applications were all deterministically based and many of these criteria and techniques are still in use today. These include percentage reserves in generation capacity planning or  $N-1$  contingency criteria in transmission planning.

The basic weakness of deterministic criteria is that they do not respond to, nor do they reflect, the probabilistic or stochastic nature of system behavior, of customer demands, or of component failures. Deterministic analysis can consider the outcome and ranking of hazards which may lead to a dangerous state or a system failure. However, a hazard, even if extremely undesirable, is of little consequence if it cannot occur or is so unlikely that it can be ignored. Planning alternatives based on such hazard analyses will lead to overinvestment. Conversely, if the hazards selected in the deterministic analysis are not very severe but have relatively large probabilities of occurrence, alternatives based on a deterministic analysis of such hazards will lead to insufficient system reliability. Probabilistic evaluation of a power system can recognize not only the severity of a state or an event and its impact on system behavior and operation, but also the likelihood or probability of its occurrence. Appropriate combination of both severity and likelihood creates indices that truly represent system risk.

The need for probabilistic evaluation of system behavior has been recognized for over forty years<sup>(2,3)</sup> and it may be questioned why such methods have not been widely used in the past. The main reasons have been lack of data, limitations of computational resources, lack of realistic techniques, aversion to the use of probabilistic techniques, and a misunderstanding of the significance and meaning of probabilistic criteria and indices. None of these reasons is valid today as most utilities have relevant reliability databases, computing facilities are greatly enhanced, evaluation techniques are highly developed, and most engineers have a working understanding of probabilistic techniques. There is, therefore, now no need to artificially constrain the inherent probabilistic or stochastic nature of a power system into a deterministic framework.

A wide range of probabilistic techniques has been developed. These include techniques for reliability and reliability worth evaluation,<sup>(4-14)</sup> probabilistic load flow,<sup>(15-17)</sup> probabilistic fault analysis,<sup>(18-20)</sup> probabilistic transient stability,<sup>(21-23)</sup> and probabilistic transmission line design.<sup>(24-27)</sup> The fundamental and common concept behind each of these developments is the need to recognize that power systems and system components behave stochastically and all input and output state and event parameters are probabilistic variables.

## 1.2. RELIABILITY EVALUATION TECHNIQUES

Power system reliability evaluation has been extensively developed utilizing probabilistic methods and a wide range of appropriate indices can be determined. A single all-purpose formula or technique does not exist. The approach used and the resulting formulas depend on the problem and the assumptions utilized. Many assumptions must be made in all practical applications of probability and statistical theory. The validity of the analysis is directly related to the validity of the models used to represent the system. Actual failure distributions seldom completely fit the analytical descriptions used in the analysis, and care must be taken to ensure that significant errors are not introduced through oversimplification. On the other hand, a potential user of reliability evaluation techniques should clearly keep in mind the objective behind the evaluation process. In generation system capacity assessment, a reference adequacy level can often be obtained in terms of historical experience of the individual utility. This generally requires a model as accurate as possible so that the resulting indices can be compared with the given target level. In evaluating composite generation and transmission systems, distribution systems, and substation configurations, however, it is generally necessary to assess the relative benefits between the various alternatives available, including the option of not doing any reinforcement at all. The level of analysis need not be any more complex than that which enables the relative merits to be assessed. The apparent ability to include a high degree of precision in the calculations should never override the inherent uncertainties in the forecast data, including load, failure rates, restoration times, etc. Absolute reliability, although an ideal objective, is virtually impossible to evaluate. This does not weaken the necessity to objectively assess the relative merits of alternate schemes.

The most important point to note is that it is absolutely necessary to have a complete understanding of the system. No amount of probability theory can circumvent this important engineering function. Probability theory is simply a tool that enables the analyst to transform knowledge of the system into a prediction of its likely future behavior. Only after this understanding has been achieved, can a model be derived and an appropriate evaluation technique chosen. Both of these must reflect and respond to the way the system operates and fails. The basic steps involved are to:

- Understand the way in which the components and system operate.
- Identify the way in which they can fail.
- Deduce the consequences of the failures.
- Derive models to represent these characteristics.
- Then select the evaluation technique.

There are two main categories of evaluation techniques: analytical and simulation. Analytical techniques represent the system by analytical models and evaluate the indices from these models using mathematical solutions. Monte Carlo simulation methods, however, estimate the indices by simulating the actual process and random behavior of the system. The method, therefore, treats the problem as a series of experiments. There are merits and demerits in both methods. In general, if complex operating conditions are not considered and/or the failure probabilities of components are quite small (i.e., the system is very reliable), the analytical techniques are more efficient. When complex operating conditions are involved and/or the number of severe events is relatively large, Monte Carlo methods are often preferable. The main advantages of Monte Carlo methods are as follows:

- In theory, they can include system effects or system processes which may have to be approximated in analytical methods.
- The required number of samples for a given accuracy level is independent of the size of the system and therefore it is suitable for large-scale system evaluation.
- They can simulate probability distributions associated with component failure and restoration activities. This generally cannot be performed using analytical methods.
- They can calculate not only reliability indices in the form of expected values of random variables, but also the distributions of these indices, which analytical techniques generally cannot.
- Nonelectrical system factors such as reservoir operating conditions, weather effects, etc. can also be simulated.

It should be appreciated that there can be considerable differences between various analytical techniques or Monte Carlo methods. The evaluated indices are only as good as the model derived for the system, the appropriateness of the evaluation technique, and the quality of the input data used in the models and techniques. This is an important point to appreciate.

### 1.3. OUTLINE OF THE BOOK

Analytical techniques for power system reliability evaluation have been highly developed and there are many technical papers and several books which summarize the developed techniques.<sup>(4-7)</sup> Developments in Monte Carlo simulation can generally be said to have occurred later than comparable analytical techniques. Considerable effort has, however, been expanded in developing Monte Carlo simulation methods, and in a number of areas

these techniques provide viable alternatives to the analytical approaches. This book provides a basic reference on this area and is based on research activities performed at the University of Saskatchewan and BC Hydro in Canada. The book does not include every known and available technique but provides a systematic description of the topic, including basic mathematical principles, and presents applications in each power system functional zone.

Chapter 2 presents basic concepts of power system reliability evaluation. These concepts are used in both analytical techniques and Monte Carlo methods. Chapter 3 describes elements of the Monte Carlo method. This description, based on the mathematical fundamentals of Monte Carlo simulation, places emphasis on the application aspects of Monte Carlo methods in system reliability evaluation. Chapters 2 and 3 are the basis for the following chapters.

Chapter 4 illustrates applications of the component state duration sampling and the system state sampling methods in generation system adequacy assessment. Both single area and multi-area generation systems are discussed. A maximum network flow approach and linear programming models are utilized in the multi-area system evaluation.

Chapter 5 illustrates applications of the system state sampling and the system state transition sampling methods in composite generation and transmission system adequacy assessment. Contingency analysis and linear programming optimal power flow techniques are utilized in this aspect. Various system problems are considered. These include considerations such as annual load duration curves, generating unit derated states, regional weather effects, transmission line common cause failures, bus load forecast uncertainty and correlation, etc. Two special aspects are discussed. The first one is consideration of steady state security in composite system adequacy assessment and the second one is possible noncoherence of composite systems.

Chapter 6 describes applications of the component state duration sampling method in distribution system and station adequacy assessment. A basic emphasis is placed on the simulation of distributions of component restoration times and the calculation of probability distributions of reliability indices.

Chapter 7 illustrates reliability cost/worth assessment of generation, composite, and distribution systems using Monte Carlo methods. Applications of reliability worth assessment in power system planning are also discussed and a minimum cost assessment method for composite system expansion planning is described.

There are four appendices provided. Appendix A presents the data for the two reliability test systems which are used in the case studies throughout the book. Appendix B provides essential elements of probability and statistics, while Appendices C and D, respectively, present basic power system

analysis techniques and the optimization methods used in the various applications.

It is important to note that although the book describes applications of Monte Carlo methods in power system reliability assessment, the basic system analysis techniques and mathematical models such as contingency analysis, optimal power flow, maximum network flow approach, linear programming models for various evaluation purposes, etc. can also be utilized in analytical applications of power system reliability assessment. The essential difference between analytical and Monte Carlo methods is basically how to select system state scenarios to be evaluated.

This book does not pretend to include all the known and available materials on this topic. It will, however, place the reader in a position whereby he/she can accommodate a wide range of problems and gain a wider and deeper appreciation of the materials that have been published and which will, no doubt, be enhanced in the future.

## 1.4. REFERENCES

1. R. Sugarman, "New York City's Blackout: A \$350 Million Drain," *IEEE Spectrum Compendium: Power Failure Analysis and Prevention*, 1979, pp. 48–50.
2. G. Calabrese, "Generating Reserve Capacity Determined by the Probability Method," *AIEE Trans.*, No. 66, 1947, pp. 1439–1450.
3. C. W. Watchorn, "The Determination and Allocation of the Capacity Benefits Resulting from Interconnecting Two or More Generating Systems," *AIEE Trans.*, No. 69, 1950, Pt. II, pp. 1180–1186.
4. R. Billinton and R. N. Allan, *Reliability Evaluation of Power Systems*, Plenum, New York, 1984.
5. R. Billinton and R. N. Allan, *Reliability Assessment of Large Electric Power Systems*, Kluwer, Boston, 1988.
6. R. Billinton, R. N. Allan, and L. Salvadori, *Applied Reliability Assessment in Electric Power Systems*, IEEE Press, New York, 1991.
7. J. Endrenyi, *Reliability Modeling in Electric Power Systems*, Wiley, Chichester, 1978.
8. R. Billinton, "Bibliography on the Application of Probability Methods in Power System Reliability Evaluation," *IEEE Trans. on PAS*, Vol. 91, 1972, pp. 649–660.
9. IEEE Committee Report, "Bibliography on the Application of Probability Methods in Power System Reliability Evaluation, 1971–1977," *IEEE Trans. on PAS*, Vol. 97, 1978, pp. 2235–2242.
10. R. N. Allan, R. Billinton, and S. H. Lee, "Bibliography on the Application of Probability Methods in Power System Reliability Evaluation, 1977–1982," *IEEE Trans. on PAS*, Vol. 103, 1984, pp. 275–282.
11. R. N. Allan, R. Billinton, S. M. Shahidehpour, and C. Singh, "Bibliography on the Application of Probability Methods in Power System Reliability Evaluation, 1982–1987," *IEEE Trans. on PS*, Vol. 3, No. 4, 1988, pp. 1555–1564.
12. R. Billinton, G. Wacker, and E. Wojczynski, "Comprehensive Bibliography of Electrical Service Interruption Costs," *IEEE Trans. on PAS*, Vol. 102, 1983, pp. 1831–1837.

13. G. Tollefson, R. Billinton, and G. Wacker, "Comprehensive Bibliography on Reliability Worth and Electrical Service Consumer Interruption Costs: 1986–1990," *IEEE Trans. on PS*, Vol. 6, No. 4, 1991, pp. 1508–1514.
14. CIGRE Working Group 38.03, "Power System Reliability Analysis—Application Guide," CIGRE Publications, Paris, 1988.
15. M. Th. Schilling, A. M. Leite da Siva, R. Billinton, and M. A. El-Kady, "Bibliography on Power System Probabilistic Analysis (1962–1988)," *IEEE Trans. on PS*, Vol. 5, No. 1, 1990, pp. 1–11.
16. B. Borkowska, "Probabilistic Load Flow," *IEEE Trans. on PAS*, Vol. 93, 1974, pp. 752–759.
17. A. M. Leite da Silva, S. M. P. Ribeiro, V. L. Arienti, R. N. Allan, and M. B. Do Coutto Filho, "Probabilistic Load Flow Techniques Applied to Power System Expansion Planning," *IEEE Trans. on PS*, Vol. 5, No. 4, 1990, pp. 1047–1053.
18. G. L. Ford and K. D. Srivastava, "Probabilistic Short Circuit Design of Substation Bus Systems," IEEE Winter Meeting, 1978, Paper A78 211–5.
19. G. L. Ford and S. S. Sengupta, "Analytical Methods for Probabilistic Short Circuit Studies," *Electric Power System Research*, Vol. 5, 1982, pp. 13–20.
20. M. D. Germani, G. L. Ford, E. G. Neudorf, M. Vainberg, M. A. El-Kady, and R. W. D. Ganton, "Probabilistic Short Circuit Uprating of Station Strain Bus System—Overview and Application," *IEEE Trans. on PWRD*, Vol. 1, 1986, pp. 111–117.
21. R. Billinton and P. R. S. Kurunganty, "A Probabilistic Index for Transient Stability," *IEEE Trans. on PAS*, Vol. 99, 1980, pp. 195–206.
22. R. Billinton and P. R. S. Kurunganty, "Probabilistic Evaluation of Transient Stability in Multimachine Power Systems," *IEE Proc. C*, Vol. 126, 1980, pp. 321–326.
23. P. M. Anderson, A. Bose, K. J. Timko, and F. E. Villaseca, "A Probabilistic Approach to Stability Analysis," EPRI Report EL-2797, 1983.
24. EPRI Report, "Reliability Based Design of Transmission Line Structures: Final Report," EL-4793, 1987.
25. E. Ghannoum and G. Orawski, "Reliability Based Design of Transmission Lines According to Recent Advances by IEC and CIGRE," in *Probabilistic Methods Applied to Electric Power Systems*, Pergamon, Oxford, 1987, pp. 125–142.
26. International Electrotechnical Commission (IEC), "Draft of IEC/TC11 Recommendations for Overhead Lines," 1985.
27. S. G. Krishnasamy and N. Ramani, "Wind Direction and Extreme Wind Loads for Overhead Power Line Design," in *Probabilistic Methods Applied to Electric Power Systems*, Pergamon, Oxford, 1987, pp. 399–411.

# 2

# Basic Concepts of Power System Reliability Evaluation

## 2.1. ADEQUACY AND SECURITY

The term *reliability* has a very wide range of meaning and cannot be associated with a single specific definition such as that often used in the mission-oriented sense.<sup>(1)</sup> It is therefore necessary to recognize this fact and to use the term to indicate, in a general rather than a specific sense, the overall ability of the system to perform its function. Power system reliability assessment can therefore be divided into the two basic aspects of system adequacy and system security as shown in Figure 2.1. The terms *adequacy* and *security* can be described as follows:

Adequacy relates to the existence of sufficient facilities within the system to satisfy the consumer load demand or system operational constraints. These includes the facilities necessary to generate sufficient energy and the associated transmission and distribution facilities required to transport the energy to the actual consumer load points. Adequacy is therefore associated with static conditions which do not include system dynamic and transient disturbances.

Security relates to the ability of the system to respond to dynamic or transient disturbances arising within the system. Security is therefore associated with the response of the system to whatever perturbations it is subject to. These include the conditions associated with both local and widespread disturbances and the abrupt loss of major generation or/and transmission

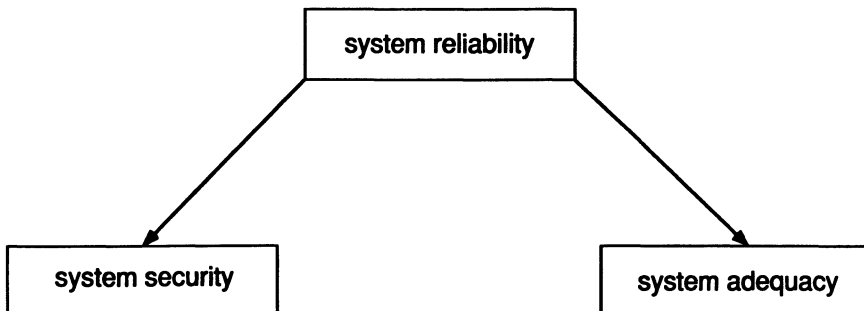


**Figure 2.1.** Subdivision of system reliability.

facilities which can lead to dynamic, transient, or voltage instability of the system.

It is important to appreciate that most of the probabilistic techniques presently available for reliability evaluation are in the domain of adequacy assessment. The ability to assess security is therefore very limited. Probabilistic transient stability evaluation<sup>(2)</sup> lies in this domain together with techniques for quantifying unit commitment and response risk.<sup>(3)</sup> This limitation is due to the complexities associated with modeling the system in the security domain. Most of the indices used at the present time are adequacy indices and not overall reliability indices. Indices which are obtained by assessing past system performance encompass the effect of all system faults and failures irrespective of cause, and therefore include the effect of insecurity as well as those due to inadequacy. This fundamental difference is an important point which should be clearly recognized.

## 2.2. FUNCTIONAL ZONES AND HIERARCHICAL LEVELS

The basic techniques for adequacy assessment can be categorized in terms of their application to segments of a complete power system. These segments are shown in Figure 2.2 and can be defined as the functional zones of generation, transmission, and distribution.<sup>(4)</sup> This division is an appropriate one as most utilities are either divided into these zones for the purposes of organization, planning, operation, and/or analysis or are solely responsible for one of these functions. Adequacy studies can be, and are, conducted in each of these three functional zones.

The functional zones shown in Figure 2.2 can be combined to give the hierarchical levels shown in Figure 2.3. These hierarchical levels can also be

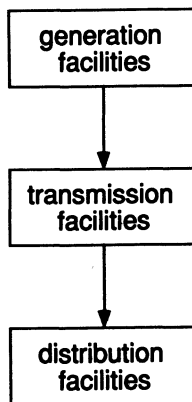


**Figure 2.2.** Basic functional zones.

used in adequacy assessment. Hierarchical Level 1 (HL1) is concerned with only the generation facilities. Hierarchical Level 2 (HL2) includes both generation and transmission facilities while HL3 includes all three functional zones in an assessment of consumer load point adequacy. HL3 studies are not usually conducted directly due to the enormity of the problem in a practical system. Analysis is usually performed in the distribution functional zone in which the input points may or may not be considered to be fully reliable.

Functional zone studies are often done which do not include the hierarchical levels above them. These studies are usually performed on a subset

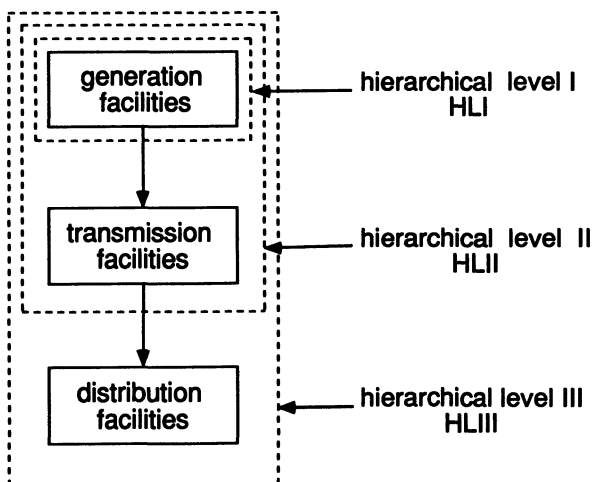


**Figure 2.3.** Hierarchical levels.

of the system in order to examine a particular configuration or topological change. These analyses are frequently undertaken in the subtransmission and distribution system functional zones as these areas are less affected by the actual location of the generating facilities. In transmission planning studies, especially for those relatively low-voltage transmission subsystems which are far away from generation sources, generation facilities are usually assumed to be 100% reliable in order to highlight effects of different transmission components and configurations on system reliability.

In composite system (HL2) adequacy studies of relatively large scale transmission systems, it is reasonable to limit a study area and, in doing so, provide more realistic results than by evaluating the whole system. This is due to the fact that the addition of a transmission facility may considerably affect a local area but have basically little impact on remote parts of the system. The contribution to overall reliability of a large system due to a local transmission line addition may be so small that it is masked by computational errors and consequently cannot be reflected in the reliability change of the whole system. This contribution, however, can be a relatively large proportion of the reliability change in the local area. When the planning task is to investigate reinforcement alternatives of the subsystem represented by the local area, evaluating reliability of the whole system may lead to a “no addition” conclusion. In this case, it is desirable to limit the size of the studied system or/and utilize system equivalent techniques. Reliability equivalence is a useful tool/concept<sup>(5)</sup> in this application area.

## 2.3. REQUIREMENTS FOR POWER SYSTEM ADEQUACY ASSESSMENT

### 2.3.1. Generation System (HL1) Studies

In a generation system study, the total system generation is examined to determine its adequacy to meet the total system load requirement. This activity is usually termed “generating capacity reliability evaluation.” The system model at this level is shown in Figure 2.4.

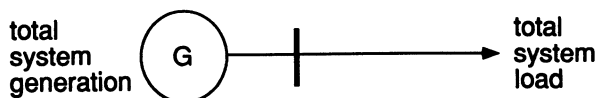


**Figure 2.4.** Hierarchical level 1 (HL1) model.

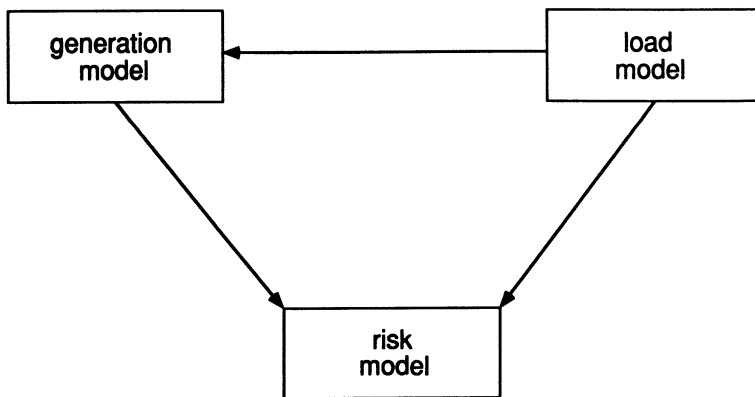


**Figure 2.5.** Conceptual tasks for HL1 evaluation.

The transmission system and its ability to move the generated energy to the consumer load points is ignored in generating system adequacy assessment. The basic concern is to estimate the generating capacity required to satisfy the system demand and to have sufficient capacity to perform corrective and preventive maintenance on the generating facilities. The basic technique, used in the past, to determine the capacity requirement was the percentage reserve method. In this approach, the required reserve is a fixed percentage of either the installed capacity or the predicted load. This and other criteria, such as a reserve equal to one or more of the largest units, have now been largely replaced by probabilistic methods which respond to and reflect the actual factors that influence the reliability of the system.<sup>(3)</sup>

The basic modeling approach<sup>(3)</sup> for an HL1 study is shown in Figure 2.5. Analytical methods and Monte Carlo simulation utilize different techniques to assess generation and load models. The essential concept shown in this figure, however, is basically the same for both techniques.

Limited transmission considerations can be, and are, included in HL1 studies. These include the modeling of remote generation facilities and interconnected systems. In the latter case, only the interconnections between adjacent systems are modeled, not the internal system connections or intra-connections. The latter is often termed multi-area generating system adequacy assessment. In the case of remote generation, the capacity model of the remote source is modified by the reliability of the transmission link before being added to the system capacity model. In the case of interconnected systems, the available assistance model should be considered. The most widely used modeling methods for a multi-area generation system are network flow (maximum flow–minimum cut) techniques.

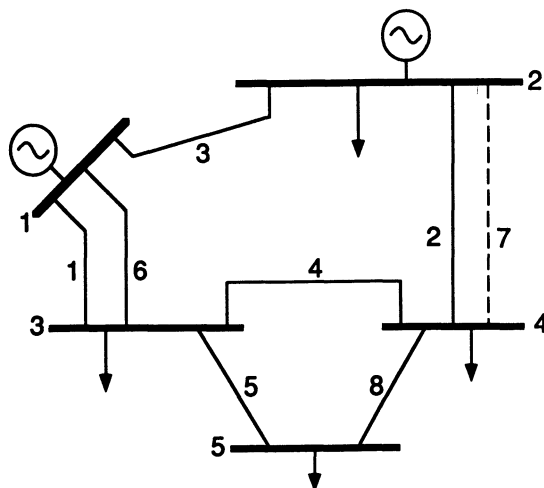


**Figure 2.6.** A sample composite system for HL2 studies.

### **2.3.2. Composite System (HL2) Studies**

In HL2 studies, the simple generation-load model shown in Figure 2.4 is extended to include bulk transmission. Adequacy analysis at this level is usually termed composite system or bulk transmission system evaluation. A sample composite system<sup>(3)</sup> is shown in Figure 2.6.

HL2 studies can be used to assess the adequacy of an existing or proposed system including the impact of various reinforcement alternatives at both the generation and transmission levels. These effects can be assessed by evaluating two sets of indices: individual bus (load points) indices and overall system indices. These indices are complementary and not alternatives. The system indices provide an assessment of overall adequacy. The bus indices show the effect at individual busbars and provide input values to subsequent distribution system adequacy evaluation (HL3). Both system and bus indices can be categorized as annualized and annual indices. Annualized indices are calculated using a single load level (normally the system peak load level) and expressed on a one-year basis. Annual indices are calculated considering detailed load variations throughout one year. In general, annualized indices provide satisfactory indications when comparing adequacies of different reinforcement alternatives. Annual indices show a more realistic and comprehensive picture of system adequacy. Annual indices should be utilized when attempting to calculate actual damage cost of system unreliability or evaluate reliability worth. Although these indices add realism by including transmission, they are still adequacy indicators. They do not

include the system dynamics or the ability of the system to respond to transient disturbances. They simply measure the ability of the system to adequately meet its requirements in a specified set of probabilistic states.

There are many complications in HL2 studies associated with load flow calculations, contingency analysis, overload alleviation, generation rescheduling, load curtailment philosophy, etc. In the area of system state selection, considerations of independent, dependent, common-cause, and station-related outages, regional weather effects, and bus load uncertainty and correlation, etc., introduce additional complexities. These aspects are discussed further in Chapter 5. It should be noted, however, that the primary indices are expected values and are highly dependent on the modeling assumptions. Adequacy assessment at HL2 is still very much in the development phase. There are many power utilities and related organizations doing interesting and innovative work in this area.

### 2.3.3. Distribution System Studies

The overall problem of HL3 evaluation can become very complex in most systems as this level involves all three functional zones, starting at the generating stations and terminating at the individual consumer load points. For this reason, the distribution functional zone is usually analyzed as a separate entity. HL3 indices can be evaluated, however, by using the HL2 load-point indices as the input values of the distribution functional zone being analyzed.

Distribution system adequacy evaluation involves assessment of suitable adequacy indices at the actual consumer load points. There are two basic types of distribution system: meshed and radial configurations. Evaluation methods for meshed distribution systems are conceptually the same as those used for composite systems. The techniques for a radial distribution system are based on failure-mode analysis including considerations of all realistic failure and restoration processes. These techniques also apply to substation adequacy assessment as a substation has similar configurations and failure modes.

Individual customer adequacy due to the overall system is reflected by HL3 indices. In most systems, inadequacy of the individual customer points is caused mainly by the distribution system. HL2 adequacy indices generally have a relatively small effect on individual customer load-point indices. The HL1 and HL2 indices are very important, however, because failures in these segments affect large sections of the system and therefore can have widespread and perhaps catastrophic consequences for both society and the

environment. Failures in the distribution system, although more frequent, have much more localized effects.

## 2.4. RELIABILITY COST/WORTH

Adequacy studies of a system are only part of the required overall assessment. The economics of alternate facilities play a major role in the decision-making process. The simplest approach which can be used to relate economics with reliability is to consider the investment cost only. In this approach, the increase in reliability due to the various alternatives is evaluated together with the investment cost associated with each scheme. Dividing this cost by the increase in reliability gives the incremental cost of reliability, i.e., how much it will cost for a per-unit increase in reliability. This approach is useful when comparing alternatives given that the reliability of a section of the power system is inadequate. In this case, the lowest incremental cost of reliability is the most cost effective. This is still a significant step forward from comparing alternatives and making major capital investment decisions using deterministic techniques.

The weakness of this approach is that it is not related to either the likely return on investment or the real benefit accruing to the consumer, utility, and society. In order to make a consistent appraisal of economics and reliability, albeit only the adequacy, it is necessary to compare the adequacy cost (the investment cost needed to achieve a certain level of adequacy) with adequacy worth (the benefit derived by the utility, consumer, and society). A step in this direction can be achieved by setting a level of incremental cost which is believed to be acceptable to consumers. Schemes costing less than this level would be considered viable but schemes costing more would be rejected. A complete solution, however, requires a detailed knowledge of adequacy worth.

This type of economic appraisal is a fundamental and important area of engineering application, and it is possible to perform this kind of evaluation at the three hierarchical levels. A goal for the future should be to extend this adequacy comparison within the same hierarchical structure to include security, and therefore to arrive at reliability-cost and reliability-worth evaluation. The extension of quantitative reliability analysis to the evaluation of service worth is deceptively simple but is fraught with potential misapplication. The basic concept is relatively simple and can be illustrated using the cost/reliability curves of Figure 2.7.

Figure 2.7 shows that utility costs will generally increase as consumers are provided with higher reliability. On the other hand, consumer costs associated with supply interruptions will decrease as the reliability increases.

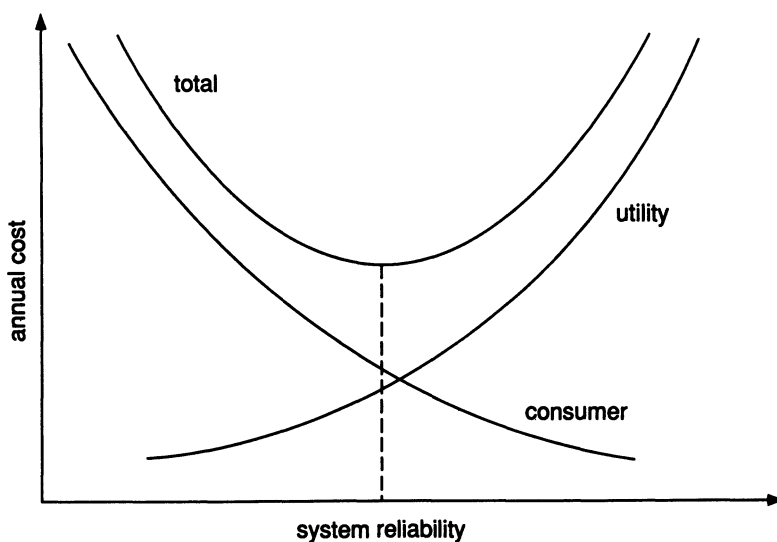


**Figure 2.7.** Consumer, utility, and total cost as a function of system reliability.

The total costs to society are the sum of these two individual costs. This total cost exhibits a minimum point at which an “optimum” or target level of reliability is achieved.

There have been many studies on the subject of interruption and outage costs.<sup>(6)</sup> These analyses show that, although trends are similar in virtually all cases, the costs vary over a wide range and depend on the country of origin and the type of consumer. It is apparent, therefore, that considerable research is still needed on power system interruption costs. This research should consider both the direct and indirect costs associated with the loss of supply.

## 2.5. RELIABILITY DATA

### 2.5.1. General Concepts

Any discussion of quantitative reliability evaluation invariably leads to a discussion of the data available and the data required to support such studies. Valid and useful data are expensive to collect, but it should be recognized that in the long run it will be even more expensive not to collect them. It is sometimes argued as to which comes first: reliability data or reliability methodology. Some utilities do not collect data because they have

not fully determined a suitable reliability methodology. Conversely, they do not conduct reliability studies because they do not have any data. It should be remembered that data collection and reliability evaluation must evolve together and that the process is therefore iterative.

In conceptual terms, data can be collected for two fundamental reasons: assessment of past performance and/or prediction of future system performance. Past assessment looks back at the past behavior of the system while predictive procedures look forward at future system behavior. In order to predict, however, it is essential to transform past experience into suitable models for future prediction. Collection of suitable data is therefore essential as it forms the input to relevant reliability models, techniques, and equations.

It should also be appreciated that the data requirements should reflect the needs of the predictive methodology. The data must be sufficiently comprehensive to ensure that the methods can be applied, but restrictive enough to ensure that unnecessary data are not collected nor irrelevant statistics evaluated. The data should therefore reflect and respond to the factors that affect system reliability and enable it to be modeled and analyzed. It should relate to the two main processes involved in component behavior, namely, the failure process and the restoration process. It cannot be stressed too strongly that, in deciding data to be collected, a utility must consider the factors that have an impact on its own planning and design considerations.

The quality of the data and the indices evaluated depend on two important factors: confidence and relevance. The quality of the data, and thus the confidence that can be placed in it, is clearly dependent on the accuracy and completeness of the information compiled by operating and maintenance personnel. It is therefore essential that they should be made fully aware of the future use of data and the importance they will play in the later development of the system. The quality of the statistical indices is also dependent on how the data are processed, how much pooling is done, and the age of the data currently stored.

## **2.5.2. Equipment Reliability Information System**

In order to establish a common reporting procedure and realize a practical database, all the major electric power utilities in Canada participate in a single data collection and analysis system called the Equipment Reliability Information System (ERIS) of the Canadian Electrical Association (CEA).<sup>(7)</sup> CEA started collecting data on generation and transmission outages in 1977 and since then has published a number of annual or periodic

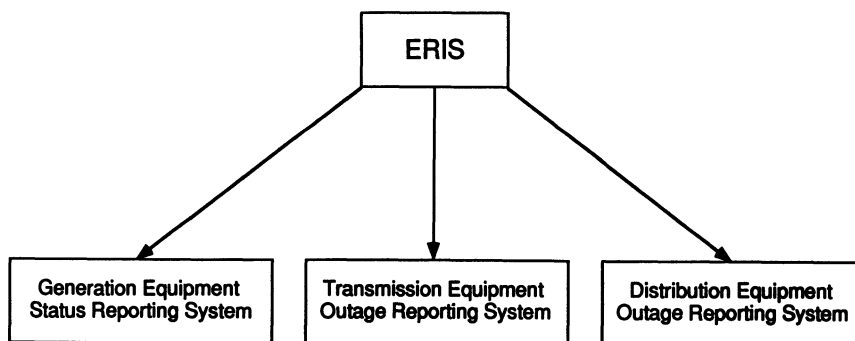


**Figure 2.8.** Basic components of the ERIS.

reports. A distribution equipment outage reporting system was initiated on January 1, 1992 and participating utilities commenced collecting data at that time. Annual reports will be issued commencing in 1993. The basic structure of ERIS is shown in Figure 2.8.

In order to provide a general indication of the basic equipment reliability parameters, selected CEA data are presented. Tables 2.1 to 2.4 show average failure rates and mean outage times of major generation and transmission components obtained from the 1990 annual ERIS reports.<sup>(8,9)</sup> These

**Table 2.1. Generating Unit Failure Data**

Unit capacity (MW)	Failure rate (occ./yr)	Mean outage time (hr/occ.)
<b>Hydraulic units</b>		
24–99	3.44	93.29
100–199	3.76	71.35
200–299	6.14	74.94
300–399	6.03	41.46
400–499	2.82	64.50
500 & over	2.42	112.58
<b>Fossil units</b>		
69–99	11.50	44.72
100–199	14.53	37.72
200–299	13.79	25.72
300–399	16.54	46.55
400–599	8.79	45.30
<b>Nuclear units</b>		
400–599	3.40	369.35
600–799	4.90	27.17
800 & over	4.49	111.64

**Table 2.2. Transmission Line Failure Data**

Voltage level (kV)	Line-related		Terminal-related	
	failure rate (occ./yr/100 km)	outage time (hr/occ.)	failure rate (occ./yr)	outage time (hr/occ.)
110–149	1.0858	6.6	0.1295	5.5
150–199	0.5513	1.6	0.0959	4.1
200–299	0.5429	12.4	0.1351	4.7
300–399	0.3010	0.8	0.0836	4.0
500–599	0.5468	22.5	0.2752	22.9
600–799	0.1689	7.3	0.1184	26.2

**Table 2.3. Transformer Failure Data**

Voltage level (kV)	Subcomponent-related		Terminal-related	
	failure rate (occ./yr)	outage time (hr/occ.)	failure rate (occ./yr)	outage time (hr/occ.)
110–149	0.0088	1293.2	0.0570	18.3
150–199	0.0484	23.5	0.0200	8.0
200–299	0.0121	495.0	0.0582	20.6
300–399	0.0245	2386.2	0.0235	32.6
500–599	0.0142	228.8	0.0477	14.4
600–799	0.0593	4545.1	0.0385	811.6

**Table 2.4. Circuit Breaker Failure Data**

Voltage level (kV)	Subcomponent-related		Terminal-related	
	failure rate (occ./yr)	outage time (hr/occ.)	failure rate (occ./yr)	outage time (hr/occ.)
110–149	0.0101	422.0	0.0268	21.2
150–199	0.0097	64.8	0.0277	274.4
200–299	0.0186	267.9	0.0369	32.4
300–399	0.0229	204.2	0.0131	304.2
500–599	0.0348	151.4	0.0638	104.1
600–799	0.0810	541.0	0.0295	424.2

data are based on statistics for the period January 1, 1986, to December 31, 1990.

### 2.5.3. System Performance Data Collection Systems

CEA has also initiated an Electric Power System Reliability Assessment (EPSRA) procedure<sup>(7)</sup> designed to provide data on the past performance of

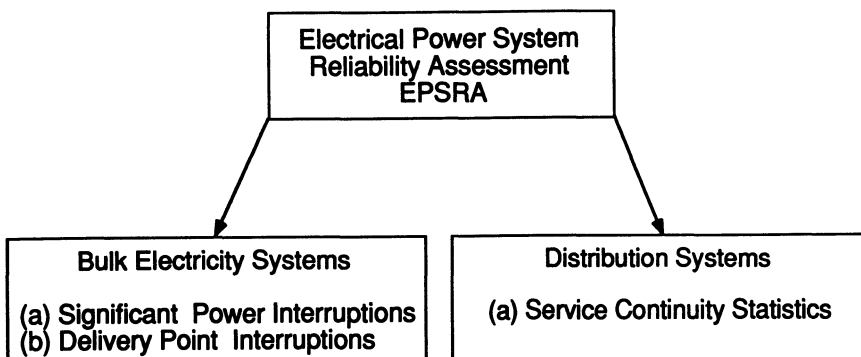


**Figure 2.9.** Basic structure of EPSRA.

an overall power system. This procedure is in the process of evolution and, at the present time, contains systems for compiling information on bulk system disturbances, bulk system delivery point performance, and customer service continuity statistics. In the latter area, these data have been collected and published for many years by the Distribution Section of the Engineering and Operating Division of CEA. The basic structure of EPSRA is shown in Figure 2.9.

The bulk electricity system (BES) parameters provide valuable HL2 data. The service continuity statistics collected at the distribution system level provide overall HL3 indices. The following is a brief description of the salient features of the EPSRA components.

**(a) BES—Significant Power Interruptions.** This is a relatively simple reporting procedure in which each participating utility provides annual data on the frequency and severity of significant power interruptions on its system. Typically, these events will involve widespread customer interruptions or localized power interruptions of an extended duration. It is expected that these events will occur infrequently. Disturbance severity is defined as the unsupplied energy in an event and is measured in MW-minutes. This is transformed into "System Minutes" by dividing the unsupplied energy by the annual peak system load.

**(b) BES—Delivery Point Interruptions.** This reporting procedure was initiated on January 1, 1988, and is intended to provide a centralized source of BES delivery point performance data at the national level which will allow utilities to compare their performance with that of other Canadian utilities. The measurement system will focus on the collection of all delivery point interruptions due to problems within the BES and therefore

**Table 2.5. Canadian Service Continuity Statistics**

System average interruption frequency index = 4.03 int/syst-cust
System average interruption duration index = 4.55 hr/syst-cust
Customer average interruption duration index = 1.13 hr/cust
Index of reliability = 0.999480

will include both adequacy and security considerations. The interruptions will be divided into momentary and sustained events. It is expected that this reporting procedure will provide some very important information for Canadian utilities.

**(c) Service Continuity Statistics.** Service continuity statistics have been collected by many Canadian utilities for over thirty years. These data were previously compiled by the Distribution Section of the CEA Engineering and Operating Division. The responsibility for the procedure was assigned to CEA headquarters in 1986. The report contains individual utility statistics and overall Canadian data and, in 1990, covered 6.5 million electric system customers. Table 2.5 shows the basic service continuity statistics on a national basis for the 1990 period.

These indices are HL3 parameters and provide a valuable indication of customer service. The report also provides a breakdown of the primary causes of interruption. Approximately 23% of the recorded customer interruptions were due to loss of supply, which is a measure of the BES contribution to customer service levels. Approximately 17% of the customer hours of interruption were attributed to loss of supply.

## 2.6. ADEQUACY INDICES

There are many possible indices which can be used to measure the adequacy of a power system at one of the three hierarchical levels and different countries/utilities use different indices. The following section presents some widely used power system adequacy indices. These indices are used in the following chapters. Most adequacy indices are basically expected values of a random variable, although the probability distribution can be calculated in some cases. There is considerable confusion both inside and outside the power industry on the specific meaning of expectation indices and the use that can be made of them. An expected value is not a deterministic parameter. It is the long-run average of the phenomenon under study. Expectation indices provides valid adequacy indicators which reflect various fac-

tors such as system component availability and capacity, load characteristics and uncertainty, system configurations and operational conditions, etc.

## 2.6.1. Adequacy Indices in HL1 Studies

The basic indices in generating system adequacy assessment are loss of load expectation (LOLE), loss of energy expectation (LOEE), loss of load frequency (LOLF), and loss of load duration (LOLD) and can be calculated using quite different approaches. Chapter 4 presents the equations for calculating these indices using Monte Carlo methods. Conceptually, these indices can be described by the following mathematical expressions:

(1) LOLE (days/yr or hr/yr)

$$\text{LOLE} = \sum_{i \in S} p_i T \quad (2.1)$$

where  $p_i$  is the probability of system state  $i$  and  $S$  is the set of all system states associated with loss of load. The LOLE is the average number of days or hours in a given period (usually one year) in which the daily peak load or hourly load is expected to exceed the available generating capacity.

It should be noted that the LOLE index in days/yr or in hr/yr has quite different meanings. When it is in days/yr,  $p_i$  depends on a comparison between the daily peak load and the available generating capacity. When it is in hr/yr,  $p_i$  depends on a comparison between the hourly load and the available generating capacity. The LOLE index does not indicate the severity of the deficiency nor the frequency nor the duration of loss of load. Despite these shortcomings, it is at present the most widely used probabilistic criterion in generating capacity planning studies.

(2) LOEE (MWh/yr)

$$\text{LOEE} = \sum_{i \in S} 8760 C_i p_i \quad (2.2)$$

where  $p_i$  and  $S$  are as defined above;  $C_i$  is the loss of load for system state  $i$ . The LOEE index is the expected energy not supplied by the generating system due to the load demand exceeding the available generating capacity.

The LOEE incorporates the severity of deficiencies in addition to the number of occasions and their duration, and therefore the impact of energy shortfalls as well as their likelihood is evaluated. It is hence believed that this index will be used more widely in the future, particularly for situations

in which alternate energy replacement sources are being considered. The complementary value of energy not supplied, i.e., energy actually supplied, can be divided by the total energy demanded to give a normalized index known as the energy index of reliability (EIR). This index can be used to compare the adequacy of systems that differ considerably in size.

(3) LOLF (occ./yr)

$$\text{LOLF} = \sum_{i \in S} (F_i - f_i) \quad (2.3)$$

where  $F_i$  is the frequency of departing system state  $i$  and  $f_i$  is the portion of  $F_i$  which corresponds to not going through the boundary wall between the loss-of-load state set and the no-loss-of-load state set.

(4) LOLD (hr/disturbance)

$$\text{LOLD} = \frac{\text{LOLE}}{\text{LOLF}} \quad (2.4)$$

Frequency and duration are a basic extension of the LOLE index in that they identify the expected frequency of encountering a deficiency and the expected duration of the deficiencies. They contain additional physical characteristics which makes them sensitive to additional generation system parameters and provide more information to power system planners. The criterion has not been used very widely in generation system reliability analysis, although the concept of frequency and duration of failures is used extensively in transmission or composite system studies.

## 2.6.2. Adequacy Indices in HL2 Studies

The adequacy index concepts used in HL1 studies can be extended to composite system adequacy assessment. More indices, however, are required to reflect composite system features. References 3 and 10 present a range of adequacy indices for HL2 studies. The following indices are used in this book:

(1) PLC—Probability of Load Curtailments

$$\text{PLC} = \sum_{i \in S} p_i \quad (2.5)$$

where  $p_i$  is the probability of system state  $i$  and  $S$  is the set of all system states associated with load curtailment.

## (2) EFLC—Expected Frequency of Load Curtailments (occ./yr).

This index has the same definition as the LOLF expressed by equation (2.3) at HL1 studies. In composite system adequacy assessment, it is a difficult task to calculate the frequency index. This is due to the fact that for each load curtailment state  $i$ , it is necessary to identify all the no-load-curtailment states which can be reached from state  $i$  in one transition. Expected Number of Load Curtailments (ENLC) is often used to replace the EFLC index:

$$\text{ENLC} = \sum_{i \in S} F_i \quad (2.6)$$

The ENLC is the sum of occurrences of load curtailment states and therefore an upper bound of the actual frequency index. It is possible to have a large difference between the EFLC and the ENLC. The ENLC may lead to an overestimation of the actual frequency. In many HL2 studies, however, absolute adequacies of the systems are not required. The basic planning task is to compare different alternatives, which only requires a relative comparison between the adequacy indices of the alternatives. In many cases, the ENLC index provides a sufficiently reasonable indication. The system state frequency  $F_i$  can be calculated by the following relationship between the frequency and the system state probability  $p_i$ :

$$F_i = p_i \sum_{k \in N} \lambda_k \quad (2.7)$$

where  $\lambda_k$  is the departure rate of the component corresponding to system state  $i$  and  $N$  is the set of all possible departure rates corresponding to state  $i$ .

## (3) EDLC—Expected Duration of Load Curtailments (hr/yr)

$$\text{EDLC} = \text{PLC} \times 8760 \quad (2.8)$$

## (4) ADLC—Average Duration of Load Curtailments (hr/disturbance)

$$\text{ADLC} = \text{EDLC}/\text{EFLC} \quad (2.9)$$

This index is similar to the LOLD index in HL1 studies.

## (5) ELC—Expected Load Curtailments (MW/yr)

$$\text{ELC} = \sum_{i \in S} C_i F_i \quad (2.10)$$

where  $C_i$  is the load curtailment in system state  $i$ .

## (6) EDNS—Expected Demand Not Supplied (MW)

$$\text{EDNS} = \sum_{i \in S} C_i p_i \quad (2.11)$$

It should be noted that the ELC and the EDNS are different indices.

## (7) EENS—Expected Energy Not Supplied (MWh/yr)

$$\text{EENS} = \sum_{i \in S} C_i F_i D_i = \sum_{i \in S} 8760 C_i p_i \quad (2.12)$$

where  $D_i$  is the duration of system state  $i$ . This index is similar to the LOEE index in HL1 studies. It is an important index in composite system adequacy assessment.

## (8) BPII—Bulk Power Interruption Index (MW/MW-yr)

$$\text{BPII} = \sum_{i \in S} C_i F_i / L \quad (2.13)$$

where  $L$  is the annual system peak load in MW. This index can be interpreted as the equivalent per-unit interruption of the annual peak load. One complete system outage during peak load conditions contributes 1.0 to this index.

## (9) BPECI—Bulk Power/Energy Curtailment Index (MWh/MW-yr)

$$\text{BPECI} = \text{EENS} / L \quad (2.14)$$

## (10) BPACI—Bulk Power-Supply Average MW Curtailment Index (MW/disturbance)

$$\text{BPACI} = \text{ELC} / \text{EFLC} \quad (2.15)$$

## (11) MBPCI—Modified Bulk Power Curtailment Index (MW/MW)

$$\text{MBPCI} = \text{EDNS} / L \quad (2.16)$$

## (12) SI—Severity Index (system min/yr)

$$\text{SI} = \text{BPECI} \times 60 \quad (2.17)$$

This index can be interpreted as the equivalent duration (in min) of the loss of all load during peak load conditions. One complete system outage during peak conditions contributes by its duration (in min) to this index.

It can be seen that items (1) to (7) are basic indices and items (8) to (12) are calculated from these basic indices. The advantage of indices (8) to (12) is that they can be used to compare adequacies of systems having

different sizes. Indices (1) to (7) can be applied to either a whole system or to one single bus. Indices (8) to (12) only apply to an overall system. These indices can be calculated at the peak load and expressed on a one-year basis (annualized index) or by considering the annual load duration curve (annual index).

### 2.6.3. Adequacy Indices in Distribution System Evaluation

There are three basic load-point indices in distribution system adequacy assessment. They are load-point failure rate  $\lambda$ , load-point outage duration  $r$ , and load-point annual unavailability  $U$ . The analytical equations and Monte Carlo simulation formulas for these three basic indices are given in Chapter 6. Overall distribution system performance indices can be calculated using the three basic load-point indices. The definitions and formulas for the system performance indices are as follows. These indices can be used to indicate the past or future performance of the system.

(1) SAIFI—System Average Interruption Frequency Index (interruptions/system customer/yr)

$$\text{SAIFI} = \frac{\sum_{i \in R} \lambda_i N_i}{\sum_{i \in R} N_i} \quad (2.18)$$

where  $\lambda_i$  and  $N_i$  are the failure rate and the number of customers at load point  $i$  respectively;  $R$  is the set of load points in the system.

(2) SAIDI—System Average Interruption Duration Index (hr/system customer/yr)

$$\text{SAIDI} = \frac{\sum_{i \in R} U_i N_i}{\sum_{i \in R} N_i} \quad (2.19)$$

where  $U_i$  is the annual unavailability or outage time (in hr/yr) at load point  $i$ .

(3) CAIFI—Customer Average Interruption Frequency Index (interruptions/customer affected/yr)

$$\text{CAIFI} = \frac{\sum_{i \in R} \lambda_i N_i}{\sum_{i \in R} M_i} \quad (2.20)$$

where  $M_i$  is the number of customers affected at load point  $i$ . The customers affected should be counted only once, regardless of the number of interruptions they may have experienced in the year. This index is particularly useful when a given calendar year is compared with other calendar years since, in any given calendar year, not all customers will be affected and many will experience complete continuity of supply.

(4) CAIDI—Customer Average Interruption Duration Index (hr/customer interruption)

$$\text{CAIDI} = \frac{\sum_{i \in R} U_i N_i}{\sum_{i \in R} \lambda_i N_i} = \frac{\text{SAIDI}}{\text{SAIFI}} \quad (2.21)$$

(5) ASAI—Average Service Availability Index

$$\text{ASAI} = \frac{\sum_{i \in R} 8760 N_i - \sum_{i \in R} U_i N_i}{\sum_{i \in R} 8760 N_i} \quad (2.22)$$

(6) ASUI—Average Service Unavailability Index

$$\text{ASUI} = \frac{\sum_{i \in R} U_i N_i}{\sum_{i \in R} 8760 N_i} \quad (2.23)$$

(7) ENS—Energy Not Supplied (kWh/yr)

$$\text{ENS} = \sum_{i \in R} P_{ai} U_i \quad (2.24)$$

where  $P_{ai}$  is the average load (in kW) connected to load point  $i$  and  $U_i$  is the annual outage time (in hr/yr) at the load point.

(8) AENS—Average Energy Not Supplied (kWh/customer/yr)

$$\text{AENS} = \frac{\text{ENS}}{\sum_{i \in R} N_i} \quad (2.25)$$

(9) ACCI—Average Customer Curtailment Index (kWh/customer affected/yr)

$$\text{ACCI} = \frac{\text{ENS}}{\sum_{i \in R} M_i} \quad (2.26)$$

## 2.6.4. Reliability Worth Indices

In general, it is not possible to measure reliability worth directly, and therefore system reliability worth is usually assessed by considering unreliability cost. Interruption costs are used as a surrogate of reliability worth. The three hierarchical level studies utilize conceptually the same reliability worth indices. They are:

- (1) EIC—Expected Interruption Cost (k\$/yr)

$$\text{EIC} = \sum_{i \in V} C_i F_i W(D_i) \quad (2.27)$$

where  $C_i$  is the load curtailment of load loss event  $i$ ;  $F_i$  and  $D_i$  are the frequency and duration of load loss event  $i$ ;  $W(D_i)$  is the unit interruption cost which is a function of the interrupted duration;  $V$  is the set of all load loss events.

- (2) IEAR—Interrupted Energy Assessment Rate (\$/kWh)

$$\text{IEAR} = \text{EIC}/\text{EENS} \quad (2.28)$$

where EENS is the expected energy not supplied. In HL1 studies, this is the LOEE index and, in distribution system studies, it is the ENS index.

It should be noted that in generation system assessment the EIC and IEAR are system indices, while in composite system and distribution system assessments they can either be system or load point (bus) indices depending on the particular focus of the study.

## 2.7. CONCLUSIONS

This chapter describes several philosophical aspects of power system reliability. These basic concepts are fundamental to an appreciation of the applications proposed in Chapters 4–7. Reliability assessment of a power system can be divided into the two aspects of system adequacy and system security. Most presently available reliability evaluation techniques are in the domain of adequacy assessment. There should be some conformity between the reliability of various segments of the system and a balance is required between the generation, transmission, and distribution functional zones. This does not imply that the reliability of each should be equal. Different levels of reliability are justified as different functional zones are associated with different impact ranges. Generation and transmission failures can cause

widespread outages while distribution failures tend to be highly localized. The most useful concept for planning purposes is to utilize a reliability cost/worth approach. The main difficulty with such a concept is the perceived uncertainty in the consumers' valuation.

Reliability data collection is an essential and important aspect of quantitative reliability evaluation. Data collection and reliability methodology should evolve together. Updating reliability data is a long-term and continuous task. Adequacy assessment at different hierarchical levels utilizes different indices, although they are fundamentally similar in a probabilistic sense. These indices are expected values of probability distributions which are not deterministic parameters. This is a very important point which should be clearly understood.

Power system reliability evaluation has been highly developed over the last twenty years and there are many publications available on this subject.<sup>(11-17)</sup> Billinton *et al.*<sup>(17)</sup> contains a collection of important publications which highlight important developments and fundamental techniques.

## 2.8. REFERENCES

1. R. Billinton and R. N. Allan, *Reliability Evaluation of Engineering Systems: Concepts and Techniques*, Plenum, New York, 1983.
2. R. Billinton and P. R. S. Kuruganty, "A Probabilistic Index for Transient Stability," *IEEE Trans. on PAS*, Vol. 99, 1980, pp. 195-207.
3. R. Billinton and R. N. Allan, *Reliability Evaluation of Power Systems*, Plenum, New York, 1984.
4. R. Billinton and R. N. Allan, *Reliability Assessment of Large Electric Power Systems*, Kluwer, Boston, 1988.
5. R. Billinton, H. J. Koglin, and E. Roos, "Reliability Equivalents in Composite System Reliability Evaluation," *IEE Proc. C*, Vol. 134, 1987, pp. 224-233.
6. R. Billinton, G. Wacker, and E. Wojcynski, "Comprehensive Bibliography of Electrical Service Interruption Costs," *IEEE Trans. on PAS*, Vol. 102, 1983, pp. 1831-1837.
7. R. Billinton, K. Debnath, M. Oprisan, and I. M. Clark, "The CEA Equipment Reliability and System Performance Reporting Procedure," *Transactions of the Canadian Electrical Association*, 1988.
8. CEA, ERIS 1990 Annual Report—Generation Equipment Status, 1991.
9. CEA, ERIS 1990 Annual Report—Forced Outage Performance of Transmission Equipment, 1991.
10. Working Group on Performance Records for Optimizing System Design, Power System Engineering Committee, "Reliability Indices for Use in Bulk Power Supply Adequacy Evaluation," *IEEE Trans. on PAS*, Vol. 97, No. 4, 1978, pp. 1097-1103.
11. R. Billinton, "Bibliography on the Application of Probability Methods in Power System Reliability Evaluation," *IEEE Trans. on PAS*, Vol. 91, 1972, pp. 649-660.
12. IEEE Committee Report, "Bibliography on the Application of Probability Methods in Power System Reliability Evaluation, 1971-1977," *IEEE Trans. on PAS*, Vol. 97, 1978, pp. 2235-2242.

13. R. N. Allan, R. Billinton, and S. H. Lee, "Bibliography on the Application of Probability Methods in Power System Reliability Evaluation, 1977–1982," *IEEE Trans. on PAS*, Vol. 103, 1984, pp. 275–282.
14. R. N. Allan, R. Billinton, S. M. Shahidehpour, and C. Singh, "Bibliography on the Application of Probability Methods in Power System Reliability Evaluation, 1982–1987," *IEEE Trans. on PS*, Vol. 3, No. 4, 1988, pp. 1555–1564.
15. G. Tollefson, R. Billinton, and G. Wacker, "Comprehensive Bibliography on Reliability Worth and Electrical Service Consumer Interruption Costs: 1986–1990," *IEEE Trans. on PS*, Vol. 6, No. 4, 1991, pp. 1508–1514.
16. CIGRE Working Group 38.03, "Power System Reliability Analysis—Application Guide," CIGRE Publications, Paris, 1988.
17. R. Billinton, R. N. Allan, and L. Salvaderi, *Applied Reliability Assessment in Electric Power Systems*, IEEE Press, New York, 1991.

# 3

# Elements of Monte Carlo Methods

## 3.1. INTRODUCTION

The Monte Carlo method is the general designation for stochastic simulation using random numbers. Monte Carlo is the name of the suburb in Monaco made famous by its gambling casino. The name was also used as the secret code for atomic bomb work performed during World War II involving random simulation of the neutron diffusion process. Monte Carlo methods have been used in many areas since that time.

The basic concept of the Monte Carlo method dates back to the 18th century when the French scientist Buffon presented the famous needle throw test method<sup>(1)</sup> to calculate  $\pi$  in 1777. The method is as follows. A needle of length  $d$  is thrown randomly onto a plane on which some parallel lines with equal width  $a$  have been drawn, where  $d < a$ . It can be shown that the probability of the needle hitting a line is  $P = 2d/\pi a$ . Since the probability can be estimated as the ratio of the number of throws hitting a line to the total number of throws, the value of  $\pi$  can be obtained by  $\pi = 2d/Pa$ . This is the earliest and most interesting example of Monte Carlo method application.

This example indicates that the Monte Carlo method can be used to solve not only stochastic but also deterministic problems. Applications of Monte Carlo techniques can be found in many fields such as complex mathematical calculations, stochastic process simulation, medical statistics, engineering system analysis, and reliability evaluation.

This book applies Monte Carlo methods to power system reliability evaluation. In this chapter, the basic concepts of the Monte Carlo method are presented and discussed from a reliability evaluation point of view.

## 3.2. GENERAL CONCEPTS

### 3.2.1. Two Simple Examples

Two simple examples are given in order to illustrate the basic concepts of the Monte Carlo method.

*Example 1:* A fair die is thrown. What is the probability of a one occurring on the upper face? This is obviously  $1/6$  as each of the six faces has equal probabilities of occurring. This probability can be estimated by sampling simulation. Throw the die  $N$  times and record the times number one occurs. Let this be  $f$  times. The estimation of the probability is  $f/N$ . As  $N$  increases sufficiently,  $f/N$  approaches  $1/6$ .

*Example 2:* Calculate the following integral by sampling simulation:

$$I = \int_0^1 g(x) dx$$

It is well known that the integral equals the shaded area in Figure 3.1. A point is thrown randomly  $N$  times in the range  $[0 \leq x \leq 1, 0 \leq y \leq 1]$  and the

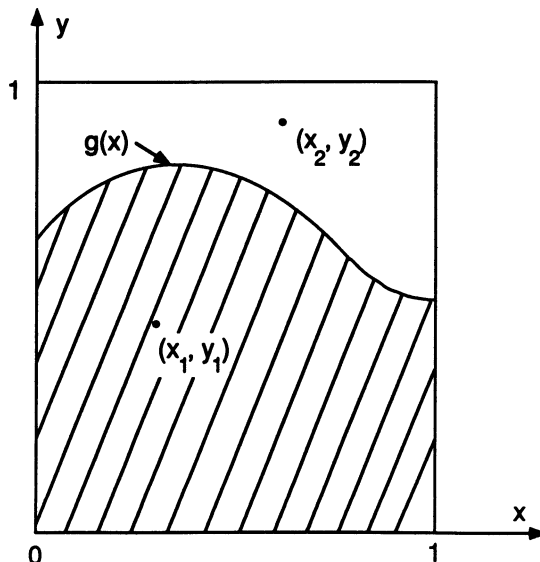


Figure 3.1. One-dimension integral by Monte Carlo simulation.

number of points hitting the shaded area is  $M$ . The integral is therefore equal to the probability of the point hitting the shaded area, namely,

$$I = p \approx \frac{M}{N}$$

The sampling simulation can be conducted on a computer. Two uniformly distributed random numbers  $x_i$  and  $y_i$  between  $[0, 1]$  can be generated and checked to see if the inequality  $y_i \leq g(x_i)$  is satisfied or not to obtain  $M$ . The most basic aspect of Monte Carlo simulation is the generation of random numbers. This is discussed in detail later in this chapter.

### 3.2.2. Features of Monte Carlo Methods in Reliability Evaluation

A fundamental parameter in reliability evaluation is the mathematical expectation of a given reliability index. Salient features of the Monte Carlo method for reliability evaluation therefore can be discussed from an expectation point of view.

Let  $Q$  denote the unavailability (failure probability) of a system and  $x_i$  be a zero-one indicator variable which states that

$$x_i = 0 \quad \text{if the system is in the up state}$$

$$x_i = 1 \quad \text{if the system is in the down state}$$

The estimate of the system unavailability is given by

$$\bar{Q} = \frac{1}{N} \sum_{i=1}^N x_i \quad (3.1)$$

where  $N$  is the number of system state samples.

The unbiased sample variance is

$$V(x) = \frac{1}{N-1} \sum_{i=1}^N (x_i - \bar{Q})^2 \quad (3.2)$$

When the sample size is large enough, equation (3.2) can be approximated by

$$V(x) = \frac{1}{N} \sum_{i=1}^N (x_i - \bar{Q})^2 \quad (3.3)$$

Because  $x_i$  is a zero-one variable, it follows that

$$\sum_{i=1}^N x_i^2 = \sum_{i=1}^N x_i \quad (3.4)$$

Substituting equations (3.1) and (3.4) into equation (3.3) yields

$$\begin{aligned} V(x) &= \frac{1}{N} \sum_{i=1}^N x_i^2 - \frac{1}{N} \sum_{i=1}^N 2x_i \bar{Q} + \frac{1}{N} \sum_{i=1}^N \bar{Q}^2 \\ &= \bar{Q} - 2\bar{Q}^2 + \bar{Q}^2 \\ &= \bar{Q} - \bar{Q}^2 \end{aligned} \quad (3.5)$$

It is important to note that equation (3.1) gives only an estimate of the system unavailability. The uncertainty around the estimate can be measured by the variance of the expectation estimate:

$$\begin{aligned} V(\bar{Q}) &= \frac{1}{N} V(x) \\ &= \frac{1}{N} (\bar{Q} - \bar{Q}^2) \end{aligned} \quad (3.6)$$

The accuracy level of Monte Carlo simulation can be expressed by the coefficient of variation, which is defined as

$$\alpha = \sqrt{V(\bar{Q})/\bar{Q}} \quad (3.7)$$

Substitution of equation (3.6) into equation (3.7) gives

$$\alpha = \sqrt{\frac{1-\bar{Q}}{N\bar{Q}}} \quad (3.8)$$

Equation (3.8) can be rewritten as

$$N = \frac{1-\bar{Q}}{\alpha^2 \bar{Q}} \quad (3.9)$$

This equation indicates two important points:

1. For a desired accuracy level  $\alpha$ , the required number of samples  $N$  depends on the system unavailability but is independent of the size of the system. Monte Carlo methods are therefore suited to large-scale system reliability evaluation. This is an important advantage of Monte Carlo methods compared to analytical enumeration techniques for reliability evaluation.
2. The unavailability (failure probability) in practical system reliability evaluation is usually much smaller than 1.0. Therefore,

$$N \approx \frac{1}{\alpha^2 \bar{Q}} \quad (3.10)$$

This means that the number of samples  $N$  is approximately inversely proportional to the unavailability of the system. In other words, in the case of a very reliable system, a large number of samples is required to satisfy the given accuracy level.

### 3.2.3. Efficiency of Monte Carlo Methods

Different Monte Carlo techniques can be used to solve the same problem. These include different random number generation methods, different sampling approaches, and different variance reduction techniques, etc. It is therefore sometimes necessary to compare the efficiency of different Monte Carlo methods.

Suppose two Monte Carlo methods are used to evaluate the same system and the expectation estimates of the reliability index obtained using these two methods are statistically the same. Let  $t_1$  and  $t_2$  denote computing times and  $\sigma_1^2$  and  $\sigma_2^2$  be the variances of the reliability index for the two methods, respectively. If the ratio

$$\eta = \frac{t_1 \sigma_1^2}{t_2 \sigma_2^2} < 1 \quad (3.11)$$

then the first method can be considered to be more efficient than the second method. The efficiency of the Monte Carlo method depends on the computing time multiplied by the variance of the estimate, but not simply on the number of required samples.

In conducting reliability evaluation of power systems using Monte Carlo methods, the computing time and the variance are directly affected by the selected sampling techniques and system analysis requirements. Sampling techniques include random number (or variate) generation methods, variance reduction techniques, and different sampling approaches and are discussed in the following sections of this chapter. The purpose of system analysis is to judge if a system state is good or bad. The system analysis requirements are different in generation (HLI), composite (HLII), and distribution system reliability evaluation and are discussed in Chapters 4, 5, and 6, respectively.

### 3.2.4. Convergence Characteristics of Monte Carlo Methods

**(a) Convergence Process.** Monte Carlo simulation creates a fluctuating convergence process as shown in Figure 3.2 and there is no guarantee

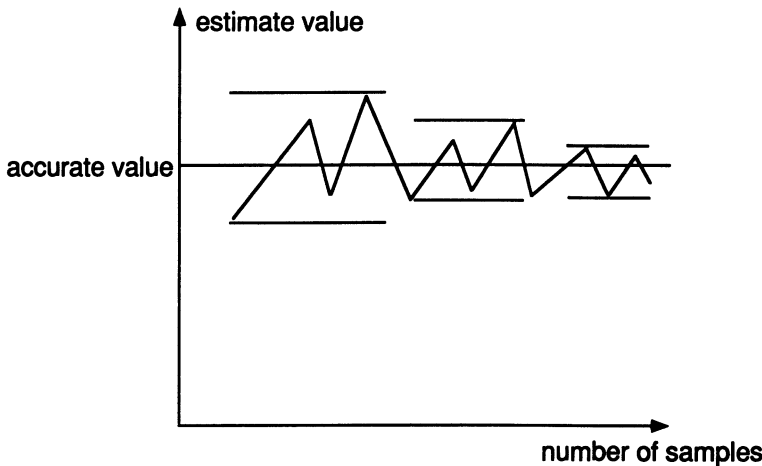


**Figure 3.2.** Convergence process in Monte Carlo simulation.

that a few more samples will definitely lead to a smaller error. It is true, however, that the error bound or the confidence range decreases as the number of samples increases.

**(b) Convergence Accuracy.** The variance of the expectation estimate is given by equation (3.6). The standard deviation of the estimate can be obtained as follows:

$$\sigma = \sqrt{V(\bar{Q})} = \frac{\sqrt{V(x)}}{\sqrt{N}} \quad (3.12)$$

This indicates that two measures can be utilized to reduce the standard deviation in a Monte Carlo simulation: increasing the number of samples and decreasing the sample variance. Variance reduction techniques can be used to improve the effectiveness of Monte Carlo simulation. The variance cannot be reduced to be zero and therefore it is always necessary to utilize a reasonable and sufficiently large number of samples.

**(c) Convergence Criteria.** The coefficient of variation shown in equation (3.7) is often used as the convergence criterion in Monte Carlo simulation. In power system reliability evaluation, different reliability indices have different convergence speeds. It has been found that the coefficient of variation of the EENS index has the lowest rate of convergence. This coefficient of variation should therefore be used as the convergence criterion in order to guarantee reasonable accuracy in a multi-index study.

## 3.3. RANDOM NUMBER GENERATION

### 3.3.1. Introduction

A random number can be generated by either a physical or a mathematical method. The mathematical method is most common as it can guarantee reproducibility and can be easily performed on a digital computer. A random number generated by a mathematical method is not really random and therefore is referred to a pseudorandom number. In principle, a pseudorandom number sequence should be tested statistically to assure its randomness.

The basic requirements for a random number generator are:

1. Uniformity: The random numbers should be uniformly distributed between  $[0, 1]$ .
2. Independence: There should be minimal correlation between random numbers.
3. Long period: The repeat period should be sufficiently long.

There is a wide range of random number generation methods. Two commonly used congruential generators are given in the following sections.

### 3.3.2. Multiplicative Congruential Generator

The multiplicative congruential generator was presented in 1949 by D. H. Lehmer<sup>(2)</sup> and is based on the following recursive relationship:

$$x_{i+1} = ax_i \pmod{m} \quad (3.13)$$

where  $a$  is a multiplier and  $m$  is the modulus;  $a$  and  $m$  have to be nonnegative integers. The module notation ( $\pmod{m}$ ) means that

$$x_{i+1} = ax_i - mk_i \quad (3.14)$$

where  $k_i = [ax_i/m]$  denotes the largest positive integer in  $ax_i/m$ . For example, assume that  $ax_i = 32$  and  $m = 30$ ,

$$\begin{array}{r} 1 \\ 30 \overline{)32} \\ 30 \\ \hline 2 \end{array}$$

therefore  $32 \pmod{30} = 2$ .

Given an initial value  $x_0$ , equation (3.13) generates a random number sequence which lies between  $[0, m]$ . A random number sequence in the interval  $[0, 1]$  can be obtained by

$$U_i = \frac{x_i}{m} \quad (3.15)$$

Obviously, such a sequence will repeat itself in at most  $m$  steps and therefore it will be periodic. If the period of the sequence equals  $m$ , the random number generator is considered to have a full period.

Different choices of the parameters  $a$  and  $m$  produce large impacts on the random number statistical features. If these parameters are properly chosen, the initial value  $x_0$  has little or no effect on the statistical features of the generated random numbers. The conventional principles in choosing the parameters are<sup>(3)</sup>

1.  $m = 2^k$  and  $k$  equals the integer word-length of the computer
2.  $a = 8d \pm 3$  and  $d$  is any positive integer
3. Initial value  $x_0$  is any odd number

These principles are, however, not completely satisfactory. When these three principles are satisfied, the maximum period length of a generated random number sequence is  $2^{k-2}$ . This means that in the interval  $[0, m-1]$ , only  $m/4$  integers can probably appear and the other  $3m/4$  integers cannot be made use of. In 1965, D. W. Hutchinson (see Zaigen<sup>(4)</sup>) proved that, if the modulus  $m$  is a prime number instead of  $2^k$ , the maximum possible period length can be  $m-1$ . When the integer word-length of the computer is 31, for example, the largest prime on the computer is  $2^{31}-1$ . Therefore  $m=2^{31}-1$  is a good choice. It is more difficult to choose a good multiplier  $a$ . A number of statistical test results indicate that the following two multiplier values produce satisfactory statistical features in the random numbers:  $a=16807$  or  $630360016$ .

An overflow problem may occur on a computer, however, when  $m=2^{31}-1$  and  $a=16807$  or  $630360016$ . This is because places of  $ax_i$  in the binary system can be as high as 46 for  $a=16807$  and 53 for  $a=630360016$ . Several alternatives have been proposed to overcome this difficulty. The following is one of these alternatives and its proof can be found in Fang Zaigen.<sup>(4)</sup>

Choose two integers  $b$  and  $c$  which satisfy

$$0 < b < m$$

$$0 \leq c < a$$

$$ab + c = m$$

The new multiplicative congruential generator is given by

$$x'_{i+1} = a(x_i \bmod b) - k_i c \quad (3.16)$$

where  $k_i = [x_i/b]$  denotes the largest positive integer in  $x_i/b$ , and

$$x_{i+1} = \begin{cases} x'_{i+1} & \text{if } x'_{i+1} > 0 \\ x'_{i+1} + m & \text{if } x'_{i+1} \leq 0 \end{cases} \quad (3.17)$$

When using equation (3.16),  $x_i \bmod b$  is calculated instead of  $ax_i \bmod m$  so that the very large integer  $ax_i$  is avoided.

### 3.3.3. Mixed Congruential Generator

In 1961, M. Greenberger generalized the multiplicative congruential generator to the mixed congruential generator, which is based on the following congruence relationship<sup>(5)</sup>:

$$x_{i+1} = (ax_i + c) \bmod m \quad (3.18)$$

It can be seen that, in addition to parameters  $a$  and  $m$ , a new parameter  $c$  is added into the multiplicative congruential generator. The quantity  $c$  is called the increment and it also has to be a nonnegative integer.

The mixed congruential generator can have a full period if and only if the following conditions are satisfied<sup>(3)</sup>:

1.  $c$  is relative prime to  $m$
2.  $a \bmod g = 1$  for every prime factor  $g$  of  $m$
3.  $a \bmod 4 = 1$  if  $m$  is a multiple of 4

These are sufficient and necessary conditions for the mixed congruential generator to have a full period. These conditions, however, do not guarantee good statistical features of generated random numbers. As in the case of the multiplicative congruential generator, the choices of parameters  $a$ ,  $c$ , and  $m$  have quite large impacts on the statistical features of the random numbers. Choosing “good” parameters is always a difficult task. D. E. Knuth suggested using the following principles in selecting the parameters<sup>(6)</sup>:

1.  $m = 2^k$  and  $k$  equals the integer word-length of a computer
2.  $a \bmod 8 = 5$  and  $a$  satisfies:

$$\frac{m}{100} < a < m - \sqrt{m}$$

3.  $c$  is an odd number and satisfies:

$$\frac{c}{m} \approx \frac{1}{2} - \frac{1}{6}\sqrt{3} \approx 0.21132$$

A number of statistical test results indicates that the following two sets of parameters give quite satisfactory statistical features in the generated random numbers:

$$\begin{aligned} m &= 2^{31}, & a &= 314159269, & c &= 453806245 \\ m &= 2^{35}, & a &= 5^{15}, & c &= 1 \end{aligned}$$

It is noteworthy that there always exists a very weak correlation between random numbers generated by the congruential generators. Greenberger showed that the correlation coefficient between  $x_i$  and  $x_{i+1}$  has the following upper and lower bounds<sup>(7)</sup>:

$$\rho = \frac{1}{a} - \left( \frac{6c}{am} \right) \left( 1 - \frac{c}{m} \right) \pm \frac{a}{m} \quad (3.19)$$

In the case of the multiplicative congruential generator (i.e.,  $c=0$ ), when  $a=\sqrt{m}$ , the correlation coefficient  $\rho$  achieves its minimum upper limit, which equals  $2/\sqrt{m}$ . This indicates that if  $m$  is large enough, correlation between generated random numbers can be very weak.

## 3.4. RANDOM VARIATE GENERATION

### 3.4.1. Introduction

A random variate refers to a random variable following a given distribution. The random number generation methods given in the previous section are essentially ones which generate a random variate following a uniform distribution between  $[0, 1]$ . Generators of random variates which follow other distributions are based on uniformly distributed random numbers between  $[0, 1]$ .

The procedures for generating nonuniformly distributed random variates can be generally categorized into three techniques: (1) inverse transform method; (2) composition method; and (3) acceptance-rejection method. There are also particular methods for specific distributions.<sup>(8)</sup> This section emphasizes the inverse transform method, which is most frequently used. The exponential and normal distributions are the most important ones in

reliability evaluation. Some techniques for generating random variates for these two distributions are therefore discussed in detail. Methods for other distributed random variates are given in Section 3.4.6.

### 3.4.2. Inverse Transform Method

The inverse transform method is based on the following proposition:

*If a random variate  $U$  follows a uniform distribution in the interval between  $[0, 1]$ , the random variate  $X = F^{-1}(U)$  has a continuous cumulative probability distribution function  $F(x)$ .*

The proof of the proposition is straightforward. Because  $X = F^{-1}(U)$ ,

$$P(X \leq x) = P(F^{-1}(U) \leq x) \quad (3.20)$$

If  $F(x)$  is a cumulative distribution function,  $F(x)$  is a monotonic increasing function. This leads to

$$P(F^{-1}(U) \leq x) = P(U \leq F(x)) \quad (3.21)$$

As  $U$  is a uniformly distributed random variate,

$$P[U \leq F(x)] = F(x) \quad (3.22)$$

Therefore

$$P(X \leq x) = F(x) \quad (3.23)$$

This means that  $F(x)$  is the cumulative distribution function of  $X$  obtained by setting  $X = F^{-1}(U)$ .

This proposition can be generalized to the case of a discrete distribution and, in this case, the inverse function of  $F(x)$  is defined as

$$X = F^{-1}(U) = \min\{x: F(x) \geq U\} \quad (0 \leq U \leq 1) \quad (3.24)$$

The proposition is clarified by Figure 3.3.

The procedure for generating random variates using the inverse transform method is as follows:

*Step 1:* Generate a uniformly distributed random number sequence  $U$  between  $[0, 1]$ .

*Step 2:* Calculate the random variate which has the cumulative probability distribution function  $F(x)$  by  $X = F^{-1}(U)$ .

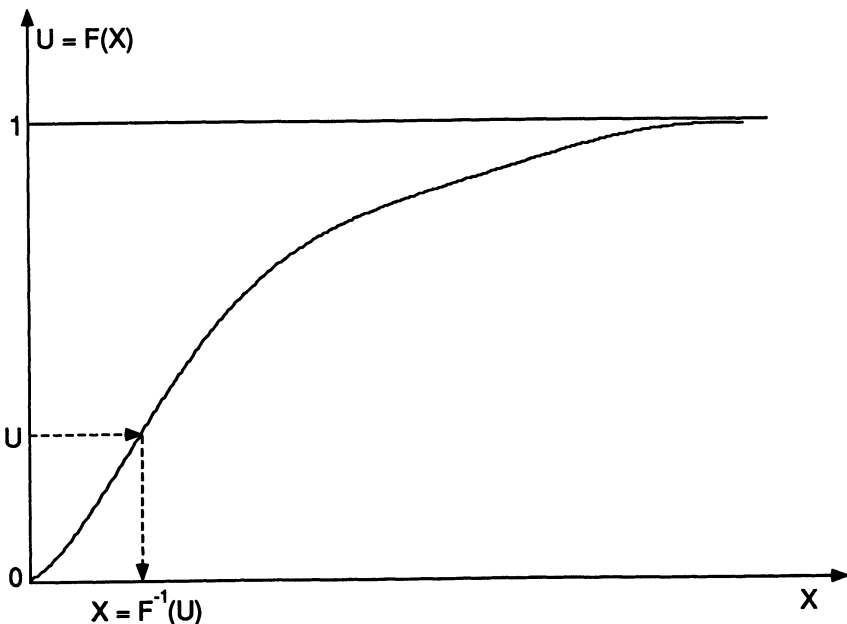


**Figure 3.3.** Explanation of the inverse transform method.

**Example:** Given the following probability density function:

$$f(x) = \begin{cases} 2x & 0 \leq x \leq 1 \\ 0 & \text{otherwise} \end{cases}$$

the cumulative probability distribution function is

$$F(x) = \begin{cases} 0 & x < 0 \\ \int_0^x 2x \, dx = x^2 & 0 \leq x \leq 1 \\ 1 & x > 1 \end{cases}$$

The random variate which follows this cumulative probability distribution function is obtained using

$$X = F^{-1}(U) = \sqrt{U} \quad (0 \leq U \leq 1)$$

where  $U$  is a uniformly distributed random number sequence between  $[0, 1]$ .

### 3.4.3. Tabulating Technique for Generating Random Variates

This is an approximate technique for generating random variates and is based on the inverse transform method. It has reasonable accuracy, but requires much less computing time than the direct inverse transform method. The tabulating technique involves two procedures: tabulating and sampling.

**(a) Tabulating Procedure.** The values of a cumulative probability distribution function range from zero to one. The interval between  $[0, 1]$  is divided into  $k$  subintervals which have the same length  $1/k$ . All values in each subinterval are represented by their midpoint value. The number  $k$  should be sufficiently large, i.e.,  $k = 500$ .

Using the inverse transform method, the  $k$  values of a random variate following the cumulative probability distribution function  $F(x)$  can be calculated using

$$x_i = F^{-1} \left( \frac{i - 0.5}{k} \right) \quad (i = 1, \dots, k) \quad (3.25)$$

This is shown in Figure 3.4. The subinterval numbers, values of the cumulative probability distribution function (CPDF), and values of the random variates (RV) are shown in Table 3.1.

**(b) Sampling Procedure.** This is a “table-look-up” procedure which can be described as follows:

*Step 1:* Generate a uniformly distributed random number between  $[0, 1]$ ,

*Step 2:* Judge in which subinterval the generated random number falls,

*Step 3:* Pick up the value of the random variate from the formed table according to the subinterval number.

The advantage of the tabulating technique is that it is not necessary to calculate the inverse function value for each sample as the  $k$  values of the inverse function of  $F(x)$  are calculated in advance. The tabulating technique is therefore much faster than the direct inverse transform method.

The tabulating technique is a discretized approach in which a continuous cumulative probability distribution function is changed into a discrete one. The purpose of the discretization, however, is to perform sampling but not to conduct enumerating. The tabulating technique involves two errors: a discretization error and a truncation error. When the number of subintervals is sufficiently large, the discretization error is smaller than the standard

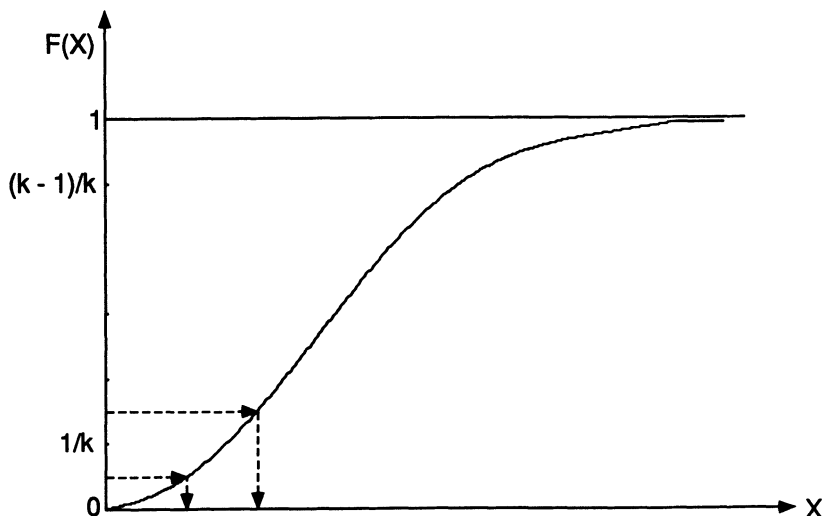


**Figure 3.4.** Calculating  $k$  values of a random variate.

deviation of sampling and therefore negligible. The truncation error is caused by the last subinterval. In order to avoid this error, the direct inverse transform method can be used only for the last subinterval. If the generated random number falls in the last interval, the inverse function value of  $F(x)$  is calculated instead of “looking up the table.” The probability of a random number falling in the last subinterval is  $1/k$  and is very small when  $k$  is sufficiently large, which leads to little increase in computing time.

The tabulating technique has sufficient accuracy for most practical applications. For example, when the number of subintervals is 500, the square root error of a normal distribution random variate obtained using the tabulating technique is 0.005.

**Table 3.1. Tabulating Technique Table**

Subinterval No.	Values of CPDF	Values of RV
1	$0.5/k$	$x_1$
2	$1.5/k$	$x_2$
3	$2.5/k$	$x_3$
...	...	...
$k$	$k - 0.5/k$	$x_k$

### 3.4.4. Generating Exponentially Distributed Random Variates

**(a) Method 1: The Inverse Transform Method.** An exponentially distributed random variate has the probability density function

$$f(x) = \lambda e^{-\lambda x} \quad (3.26)$$

Its cumulative probability distribution function is

$$F(x) = 1 - e^{-\lambda x} \quad (3.27)$$

By the inverse transform method

$$U = F(x) = 1 - e^{-\lambda x}$$

so that

$$X = F^{-1}(U) = -\frac{1}{\lambda} \ln(1 - U) \quad (3.28)$$

Since  $(1 - U)$  distributes uniformly in the same way as  $U$  in the interval  $[0, 1]$ ,

$$X = -\frac{1}{\lambda} \ln U \quad (3.29)$$

where  $U$  is a uniformly distributed random number sequence and  $X$  follows an exponential distribution.

**(b) Method 2: Alternate Method.** In reliability evaluation, it is sometimes necessary to simultaneously generate several exponentially distributed random variates. In this case, the inverse transform method requires calculation of the natural logarithm for each variate. An alternate method can be used which requires only one computation of the natural logarithm for generating  $n$  exponential distribution random variates. This alternate method is based on the following proposition<sup>(1)</sup>:

*$U_1, \dots, U_n, U_{n+1}, \dots, U_{2n-1}$  are independent and uniformly distributed random numbers. If  $U'_1, \dots, U'_{n-1}$  represent the order statistics corresponding to the random numbers  $U_{n+1}, \dots, U_{2n-1}$  and define  $U'_0=0$  and  $U'_n=1$ , then*

the random variates

$$Y_k = (U'_{k-1} - U'_k) \ln \prod_{i=1}^n U_i \quad (k = 1, \dots, n) \quad (3.30)$$

are independent and follow standard exponential distributions.

According to the proposition, the algorithm generating  $n$  standard exponential distribution random variates can be stated as follows:

*Step 1:* Generate  $2n-1$  uniformly distributed random numbers

$$U_1, \dots, U_n, U_{n+1}, \dots, U_{2n-1},$$

*Step 2:* Arrange the random numbers  $U_{n+1}, \dots, U_{2n-1}$  in the order of increasing magnitudes to obtain  $U'_1, \dots, U'_{n-1}$ ,

*Step 3:* Calculate  $Y_k$  ( $k = 1, \dots, n$ ) in terms of equation (3.30).

### 3.4.5. Generating Normally Distributed Random Variates

#### (a) Method 1: The Approximate Inverse Transform

**Method.** A normally distributed random variate cannot be generated by the accurate inverse transform method as there exists no analytical inverse function of the normal cumulative probability distribution function  $F(x)$ . The inverse function of  $F(x)$ , however, has the following approximate expression<sup>(9)</sup>:

$$z = t - \frac{\sum_{i=0}^2 c_i t^i}{1 + \sum_{i=1}^3 d_i t^i} \quad (3.31)$$

where

$$t = \sqrt{-2 \ln Q} \quad (3.32)$$

$$c_0 = 2.515517 \quad d_1 = 1.432788$$

$$c_1 = 0.802853 \quad d_2 = 0.189269$$

$$c_2 = 0.010328 \quad d_3 = 0.001308$$

The implications of  $z$  and  $Q$  are shown in Figure 3.5, where  $f(z)$  is the standard normal probability density function:

$$f(z) = \frac{1}{\sqrt{2\pi}} \exp\left(-\frac{z^2}{2}\right) \quad (3.33)$$

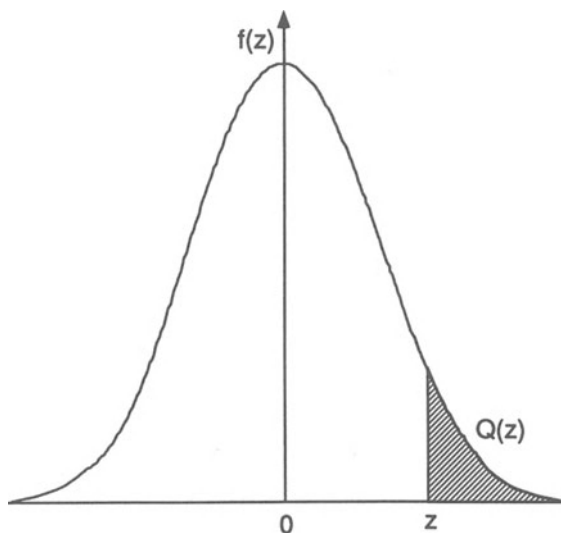


**Figure 3.5.** Area under normal density function,  $Q(z)$ .

The algorithm for generating a normally distributed random variate can be stated as follows:

*Step 1:* Generate a uniformly distributed random number sequence  $U$  between  $[0, 1]$ ,

*Step 2:* Calculate the normally distributed random variate  $X$  by

$$X = \begin{cases} z & \text{if } 0.5 < U \leq 1.0 \\ 0 & \text{if } U = 0.5 \\ -z & \text{if } 0 \leq U < 0.5 \end{cases}$$

where  $z$  is obtained using equations (3.31) and (3.32) and  $Q$  in equation (3.32) is given by

$$Q = \begin{cases} 1 - U & \text{if } 0.5 < U \leq 1.0 \\ U & \text{if } 0 \leq U \leq 0.5 \end{cases}$$

The maximum absolute error in equation (3.31) is smaller than  $0.45 \times 10^{-4}$  and is generally negligible.

**(b) Method 2: The Box–Müller Method.** Box and Müller presented the following proposition<sup>(10)</sup>:

*If  $U_1$  and  $U_2$  are two independent, uniformly distributed random numbers between  $[0, 1]$ , then*

$$X_1 = \sqrt{-2 \ln U_1} \cos(2\pi U_2) \quad \text{and} \quad X_2 = \sqrt{-2 \ln U_1} \sin(2\pi U_2) \quad (3.34)$$

*are two independent, normally distributed random variates.*

The algorithm for generating two normally distributed random variates simultaneously is as follows:

*Step 1:* Generate two uniformly distributed random number sequences between  $[0, 1]$ ,

*Step 2:* Calculate  $X_1$  and  $X_2$  using equation (3.34).

### 3.4.6. Generating Other Distribution Random Variates

In this section, algorithms for generating log-normal, gamma, and Weibull distributed random variates, which are useful in power system reliability evaluation, are presented.

**(a) Log-Normal Distributed Random Variate.** In reliability evaluation, the time to repair a component is sometimes considered as a random variate from a log-normal distribution with the following probability density function:

$$f(y) = \begin{cases} \frac{1}{\sqrt{2\pi}\sigma y} \exp\left[-\frac{(\ln y - \mu)^2}{2\sigma^2}\right] & (0 < y < \infty) \\ 0 & (y \leq 0) \end{cases} \quad (3.35)$$

If  $X$  follows a normal distribution, then  $Y = e^X$  follows the log-normal distribution. This is because equation (3.35) can be obtained from the general relationship between probability density functions of  $Y$  and  $X$  which is given by equation (B.11) in Appendix B when  $Y = e^X$  and  $X$  has a normal distribution density function. Note that  $\mu$  and  $\sigma$  in equation (3.35) are not the mean and the standard deviation of the log-normal distribution. They are the mean and the standard deviation of the normal distribution corresponding to the log-normal distribution. The mean and the variance of the log-normal

distribution should be calculated using equations (B.22) and (B.23) in Appendix B.

The algorithm for generating a log-normally distributed random variate is as follows:

*Step 1:* Generate a random variate  $Z$  following a standard normal distribution.

*Step 2:*  $X = \mu + \sigma Z$ , where  $\mu$  and  $\sigma$  are the parameters given in the equation (3.35). If the mean and variance of the log-normal distribution are specified, the parameters  $\mu$  and  $\sigma$  can be calculated using equations (B.24) and (B.25) in Appendix B.

*Step 3:*  $Y = e^X$  where  $Y$  is a log-normally distributed random variate.

**(b) Weibull Distributed Random Variate.** The Weibull distribution has the following probability density function:

$$f(x) = \frac{\beta}{\alpha^\beta} x^{\beta-1} \exp\left[-\left(\frac{x}{\alpha}\right)^\beta\right] \quad (3.36)$$

where  $0 \leq x < \infty$ ,  $\alpha > 0$ , and  $\beta > 0$ . The cumulative probability distribution function is

$$F(x) = 1 - \exp\left[-\left(\frac{x}{\alpha}\right)^\beta\right] \quad (3.37)$$

By the inverse transform method,

$$U = F(x) = 1 - \exp\left[-\left(\frac{x}{\alpha}\right)^\beta\right]$$

and

$$X = \alpha[-\ln(1 - U)]^{1/\beta} \quad (3.38)$$

where  $U$  is a uniformly distributed random variate between  $[0, 1]$ . Since  $1 - U$  is also a uniformly distributed random variate between  $[0, 1]$ , equation (3.38) becomes

$$X = \alpha(-\ln U)^{1/\beta} \quad (3.39)$$

The algorithm for generating Weibull distributed random variates is as follows:

*Step 1:* Generate a uniformly distributed random number sequence  $U$  between  $[0, 1]$ ;

*Step 2:* Calculate  $X$  by equation (3.39).

**(c) Gamma Distributed Random Variate.** The gamma distribution has the following probability density function:

$$f(x) = \frac{x^{\beta-1}}{\alpha^\beta \Gamma(\beta)} \exp\left(-\frac{x}{\alpha}\right) \quad (3.40)$$

where  $0 \leq x < \infty$ ,  $\alpha > 0$ , and  $\beta > 0$ , and it is denoted by  $G(\beta, \alpha)$ . When  $\beta = 1$ , the gamma distribution becomes the exponential distribution with parameter  $1/\alpha$ . When  $\beta$  equals an integer, the gamma distribution is known as the Erlangian distribution. It has been shown<sup>(1)</sup> that if  $X_i$  ( $i=1, \dots, n$ ) is a sequence of independent random variates following  $G(\beta_i, \alpha)$ , then  $X = \sum_{i=1}^n X_i$  is a random variate following  $G(\beta, \alpha)$  where  $\beta = \sum_{i=1}^n \beta_i$ . The Erlangian distribution with parameter  $\beta = n$  therefore can be obtained by summing  $n$  independent exponential random variates with parameter  $1/\alpha$ , that is,

$$X = \alpha \sum_{i=1}^n (-\ln U_i) = -\alpha \ln \prod_{i=1}^n U_i \quad (3.41)$$

The algorithm for generating gamma distributed random variates is as follows:

*Step 1:* Generate  $n$  independent, uniformly distributed random number sequences  $U_i$  ( $i=1, \dots, n$ ) between  $[0, 1]$  where  $n$  is the integer  $\beta$ ,

*Step 2:* Calculate  $X$  by equation (3.41).

## 3.5. VARIANCE REDUCTION TECHNIQUES

### 3.5.1. Introduction

Equation (3.12) shows that reducing the sample variance can decrease the standard deviation of the Monte Carlo estimator and that decreasing the sample variance has a similar effect on the accuracy of a Monte Carlo simulation as increasing the number of samples. The application of variance reduction techniques is an important concept in Monte Carlo simulation. The following points, however, should be clearly understood:

1. Variance reduction is simply a means to use known information about the problem. Before variance reduction is achieved, a price has to be paid to obtain and deal with required information.
2. Not all theoretical variance reduction techniques can be applied effectively in power system reliability evaluation.

Five variance reduction techniques which are useful in power system reliability evaluation are discussed in this section. They are: control variates, importance sampling, stratified sampling, antithetic variates, and dagger sampling.

### 3.5.2. Control Variates

The basic feature of the control variate technique is the use of information obtained from an analytical model to reduce the variance. If the problem contains a part which can be solved by means of an analytical model, then Monte Carlo simulation is only used to calculate the difference between the solution of the problem and this part.<sup>(11)</sup>

If  $Z$  is a random variate which is strongly correlated with another random variate  $F$ , define a new random variate  $Y$ :

$$Y = F - Z + E(Z) \quad (3.42)$$

where the mean value  $E(Z)$  can be obtained by an analytical model.

It can be seen that  $Y$  and  $F$  have the same expected value because

$$E(Y) = E(F) - E(Z) + E(Z) = E(F) \quad (3.43)$$

The variance of  $Y$  is given by

$$V(Y) = V(F) + V(Z) - 2 \operatorname{cov}(F, Z) \quad (3.44)$$

where  $\operatorname{cov}(F, Z)$  is the covariance between  $F$  and  $Z$ . Since  $F$  and  $Z$  are strongly correlated, the absolute value of the negative term in equation (3.44) may be larger than the positive term  $V(Z)$ . In this case, therefore, the variance of  $Y$  is smaller than the variance of  $F$ . Variate  $Z$  is called the control variate.

This variance reduction technique can be used to evaluate system indices of a composite generation and transmission system. Let the load curtailment due to the generating capacity shortage be the control variate  $Z$  and that due to the composite generation and transmission system be the variate  $F$ . Quantities  $Z$  and  $F$  are strongly correlated and  $E(Z)$  can be easily obtained by an analytical model such as the generating capacity outage table. The technique cannot be used to evaluate bus indices of composite systems unless a proper control variate for this purpose can be found.

### 3.5.3. Importance Sampling

Importance sampling is a procedure for changing the probability density function of sampling in such a way that the events which make greater

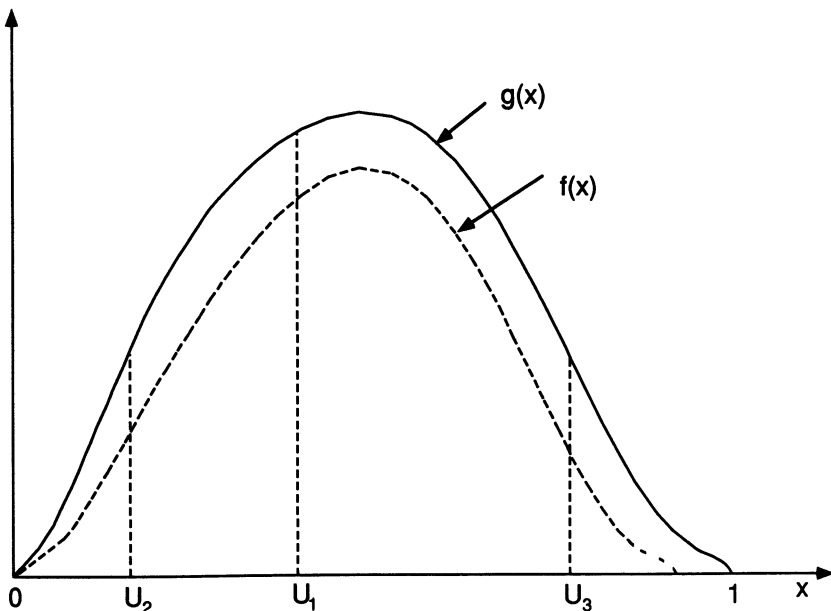


**Figure 3.6.** Explanation of importance sampling.

contributions to the simulation results have greater occurrence probabilities.<sup>(12)</sup>

An integral can represent an expected value of a parameter and therefore the problem of estimating an integral by the Monte Carlo method is equivalent to the problem of estimating an adequacy index in reliability evaluation. The importance sampling technique can be illustrated using the problem of estimating an integral.

Consider the following integral between  $[0, 1]$ :

$$I = \int_0^1 g(x) dx \quad (3.45)$$

Using the expected value estimation method, the integral can be estimated by

$$I = E(g(U)) \approx \frac{1}{N} \sum_{i=1}^N g(x_i) \quad (3.46)$$

where  $U$  is a uniformly distributed random number sequence between  $[0, 1]$ .

As shown in Figure 3.6, three random numbers  $U_1$ ,  $U_2$ , and  $U_3$  of  $x$  are obtained by uniform sampling between  $[0, 1]$ . These three random

numbers make different contributions to the integral value;  $U_1$  has a greater contribution than  $U_2$  and  $U_3$ , which indicates that uniform sampling is unreasonable. If the probability density function for sampling is changed from the uniform distribution to  $f(x)$ , which has the same shape as  $g(x)$ , then the random numbers which can make a greater contribution to the integral value have larger occurrence probabilities.

Multiplying and dividing  $g(x)$  by  $f(x)$ , the integral given in equation (3.45) can be rewritten as

$$I = \int_0^1 \frac{g(x)}{f(x)} f(x) dx$$

The new probability density function  $f(x)$  is called the importance sampling density function.

Let  $\theta = g(x)/f(x)$ . According to the definition of the expected value, the integral equals the expected value of  $\theta$ :

$$I = E[g(x)/f(x)] \quad (3.47)$$

This means that if a random variate is sampled, which has the importance sampling density function  $f(x)$  instead of a uniformly distributed random variate, the integral can be obtained by calculating the expected value of  $\theta$ .

The variance of  $\theta$  is

$$V(\theta) = \int_0^1 \frac{g^2(x)}{f^2(x)} f(x) dx - I^2 \quad (3.48)$$

If  $f(x) = g(x)/I$ , the variance of  $\theta$  would be zero:

$$V(\theta) = I \int_0^1 g(x) dx - I^2 = 0$$

It is impossible to make  $f(x) = g(x)/I$  because  $I$  is unknown. The variance, however, can be considerably reduced if  $f(x)$  has a shape similar to the shape of  $g(x)$ .

In power system reliability evaluation, the importance sampling technique can be used to sample load or hydrological states. It is a relatively difficult problem in practical application to find a proper importance sampling density function  $f(x)$ . A trial Monte Carlo sampling can be conducted to develop an importance sampling density function  $f(x)$ . This requires additional computing time.

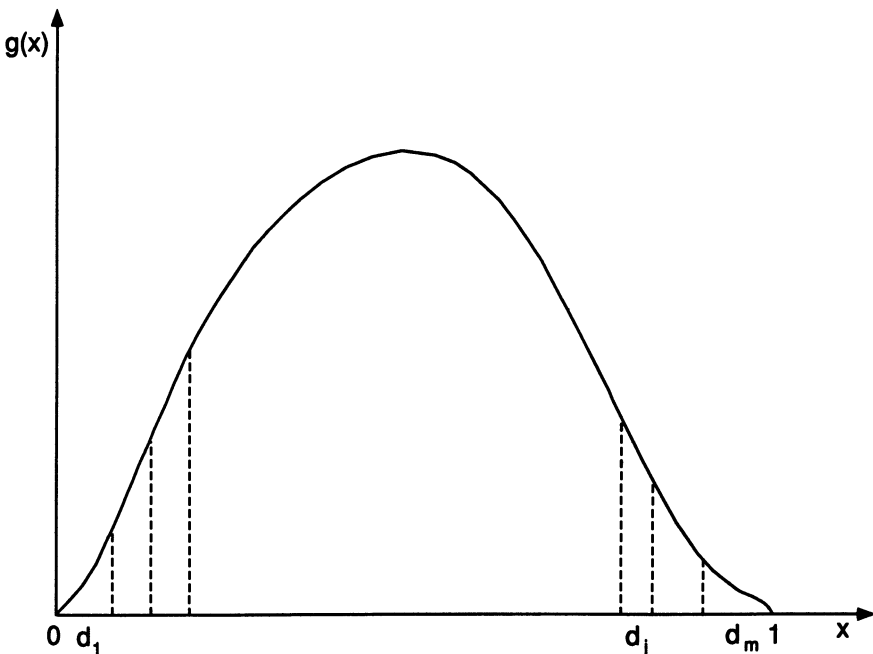


**Figure 3.7.** Explanation of stratified sampling.

### 3.5.4. Stratified Sampling

The idea of stratified sampling is similar to that of importance sampling. In order to reduce the variance, more samples are drawn in the subintervals which make greater contributions to the simulation results.<sup>(13)</sup>

Consider the integral between  $[0, 1]$  given in equation (3.45). The interval  $[0, 1]$  is divided into  $m$  disjoint subintervals  $d_j$  ( $j = 1, \dots, m$ ), as shown in Figure 3.7. The total integral can be expressed as

$$I = \int_0^1 g(x) dx = \sum_{j=1}^m I_j \quad (3.49)$$

where  $I_j$  is the integral in the  $j$ th subinterval. By the expected value estimation method,  $I_j$  can be estimated by

$$I_j = d_j E[g(U_j)] \approx \frac{d_j}{N_j} \sum_{i=1}^{N_j} g(x_i) \quad (3.50)$$

where  $U_j$  is a uniformly distributed random number sequence in the  $j$ th subinterval and  $N_j$  is the number of random numbers in the  $j$ th subinterval. The total integral therefore can be estimated by

$$\begin{aligned}
 E(\theta) &= E\left[\sum_{j=1}^m \frac{d_j}{N_j} \sum_{i=1}^{N_j} g(x_i)\right] \\
 &= \sum_{j=1}^m \frac{d_j}{N_j} \sum_{i=1}^{N_j} E[g(U_j)] \\
 &= \sum_{j=1}^m \frac{d_j}{N_j} \sum_{i=1}^{N_j} \frac{I_j}{d_j} \\
 &= \sum_{j=1}^m I_j = I
 \end{aligned} \tag{3.51}$$

This indicates that  $\theta$  is the unbiased estimator of  $I$ . The variance of  $\theta$  is

$$\begin{aligned}
 V(\theta) &= \text{var}\left[\sum_{j=1}^m \frac{d_j}{N_j} \sum_{i=1}^{N_j} g(x_i)\right] \\
 &= \sum_{j=1}^m \frac{d_j^2}{N_j^2} \sum_{i=1}^{N_j} \text{var}[g(U_j)] \\
 &= \sum_{j=1}^m \frac{d_j^2}{N_j} \text{var}[g(U_j)]
 \end{aligned} \tag{3.52}$$

where the estimation of  $\text{var}[g(U_j)]$  can be obtained by

$$V[g(U_j)] = \frac{1}{N_j - 1} \sum_{i=1}^{N_j} g^2(x_i) - \frac{I_j^2}{d_j^2} \tag{3.53}$$

It has been shown that if the sample size  $N_j$  in each subinterval is proportional to  $d_j$ , then the variance of the stratified sampling given in equation (3.52) is smaller than or at most equal to the variance obtained when applying the expected value estimation method to the whole interval  $[0, 1]$ . When

$$N_j = N \frac{d_j \sigma_j}{\sum_{j=1}^m d_j \sigma_j}$$

where  $N = \sum_{j=1}^m N_j$  and  $\sigma_j = \{\text{var}[g(U_j)]\}^{1/2}$ ,  $V(\theta)$  achieves its minimum value. In other words, the minimum  $V(\theta)$  occurs when the  $N_j$  are proportional to  $d_j \sigma_j$ .

In power system reliability evaluation, high load level points in the annual load curve make greater contributions to unreliability indices than low load level points. The idea of stratified sampling therefore can be used when considering the annual load curve.

### 3.5.5. Antithetic Variates

This technique is based on the following concept.<sup>(14)</sup> If there are two unbiased estimators  $\theta_1$  and  $\theta_2$ , then

$$\theta = \frac{1}{2}(\theta_1 + \theta_2) \quad (3.54)$$

is still an unbiased estimator. The variance of  $\theta$  is

$$V(\theta) = \frac{1}{4}V(\theta_1) + \frac{1}{4}V(\theta_2) + \frac{1}{2}\text{cov}(\theta_1, \theta_2) \quad (3.55)$$

If  $\text{cov}(\theta_1, \theta_2)$  is strongly negative, the estimator (3.54) can lead to reduction of the variance.

For example, the integral given in equation (3.45) can be calculated by

$$I = \frac{1}{2} \int_0^1 [g(x) + g(1-x)] dx \quad (3.56)$$

Therefore, it can be estimated by

$$\begin{aligned} \theta &= \frac{1}{2}E[g(U) + g(1-U)] \\ &= \frac{1}{2N} \sum_{i=1}^N [g(x_i) + g(1-x_i)] \end{aligned} \quad (3.57)$$

where  $U$  is a uniformly distributed random number sequence between  $[0, 1]$ . Since  $U$  and  $1 - U$  are strongly negatively correlated, the estimator (3.57) has smaller variance than the estimator (3.46). Note that the computing time required by equation (3.57) is twice that required by equation (3.46). Therefore, the estimator (3.57) is more effective than the estimator (3.46) only if the variance corresponding to the former is smaller than half of that corresponding to the latter. This can be guaranteed if  $g(x)$  is a monotonic function.

### 3.5.6. Dagger Sampling

This technique is suited to two-state variables and small probability events.<sup>(15)</sup> In power system reliability evaluation, system component states

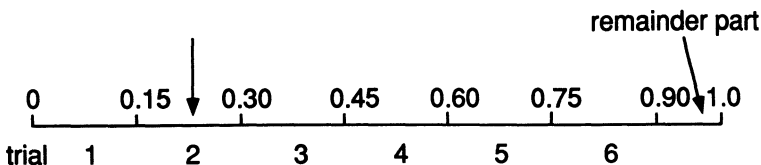


Figure 3.8. Explanation of dagger sampling.

can be simulated by a two-state (up and down) variable and system component failure events are usually small probability events. This technique is discussed from a reliability evaluation point of view.

Suppose that a system component has failure probability  $p$ . Generate a uniformly distributed random number  $U$  between  $[0, 1]$ . If  $U \leq p$ , the component is in the failure state, and if  $U > p$ , it is in the normal state. Each random number therefore corresponds to one trial of the component state. This form of sampling is called direct Monte Carlo sampling.

Let  $S$  be the largest integer not larger than  $1/p$ . The interval between  $[0, 1]$  is divided into  $S$  equal subintervals and the length of each subinterval is  $p$ . For example, the failure probability of a component  $p = 0.15$ ,  $1/p = 6.66$ , and  $S = 6$ . In this case, as shown in Figure 3.8, there are six subintervals, the length of each subinterval is 0.15, and there is also a remainder part. In dagger sampling, each subinterval corresponds to a trial of the component. If the generated random number falls in subinterval  $i$ , the component failure is assumed to occur in trial  $i$  and not to occur in other trials. In this example, there are six trials associated with one random number. If the random number falls in the second subinterval, the component failure occurs in trial 2 but not in the other five trials. If the random number falls in the remainder part beyond all the subintervals, then the component failure does not take place in any of the six trials. In this sampling procedure, only one uniform random number determines  $S$  trials of the component state. It is as if one uniform random number pierces in  $S$  subintervals and therefore this method is called "dagger sampling."

Combination of all component states provides a system state vector. Let  $Z_1, Z_2, \dots, Z_N$  be  $N$  system state vectors obtained by dagger sampling. The system unavailability can be estimated by

$$Q = \frac{1}{N} \sum_{i=1}^N X(Z_i) \quad (3.58)$$

where  $X$  is an indicator variable:

$$X(Z_i) = 0 \quad \text{if } Z_i \text{ is a nonfailure state vector}$$

$$X(Z_i) = 1 \quad \text{if } Z_i \text{ is a failure state vector}$$

Generally, the variance of  $Q$  can be calculated by

$$V(Q) = \frac{1}{N^2} \left\{ \sum_{i=1}^N V[X(Z_i)] + \sum_{i \neq j} \text{cov}[X(Z_i), X(Z_j)] \right\} \quad (3.59)$$

In the case of direct Monte Carlo sampling, there is no correlation between different random vectors. The variance of the direct Monte Carlo sampling is the first term of equation (3.59), that is,

$$V(Q_D) = \frac{1}{N^2} \sum_{i=1}^N V[X(Z_i)] \quad (3.60)$$

Here, the subscript D denotes direct Monte Carlo sampling.

In dagger sampling, different random vectors are correlated. If a component failure occurs in a trial, then it definitely does not occur in all other trials corresponding to the common random number. If  $Z_{ik}$  and  $Z_{jk}$  are two elements associated with component  $k$  in the system state vectors  $Z_i$  and  $Z_j$ , respectively, and the trials  $i$  and  $j$  are generated by a common random number for component  $k$ , then they have a negative covariance:

$$\text{cov}(Z_{ik}, Z_{jk}) = E(Z_{ik}Z_{jk}) - E(Z_{ik})E(Z_{jk}) = -p_k^2 < 0 \quad (3.61)$$

This indicates that the correlation between two system state random vectors is negative as long as these two vectors have some elements corresponding to a common random number. Because variable  $X(Z_i)$  is an indicator variable, the negative correlation between  $Z_i$  and  $Z_j$  also applies to  $X(Z_i)$  and  $X(Z_j)$ . Therefore, the dagger sampling has smaller variance than direct Monte Carlo sampling.

## 3.6. THREE SIMULATION APPROACHES IN RELIABILITY EVALUATION

The basic principles of three simulation approaches<sup>(16-20)</sup> are described in this section. Further discussion and their application to power system reliability evaluation are developed in the following chapters.

### 3.6.1. State Sampling Approach

A system state depends on the combination of all component states and each component state can be determined by sampling the probability that the component appears in that state.<sup>(21,22)</sup>

The behavior of each component can be described by a uniform distribution between [0, 1]. Assume that each component has two states of failure and success and that component failures are independent events. Let  $S_i$  denote the state of the  $i$ th component and  $\text{PF}_i$  denotes its failure probability. Draw a random number  $U_i$  distributed uniformly between [0, 1] for the  $i$ th component,

$$S_i = \begin{cases} 0 & (\text{success state}) \quad \text{if } U_i \geq \text{PF}_i \\ 1 & (\text{failure state}) \quad \text{if } 0 \leq U_i < \text{PF}_i \end{cases} \quad (3.62)$$

The state of the system containing  $m$  components is expressed by the vector  $S$ ,

$$S = (S_1, \dots, S_i, \dots, S_m) \quad (3.63)$$

Assuming that each system state has the probability  $P(S)$  and the reliability index function  $F(S)$ , the mathematical expectation of the index function of all system states is given by

$$E(F) = \sum_{S \in G} F(S)P(S) \quad (3.64)$$

where  $G$  is the set of system states.

Substituting the sampling frequency of the state  $S$  for its probability  $P(S)$  gives

$$E(F) = \sum_{S \in G} F(S) \frac{n(S)}{N} \quad (3.65)$$

where  $N$  is the number of samples and  $n(S)$  is the number of occurrences of state  $S$ ;  $F(S)$  can be obtained by appropriate system analysis. The advantages of the state sampling approach are:

1. Sampling is relatively simple. It is only necessary to generate uniformly distributed random numbers between [0, 1]. It is not necessary to sample a distribution function.
2. Required basic reliability data are relatively few. Only the component-state probabilities are required.
3. The idea of state sampling not only applies to component failure events but also can be easily generalized to sample states of other parameters in power system reliability evaluation, such as load, hydrological, and weather states, etc.

The disadvantage of this approach is that it cannot be used by itself to calculate the actual frequency index.

### 3.6.2. State Duration Sampling Approach

The state duration sampling approach is based on sampling the probability distribution of the component state duration. In this approach, chronological component state transition processes for all components are first simulated by sampling. The chronological system state transition process is then created by combination of the chronological component state transition processes.<sup>(23,24)</sup>

This approach uses the component state duration distribution functions. In a two-state component representation, these are the operating and repair state duration distribution functions and are usually assumed to be exponential. Other distributions, however, can be easily used.

The state duration sampling approach can be summed up in the following steps:

*Step 1:* Specify the initial state of each component. Generally, it is assumed that all components are initially in the success or up state.

*Step 2:* Sample the duration of each component residing in its present state. For example, given an exponential distribution, the sampling value of the state duration is

$$T_i = -\frac{1}{\lambda_i} \ln U_i$$

where  $U_i$  is a uniformly distributed random number between  $[0, 1]$  corresponding to the  $i$ th component; if the present state is the up state,  $\lambda_i$  is the failure rate of the  $i$ th component; if the present state is the down state,  $\lambda_i$  is the repair rate of the  $i$ th component.

*Step 3:* Repeat Step 2 in the given time span (yr) and record sampling values of each state duration for all components. Chronological component state transition processes in the given time span for each component can be obtained and have the forms shown in Figure 3.9.

*Step 4:* The chronological system state transition process can be obtained by combining the chronological component state transition processes of all components. The chronological system state transition process for the two components is shown in Figure 3.10.

*Step 5:* Conduct system analysis for each different system state to obtain the reliability index  $F(S)$  and use the concept given in equation (3.64) to calculate  $E(F)$ .

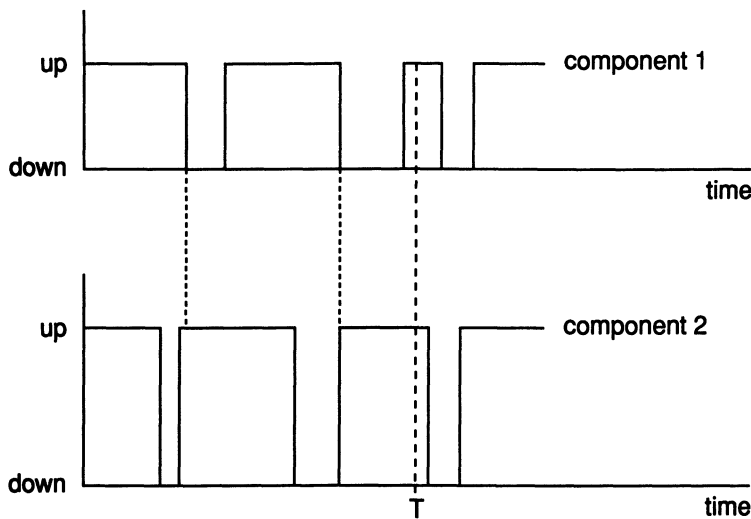


**Figure 3.9.** Chronological component state transition process.

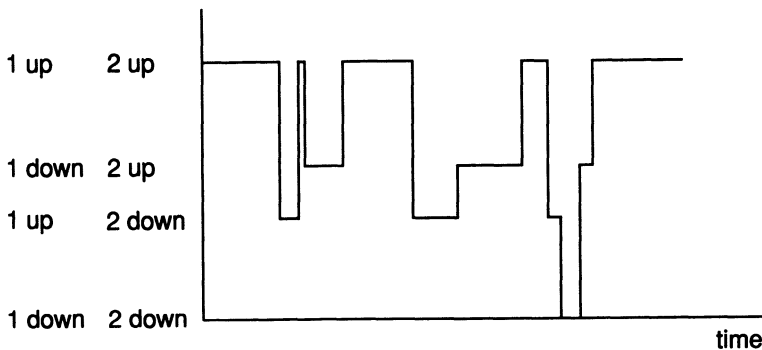


**Figure 3.10.** Chronological system state transition process.

The advantages of the state duration sampling approach are:

1. It can be easily used to calculate the actual frequency index.
2. Any state duration distribution can be easily considered.
3. The statistical probability distributions of the reliability indices can be calculated in addition to their expected values.

The disadvantages of this approach are:

1. Compared to the state sampling approach, it requires more computing time and storage because it is necessary to generate a random

- variate following a given distribution for each component and store information on chronological component state transition processes of all components in a long time span.
2. This approach requires parameters associated with all component state duration distributions. Even under a simple exponential assumption, these are all transition rates between states of each component. In some case, especially for a multistate component representation, it might be quite difficult to provide all these data in an actual system application.

### 3.6.3. System State Transition Sampling Approach

This approach focuses on state transition of the whole system instead of component states or component state transition processes.<sup>(21,25)</sup>

Assume that a system contains  $m$  components and that the state duration of each component follows an exponential distribution. The system can experience a system state transition sequence  $\{S^{(1)}, \dots, S^{(n)}\} = G$  where  $G$  is the system state space. Let us suppose that the present system state is  $S^{(k)}$  and the transition rate of each component relating to  $S^{(k)}$  is  $\lambda_i$  ( $i = 1, \dots, m$ ). The state duration  $T_i$  of the  $i$ th component corresponding to system state  $S^{(k)}$  therefore has the probability density function:  $f_i(t) = \lambda_i \exp(-\lambda_i t)$ . Transition of the system state depends randomly on the state duration of the component which departs earliest from its present state, i.e., the duration  $T$  of the system state  $S^{(k)}$  is a random variable which can be expressed by

$$T = \min_i \{T_i\} \quad (3.66)$$

It can be proved that since the state duration of each component  $T_i$  follows an exponential distribution with parameter  $\lambda_i$ , the random variable  $T$  also follows an exponential distribution with the parameter  $\lambda = \sum_{i=1}^m \lambda_i$ , i.e.,  $T$  has the probability density function

$$f(t) = \sum_{i=1}^m \lambda_i \exp\left(-\sum_{i=1}^m \lambda_i t\right)$$

Assume that system state  $S^{(k)}$  starts at instant 0 and the transition of the system state from  $S^{(k)}$  to  $S^{(k+1)}$  takes place at instant  $t_0$ . The probability that this transition is caused by departure of the  $j$ th component from its present state is the following conditional probability:  $P_j = P(T_j = t_0 / T = t_0)$ . According to the definition of conditional probability and equation (3.66),

it follows that

$$\begin{aligned}
 P_j &= P(T_j = t_0 / T = t_0) \\
 &= P(T_j = t_0 \cap T = t_0) / P(T = t_0) \\
 &= P[T_j = t_0 \cap (T_i \geq t_0, i = 1, \dots, m)] / P(T = t_0) \\
 &= P(T_j = t_0) \prod_{i=1, i \neq j}^m P(T_i \geq t_0) / P(T = t_0)
 \end{aligned} \tag{3.67}$$

Since  $T_i$  ( $i = 1, \dots, m$ ) and  $T$  follow exponential distributions,

$$P(T_i \geq t_0) = \int_{t_0}^{\infty} \lambda_i e^{-\lambda_i t} dt = e^{-\lambda_i t_0} \tag{3.68}$$

$$P(T_j = t_0) = \lim_{\Delta t \rightarrow 0} (\lambda_j e^{-\lambda_j t_0}) \Delta t \tag{3.69}$$

$$P(T = t_0) = \lim_{\Delta t \rightarrow 0} \left( \sum_{i=1}^m \lambda_i e^{-\sum_{i=1}^m \lambda_i t_0} \right) \Delta t \tag{3.70}$$

Substituting equations (3.68), (3.69), and (3.70) into equation (3.67) yields

$$P_j = P(T_j = t_0 / T = t_0) = \lambda_j \left/ \sum_{i=1}^m \lambda_i \right. \tag{3.71}$$

State transition of any component in the system may lead to system state transition. Consequently, starting from state  $S^{(k)}$ , the system containing  $m$  components has  $m$  possible reached states. The probability that the system reaches one of these possible states is expressed by equation (3.71) and obviously

$$\sum_{j=1}^m P_j = 1 \tag{3.72}$$

Therefore, the next system state can be determined by the following simple sampling. The probabilities of  $m$  possible reached states are successively placed in the interval  $[0, 1]$  as shown in Figure 3.11. Generate a

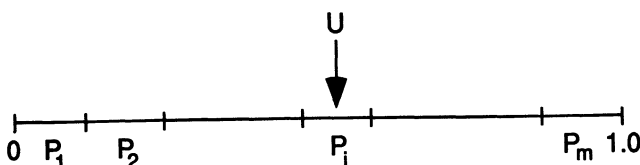


**Figure 3.11.** Explanation of system state transition sampling.

uniformly distributed random number  $U$  between  $[0, 1]$ . If  $U$  falls into the segment corresponding to  $P_j$ , this means that transition of the  $j$ th component leads to the next system state. A long system state transition sequence can be obtained by a number of samples and the reliability of each system state can be evaluated.

The advantages of the system state transition sampling approach are:

1. It can be used to calculate the exact frequency index without the need to sample the distribution function and storing chronological information as in the state duration sampling approach.
2. In the state sampling approach,  $m$  random numbers are required to obtain a system state for an  $m$ -component system. This approach requires only a random number to produce a system state.

The disadvantage of this approach is that it only applies to exponentially distributed component state durations. It should be noted, however, that the exponential distribution is the most commonly used distribution in reliability evaluation.

### **3.7. EVALUATING SYSTEM RELIABILITY BY MONTE CARLO SIMULATION**

In order to illustrate the utilization of Monte Carlo techniques in reliability evaluation, two simple examples are given in this section.<sup>(26,27)</sup>

#### **3.7.1. Example 1**

Two independent repairable components, A and B, operate in parallel. System operation requires at least one component in service. The state durations of both A and B follow exponential distributions. Their failure rates are denoted by  $\lambda_A$  and  $\lambda_B$  and repair rates by  $\mu_A$  and  $\mu_B$  respectively.

**(a) Calculate the System Reliability  $R_s$  for a Mission Time of 7.** The reliability of the system without considering repair can be obtained using the following analytical expression:

$$R_s = 1 - (1 - e^{-\lambda_A T})(1 - e^{-\lambda_B T}) \quad (3.73)$$

If repairs are taken into consideration, the problem is relatively complex to solve by an analytical method. It can be handled easily, however, by Monte Carlo simulation.

The reliability of the system can be estimated by observing the results of random experiments. An experiment is designed as a system behavior before time  $T$ . The first step is to simulate the transition processes of the two components as stated in Section 3.6.2. If there is no overlapping repair in the time interval  $[0, T]$ , the experiment is said to be a “success” (see Figure 3.9); otherwise, it is a “failure.” By defining the following indicator variables:

$$X_i = \begin{cases} 0 & \text{if the } i\text{th experiment is a “success”} \\ 1 & \text{if the } i\text{th experiment is a “failure”} \end{cases}$$

the reliability of the system for a mission time of  $T$  can be obtained by

$$R_s = 1 - \frac{\sum_{i=1}^N X_i}{N} \quad (3.74)$$

where  $N$  is the number of experiments.

Consider the following data:  $\lambda_A = 0.001$  failures/hr,  $\lambda_B = 0.0024$  failures/hr,  $\mu_A = 0.003$  repairs/hr,  $\mu_B = 0.005$  repairs/hr and  $T = 1000$  hr. In the case of no repair being considered, the analytical solution using equation (3.73) is  $R_s = 0.425224$  and the estimated value by Monte Carlo simulation ( $10^6$  samples) is  $R_s = 0.425057$ . In the case where repairs of the two components are considered, the estimated reliability of the system is  $R_s = 0.61167$ . Figure 3.12 shows the Monte Carlo convergence process as the number of experiments,  $N$ , increases.

**(b) Calculate the System Availability  $A_s$ .** The availability of the system can be calculated analytically using

$$A_s = 1 - \left( \frac{\lambda_A}{\lambda_A + \mu_A} \right) \left( \frac{\lambda_B}{\lambda_B + \mu_B} \right) \quad (3.75)$$

The availability of the system using Monte Carlo simulation can be estimated by observing the chronological system state transition process over a sufficiently long time as shown in Figure 3.10. The value of  $A_s$  can be calculated using

$$A_s = \frac{\text{Total system up time}}{\text{Total simulation time}} \quad (3.76)$$

Using the data of  $\lambda_A$ ,  $\lambda_B$ ,  $\mu_A$ , and  $\mu_B$  given earlier, the analytical value for the system availability by equation (3.75) is  $A_s = 0.918919$  and the estimated value by Monte Carlo simulation with the total simulation time of  $10^6$  hr is  $A_s = 0.915562$ . Figure 3.13 shows the Monte Carlo convergence process.

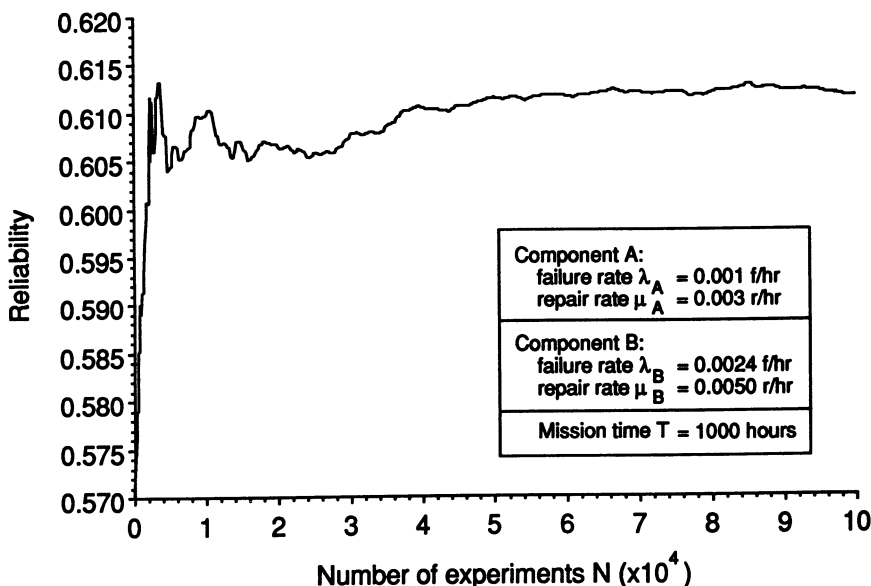


**Figure 3.12.** Reliability of the two repairable component parallel system vs. the number of experiments.

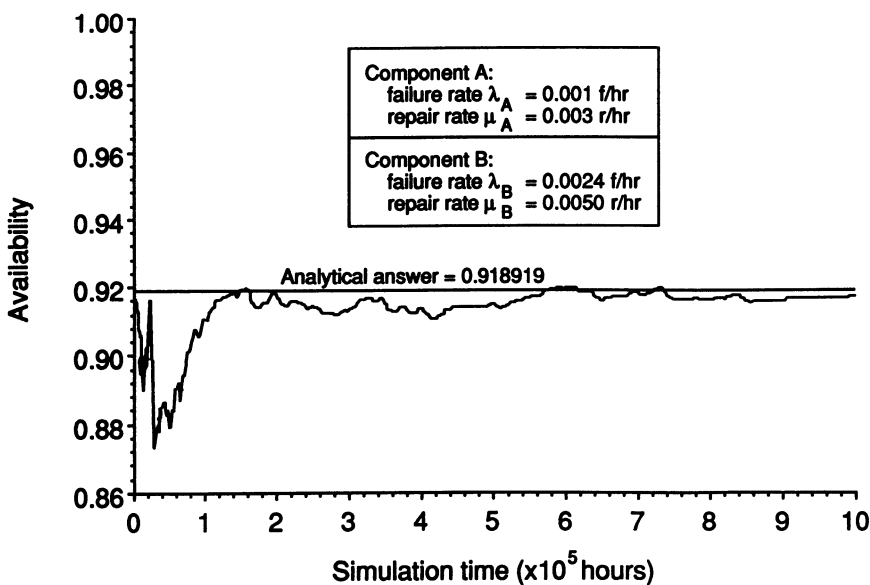


**Figure 3.13.** Availability of the two repairable component parallel system vs. simulation time.

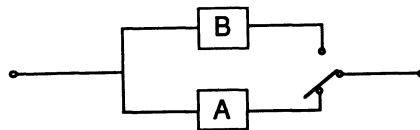


**Figure 3.14.** A two repairable component standby system.

### 3.7.2. Example 2

A standby system which contains two independent repairable components, A and B, is shown in Figure 3.14. When the normally operating component A fails, component B is switched in and component A is placed in the standby mode after being repaired. The switch is assumed to be fully reliable and switching time is negligible. It is assumed that a component cannot fail in a standby mode. The state durations of the two components follow an exponential distribution.

**(a) Calculate the System Reliability  $R_s$  for a Mission Time of  $T$ .** The analytical method to solve this problem involves the solution of Markov differential equations using a numerical algorithm. The Monte Carlo technique can be easily applied by considering a series of experiments which simulate the system behavior before time  $T$ . As shown in Figure 3.15, the sequential time to failure (TTF) chain is generated first starting with

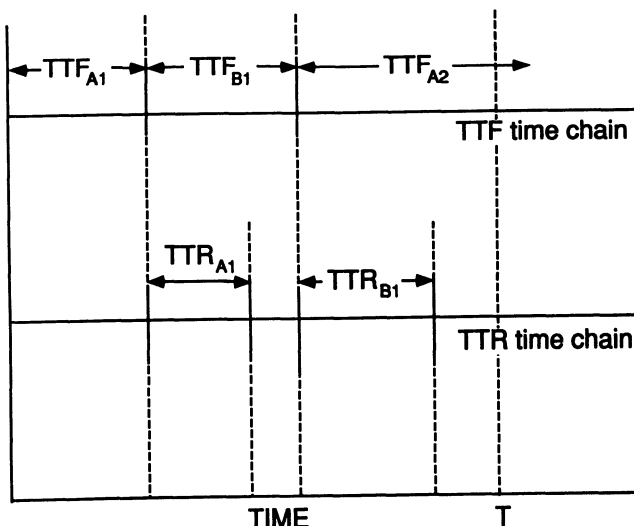


**Figure 3.15.** Simulation of the TTF and the TTR time chains.

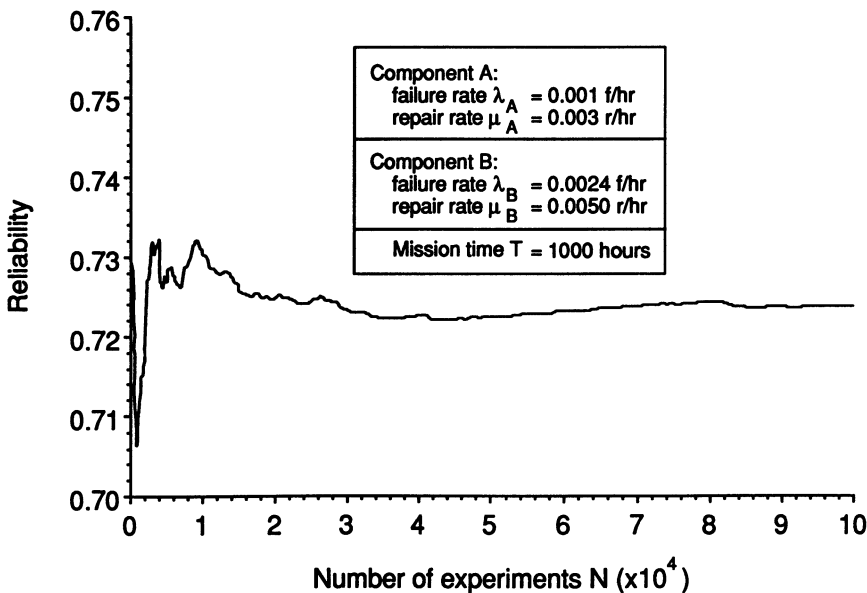


**Figure 3.16.** Reliability of the two repairable component standby system vs. the number of experiments.

component A. Another time chain associated with repair is also created starting with component A and originates from the end of  $TTF_{A1}$ . If the time to repair (TTR) of a failed component is greater than the TTF of the operating component, then that failed component cannot be repaired before the other fails. Thus, the experiment is a “failure.” Otherwise, it can be considered a “success.” Similarly, by defining indicator variables  $X_i$  as in the first example, system reliability can be estimated using equation (3.74).

Using the same data for  $\lambda_A$ ,  $\lambda_B$ ,  $\mu_A$ ,  $\mu_B$ , and  $T$  as given in the first example, the estimated value of the system reliability with repairs ( $10^5$  samples) is  $R_s = 0.72399$ . The reliability of the system without repairs is 0.56585. Figure 3.16 shows the Monte Carlo convergence process in this case with repairs.

**(b) Calculate the System Availability  $A_s$ .** The Monte Carlo procedure for estimating the availability of the system is the same as that discussed in the first example using equation (3.76). The calculation of system down time, however, is different. As shown in Figure 3.17, the operating time is first simulated. The component repair time is simulated according to the operating time sequence. Whenever the repair time TTR of the failed component is longer than the operating time TTF of the operating

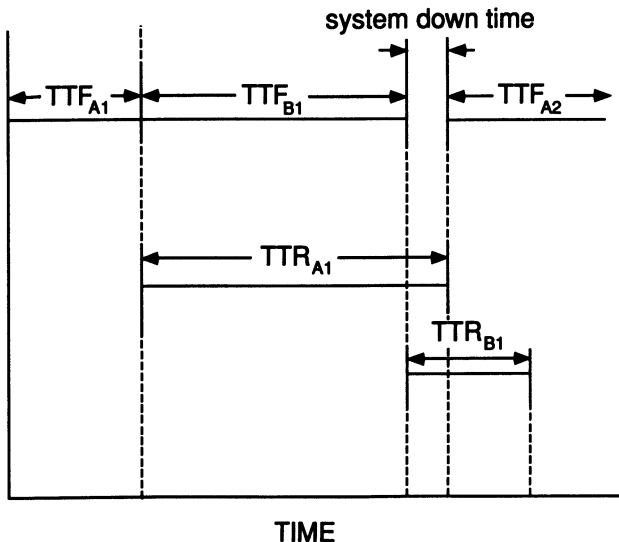


**Figure 3.17.** Calculation of the system down time.

component, a random repair time of the operating component is drawn. The system down time is then equal to the overlapping repair time.

With the same data given earlier, the system availability  $A_s$  for a total simulation time of  $10^6$  hr is  $A_s = 0.9408385$ . Figure 3.18 shows the Monte Carlo convergence process in this case. The analytical solution for the system availability is  $A_s = 0.943109$ .

It can be seen from the above two examples that Monte Carlo simulation provides considerable flexibility in evaluating system reliability. Successful application relies on a complete understanding of the problem.

### 3.8. CONCLUSIONS

This chapter describes the basic elements of Monte Carlo simulation. In general, random number/variante generation and variance reduction techniques are the most basic and important aspects of the Monte Carlo simulation method. These elements are discussed in Sections 3.3, 3.4, and 3.5. This material is not intended to be an exhaustive description of these concepts but to provide a sufficient introduction. Readers can find more material in specialized texts and papers on Monte Carlo simulation. Monte Carlo methods are also discussed from a reliability application point of view in Sections 3.2 and 3.6. These considerations include convergence

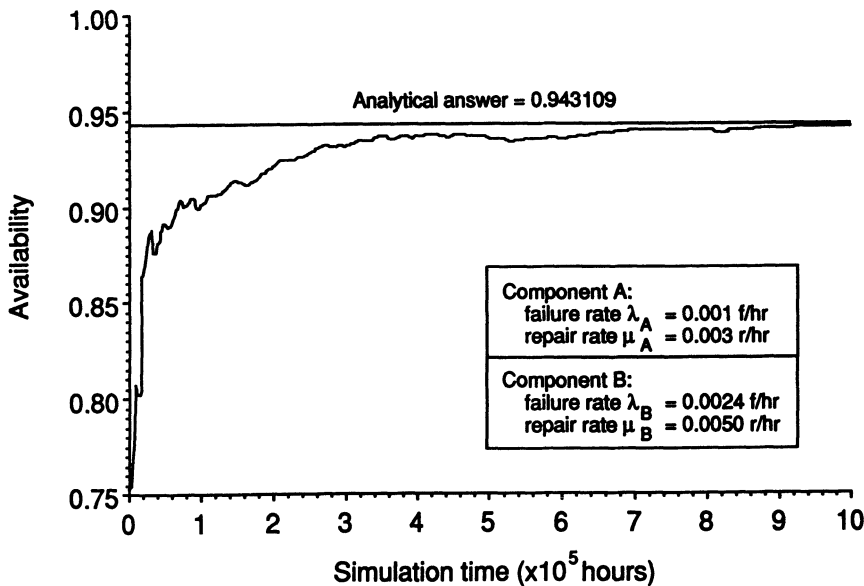


**Figure 3.18.** Availability of the two repairable component standby system vs. simulation time.

characteristics and criteria and three basic sampling approaches for reliability evaluation. The material in this chapter provides the theoretical fundamentals required to apply Monte Carlo methods to reliability assessment. There is no unified mode or procedure for any given problem and two simple illustrative examples for general application are given in Section 3.7.

### 3.9. REFERENCES

1. R. Y. Rubinstein, *Simulation and the Monte Carlo Method*, Wiley, New York, 1981.
2. D. H. Lehmer, "Mathematical Methods in Large-Scale Computing Units," *Ann. Comp. Lab., Harvard Univ.*, 1951, No. 26, pp. 141-146.
3. B. J. T. Morgan, *Computer Simulation and Monte Carlo Method*, Chapman and Hall, London, 1984.
4. Fang Zaigen, *Computer Simulation and Monte Carlo Method*, Publishing House of Beijing Industrial Institute, 1988.
5. M. Greenberger, "Notes in a New Pseudo-Random Number Generator," *J. Assoc. Comp. Math.*, No. 8, 1961, pp. 163-167.
6. D. E. Knuth, *The Art of Computer Programming: Seminumerical Algorithms*, Vol. 2, Addison-Wesley, Massachusetts, 1969.
7. M. Greenberger, "An a Priori Determination of Serial Correlation in Computer Generated Random Numbers," *Math. Comp.*, No. 15, 1961, pp. 383-389.

8. A. M. Law and W. D. Kelton, *Simulation Modelling and Analysis*, McGraw-Hill, New York, 1982.
9. M. Abramovitz and I. A. Stegun, *Handbook of Mathematical Functions*, National Bureau of Standards, 1968.
10. G. E. P. Box and M. E. Müller, "A Note on the Generation of Random Normal Deviates," *Ann. Math. Stat.*, No. 29, 1958, pp. 610–611.
11. J. M. Hammersley and D. C. Handscomb, *Monte Carlo Methods*, Wiley, New York, 1964.
12. A. W. Marshall, "The Use of Multi-Stage Sampling Schemes in Monte Carlo Computations," in *Symposium on Monte Carlo Methods*, Wiley, New York, 1956, pp. 123–14.
13. W. S. Cochran, *Sampling Techniques*, Wiley, New York, 1966.
14. J. M. Hammersley and K. W. Morton, "A New Monte Carlo Technique: Antithetic Variates," *Proc. Cambridge Philos. Soc.*, No. 52, 1956, pp. 449–474.
15. H. Kumamoto, K. Tanaka, K. Inoue, and E. J. Henley, "Dagger-Sampling Monte Carlo for System Unavailability Evaluation," *IEEE Trans. on Reliability*, R-29, No. 2, 1980.
16. G. Fishman, *Principles of Discrete Event Simulation*, J. Wiley, New York, 1978.
17. L. T. Blank, *Statistical Procedures for Engineering, Management and Science*, McGraw-Hill, New York, 1980.
18. A. M. Mood, F. A. Graybill, and D. C. Boes, *Introduction to the Theory of Statistics*, McGraw-Hill, New York, 1974.
19. S. J. Yakowitz, *Computational Probability and Simulation*, Addison-Wesley, Massachusetts, 1977.
20. J. Banks and J. S. Carson, *Discrete Event System Simulation*, Prentice-Hall, Englewood Cliffs, NJ, 1984.
21. E. J. Henley and H. Kumamoto, *Probabilistic Risk Assessment: Reliability Engineering, Design, and Analysis*, IEEE Press, New York, 1992.
22. R. Billinton and W. Li, "Hybrid Approach for Reliability Evaluation of Composite Generation and Transmission Systems Using Monte Carlo Simulation and Enumeration Technique," *IEE Proc. C*, Vol. 138, No. 3, 1991, pp. 233–241.
23. J. Endrenyi, *Reliability Modeling in Electric Power Systems*, Wiley, New York, 1978.
24. J. Kleijnen, *Statistical Techniques in Simulation: Part I and II*, Marcel Dekker, New York, 1975.
25. R. Billinton and W. Li, "A System Transition Sampling Method for Composite System Reliability Evaluation," *IEEE Trans. on PS*, Vol. 8, No. 3, 1993, pp. 761–770.
26. L. Gan, "Multi-Area Generation System Adequacy Assessment by Monte Carlo Simulation," M.Sc. Thesis, University of Saskatchewan, 1991.
27. R. Billinton and R. N. Allan, *Reliability Evaluation of Engineering Systems: Concepts and Techniques* (2nd edition), Plenum, New York, 1992.

# 4

# Generating System Adequacy Assessment

## 4.1. INTRODUCTION

Generating system adequacy assessment (HL1) is used to evaluate the ability of the system generating capacity to satisfy the total system load. This assessment can be conducted using either an analytical technique or the Monte Carlo method. A considerable number of papers involving analytical techniques are listed in References.<sup>(1-7)</sup> This chapter does not attempt to reiterate these analytical techniques but focuses an application of the Monte Carlo method in generating system adequacy assessment. Monte Carlo simulation can be considered to be more preferable than an analytical approach in situations which involve, for example, the following considerations:

1. Time-dependent or chronological issues are considered.
2. The duty cycle of peaking units are modeled.
3. Nonexponential component state duration distributions are considered.
4. Distributions of reliability indices are required.
5. A large unacceptable set of states (unfeasible range) in multi-area generation system studies is involved.

Generating system adequacy assessment is normally divided into two aspects: single-area and multi-area generating systems. Modeling a single-area generating system provides the basis for modeling multi-area systems. Two fundamental simulation methods—state duration sampling and system

state sampling—are described by application to single-area generating systems in Sections 4.2 and 4.3.

Most electric power companies operate as members of an interconnected power system because of the mutual benefits associated with interconnected operation and planning. Multi-area generating system adequacy assessment is therefore as important but also more complex than a single area analysis. It involves not only generating capacity models and load models of each area, but also tie line models and supporting policies between areas. A maximum flow algorithm and a linear programming model for multi-area generating system adequacy assessment are presented in Sections 4.4 and 4.5, respectively. A wide variety of supporting policies and their effects on multi-area system reliability indices are discussed in Section 4.6.

## **4.2. SINGLE-AREA GENERATING SYSTEM ADEQUACY ASSESSMENT—STATE DURATION SAMPLING METHOD**

As described in Section 3.6, there are three basic simulation methods in reliability evaluation. State duration sampling and system state transition sampling are often called sequential methods because they advance time or system states sequentially. Correspondingly, system state sampling can be called a nonsequential method because it considers each time point or system state independent of another. In this section, the state duration sampling method is applied to single-area generating system adequacy assessment. The main advantages of this method are as follows:

1. Frequency indices can be easily calculated.
2. Nonexponential distributions of generating unit state duration can be considered.
3. Peaking unit operating cycle can be easily modeled.

### **4.2.1. General Steps**

The state duration sampling method for single-area generating system adequacy assessment can be illustrated as follows.<sup>(8)</sup>

The first step is to generate operating histories for each generating unit by drawing sample values of TTF (Time-to-Failure) and TTR (Time-to-Repair) of the unit. The operating history of each unit is in the form of chronological up-down-up or up-derated-down-up operating cycles. The sys-

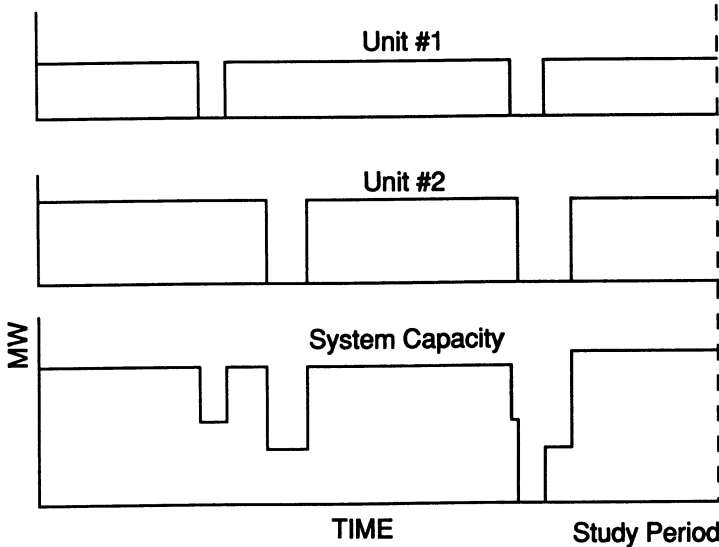


**Figure 4.1.** Available capacity models of each unit and the system.

tem available capacity can then be obtained by combining the operating cycles of all units. Figure 4.1 shows the combination.

The second step is to superimpose the system available capacity curve on the chronological hourly load curve to obtain the system available margin model. A positive margin denotes that the system generation is sufficient to meet the system load, while a negative margin implies that the system load has to be curtailed. Figure 4.2 shows the superimposition.

The third step is to calculate appropriate reliability indices. In each sampled year, for example in year  $i$ , the loss of load duration ( $LLD_i$ ) in hr, the loss of load occurrence ( $LLO_i$ ), and the energy not supplied ( $ENS_i$ ) in MWh can be obtained by observing the available margin model. The reliability indices in  $N$  sampling years therefore can be estimated using the following equations:

- (1) Loss of Load Expectation (LOLE), hr/yr

$$LOLE = \frac{\sum_{i=1}^N LLD_i}{N} \quad (4.1)$$

- (2) Loss of Energy Expectation (LOEE), MWh/yr

$$LOEE = \frac{\sum_{i=1}^N ENS_i}{N} \quad (4.2)$$

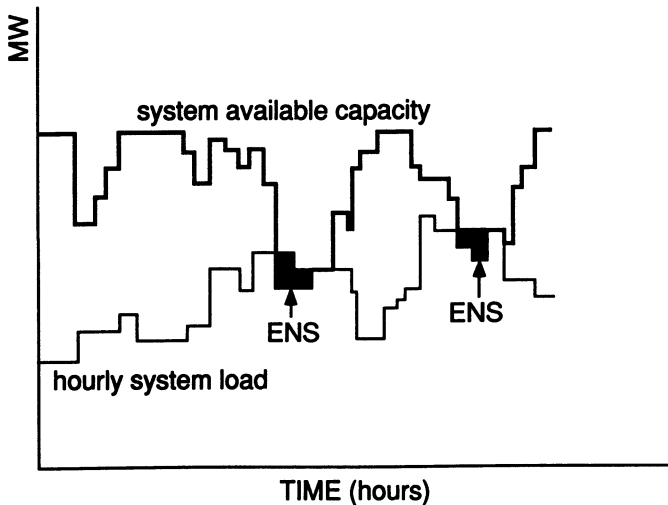


**Figure 4.2.** Superimposition of the system available capacity model on the load model.

(3) Loss of Load Frequency (LOLF) occ./yr

$$\text{LOLF} = \frac{\sum_{i=1}^N \text{LLO}_i}{N} \quad (4.3)$$

The mean value obtained by equations (4.1) to (4.3) are expectation estimates of the index over a period of  $N$  sampling years. The variance of the estimate of a reliability index can be obtained by

$$\sigma^2 = \frac{1}{N(N-1)} \sum_{i=1}^N [X_i - E(X)]^2 \quad (4.4)$$

where  $E(X)$  denotes the estimated expectation of any index and  $X_i$  is the sample value of the index in year  $i$ .

### 4.2.2. Generating Unit Modeling

It can be seen from the above general steps that the most important factor is generating unit modeling. Other work is nothing more than the combination of the operating cycles of all units, superimposition of the system available capacity curve on the chronological load curve, records of observed values, and simple calculations. The generating unit model provides an artificial operating history of the unit in state duration sampling simulation.

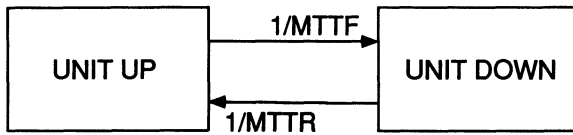


**Figure 4.3.** Two-state model for a base load unit.

Generating units can be divided into two types: base load units and peaking units. Base load units have long operating cycles while peaking units have short operating cycles. Both types of unit can be modeled using their state space diagrams based upon state durations. The development of the state space diagram of a unit requires an understanding of the physical and logical operation of the unit.

**(a) Two-State Model for Base Load Units.** A conventional two-state model for a base load unit is shown in Figure 4.3 in which both the operating and repair times are exponentially distributed. In this figure, MTTF is the mean time to failure and MTTR the mean time to repair. Sampling values of the TTF (time to failure) and the TTR (time to repair) can be obtained by drawing random variates following the exponential distributions with parameters  $\lambda = 1/\text{MTTF}$  and  $\mu = 1/\text{MTTR}$ , respectively, i.e.,

$$\text{TTF} = -\text{MTTF} \ln U \quad (4.5)$$

and

$$\text{TTR} = -\text{MTTR} \ln U' \quad (4.6)$$

where  $U$  and  $U'$  are two uniformly distributed random number sequences between  $[0, 1]$ .

An up-and-down cycle of a two-state unit can be generated starting from an initial state by sampling values of the TTF and TTR, as shown in Figure 4.4.

**(b) Derated State Model for Base Load Units.** A generating unit can operate at a reduced-capacity state designated as a derated state. The state space diagram of the three-state model of a unit is shown in Figure 4.5, where  $\lambda_{ij}$  denotes the transition rate from state  $i$  to state  $j$ .

Assuming that the unit resides in the up state at the beginning of the simulation, there are two possible states to follow: the derated state or the down state. If the unit transits to the derated state, the sampling value of

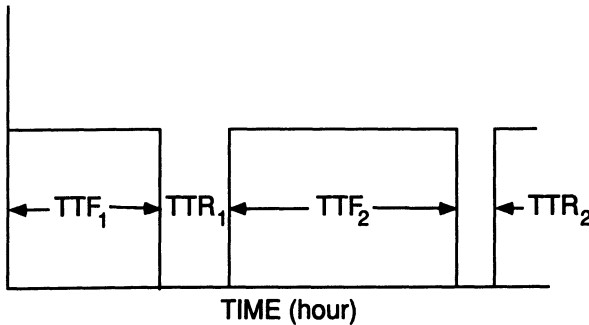


**Figure 4.4.** Up-down-up cycle of a two-state unit.

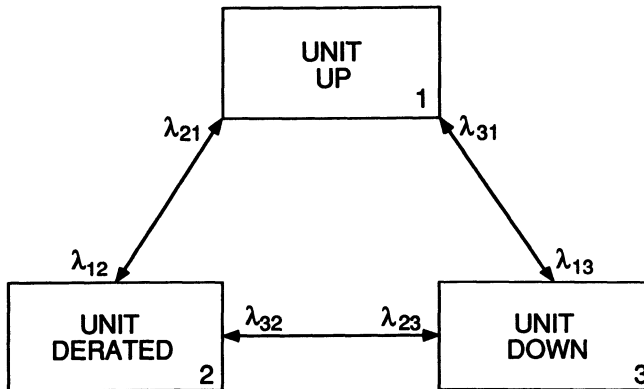


**Figure 4.5.** Three-state model for a base load unit.

the up-state duration is given by

$$T_{up1} = -\frac{1}{\lambda_{12}} \ln U_1 \quad (4.7)$$

If the unit transits to the down state, the sampling value of the up-state duration is given by

$$T_{up2} = -\frac{1}{\lambda_{13}} \ln U_2 \quad (4.8)$$

where  $U_1$  and  $U_2$  are two uniformly distributed random numbers. The sampling value of the up-state duration is given by

$$T_{up} = \min(T_{up1}, T_{up2}) \quad (4.9)$$

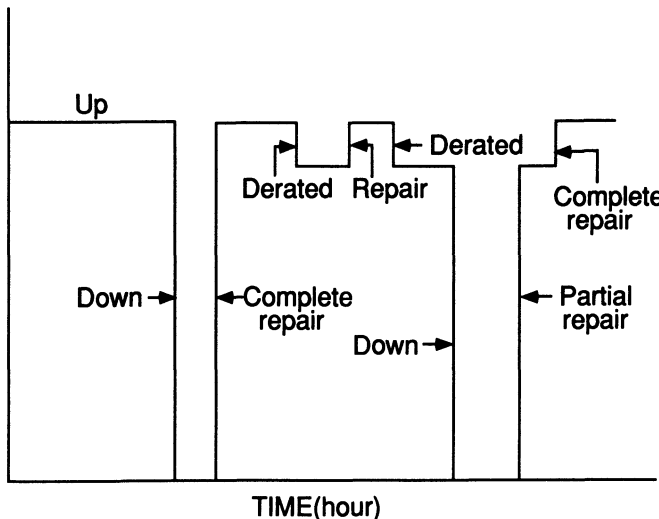


**Figure 4.6.** Operating cycle of a three-state unit.

Equation (4.9) also indicates the next state of the unit. If  $T_{up} = T_{up1}$ , the next state is the derated state. If  $T_{up} = T_{up2}$ , the next state is the down state. When the unit resides in the derated or the down state, similar sampling can be conducted. A unit operating cycle can therefore be obtained by simulating the state duration, as shown in Figure 4.6. This simulation technique can be generalized to a multiderated-state case.

**(c) Peaking Unit Model.** The model of a base load unit is inadequate for modeling peaking units. This is due to the fact that when the unit is forced out of service, it may not be needed by the system, and when it is in the operating state, periods of service may be interrupted by reserve shutdown. The IEEE Task Group on Models for Peaking Service Units proposed the four-state model<sup>(9)</sup> shown in Figure 4.7.

The parameters in Figure 4.7 are:  $T$ , average reserve shutdown time between periods of need, excluding scheduled outage;  $S$ , average in-need time per occasion of demand;  $m$ , average in-service time between occasions of forced outage, excluding forced outage as a result of failure to start;  $r$ , average repair time per forced outage occurrence;  $P_s$ , probability of a starting failure resulting in inability to serve load during all or part of a demand period; a repeated attempt to start during one demand period should not be counted as more than one failure to start.

The simulation procedure for peaking units can be explained as follows: A system available capacity margin model, as shown in Figure 4.2, without

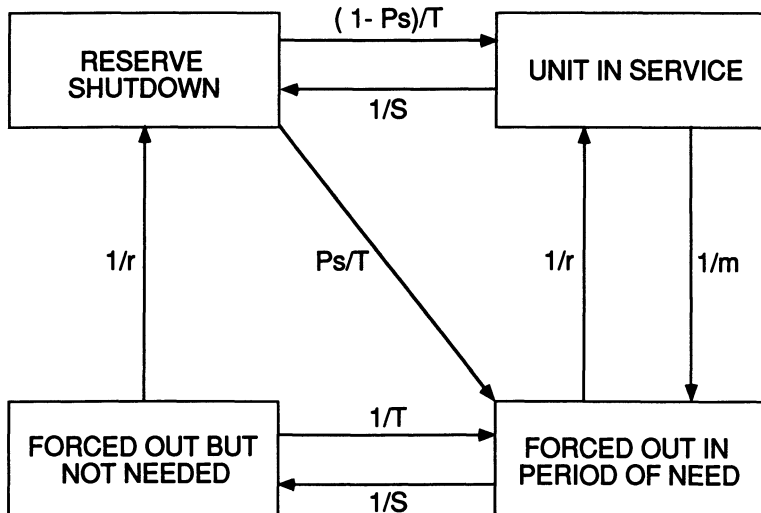


**Figure 4.7.** Four-state model for a peaking unit.

considering the peaking units, can be obtained first. The starting instants and in-need times (corresponding to  $S$ ) requiring peaking units can be determined from this model (see the shaded parts). Peaking units can then be incorporated to modify the system available capacity margin model. Whenever a peaking unit is needed, a uniformly distributed random number between  $[0, 1]$  is generated. If this random number is smaller than  $P_s$ , then the unit fails to start up. Otherwise, it starts. If the unit starts, a sampling value of time to failure corresponding to  $m$  is drawn. If the unit becomes unnecessary before the failure event occurs (i.e., the in-need time is less than the time to failure), this peaking unit is in service only during the in-need time. If the unit fails to start during the in-need time, a sampling value of time to repair corresponding to  $r$  is drawn. If the unit becomes unnecessary before the repair event occurs, this peaking unit is out of service during the whole or part of the in-need time. When the unit is in the forced out but not needed state, the reserve shutdown time (the duration between two starting instants requiring peaking units) is compared with the repair completion time and the most imminent event is applied. This procedure applies to all starting instants requiring a peaking unit. The start-up duration is assumed to be so short that it is negligible. If the system has more than one peaking unit, a “one-by-one” policy is used.

**(d) Nonexponential Distributions of State Durations.** The general steps are the same as described earlier when nonexponential distribu-

tions for the state duration are considered. The unique difference is that sampling values of the state durations are obtained by drawing random variates following the given distribution. For example, the generating unit repair times can be modeled by log-normal distributions. In this case, not only the mean value of the repair time of a unit but also its standard deviation should be specified. The sampling values of the repair time can be calculated using the procedures given in Section 3.4.6(a) instead of equation (4.6). Similarly, if the operating time or repair time is modeled by other distributions, the sampling values of the state duration can be obtained using the procedures corresponding to the specific distribution, which are given in Sections 3.4.5 and 3.4.6.

### 4.2.3. Stopping Rules

Monte Carlo simulation is a fluctuating convergence process. As the simulation proceeds, the estimated indices will approach their “real” values. The simulation should be terminated when the estimated reliability indices achieve a specified degree of confidence. The purpose of a stopping rule is to provide a compromise between the accuracy needed and the computation cost.

As noted in Section 3.2.4, the coefficient of variation is often used as the convergence criterion in Monte Carlo simulation. The coefficient of variation of an index is defined as

$$\alpha = \sigma/E(X) \quad (4.10)$$

where  $E(X)$  is the estimated expectation of the index and  $\sigma$  the standard deviation of the estimated expectation obtained from equation (4.4). A number of calculations indicate that the coefficient of variation for the LOEE index has the lowest convergence speed compared to other indices. It is therefore advisable when calculating multiple indices to use the LOEE coefficient of variation as the convergence criterion.

Two stopping rules can be used:

1. The simulation stops when the coefficient of variation is less than the prespecified tolerance value.
2. The simulation pauses at a given number of samples and it is checked to see if the coefficient of variation is acceptable. If not, the number of samples can be increased.

These two stopping rules are quite general. The basic idea presented here is applied in all the other applications in this book.

#### 4.2.4. IEEE RTS Studies

The IEEE RTS has 32 generating units ranging from 12 MW to 400 MW. The annual load curve consists of 8736 hourly load points. All the data for the IEEE RTS are given in Appendix A.1.

**(a) Base Case.** In this case, the generating unit state durations are assumed to be exponential and no derated states are considered.

The system available capacity is obtained by combining the operating cycles of all the units. Figure 4.8 shows the system available capacity model in a typical sample year. The annual load model for the IEEE RTS is shown in Figure 4.9. Figure 4.10 shows the system available margin model in the typical sample year.

The estimated reliability indices are given in Table 4.1. These results are for 2500 sampling years. Figures 4.11, 4.12, and 4.13 show the convergence processes of the LOLE, LOEE, and LOLF indices, respectively, as the number of sample years increases. It can be seen that of these indices, the LOEE index has the most difficulty in converging and the LOLF index takes the shortest time to stabilize.

The distribution of an index can be obtained from the simulated history of the index. Figures 4.14, 4.15, and 4.16 show the distributions of LOLE, LOEE, and LOLF indices, respectively, for a system peak load of 2850 MW.

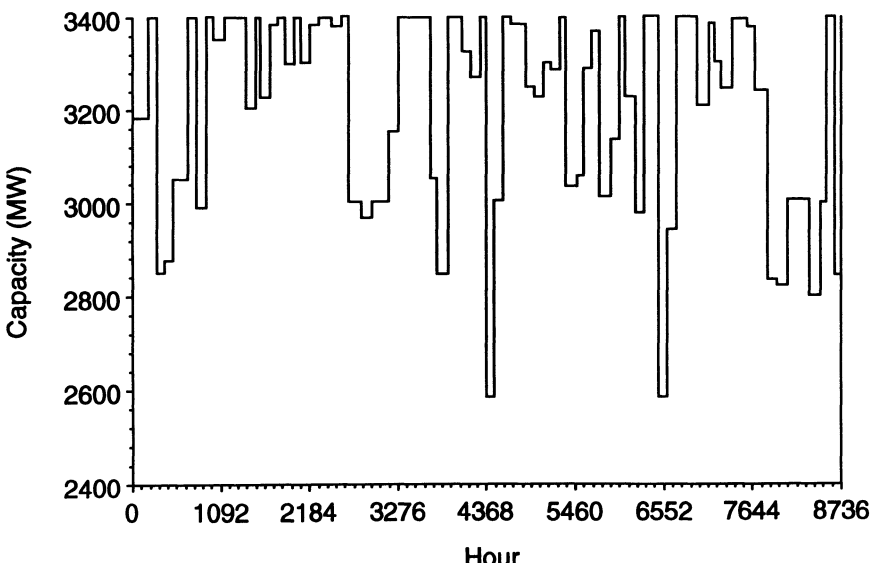


**Figure 4.8.** System available capacity model in a typical sample year.

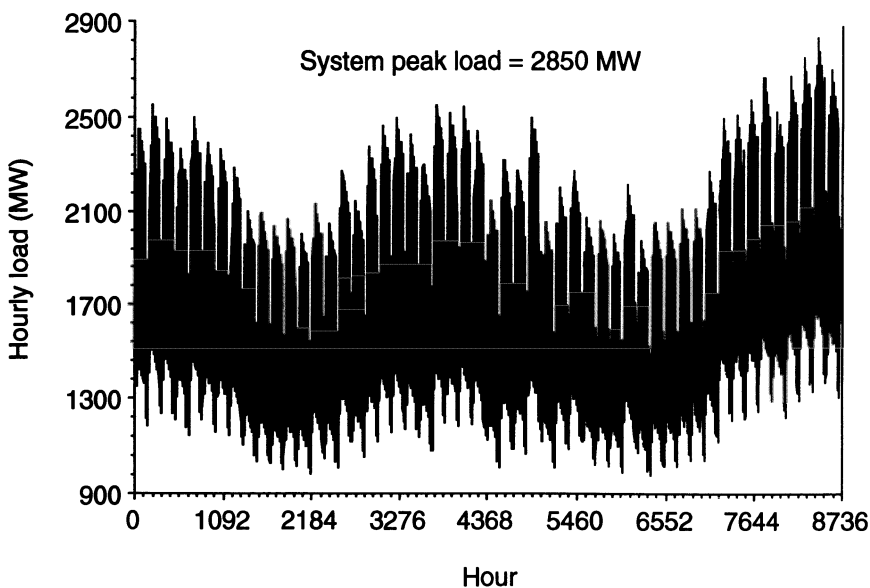


Figure 4.9. Annual hourly load model for the IEEE RTS.

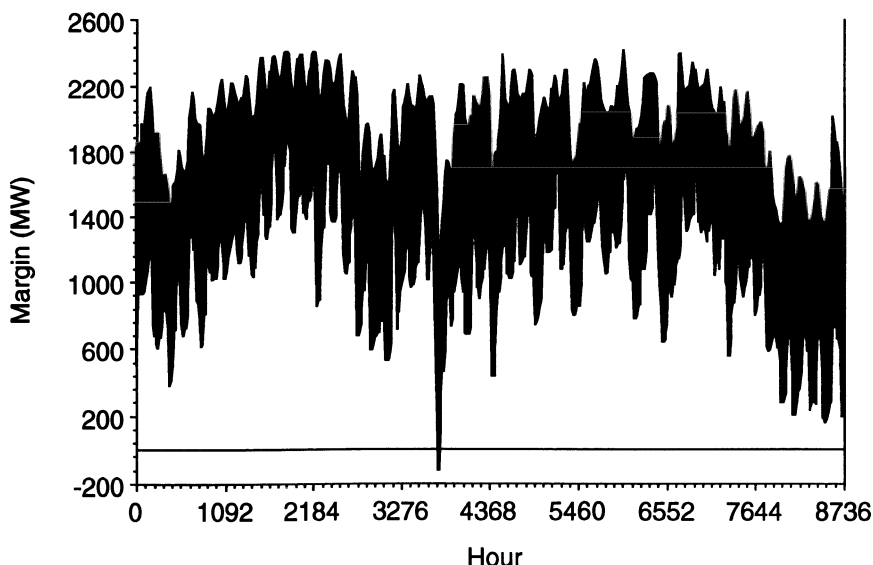
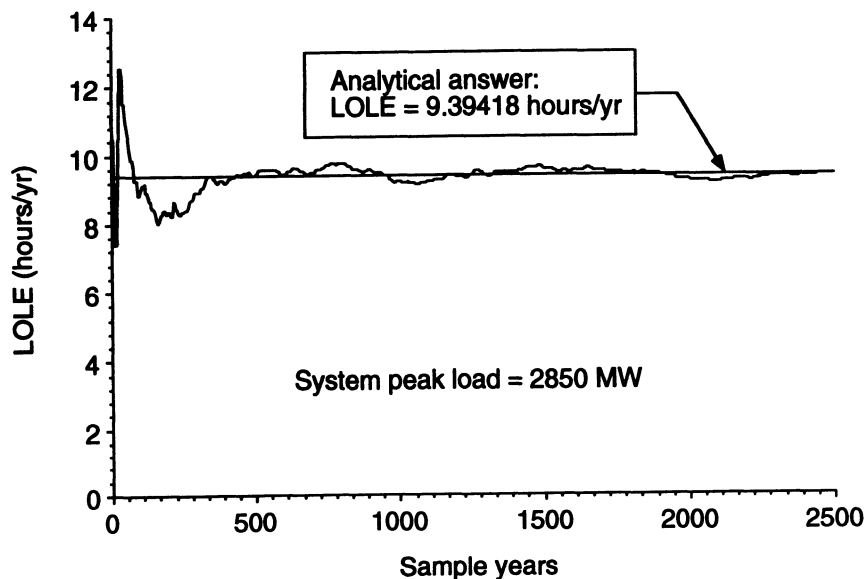


Figure 4.10. System available margin model in a typical sample year.

**Table 4.1. IEEE RTS Reliability Indices**

Index	Annual system peak load (MW)			
	2750	2850	2950	3050
LOLE (hr/yr)	4.8516	9.3716	17.3696	30.7172
LOEE (MWh/yr)	586.4907	1197.4448	2335.7295	4384.6909
LOLF (occ./yr)	1.0348	1.9192	3.4228	5.8652

**Figure 4.11. LOLE vs. the number of sample years.**

Note that these distributions are not probability densities. Instead, they are in the number of years. The probability density can be obtained by dividing the number of years by the total number of sample years (2500). The distribution of each index provides interesting and important insight into the random behavior of the system. For instance, it can be seen from Figure 4.14 that among the 2500 sample years, about 1560 years actually experience loss of load for less than 0.5 hr (including 0 hr).

**(b) Derated State Case.** This case is the same as the base case, except that the 350 MW and 400 MW units are assumed to be able to operate at 50% derated capacities. The unit derating data are given in Table 4.2. These derating data are such that the derating-adjusted two-state model of a unit is identical to that in the base case.<sup>(10)</sup> The simulation results for 2500

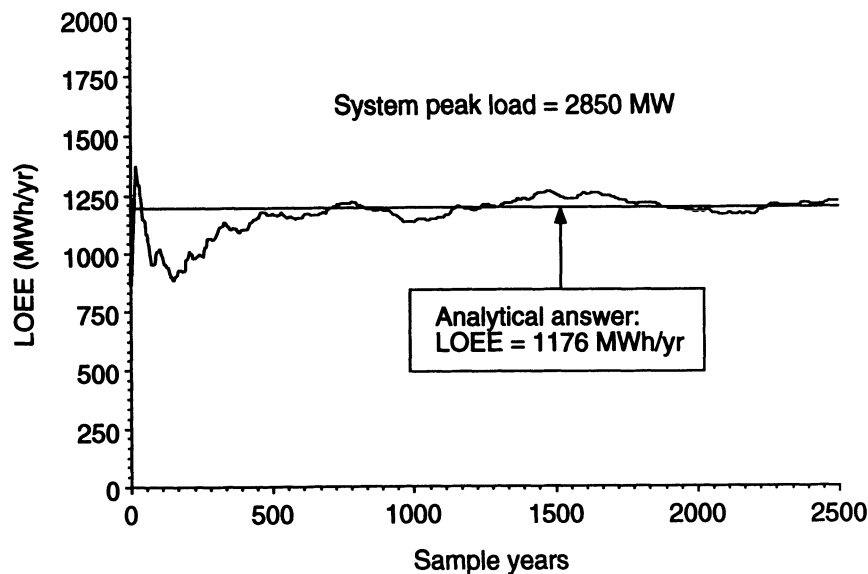


Figure 4.12. LOEE vs. the number of sample years.

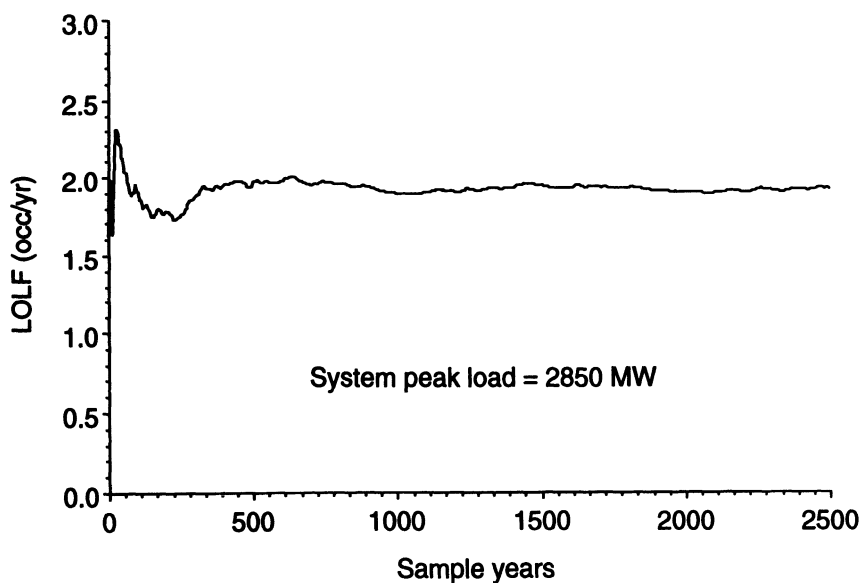


Figure 4.13. LOLF vs. the number of sample years.

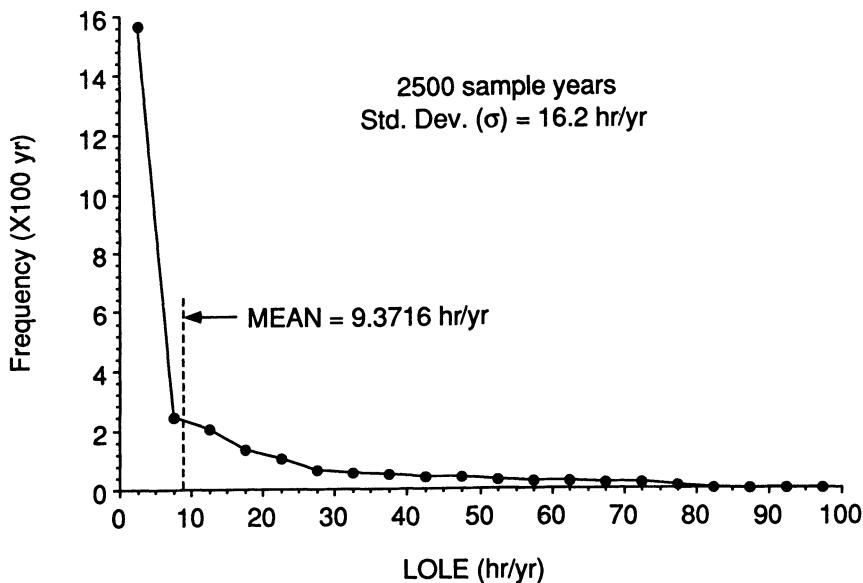


Figure 4.14. Distribution of the LOLE index.

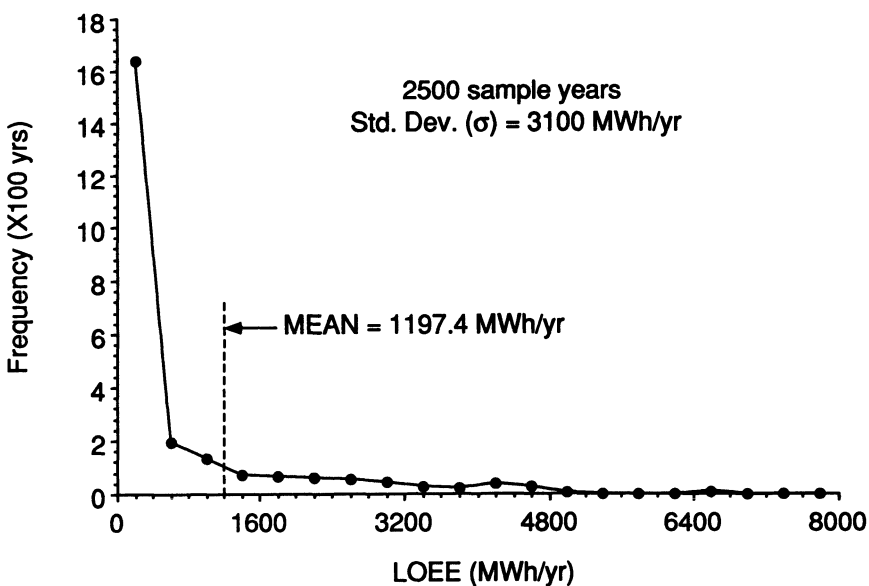


Figure 4.15. Distribution of the LOEE index.

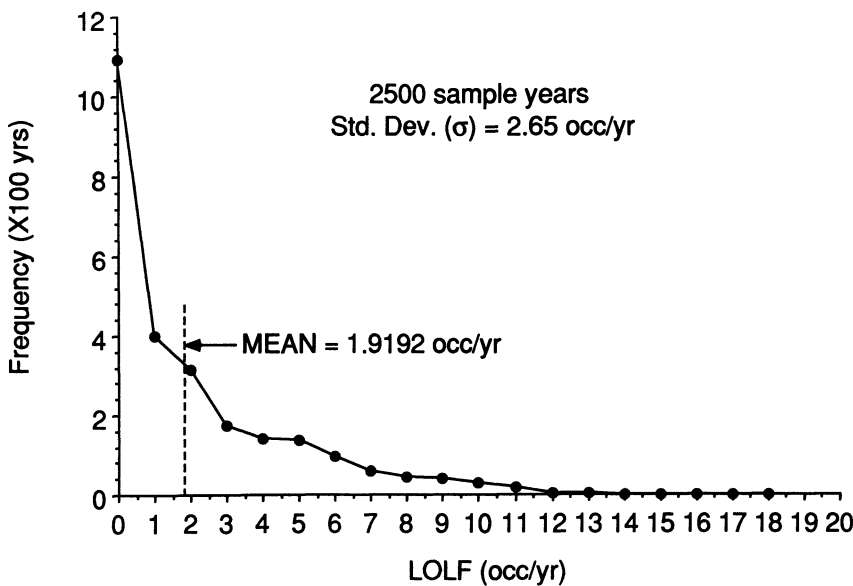


Figure 4.16. Distribution of the LOLF index.

sample years are shown in Table 4.3. It can be seen, by comparing the results in Tables 4.1 and 4.3, that including the unit derated states provides a more optimistic appraisal of generating system adequacy.

**(c) Peaking Unit Case.** This case is the same as the base case for the annual peak load of 2850 MW, except that additional 25-MW gas turbine

Table 4.2. Unit Derating Data for the IEEE RTS

Unit size (MW)	Derated capacity (MW)	Mean duration (hr)		
		Up	Derated	Down
350	175	1150	60	70
400	200	1100	100	100

Table 4.3. IEEE RTS Reliability Indices for the Derated State Case

Index	Annual system peak load (MW)			
	2750	2850	2950	3050
LOLE (hr/yr)	2.6860	5.5404	11.0608	21.0664
LOEE (MWh/yr)	290.4749	642.0654	1350.1066	2729.4775
LOLF (occ./yr)	0.5952	1.2140	2.3748	4.3752

**Table 4.4. Peaking Unit Data for the IEEE RTS**

Capacity (MW)	Mean time to failure (hr)	Average repair time (hr)	Starting failure probability
25	550	75	0.01

**Table 4.5. IEEE RTS Reliability Indices for the Peaking Unit Case**

Index	Number of peaking units added		
	Zero units	One unit	Two units
LOLE (hr/yr)	9.3716	7.9108	6.6132
LOEE (MWh/yr)	1197.4448	990.0966	817.2875
LOLF (occ./yr)	1.9192	1.6208	1.3876

units are installed as peaking units. The data for the peaking units are given in Table 4.4. The simulation results for 2500 sample years are shown in Table 4.5. The addition of peaking units improves the generating system adequacy.

**(d) Nonexponential Distribution Case.** This case is the same as the base case for the annual peak load of 2850 MW, except that unit operating durations or repair durations are assumed to be nonexponential. The following four conditions were considered:

1. Times to failure of all units follow a Weibull distribution with the mean value = MTTF and the shape parameter  $\beta = 0.5$ .
2. Times to repair of all units follow a Weibull distribution with the mean value = MTTR and the shape parameter  $\beta = 4.0$ .
3. Times to repair of all units follow a normal distribution with the standard deviation which equals one-third of the mean value (MTTR).
4. Times to repair of all units follow a log-normal distribution with the standard deviation which equals one-third of the mean value (MTTR).

The simulation results for 2500 sample years are shown in Table 4.6. It is interesting to note that the reliability indices of the generating system in a mean value sense do not display great differences when the generating unit state durations are assumed to follow different distributions.

**Table 4.6. IEEE RTS Reliability Indices Considering Nonexponential Distributions of Generating Unit State Durations**

Index	Cond. 1	Cond. 2	Cond. 3	Cond. 4
LOLE (hr/yr)	9.7388	9.2260	9.2407	9.1866
LOEE (MWh/yr)	1231.6710	1135.4628	11181.0088	1157.0930
LOLF (occ./yr)	1.9388	1.9096	1.8890	1.8883

### 4.3. SINGLE-AREA GENERATING SYSTEM ADEQUACY ASSESSMENT—STATE SAMPLING METHOD

This section describes the application of the state sampling method in single-area generating system adequacy assessment. Compared to the state duration sampling method, this method cannot be used to calculate the frequency index in a strict sense. However, it has the following advantages:

1. It requires less computing time and memory storage than the state duration sampling method, particularly for a large-scale system.
2. Basic data are the generating unit state probabilities and no transition rates between generating unit states nor other data are required. It is easier for an electric power company to provide generating unit state probabilities than transition rates between possible generating unit states, particularly in the case of multistate generating unit representations.

#### 4.3.1. Single Load Level Case

For a single load level, generating system adequacy depends on the possible generating capacity states of the system. A system state is a random combination of all generating unit states. The behavior of each generating unit can be simulated by a uniformly distributed random number sequence in  $[0, 1]$ . In the case of a two-state representation, let  $S_i$  denote the state of the  $i$ th generating unit and  $FU_i$  be its forced unavailability. A uniformly distributed random number  $U_i$  is drawn in  $[0, 1]$  for the  $i$ th generating unit,

$$S_i = \begin{cases} 0 & (\text{up state}) & \text{if } U_i \geq FU_i \\ 1 & (\text{down state}) & \text{if } 0 \leq U_i < FU_i \end{cases} \quad (4.11)$$

In situations in which generating unit derated states are considered, let  $PDR_i$  be the probability of a single derated state of the  $i$ th generating unit,

$$S_i = \begin{cases} 0 & (\text{up state}) & \text{if } U_i \geq PDR_i + FU_i \\ 1 & (\text{down state}) & \text{if } PDR_i \leq U_i < PDR_i + FU_i \\ 2 & (\text{derated state}) & \text{if } 0 \leq U_i < PDR_i \end{cases} \quad (4.12)$$

The above state sampling technique can be easily extended to the case of multiderated states of generating units without any increase in computation effort.

The available capacity of each generating unit can be determined according to its state. The generating capacity state of the system can be expressed using a generation capacity vector  $\{G_{ik}, i=1, \dots, m\}$ , where  $G_{ik}$  is the available capacity of the  $i$ th generating unit in the  $k$ th sampling and  $m$  is the number of generating units. For a given load level  $D$ , the demand not supplied due to insufficient generating capacity in the  $k$ th sampling is given by

$$DNS_k = \max \left\{ 0, D - \sum_{i=1}^m G_{ik} \right\} \quad (4.13)$$

The estimates of the annualized reliability indices for  $N$  samples can be calculated using the following equations:

(1) Expected Demand Not Supplied (EDNS), MW

$$EDNS = \frac{\sum_{k=1}^N DNS_k}{N} \quad (4.14)$$

(2) Loss of Energy Expectation (LOEE), MWh/yr

$$LOEE = \frac{\sum_{k=1}^N DNS_k \times 8760}{N} \quad (4.15)$$

(3) Loss of Load Expectation (LOLE), hr/yr

$$LOLE = \frac{\sum_{k=1}^N I_k(DNS_k)}{N} \times 8760 \quad (4.16)$$

where  $I_k$  is an indicator variable which means that

$$I_k = \begin{cases} 0 & \text{if } DNS_k = 0 \\ 1 & \text{if } DNS_k \neq 0 \end{cases}$$

The variance of the estimate of a reliability index can be calculated by

$$\sigma^2 = \frac{1}{N(N-1)} \sum_{k=1}^N [X_k - E(X)]^2 \quad (4.17)$$

where  $E(X)$  denotes the expected estimate of any index and  $X_k$  is the  $k$ th sample value of the index. It should be noted that equations (4.4) and (4.17) have the same form, but  $N$  in these two equations is different;  $N$  in equation (4.4) is the number of sample years and  $N$  in equation (4.17) is the number of samples.

### 4.3.2. Modeling an Annual Load Curve

The most basic approach to consider the annual load curve is to scan all hourly points of the chronological load curve. This is, however, not practical because of computational requirements. The following three alternatives can be used to model the annual load curve:

1. Sample load states in terms of the chronological load curve. Each hourly load in one year has an equal occurrence probability. A uniformly distributed random number therefore can be drawn to select a particular load state. This load state and the drawn states of all generating units form a sample of the system state.

2. Create a multistep model of the annual load curve. The chronological load curve can be changed into the load duration curve in a load level descending order. And the load duration curve can be approximated by a multistep model as shown in Figure 4.17. The method given in the previous subsection for a single load level can be used directly for each load level step. Annual reliability indices can be obtained by weighting the annualized indices for each load level by the load step probability. Assume that the load duration curve is divided into  $NL$  level steps and the  $i$ th step includes  $NI_i$  load points. The probability of the  $i$ th load step is

$$P_i = \frac{NI_i}{8760} \quad (4.18)$$

The annual reliability indices considering the multistep model of the annual load curve can be obtained using

$$EDNS = \sum_{i=1}^{NL} EDNS_i P_i \quad (4.19)$$

$$LOEE = \sum_{i=1}^{NL} LOEE_i P_i \quad (4.20)$$

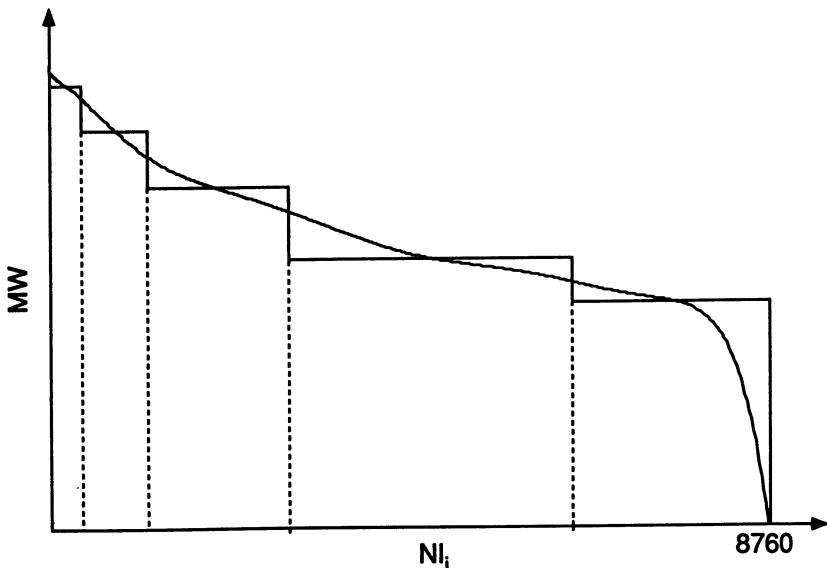


**Figure 4.17.** A multistep model of the load duration curve.

$$\text{LOLE} = \sum_{i=1}^{NL} \text{LOLE}_i P_i \quad (4.21)$$

where  $\text{EDNS}_i$ ,  $\text{LOEE}_i$ , and  $\text{LOLE}_i$  are the annualized indices for the  $i$ th load level step.

3. Sample the load levels using the multistep model. The probabilities of all steps  $P_i$  are put successively in the interval  $[0, 1]$ . Draw a uniformly distributed random number in  $[0, 1]$ . A load level can be determined in each sample according to the location of the random number as shown in Figure 4.18.

Method 2 is more effective than Method 1 or 3 from a computational point of view. This is mainly due to the fact that load points in the flat segments of a load duration curve provide almost the same contribution to the total indices and that a number of the low load points, which may have

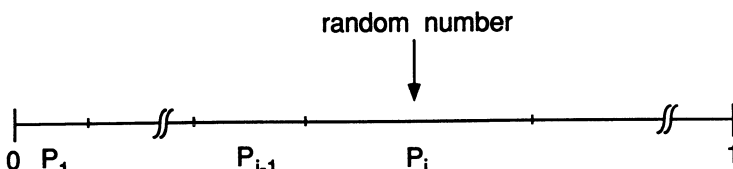


**Figure 4.18.** Explanation of how to sample load levels.

relatively high probabilities of occurrence, make little or no contribution to the total indices. Method 2 requires enumeration of load level steps. Essentially, however, it is still a Monte Carlo simulation method because sampling of generating unit capacity states is conducted for each load level. It can be seen as a variance reduction technique as it makes use of analytical load level step probabilities.

Different load level steps make different contributions to the total annual indices. It is therefore possible to use different tolerance values for the coefficient of variation convergence criteria in the different load level steps. This is similar to a stratified sampling approach. The low load level steps, which make little or no contribution to the total indices, can often be excluded from enumeration. The following discussion focuses on Method 2 and the numerical results given in Section 4.3.5 are based on this method.

### 4.3.3. Cluster Technique for a Multistep Load Model

The cluster technique<sup>(11,12)</sup> can be used to create a multistep model of the annual load duration curve. This technique is called the  $K$ -mean algorithm or nearest centroid sorting. Assume that the load duration curve is divided into  $NL$  load levels. This corresponds to grouping 8760 load points into  $NL$  clusters. Each load level is the mean value of those load points in a cluster. This analysis can be conducted in the following steps:

*Step 1:* Select initial cluster means  $M_i$  where  $i$  denotes cluster  $i$  ( $i = 1, \dots, NL$ ).

*Step 2:* Calculate the distance  $D_{ki}$  from each hourly load point  $L_k$  ( $k = 1, \dots, 8760$ ) to each cluster mean  $M_i$  by

$$D_{ki} = |M_i - L_k| \quad (4.22)$$

*Step 3:* Group load points by assigning them to the nearest cluster and calculate new cluster means by

$$M_i = \frac{\sum_{k \in IC} L_k}{NI_i} \quad (4.23)$$

where  $NI_i$  is the number of load points in the  $i$ th cluster and  $IC$  denotes the set of the load points in the  $i$ th cluster.

*Step 4:* Repeat Steps 2 and 3 until all cluster means remain unchanged between iterations.

The obtained  $M_i$  and  $NI_i$  are the load level (in MW) and the time length (in hr) for the  $i$ th step in the multistep load model, respectively.

It should be noted that, theoretically, the cluster technique is a local optimal sorting approach and therefore may lead to multisolutions. It is important to specify the proper number of clusters (steps) and initial cluster means. This can be determined by testing for a given annual load curve. Generally, selecting relatively high initial cluster means is beneficial.

#### 4.3.4. Stopping Rules

The two general stopping rules in Monte Carlo simulation are given in Section 4.2.3. In order to obtain the coefficient of variation expressed in equation (4.10), the variance of the estimate of a reliability index has to be first calculated. In the case of a single load level it can be estimated directly by equation (4.17). In the case of a multistep model of the annual load curve, the following equation similar to that used in stratified sampling can be applied:

$$\sigma^2 = \sum_{i=1}^{NL} \frac{P_i^2}{N_i(N_i-1)} \sum_{k=1}^{N_i} [X_k - E_i(X)]^2 \quad (4.24)$$

where  $NL$  is the number of load levels;  $N_i$ ,  $P_i$ , and  $E_i(X)$  are the number of samples, the probability, and the expected estimate of any index for the  $i$ th load level, respectively; and  $X_k$  is the  $k$ th sample value of the index. Equation (4.24) can also be rewritten as

$$\sigma^2 = \sum_{i=1}^{NL} P_i^2 \sigma_i^2 \quad (4.25)$$

where  $\sigma_i^2$  is the variance of the estimate of the reliability index associated with the  $i$ th load level.

Generally, the relatively high load level steps make greater contributions to the total annual indices than to those at relatively low load levels. A smaller coefficient of variation tolerance can be used as the stopping criterion for the high load level steps and larger ones for the low load level steps.

#### 4.3.5. IEEE RTS Studies

The 8736 hourly load points given in Appendix A.1 were replaced by a 20-step load level model obtained using the cluster technique. The 20-step load level model is given in Table 4.7. The load levels are in per unit of the annual peak load.

**Table 4.7. The 20-Step Load Level Model for the IEEE RTS**

Step No.	Load level (p.u.)	Probability	Step No.	Load level (p.u.)	Probability
1	0.9900	0.0006	11	0.6792	0.0711
2	0.9505	0.0034	12	0.6481	0.0738
3	0.9210	0.0061	13	0.6179	0.0754
4	0.8896	0.0171	14	0.5866	0.0630
5	0.8612	0.0236	15	0.5519	0.0695
6	0.8348	0.0371	16	0.5184	0.0805
7	0.8068	0.0482	17	0.4864	0.0949
8	0.7782	0.0499	18	0.4512	0.0769
9	0.7467	0.0517	19	0.4149	0.0690
10	0.7126	0.0590	20	0.3733	0.0292

**(a) Base Case.** In this case, no generating unit derated states are considered. The stopping rule includes the following two aspects:

1. Two criteria are specified for each load level step. The maximum number of samples is 80,000 and the LOEE index coefficient of variation tolerance is 0.05. When either of them is reached, the simulation in a particular load level step ends.
2. When the contribution of a load level step to the total LOEE index is smaller than 3%, all load steps lower than this level are ignored.

Tables 4.8 and 4.9 show the results for annual peak loads of 2850 MW and 3050 MW, respectively. It can be seen that the LOLE and LOEE indices obtained using the state sampling method are consistent with those obtained using the state duration sampling method. The coefficients of variation for the system LOEE are quite small (0.0227 and 0.0189, respectively), which indicates that the calculated results have sufficient accuracy. The stopping rule given earlier is reasonable. The relatively high load level steps, which make major contributions to the total reliability indices, are associated with the relatively small coefficients of variation. On the other hand, although the relatively low load level steps have relatively large coefficients of variation, this does not materially affect the accuracy of the total system indices as their contributions are quite small. For example, in the case of the 2850 MW annual peak load, the coefficient of variation for the LOEE in Step 9 is quite high (0.2089). It has, however, no great impact on the accuracy of the total system index because its contribution is only 2.27%. The contributions due to Steps 10–20 are very small and therefore have been neglected.

**Table 4.8. The Results for an Annual Peak Load of 2850 MW**

	LOLE (hr/yr)	LOEE (MWh/yr)	Coefficient of variation for LOEE index
Index	9.2185	1147.3279	0.0227
<b>Contributions of Each Load Step (p.u.)</b>			
Step 1	0.0545	0.0406	0.0438
Step 2	0.1586	0.1444	0.0487
Step 3	0.1556	0.1499	0.0482
Step 4	0.2183	0.2128	0.0490
Step 5	0.1565	0.1641	0.0578
Step 6	0.1223	0.1165	0.0776
Step 7	0.0720	0.0976	0.1038
Step 8	0.0466	0.0514	0.1388
Step 9	0.0156	0.0227	0.2089
Step 10–20	0.0000	0.0000	

**Table 4.9. The Results for an Annual Peak Load of 3050 MW**

	LOLE (hr/yr)	LOEE (MWh/yr)	Coefficient of variation for LOEE index
Index	30.4516	4379.6152	0.0189
<b>Contributions of Each Load Step (p.u.)</b>			
Step 1	0.0441	0.0437	0.0442
Step 2	0.1372	0.1103	0.0413
Step 3	0.1347	0.1208	0.0463
Step 4	0.2389	0.2155	0.0493
Step 5	0.1552	0.1701	0.0490
Step 6	0.1445	0.1525	0.0480
Step 7	0.0780	0.1084	0.0577
Step 8	0.0482	0.0494	0.0758
Step 9	0.0192	0.0293	0.1100
Step 10–20	0.0000	0.0000	

**(b) Derated State Case.** In this case, the derated states of the 350-MW and two 400-MW units are considered. The unit derating data are given in Table 4.2. The state probabilities for these generating units were obtained using their state space model and are shown in Table 4.10. The stopping rule is the same as that in the base case. The calculated results are given in Tables 4.11 and 4.12.

**Table 4.10. The State Probabilities of the Two Three-State Generating Units**

Unit size (MW)	State probability		
	up	50% derated	down
350	0.84616	0.07692	0.07692
400	0.89843	0.04688	0.05469

**Table 4.11. The Results Considering Derated States for the Annual Peak Load of 2850 MW**

	LOLE (hr/yr)	LOEE (MWh/yr)	Coefficient of variation for LOEE index
Index	5.4591	613.7520	0.0263
<b>Contributions of Each Load Step (p.u.)</b>			
Step 1	0.0704	0.0588	0.0440
Step 2	0.1840	0.1643	0.0467
Step 3	0.1728	0.1651	0.0490
Step 4	0.2304	0.2223	0.0532
Step 5	0.1489	0.1638	0.0764
Step 6	0.1073	0.1166	0.1052
Step 7	0.0582	0.0800	0.1502
Step 8	0.0280	0.0300	0.2626
Step 9–20	0.0000	0.0000	

**Table 4.12. The Results Considering Derated States for the Annual Peak Load of 3050 MW**

	LOLE (hr/yr)	LOEE (MWh/yr)	Coefficient of variation for LOEE index
Index	21.2280	2741.4656	0.0196
<b>Contributions of Each Load Step (p.u.)</b>			
Step 1	0.0573	0.0528	0.0472
Step 2	0.1655	0.1424	0.0443
Step 3	0.1543	0.1473	0.0448
Step 4	0.2432	0.2237	0.0490
Step 5	0.1461	0.1544	0.0498
Step 6	0.1227	0.1298	0.0495
Step 7	0.0658	0.0945	0.0751
Step 8	0.0311	0.0352	0.1140
Step 9	0.0140	0.0199	0.1695
Step 10–20	0.0000	0.0000	

## 4.4. MULTI-AREA GENERATING SYSTEM ADEQUACY ASSESSMENT— MAXIMUM FLOW ALGORITHM

The generating capacity adequacy of a power system can be improved by interconnecting the system to other power utilities. When the total available capacity in an area is insufficient to meet its load, assistance can be received from neighboring areas. The amount of assistance depends on the following four factors:

1. The load level of the supported area
2. The available generating capacities of the supporting areas
3. The tie line constraints
4. The import/export agreement between the areas

Two different fundamental approaches to deal with assistance between areas and tie line constraints are presented in this section and in the next section, respectively. The problem of import/export agreements is discussed in Section 4.6.

### 4.4.1. Basic Procedure

The multi-area generating system adequacy assessment approach described in this section is based on a combination of the state duration sampling method and the maximum flow algorithm.<sup>(13,14)</sup> It consists of the following general steps:

1. Construct a generating capacity model and an appropriate load model for each area.
2. Combine the generating capacity model and the load model to obtain an available capacity margin model for each area.
3. Incorporate the tie line network and the supporting policy, and calculate the reliability indices for each area and the total system.

Steps 1 and 2 have been clearly explained in Section 4.2. A tie line can also be simulated using state duration sampling to obtain the up-down-up operating cycles. Given an initial state, a chain of time to failure and time to repair can be generated by random samplings, which are similar to the simulation of a generating unit. The operating cycles of the tie lines and the available capacities of the tie lines are then used to modify the available capacity margin models for each area. This can be done using the maximum flow algorithm described in the next subsection.

The reference period, as in the case of a single system study, is 1 yr. Each sample year is divided into 8760 hr and therefore the time unit is 1 hr. The maximum flow algorithm is applied for all hourly points where at least one area has a negative capacity margin. A loss of load situation is considered to arise in an area when the available assistance through interconnections cannot offset the capacity deficiency of the area. Consequently, the available capacity margin model for each area can be modified. The reliability indices in each sample year, that is, the loss of load duration ( $LLD_i$ ) in hr, the loss of load occurrence ( $LLO_i$ ), and the energy not supplied ( $ENS_i$ ) in MWh for an area considering interconnections, can be obtained by observing the modified available capacity margin model of the area. The estimates of the area reliability indices in  $N$  sample years can be calculated using equations (4.1)–(4.3). The LOLE and LOEE indices reflecting the overall system reliability can be calculated using

$$LOLE_s = \frac{\sum_{i=1}^N LLD_{si}}{N} \quad (4.26)$$

and

$$LOEE_s = \frac{\sum_{k=1}^m \sum_{i=1}^N ENS_{ki}}{N} \quad (4.27)$$

where  $N$  is the number of sample years,  $m$  is the number of areas,  $LLD_{si}$  is the total system state duration when one or more areas are in the loss of load situation in sample year  $i$ , and  $ENS_{ki}$  is the energy not supplied of area  $k$  in sample year  $i$ .

#### 4.4.2. Modifying the Area Available Margin Model Using the Maximum Flow Algorithm

A multi-area generating system can be modeled by a transportation network with stochastic branch capacities.<sup>(8,13,14)</sup> A tie line is represented by a branch, which may be either unidirectional or bidirectional depending on the allowable orientation of power transfer. Each area is represented by a node. Two additional fictitious nodes are introduced: a generation source node  $s$  and a load sink node  $t$ . Node  $s$  is assumed to have an infinite installed capacity. A fictitious unidirectional branch from node  $s$  to each area node is introduced to represent the maximum available area assistance. A fictitious unidirectional branch from each area node to node  $t$  is created to represent the required supported demand. For simplicity, all the branches can be

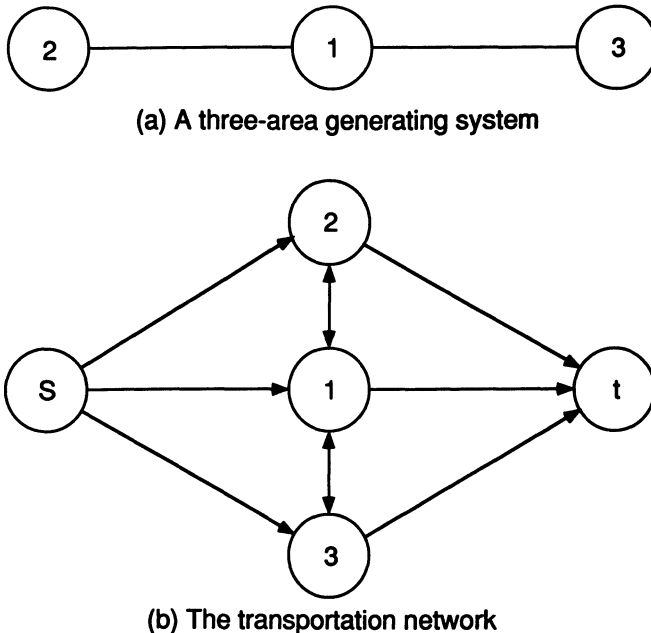


**Figure 4.19.** A three-area generating system and its transportation network.

assumed to be bi-directional and therefore a pair of capacities  $(C_{ij}, C_{ji})$  are associated with each branch  $(i, j)$ . For the unidirectional branches,  $C_{ij}=0$  or  $C_{ji}=0$ . Capacity  $C_{ij}$  is not necessarily equal to capacity  $C_{ji}$  for bidirectional branches. As an example, Figure 4.19 shows a three-area generating system and its transportation network.

The capacity pair of each branch  $(i, j)$  ( $i, j \neq s, t$ ) at a time point is either  $(C_{ij}, C_{ji})$  or  $(0, 0)$ , depending on the state of the corresponding tie line at that time point. If tie line  $(i, j)$  is in an operating state, the capacity of branch  $(i, j)$  is  $(C_{ij}, C_{ji})$ ; otherwise, it is  $(0, 0)$ . The capacity of each fictitious branch  $(s, i)$  or  $(i, t)$  at a time point is determined by the available capacity margin of area  $i$  ( $i \neq s, t$ ) at the time point. Let  $d_i$  denote the available capacity margin of area  $i$ ,  $C_{si}$  and  $C_{ti}$  are obtained by the following rules:

$$C_{si} = \begin{cases} d_i & \text{if } d_i > 0 \\ 0 & \text{if } d_i \leq 0 \end{cases} \quad (4.28)$$

and

$$C_{ti} = \begin{cases} -d_i & \text{if } d_i < 0 \\ 0 & \text{if } d_i \geq 0 \end{cases} \quad (4.29)$$

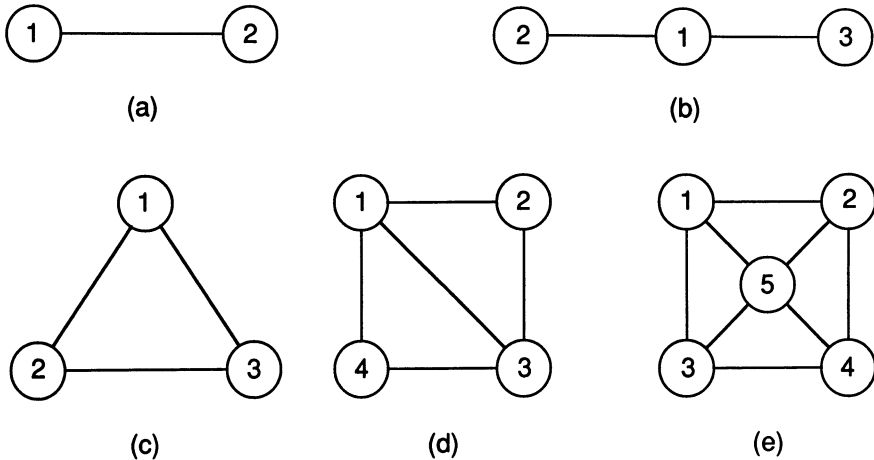


**Figure 4.20.** Five multi-area systems.

After the transportation network is constructed, the maximum flow algorithm, which is described in Appendix D.2, can be used to calculate supporting power. For a supported area  $i$ , a failure occurs when

$$x_{it} < -d_i$$

where  $x_{it}$  is the calculated supporting power for area  $i$ . The available capacity margin model of each area without considering interconnection can be modified in terms of the results obtained by the maximum flow algorithm.

It can be seen that the transportation network topology is fixed all the time. The only changeable item is the branch capacity  $C_{ij}$ , which is determined by the state of a tie line or the available capacity margin of an area. At a time point in a sampling year, where the available capacities of one or more area cannot meet the loads, the maximum flow algorithm is utilized to find the maximum available assistance for the supported areas.

### 4.4.3. Case Studies

In order to demonstrate the application of the maximum flow algorithm to multi-area generating system adequacy assessment, five multi-area configurations created by connecting identical IEEE RTSs are considered. These configurations are shown in Figure 4.20. Each area in Figure 4.20 is an IEEE RTS with 32 generating units. The annual peak load is 2850 MW.

**Table 4.13. Reliability Indices for the Two-Area System**

	LOLE (hr/yr)	LOEE (MWh/yr)	LOLF (occ./yr)
Area 1	4.534	542.696	0.9617
Area 2	4.542	535.751	0.9731
System	8.568	1078.457	

Each tie line is represented by a two-state model with  $MTTF = 4380$  hr and  $MTTR = 10$  hr. The capacity of each tie line is  $C_{ij} = C_{ji} = 100$  MW.

**(a) Two-Area System.** The estimated reliability indices for the two-area system are given in Table 4.13. The number of sample years is 10,000. Figures 4.21, 4.22, and 4.23 show the area LOLE, LOEE, and LOLF indices as functions of sample years, respectively. It can be observed from these figures that the rough location at which the estimated mean value begins to stabilize is about 2000 sample years. This can be compared to about 800 sample years in a single-area IEEE RTS study (see Figures 4.11, 4.12, and 4.13). The required simulation time for multi-area system analysis is normally longer than that required in single-area system studies. This is due to the fact that a multi-area system is more reliable than a single-area system.

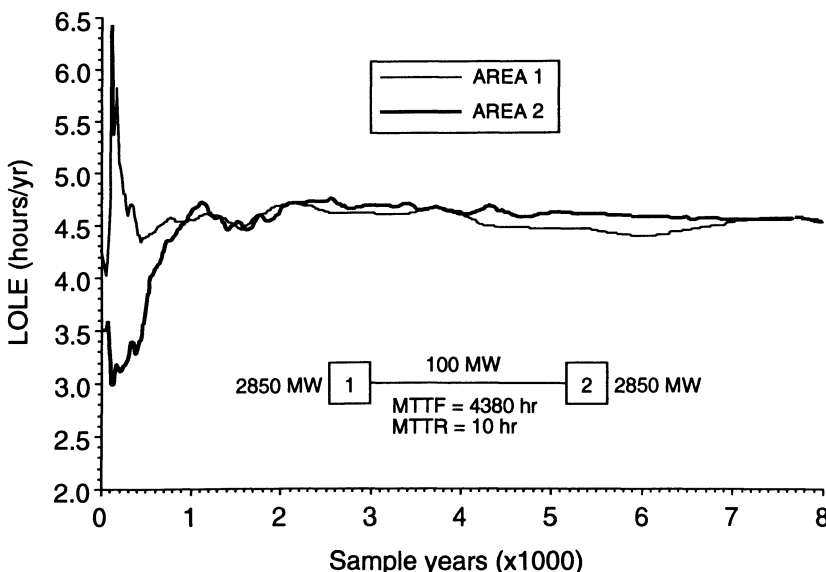


**Figure 4.21.** Area LOLE vs. the number of sample years.

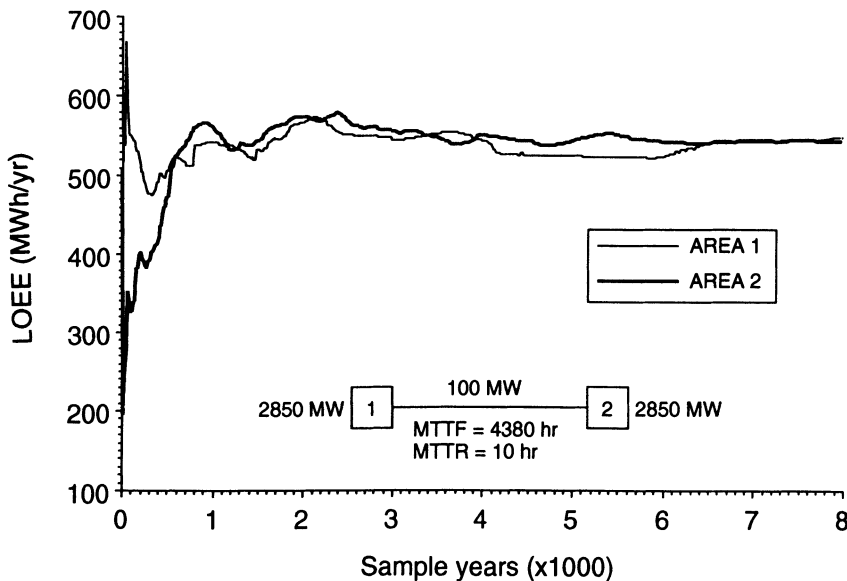


Figure 4.22. Area LOEE vs. the number of sample years.

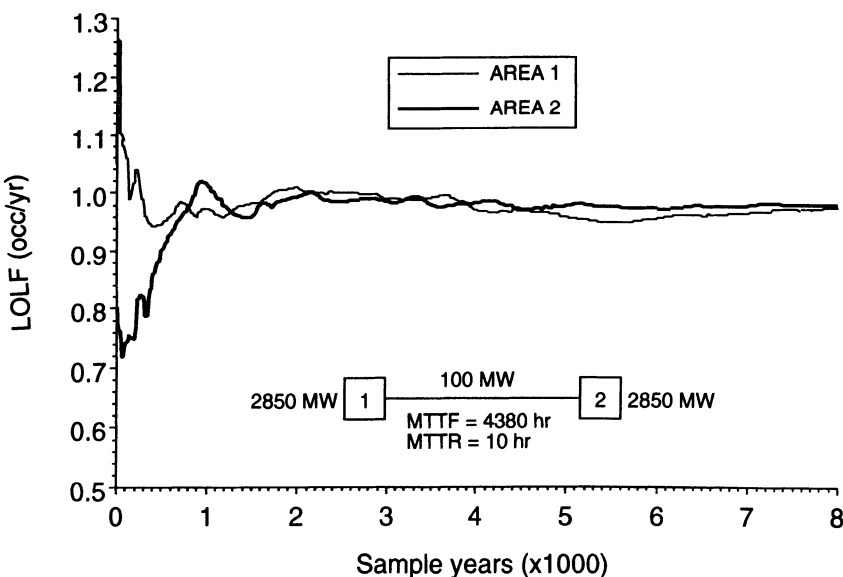


Figure 4.23. Area LOLF vs. the number of sample years.

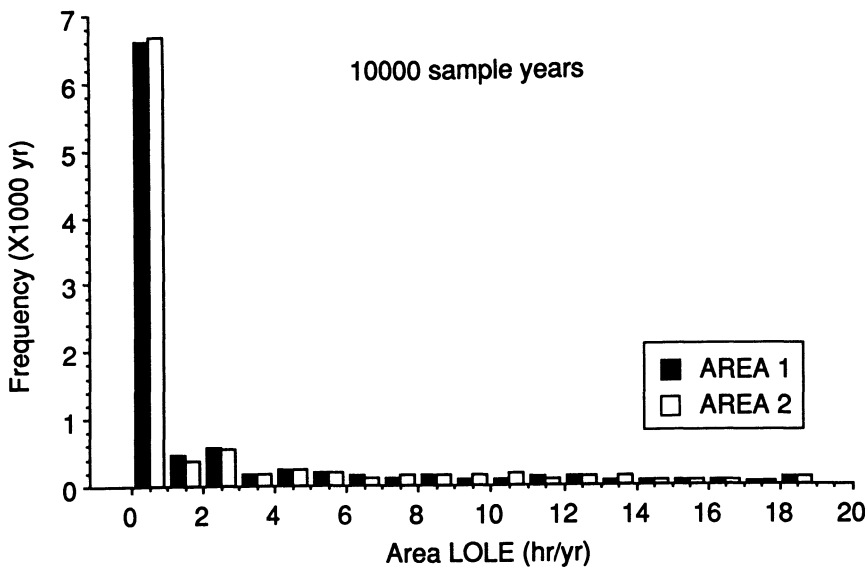


Figure 4.24. Distribution of the area LOLE index.

Figures 4.24, 4.25, and 4.26 show the distributions of the area LOLE, LOEE, and LOLF indices for a sampling period of 10,000 years.

**(b) Other Multi-Area Systems.** The multi-area systems shown in Figure 4.20b, c, d, and e were simulated using the maximum flow algorithm under the same conditions as those used for the two-area system but for the different configurations. The obtained reliability indices for 10,000 sample years for these four multi-area systems are shown in Tables 4.14, 4.15, 4.16, and 4.17, respectively.

## 4.5. MULTI-AREA GENERATING SYSTEM ADEQUACY ASSESSMENT—LINEAR PROGRAMMING MODEL

### 4.5.1. Basic Procedure

This section describes a method for multi-area generating system adequacy assessment based on a combination of the state sampling technique and a linear programming model.<sup>(15)</sup> The basic steps of the method can be

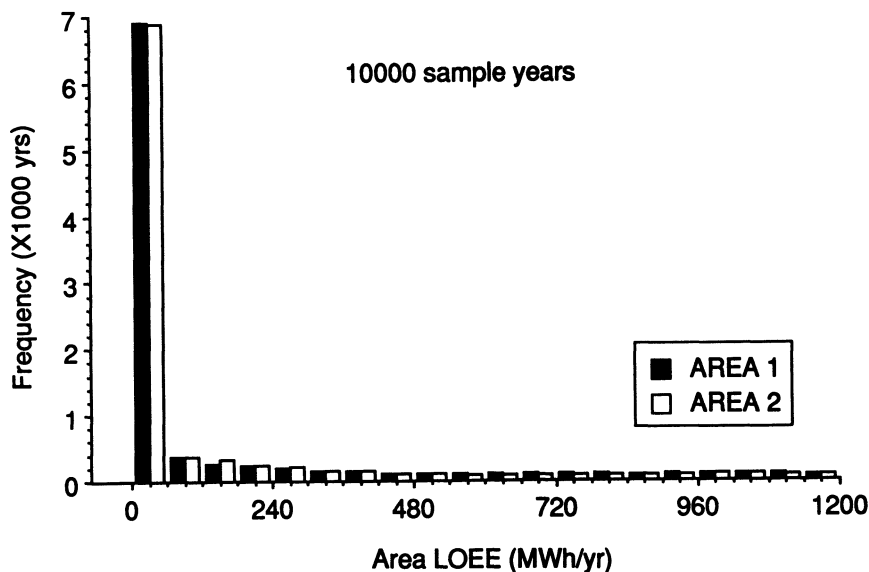


Figure 4.25. Distribution of the area LOEE index.

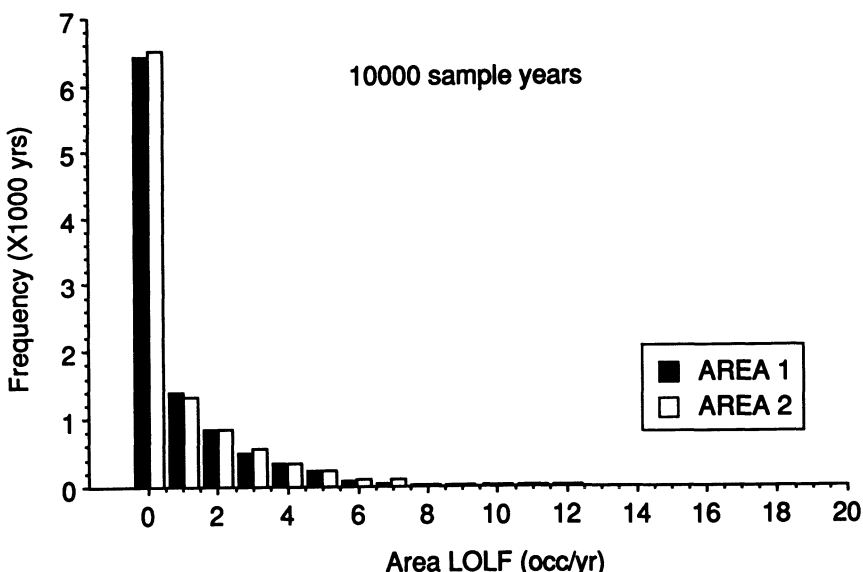


Figure 4.26. Distribution of the area LOLF index.

**Table 4.14. Reliability Indices for the Radially Connected Three-Area System**

	LOLE (hr/yr)	LOEE (MWh/yr)	LOLF (occ./yr)
Area 1	2.203	228.234	0.4700
Area 2	4.478	526.761	0.9626
Area 3	4.349	498.581	0.9546
System	10.629	1253.576	

**Table 4.15. Reliability Indices for the Delta-Connected Three-Area System**

	LOLE (hr/yr)	LOEE (MWh/yr)	LOLF (occ./yr)
Area 1	2.012	228.013	0.4549
Area 2	2.041	226.795	0.4607
Area 3	1.972	217.444	0.4530
System	5.888	672.252	

**Table 4.16. Reliability Indices for the Four-Area System**

	LOLE (hr/yr)	LOEE (MWh/yr)	LOLF (occ./yr)
Area 1	0.860	94.473	0.2030
Area 2	2.010	222.325	0.4518
Area 3	0.835	86.500	0.2028
Area 4	1.978	218.994	0.4467
System	5.568	622.291	

**Table 4.17. Reliability Indices for the Five-Area System**

	LOLE (hr/yr)	LOEE (MWh/yr)	LOLF (occ./yr)
Area 1	0.836	91.757	0.1951
Area 2	0.854	87.702	0.2050
Area 3	0.812	83.489	0.1957
Area 4	0.831	87.104	0.1971
Area 5	0.303	30.104	0.0808
System	3.557	380.156	

stated as follows:

1. Select a system state  $S = (S_1, S_2, \dots, S_n)$  by sampling techniques, where  $S_i$  is the state of the  $i$ th component. The set of  $n$  components includes the generating units in each area, the load levels of each area, and all the tie lines.
2. Evaluate a reliability index  $R(S)$  for system state  $S \in G$  by a linear programming model, where  $G$  denotes the set of all sampled system states and  $R(S)$  represents the selected reliability index for the overall system or each area.
3. Calculate the expected value of  $R(S)$  by

$$E(R) = \sum_{S \in G} R(S) \frac{n(S)}{N} \quad (4.30)$$

where  $N$  is the number of samples and  $n(S)$  is the number of occurrences of system state  $S$ .

The sampling technique used to select a generating unit state is described in Section 4.3.1. After all the generating unit states in each area are determined by sampling, a generation capacity level for the area can be obtained. A similar sampling technique can also be used to select the tie line states in a multi-area system. Selection of a load level state and the linear program model for multi-area reliability evaluation are discussed in the following sections.

#### 4.5.2. Load Model of a Multi-Area System

The load model of a multi-area system involves two phases. In the first step, the 8760 hourly load points representing a year are grouped into several clusters and the mean values of the load points for each area in each cluster obtained by the  $K$ -mean algorithm. In the second step, the area load uncertainty and correlation can be incorporated by a normal distribution sampling technique and a correlation sampling technique.

**(a) The  $K$ -Mean Algorithm.**<sup>(11,12)</sup> The  $K$ -mean algorithm described here is an extension to a multi-area system of the cluster technique for the single-area system given in Section 4.3.3. It therefore has the similar basic steps:

*Step 1:* Select initial values of cluster means  $M_{ij}$ , where  $i$  and  $j$  denote cluster  $i$  and area  $j$ .

*Step 2:* Calculate Euclidean distances from each hourly load point to each cluster mean by

$$D_{ki} = \left[ \sum_{j=1}^{NA} (M_{ij} - L_{kj})^2 \right]^{1/2} \quad (4.31)$$

where  $D_{ki}$  denotes the Euclidean distance from the  $k$ th load point to the  $i$ th cluster mean,  $L_{kj}$  the  $k$ th load value in the  $j$ th area, and  $NA$  is the number of areas.

*Step 3:* Regroup the points by assigning them to the nearest cluster and calculate the new cluster means by

$$M_{ij} = \frac{\sum_{k \in IC} L_{kj}}{NI_i} \quad (4.32)$$

where  $NI_i$  is the number of load points in the  $i$ th cluster and  $IC$  denotes the set of the load points in the  $i$ th cluster.

*Step 4:* Repeat Steps 2 and 3 until all cluster means maintain unchanged between iterations.

The cluster means  $M_{ij}$  are then used as the load levels for each area in each cluster. Each load level represents  $NI_i$  load points in the corresponding cluster in a mean value sense. Correlation between mean values of area load points in each cluster is captured in the  $K$ -mean algorithm. The captured correlation is approximate since it reflects correlative relation between cluster means. After the reliability indices for each cluster are calculated, annual reliability indices can be obtained by weighting the indices for each cluster by  $(NI_i/8760)$ .

**(b) Area Load Uncertainty and Correlation.** Load uncertainty and correlation always exist in an actual power system and it has long been recognized that they can have a great impact in power system reliability evaluation.

Load uncertainty can be modeled using a normal distribution and therefore it is necessary to draw normally distributed random numbers in order to simulate area load uncertainty. A normal distribution has two parameters: mean value and standard deviation. The mean values are the cluster means obtained by the  $K$ -mean algorithm and the standard deviation is assigned according to the perceived load forecast uncertainty, such as 5%. The normal distribution sampling techniques given in Section 3.4.5 can be used to create normally distributed random numbers.

If all the area loads are completely dependent, the cluster means of all the area loads are the same for a cluster. In this case, only one normally distributed random number is required for each cluster in order to determine

the load states of all areas. If all area loads are not completely dependent but are correlated to some extent, it is necessary to generate a normally distributed random vector for each cluster, in which each component corresponds to the load state of a particular area and whose components satisfy the correlation between the loads of different areas in the same cluster. The correlation matrix corresponding to each cluster can be calculated as follows.

According to the statistical definitions of variance, covariance, and correlation coefficient, the element of the correlation matrix corresponding to area  $n$  and area  $m$  for the  $i$ th cluster is

$$\rho_{nm} = \frac{(\sum_{k \in IC} L_{kn}L_{km}/NI_i) - M_{in}M_{im}}{[\sum_{k \in IC} (L_{kn} - M_{in})^2 \sum_{k \in IC} (L_{km} - M_{im})^2]^{1/2}/NI_i} \quad (4.33)$$

The covariance matrix  $C$  corresponding to the correlation matrix  $\rho$  can be obtained by

$$C = \begin{bmatrix} \sigma_1^2 \rho_{11} & \sigma_1 \sigma_2 \rho_{12} & \dots & \sigma_1 \sigma_n \rho_{1n} \\ \vdots & \vdots & \vdots & \vdots \\ \sigma_n \sigma_1 \rho_{n1} & \sigma_n \sigma_2 \rho_{n2} & \dots & \sigma_n^2 \rho_{nn} \end{bmatrix} \quad (4.34)$$

where  $\sigma_i$  is the standard deviation for the  $i$ th area load uncertainty. The same standard deviation is usually assumed for all area loads. In this case, equation (4.34) is simply written as

$$C = \sigma^2 \rho \quad (4.35)$$

After the covariance matrix  $C$  between area loads for each cluster is obtained, the following load correlation sampling technique can be used to simulate area load uncertainty and correlation.

Let  $H$  be an NA (number of areas) dimensional normally distributed random vector with mean vector  $B$  and covariance matrix  $C$ . Let  $G$  be an NA dimensional normally distributed random vector whose components are independent of each other and each component has a mean of zero and a variance of unity. Linear combination of normal distributions is still a normal distribution. There exists therefore a matrix  $A$  which can create the following transformation relationship between  $H$  and  $G$ <sup>(16)</sup>:

$$H = AG + B \quad (4.36)$$

The mean value vector  $B$  and the covariance matrix  $C$  of  $H$  can be calculated from equation (4.36) as follows:

$$E(H) = AE(G) + B = A0 + B = B \quad (4.37)$$

$$E[(H - B)(H - B)^T] = E(AGG^TA^T) = AA^T = C \quad (4.38)$$

Equation (4.38) gives the relation between matrix  $A$  and matrix  $C$ . On the other hand, covariance matrix  $C$  is a nonnegative definite symmetric matrix and therefore matrix  $C$  can be triangularized into the unique lower triangular matrix multiplied by its transposed matrix. Consequently, in the following equation,

$$C = AA^T \quad (4.39)$$

where  $A$  is a lower triangular matrix. As a result, the following recursive formulas can be derived from equation (4.39) to calculate the elements of matrix  $A$  from those of matrix  $C$ :

$$A_{ii} = \frac{C_{ii}}{(C_{11})^{1/2}} \quad (1 \leq i \leq NA) \quad (4.40)$$

$$A_{ii} = \left( C_{ii} - \sum_{k=1}^{i-1} A_{ik}^2 \right)^{1/2} \quad (1 < i \leq NA) \quad (4.41)$$

$$A_{ij} = \frac{C_{ij} - \sum_{k=1}^{j-1} A_{ik} A_{jk}}{A_{jj}} \quad (1 < j < i \leq NA) \quad (4.42)$$

The area load correlation sampling technique can be summarized in the following steps:

- Step 1:* Calculate the area load covariance matrix  $C$  according to equations (4.33) and (4.34) from the information obtained by the  $K$ -mean algorithm.
- Step 2:* Calculate the low triangular matrix  $A$  according to equations (4.40)–(4.42).
- Step 3:* Draw an NA dimensional, normally distributed random vector  $G$ . All its components have a mean of zero and a variance of unity.
- Step 4:* Create an NA dimensional correlative normally distributed random vector  $H$  from equation (4.36) in which  $B$  is a mean value vector whose components are the cluster means. Both area load uncertainty and the correlation defined by matrix  $C$  are included in the random vector  $H$ .

### 4.5.3. Linear Programming Model for Multi-Area Reliability Evaluation

After the area generating capacity levels, area load states, and tie line states are selected using the sampling techniques described earlier, it is necessary to evaluate the reliability indices of the selected multi-area system state.

All areas can be divided into two sets of supporting and supported areas. In the supporting set, the available area generating capacity is larger than the area load. A “generator variable” is defined for each area in the supporting set. The upper limit of each “generator variable” is the difference between the available area generating capacity and the area load. In the supported set, the available area generating capacity is smaller than the area load. A “required load” is defined for each area in the supported set, which equals the difference between the area load and the available area generating capacity. A “fictitious generator variable” is also defined for each area in the supported set. When the “required load” at each area cannot be completely satisfied due to the insufficient total available generating capacity in the supporting set or/and limits of tie line capacities, the “fictitious generator variables” can provide the unsatisfied parts of the “required load” such that power balance in each area is always guaranteed. Essentially, the “fictitious generator variables” are load curtailment variables in the supported areas and therefore the upper limit of each “fictitious generator variable” is assigned as the relative “required load.”

The “generator variables,” the “fictitious generator variables,” the “required loads,” and tie lines constitute a new small “generation–transmission” system. The basic objective is to minimize the total load curtailment while satisfying the power balance at each node (area) and upper limits of the tie line capacities, the “generator variables,” and the “fictitious generator variables.” The following linear programming model can be used for this purpose:

$$\min \sum_{i \in ND} \alpha_i GF_i \quad (4.43)$$

subject to

$$\sum_{j \rightarrow i} TP_j + GP_i = 0 \quad (i \in NG) \quad (4.44)$$

$$\sum_{j \rightarrow i} TP_j + GF_i = DP_i \quad (i \in ND) \quad (4.45)$$

$$|TP_j| \leq T_j^{\max} \quad (j \in NT) \quad (4.46)$$

$$0 \leq GP_i \leq SP_i \quad (i \in NG) \quad (4.47)$$

$$0 \leq GF_i \leq DP_i \quad (i \in ND) \quad (4.48)$$

where  $GP_i$  and  $GF_i$  denote the “generator variables” and the “fictitious generator variables” at the  $i$ th node, respectively; “ $j \rightarrow i$ ” indicates that  $j$  belongs to the line set in which all lines are connected to node  $i$ ;  $TP_j$  is the tie line power on line  $j$  and it is positive when entering node  $i$  and negative

when issuing from node  $i$ ;  $DP_i$  is the “required load” at the  $i$ th node;  $SP_i$  is the upper limit of the  $i$ th “generator variable”;  $T_j^{\max}$  is the capacity limit of the  $j$ th tie line;  $NG$ ,  $ND$ , and  $NT$  are the sets of the “generator variables,” the “fictitious generator variables,” and tie lines, respectively;  $\alpha_i$  is the weighting factor for the  $i$ th “fictitious generator variable.”

There is a wide variety of possible supporting policies in multi-area generating system reliability assessment. One advantage of a linear programming model such as that described is that variable supporting policies can be easily incorporated. Different supporting policies and their effects are discussed in Section 4.6. A priority order supporting policy which is most commonly used, is considered first. This can be incorporated by assigning different values of weighting factors  $\alpha_i$ . The supported area with the first priority has a maximum value of  $\alpha_i$ , the supported area in the next priority has a second maximum value of  $\alpha_i$ , etc. These values of  $\alpha_i$  are specified in terms of their relative magnitudes and therefore it is easy to select these values.

Another advantage of the linear programming model is that the LOEE sensitivity indices of both system and area to area generation and tie line capacities can be calculated. These sensitivity indices can provide information about which tie line or which area generation capacity should be reinforced from an overall system and each area point of view. It should be noted that it is not possible to obtain the area sensitivity indices merely by using the concept of dual variables. Calculation of the area sensitivity indices can be explained as follows. For a standard linear programming problem

$$\min C^T X \quad (4.49)$$

subject to

$$AX = b \quad (4.50)$$

$$X \geq 0 \quad (4.51)$$

its optimal and feasible solution can be expressed by

$$X_b = B^{-1}b \quad (4.52)$$

where  $B$  is the optimal basis at the optimal and feasible solution and  $X_b$  is the basic variable subvector. The value of  $B$  will remain unchanged if the right-hand term  $b$  has a sufficiently small change. Therefore

$$\Delta X_b = B^{-1} \Delta b \quad (4.53)$$

which means

$$\frac{\partial(X_b)_i}{\partial b_j} = (B^{-1})_{ij} \quad (4.54)$$

where  $(B^{-1})_{ij}$  is the element of  $B^{-1}$ .

Equation (4.54) indicates that the elements in the optimal basis are the sensitivities of the basic variables to the elements in the right-hand term of the constraints. Area sensitivity indices to area generations and tie line capacities can therefore be obtained by solving the linear programming model expressed by equations (4.43)–(4.48). The basic concepts and solution techniques of linear programming are given in Appendix D.1 for the convenience of the reader.

#### 4.5.4. Case Studies

**(a) The Test System.** A four-area system shown in Figure 4.27 is considered as the test system. Area 1 is the basic IEEE RTS. The annual peak load is 2850 MW. Areas 2, 3, and 4 are three modified RTSs. The modifications are as follows:

Area 2: Three 197-MW generators are removed and the annual peak load is reduced to 2280 MW.

Area 3: One 800-MW generator with forced unavailability  $FU=0.18$  is added and the annual peak load is increased to 3575 MW.

Area 4: One 800-MW generator with  $FU=0.18$  and one 600-MW generator with  $FU=0.15$  are added and the annual peak load is increased to 4180 MW.

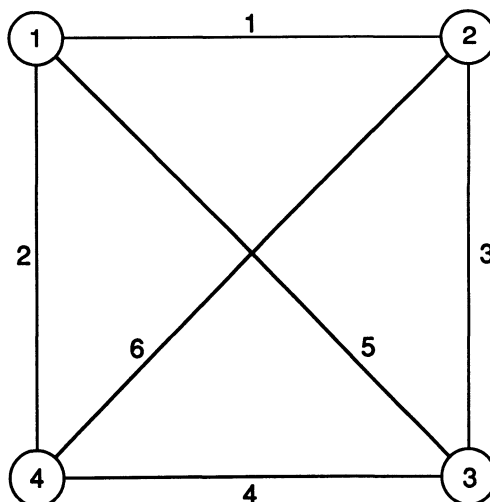


Figure 4.27. A four-area generating system.

**Table 4.18. The Tie Line Data of the Test System**

No.	From area to area	Capacity (MW)	FU
1	1–2	100	0.0005
2	1–4	200	0.0005
3	2–3	100	0.0005
4	3–4	200	0.0005
5	1–3	200	0.0005
6	2–4	200	0.0005

The tie line data are given in Table 4.18.

When the area loads are considered to be completely dependent, the same annual load curve data of the IEEE RTS given in Appendix A.1 are applied to the four areas. When correlation between area loads (noncompletely dependent) is considered, the area load curve in Area 1 remains unchanged and the area load curves in Areas 2, 3, and 4 were obtained by displacing the hourly load values of Area 2 ahead by 4 hr, those of Area 3 ahead by 2 hr, and those of Area 4 backward by 2 hr, respectively.

In order to include generating unit derated states, the 350-MW and the two 400-MW generators were derated to 50% capacity with the derated state probabilities given in Table 4.10. The state probabilities of the derated models are such that the derating-adjusted two-state model data are identical to those given in Appendix A.1. The specified supported priority order is: Area 4–Area 3–Area 2–Area 1.

**(b) LOLE and LOEE Indices.** The following eight cases were studied:

*Case 1:* Completely dependent area loads, no load uncertainty, and no generating unit derated states.

*Case 2:* Correlation between area loads, no load uncertainty, and no generating unit derated states.

*Case 3:* Completely dependent area loads, load uncertainty (5% standard deviation), and no generating unit derated states.

*Case 4:* Correlation between area loads, load uncertainty (5% standard deviation), and no generating unit derated states.

Cases 5 to 8 correspond to Cases 1 to 4, respectively, with the difference that derated states of 50% capacity for the 350-MW and the two 400-MW generators in each area are included.

One 20-step load model was created using the *K*-mean algorithm to represent the annual load curve in the cases of completely dependent area loads while four 20-step load models for the four areas were created when

correlation between area loads was considered. The stopping rule used in the studies is that the simulation in one load level step ends when either 16,000 samples of the system states have been simulated or the coefficient of variation for the system LOEE is less than 0.1. The results for these studies are shown in Tables 4.19–4.22.

It can be seen from the results in Tables 4.19 to 4.22 that the indices in the cases of completely dependent area loads are larger than those in the cases of correlation between area loads under the same conditions of load uncertainty and/or generating unit derated states. Area load uncertainty can

**Table 4.19. LOLE Indices for Cases 1 to 4 (hr/yr)**

	Case 1	Case 2	Case 3	Case 4
Area 1	0.5200	0.1856	1.5071	0.5683
Area 2	0.6572	0.2879	1.2968	0.5493
Area 3	4.6784	3.2533	6.8250	4.6746
Area 4	6.7150	5.6493	9.9241	8.1607
System	11.6947	9.0490	17.1283	13.3346

**Table 4.20. LOEE Indices for Cases 1 to 4 (MWh/yr)**

	Case 1	Case 2	Case 3	Case 4
Area 1	48.5333	11.2750	212.6279	61.2335
Area 2	73.9207	18.0256	162.8383	32.2251
Area 3	736.5811	388.3348	1222.5161	648.8776
Area 4	1309.9360	1064.9319	1972.3239	1501.6836
System	2168.9714	1482.5678	3570.3071	2244.0203

**Table 4.21. LOLE Indices for Cases 5 to 8 (hr/yr)**

	Case 5	Case 6	Case 7	Case 8
Area 1	0.1626	0.0413	0.8033	0.2745
Area 2	0.5423	0.2879	1.0867	0.4558
Area 3	2.1571	1.0869	3.7754	2.2162
Area 4	3.1756	2.4964	5.1385	4.3451
System	5.7332	3.8505	9.3108	6.9754

**Table 4.22. LOEE Indices for Cases 5 to 8 (MWh/yr)**

	Case 5	Case 6	Case 7	Case 8
Area 1	18.5329	2.4349	115.8170	26.6675
Area 2	53.7787	18.9414	133.9687	29.9503
Area 3	298.2609	106.2488	608.0114	262.7329
Area 4	532.6486	391.9146	1010.1765	694.6565
System	903.2213	519.5398	1867.9736	1014.0071

**Table 4.23. LOEE Sensitivity Indices of System and Areas to Area Generation and Tie Line Capacities in Case 1 (MWh/yr/MW)**

	Area 1	Area 2	Area 3	Area 4	System
Area 1	-0.5154	-0.0087	-0.1747	-0.0699	-0.7688
Area 2	-0.0175	-0.6552	-0.0437	-0.0349	-0.7513
Area 3	-0.1048	-0.0262	-4.6738	-0.0699	-4.8747
Area 4	-0.0699	-0.1048	-0.5416	-6.7093	-7.4256
Line 1	-0.3407	-0.5591	-0.0437	-0.0699	-1.0134
Line 2	-0.2097	-0.0786	-0.3145	-6.4035	-7.0063
Line 3	-0.0874	-0.5591	-4.4554	-0.1136	-5.2154
Line 4	-0.0087	-0.0699	-3.6953	-6.1239	-9.8979
Line 5	-0.1485	-0.0087	-4.1758	-0.0000	-4.3331
Line 6	-0.0437	-0.4543	-0.4630	-6.6132	-7.5741

have a great impact on the calculated reliability indices and always provides a more pessimistic appraisal of multi-area system reliability. Utilization of derated state models for large-capacity generating units provides a more optimistic estimation of multi-area system reliability compared to the utilization of a derating-adjusted two-state model.

**(c) Sensitivity Indices.** The LOEE sensitivity indices for Cases 1 to 4 are listed in Tables 4.23 to 4.26. It should be noted that Area No. or “System” in the first row corresponds to incremental variations of LOEE in the sensitivity indices, while Area No. or Line No. in the first column corresponds to incremental variations of area generations or tie line capacities. For example, the value -0.1747 in the second row and the fourth column indicates that if the generation of Area 1 is increased by 1 MW, the LOEE index of Area 3 is decreased by 0.1747 MWh/year.

**Table 4.24. LOEE Sensitivity Indices of System and Areas to Area Generation and Tie Line Capacities in Case 2 (MWh/yr/MW)**

	Area 1	Area 2	Area 3	Area 4	System
Area 1	-0.1835	-0.0000	-0.0961	-0.0349	-0.3145
Area 2	-0.0000	-0.2796	-0.0000	-0.0000	-0.2796
Area 3	-0.0612	-0.0000	-3.2498	-0.0000	-3.3109
Area 4	-0.0349	-0.0349	-0.2883	-5.6435	-6.0016
Line 1	-0.1835	-0.2621	-0.0000	-0.0000	-0.4455
Line 2	-0.0786	-0.0349	-0.1922	-5.5212	-5.8269
Line 3	-0.0612	-0.2621	-3.2323	-0.0349	-3.5905
Line 4	-0.0175	-0.0349	-2.7693	-5.4600	-8.2817
Line 5	-0.0612	-0.0000	-3.0489	-0.0000	-3.1100
Line 6	-0.0350	-0.2184	-0.2883	-5.6260	-6.1676

**Table 4.25. LOEE Sensitivity Indices of System and Areas to Area Generation and Tie Line Capacities in Case 3 (MWh/yr/MW)**

	Area 1	Area 2	Area 3	Area 4	System
Area 1	-1.5026	-0.0524	-0.4543	-0.4106	-2.4199
Area 2	-0.1310	-1.2929	-0.2184	-0.3320	-1.9743
Area 3	-0.3145	-0.1398	-6.8228	-0.2359	-7.5130
Area 4	-0.2970	-0.2883	-1.1532	-9.9241	-11.6626
Line 1	-0.8649	-0.8387	-0.0961	-0.1747	-1.9743
Line 2	-0.4717	-0.2009	-0.5766	-8.8059	-10.0551
Line 3	-0.1660	-0.7688	-5.8706	-0.2184	-7.0237
Line 4	-0.1223	-0.2097	-4.7349	-8.6312	-13.6981
Line 5	-0.4543	-0.0437	-5.3639	-0.0349	-5.8968
Line 6	-0.1747	-0.5242	-0.8125	-9.2077	-10.7191

**Table 4.26. LOEE Sensitivity Indices of System and Areas to Area Generation and Tie Line Capacities in Case 4 (MWh/yr/MW)**

	Area 1	Area 2	Area 3	Area 4	System
Area 1	-0.5678	-0.0000	-0.0262	-0.0524	-0.6465
Area 2	-0.0000	-0.5416	-0.0000	-0.0262	-0.5678
Area 3	-0.1310	-0.0262	-4.6738	-0.0262	-4.8572
Area 4	-0.0349	-0.1048	-0.1922	-8.1594	-8.4914
Line 1	-0.5329	-0.5416	-0.0000	-0.0262	-1.1007
Line 2	-0.3145	-0.1048	-0.1660	-7.7925	-8.3778
Line 3	-0.1310	-0.4892	-4.5078	-0.0524	-5.1805
Line 4	-0.1136	-0.0786	-4.2020	-7.8275	-12.2217
Line 5	-0.3494	-0.0262	-4.4816	-0.0000	-4.8572
Line 6	-0.0349	-0.3757	-0.1922	-8.0721	-8.6749

It can be seen from the results in Tables 4.23 to 4.26 that although the values of the sensitivity indices are different in the various cases considering completely dependent area loads or correlation between area loads and area load uncertainty or no load uncertainty, their ranking order in these cases are basically the same. On the other hand, the ranking order of the sensitivity indices for the overall system and each area are different. From the overall system point of view, the best choice is to reinforce Tie-line 4, followed by Tie-line 6 and the generating capacity in Area 4. From an Area 4 point of view, the best choice is to reinforce the generating capacity in Area 4, followed by Tie-lines 6 and 2. From an Area 3 point of view, the best choice is to reinforce the generating capacity in Area 3, followed by Tie-lines 3 and 5. From an Area 2 point of view, the best choice is to reinforce the generating capacity in Area 2, followed by Tie-lines 1 and 3. From an Area 1 point of view, the best choice is to reinforce the generating capacity in Area 1, fol-

lowed by Tie-line 1. Increasing the generating capacity of each area naturally has the greatest impact on improving the reliability of each area itself. It is interesting to note that for the overall system, the first choice should be to reinforce two tie lines instead of increasing the generating capacity of the multi-area system.

## **4.6. DIFFERENT SUPPORTING POLICIES IN MULTI-AREA GENERATING SYSTEM ADEQUACY ASSESSMENT**

A power system pool or interconnected system configuration is usually represented by a group of areas each of which is associated with a specific utility company or a jointly owned generation facility. It is therefore important to calculate area indices which indicate area reliability. In order to obtain realistic area indices, a supporting policy must be clearly specified. Different supporting policies can lead to different area indices and therefore a different appreciation of area reliability. This section discusses how to incorporate different supporting policies into the linear programming model presented in Section 4.5.3 and examines their effects in multi-area generating system adequacy assessment.<sup>(17)</sup>

### **4.6.1. Incorporation of Different Supporting Policies**

There is a wide variety of supporting policies. A firm interchange contract can be considered by adjusting the area load levels and the relative tie line capacity. The following two basic emergency action philosophies can be used in a loss-of-load situation.

- The load loss sharing philosophy: Each area shares the unserved demand according to a supporting policy, recognizing tie line constraints.
- The no-load-loss sharing philosophy: Each area attempts to meet its own demand. If there is excess capacity, it is supplied to supported areas in accordance with an agreed supporting policy.

The basic emphasis here is not on the fundamental difference between these two philosophies but on the effects due to possible variations of supporting policies which can be used in both philosophies. Different supporting policies will lead to different area reliability evaluation even if the same

basic philosophy is used. The linear programming model presented earlier corresponds to the general no-load-loss sharing philosophy. In the case of the loss-load sharing philosophy, the required linear programming model has the same mathematical form but it is necessary to define “generator variables” and “required loads” at both supporting and supported area sets. The following discussion therefore applies to both philosophies. Four supporting policies are specifically considered but additional supporting policies can be introduced by similar techniques.

**(a) Priority Order Policy.** This supporting policy has been described in Section 4.5.3. A priority order can be considered by assigning different values of the weighting factors  $\alpha_i$  in equation (4.43).

**(b) Shortest Distance Policy.** This supporting policy states that excess capacities in supporting areas should be supplied to the nearest supported areas first. It also states that line power losses caused by supporting power flowing on tie lines are minimized. In order to incorporate this supporting policy, lengths of tie lines must be included in the input data. The objective function given in equation (4.43) is changed into equation (4.55):

$$\min \sum_{j \in NT} \beta_j |TP_j| + \alpha \sum_{i \in ND} GF_i \quad (4.55)$$

where  $\beta_j$  denotes the perceived length (in km or mile) of the  $j$ th tie line and the value of  $\alpha$  satisfies

$$\alpha \gg \max_{j \in NT} \{\beta_j\}$$

Equations (4.44) and (4.45) guarantee power balance at each area. Selecting a large value of  $\alpha$  in equation (4.55) guarantees that load curtailments will be zero if avoidable or minimized if unavoidable. Introduction of the first term in equation (4.55) enables the supporting power to trace the shortest path.

**(c) Priority Order Plus Path Order Policy.** This supporting policy includes two conditions: (a) excess capacities in a supporting area set are supplied to supported areas according to a specified priority; (b) when supporting power cannot directly reach the privileged supported

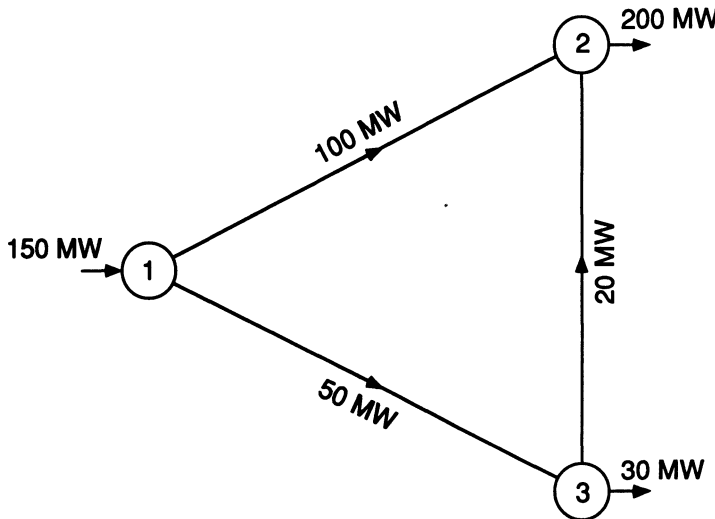


**Figure 4.28.** Explanation of supporting policy 3.

area due to tie line capacity limits, it should be supplied to supported areas according to the path order. A simple example is given to illustrate this policy. As shown in Figure 4.28, Area 1 has excess capacity of 150 MW while Areas 2 and 3 have shortage capacities of 200 MW and 30 MW, respectively.

The capacity limit of each tie line is 100 MW. Area 2 is assumed to have the supported privilege. According to Condition (a), 100 MW flows directly from Area 1 to Area 2. According to Condition (b), another 50 MW flows from Area 1 to Area 3 and then 30 MW are left for Area 3 while the remaining 20 MW supports Area 2.

In order to incorporate this supporting policy into the linear programming model, the tie line set NT is divided into three subsets of NT<sub>1</sub>, NT<sub>2</sub>, and NT<sub>3</sub>. The lines connecting two supporting areas belong to NT<sub>1</sub>, those connecting one supporting area and one supported area belong to NT<sub>2</sub>, and those connecting two supported areas belong to NT<sub>3</sub>. The objective function given in equation (4.43) is changed into equation (4.56):

$$\min \sum_{j \in NT_1} \beta_j |TP_j| + \sum_{k \in NT_2} \beta_k |TP_k| + \sum_{m \in NT_3} \beta_m |TP_m| + \sum_{i \in ND} \alpha_i GF_i \quad (4.56)$$

The coefficients in the new objective function (4.56) meet the following four requirements:

1.  $\beta_j = 0$  ( $j \in NT_1$ ).

2. The value of  $\beta_k$  ( $k \in NT_2$ ) are specified in such a way that  $\beta_k$  of the lines connecting the first priority supported area have minimum values, those connecting the second priority supported area have the second minimum values, etc.
3. The values of  $\beta_m$  ( $m \in NT_3$ ) satisfy

$$\min_{m \in NT_3} \{\beta_m\} > \max_{k \in NT_2} \{\beta_k\}$$

4. The values of  $\alpha_i$  are specified using the same principle as in the priority order policy and satisfy

$$\min_{i \in ND} \{\alpha_i\} \gg \max_{m \in NT_3} \{\beta_m\}$$

The priority order plus path order policy can be implemented automatically in the linear programming approach by selecting the coefficients which meet the four requirements.

**(d) Proportional Policy.** This supporting policy includes two aspects:

1. In those states where the total excess capacity in the supporting areas is larger than the total shortage capacity in the supported areas, the shortage capacity of each supported area can be compensated despite the supporting priority and path if the tie lines are capable of transmitting the supporting power. In other words, the area load curtailment depends only on the tie line capacity limits. The objective function given in equation (4.43) is changed into equation (4.57):

$$\min \alpha \sum_{i \in ND} GF_i \quad (4.57)$$

This means that each supported area has an equal opportunity for load curtailment in the objective function. Whether load curtailments occur depends only on the constraints expressed by equation (4.46).

2. In those states where the total excess capacity in the supporting areas is smaller than the total shortage capacity in the supported areas, load curtailments are unavoidable. A proportional curtailment principle can be designed. The supporting-supported ratio principle is used here and other possible proportional principles can be treated similarly. Each load curtailment variable  $GF_i$  is divided into two subvariables which are expressed by  $GF_{i1}$  and  $GF_{i2}$  and have different weighting factors in the objective function and different upper limits in the constraints. The linear programming model

given by equations (4.43) to (4.48) is changed into

$$\min \alpha \sum_{i \in ND} GF_{i1} + \sum_{i \in ND} \beta_i GF_{i2} \quad (4.58)$$

subject to

$$\sum_{j \rightarrow i} TP_j + GP_i = 0 \quad (i \in NG) \quad (4.59)$$

$$\sum_{j \rightarrow i} TP_j + \sum_{k=1}^2 GF_{ik} = DP_i \quad (i \in ND) \quad (4.60)$$

$$|TP_j| \leq T_j^{\max} \quad (j \in NT) \quad (4.61)$$

$$0 \leq GP_i \leq SP_i \quad (i \in NG) \quad (4.62)$$

$$0 \leq GF_{i1} \leq DP_i R \quad (i \in ND) \quad (4.63)$$

$$0 \leq GF_{i2} \leq DP_i(1 - R) \quad (i \in ND) \quad (4.64)$$

where  $R$  denotes the supporting-supported ratio which is defined as

$$R = \frac{\sum_{i \in NG} SP_i}{\sum_{i \in ND} DP_i} \quad (4.65)$$

$GF_{i1}$  corresponds to the portion which can be compensated when tie line capacity limits are not reached, and  $GF_{i2}$  the portion which may be supplementarily compensated in the case that  $GF_{i1}$  cannot be compensated in some areas because of tie line capacity limits;  $\alpha$  and  $\beta_i$  satisfy

$$\alpha > \max_{i \in ND} \{\beta_i\}$$

Such a selection guarantees that the total excess capacity attempts to compensate each supported area in terms of the proportion  $R$ . If this cannot be reached because of tie line limits, the surplus capacity can compensate parts reflected in the proportion  $(1 - R)$ .

## 4.6.2. Case Studies

Studies were conducted using two test systems. Test System 1 is shown in Figure 4.27 and all data are given in Section 4.5.4. Test System 2 is obtained by modifying Test System 1 in such a way that it has relatively low generation reserve margin and relatively high tie line capacity limits:

**Table 4.27. The Tie Line Data for the Two Systems**

No.	From area to area	Length (km)	Capacity (MW)		
			System 1	System 2	FU
1	1-2	100	100	100	0.0005
2	1-4	250	200	300	0.0005
3	2-3	100	100	200	0.0005
4	3-4	250	200	300	0.0005
5	1-3	150	200	200	0.0005
6	2-4	300	200	300	0.0005

- Modification 1: The annual peak loads of Areas 1 and 2 are increased to 3000 MW and 2500 MW, respectively.
- Modification 2: The tie line capacities are modified as shown in Table 4.27.

The following four cases were studied for both test systems. The reliability index selected for these studies is the Loss Of Energy Expectation (LOEE).

- Case 1: Completely dependent area loads and no load uncertainty
- Case 2: Correlation between area loads and no load uncertainty
- Case 3: Completely dependent area loads and load uncertainty (5% standard deviation)
- Case 4: Correlation between area loads and load uncertainty (5% standard deviation)

In each case, the four supporting policies presented in the previous subsection were considered. The specified supported priority is: Area 4–Area 3–Area 2–Area 1. The stopping rule for the simulation is the same as that used in Section 4.5.4.

It can be seen from the results in Tables 4.28 to 4.35 that considering load uncertainty provides a higher estimate of system and area reliability indices while considering correlation between area loads can lead to a lower estimate of these indices. This impact is greater on Test System 2, which has a lower generation reserve margin compared to Test System 1. Different supporting policies create the same system indices, but they can provide different area reliability indices depending on tie line parameters and configurations. The area indices due to different supporting policies are quite close for Test System 1 and have relatively large differences for Test System 2. This is caused by the fact that Test System 2 has higher tie line capacities and therefore different supporting situations are less constrained by the tie lines. When the tie lines have low capacities, such as in the case of Test

**Table 4.28. LOEE Indices in Case 1 for Test System 1 (MWh/yr)**

	Supporting policies			
	(a)	(b)	(c)	(d)
Area 1	48.5333	15.8760	18.9144	37.2703
Area 2	73.9207	61.0366	61.1564	58.2003
Area 3	736.5811	662.6406	674.6348	665.7415
Area 4	1309.9360	1429.4180	1414.2658	1407.7592
System	2168.9714	2168.9714	2168.9714	2168.9714

**Table 4.29. LOEE Indices in Case 2 for Test System 1 (MWh/yr)**

	Supporting policies			
	(a)	(b)	(c)	(d)
Area 1	11.2750	1.0111	1.0111	6.5628
Area 2	18.0256	16.6377	16.6377	15.0702
Area 3	388.3348	353.2820	361.5459	361.0461
Area 4	1064.9319	1111.6367	1103.3728	1099.8884
System	1482.5678	1482.5678	1482.5678	1482.5678

**Table 4.30. LOEE Indices in Case 3 for Test System 1 (MWh/yr)**

	Supporting policies			
	(a)	(b)	(c)	(d)
Area 1	212.6279	91.9890	109.3441	136.7954
Area 2	162.8382	101.7723	121.9547	110.0646
Area 3	1222.5161	1099.6311	1155.6234	1098.3940
Area 4	1972.3239	2276.9138	2183.3840	2225.0520
System	3570.3071	3570.3071	3570.3071	3570.3071

**Table 4.31. LOEE Indices in Case 4 for Test System 1 (MWh/yr)**

	Supporting policies			
	(a)	(b)	(c)	(d)
Area 1	61.2335	28.6084	28.6084	41.7482
Area 2	32.2251	24.4907	24.4907	24.2376
Area 3	648.8776	614.1002	621.5178	623.6267
Area 4	1501.6836	1576.8206	1569.4031	1554.4074
System	2244.0203	2244.0203	2244.0203	2244.0203

**Table 4.32. LOEE Indices In Case 1 for Test System 2 (MWh/yr)**

	Supporting policies			
	(a)	(b)	(c)	(d)
Area 1	123.3989	63.7031	98.3037	75.6751
Area 2	128.4102	94.0824	109.1272	93.0787
Area 3	337.1798	236.1089	317.9130	281.0001
Area 4	333.2816	528.3761	396.9266	472.5166
System	922.2706	922.2706	922.2706	922.2706

**Table 4.33. LOEE Indices in Case 2 for Test System 2 (MWh/yr)**

	Supporting policies			
	(1)	(2)	(3)	(4)
Area 1	33.1458	15.0634	22.5880	18.1044
Area 2	27.1487	22.5329	21.4571	23.1804
Area 3	114.9670	77.9003	103.6966	90.9659
Area 4	166.8760	226.6410	194.3958	209.8867
System	342.1375	342.1375	342.1375	342.1375

**Table 4.34. LOEE Indices in Case 3 for Test System 2 (MWh/yr)**

	Supporting policies			
	(a)	(b)	(c)	(d)
Area 1	498.1291	292.8050	424.1649	315.0927
Area 2	448.1004	317.5350	405.0695	326.6522
Area 3	830.8882	617.5696	833.0615	758.6989
Area 4	854.4456	1403.6537	969.2673	1231.1194
System	2631.5635	2631.5635	2631.5635	2631.5635

**Table 4.35. LOEE Indices in Case 4 for Test System 2 (MWh/yr)**

	Supporting policies			
	(a)	(b)	(c)	(d)
Area 1	137.7941	68.8414	76.9299	75.3196
Area 2	55.9805	34.7817	40.8426	39.6034
Area 3	202.4308	167.8020	195.3536	186.5768
Area 4	292.8550	417.6354	375.9344	387.5604
System	689.0602	689.0602	689.0602	689.0602

System 1, the range of possible supporting scenarios becomes relatively narrow and therefore different supporting policies do not create large differences in the area indices.

## 4.7. CONCLUSIONS

This chapter discusses the application of Monte Carlo methods in both single-area and multi-area generating system adequacy assessment. Two basic approaches—the state duration sampling method and the state sampling method—are presented. In the case of the state duration sampling method, the load model is relatively simple and is the direct chronological hourly load curve. The major focus is therefore on generating unit modeling. The crucial aspect in this method is how to obtain an operating cycle of a particular generating unit model by sampling. In the case of the state sampling method, however, the generating unit model is relatively simple as the state of a generating unit can be simulated by a uniformly distributed random number. Emphasis is therefore placed on the load model in this method. The cluster technique can be used to create a multistep load level model for both single-area and multi-area systems. A normal distribution sampling technique and a correlation sampling technique can be used to simulate load uncertainty and correlation between area loads.

In the case of a multi-area system, it is necessary to model the assistances between areas and the tie line constraints. Two techniques in the form of a maximum flow algorithm and a linear programming model are presented for this purpose. One of the advantages of the linear programming model is that the LOEE sensitivity indices of both system and area to area generation and tie line capacities can be obtained. These sensitivity indices provide information about which tie line or which area generating capacity should be reinforced. A further advantage is that a wide variety of supporting policies can be readily incorporated into the model. Four supporting policies and their effects on multi-area system reliability evaluation are presented and discussed. Readers can use similar techniques to consider other possible supporting policies.

Selection of a stopping rule is an important factor in Monte Carlo simulation. The stopping criterion can be the prespecified number of samples, or the coefficient of variation tolerance, or a combination of both. A large prespecified number of samples or/and a small tolerance coefficient can provide relatively high accuracy in reliability indices with an attendant increase in CPU time. A reasonable stopping criterion should be specified for a particular system in order to provide a compromise between the accur-

acy and computing time. This may need to be examined in some detail for the configuration in question.

## 4.8. REFERENCES

1. R. Billinton, "Bibliography on Application of Probability Methods in the Evaluation of Generating Capacity Requirements," IEEE/PES Winter Meeting, 1966, paper 31 CP 66-62.
2. R. Billinton, "Bibliography on the Application of Probability Methods in Power System Reliability Evaluation," *IEEE Trans. on PAS*, Vol. 91, 1972, pp. 649-660.
3. IEEE Committee Report, "Bibliography on the Application of Probability Methods in Power System Reliability Evaluation, 1971-1977," *IEEE Trans. on PAS*, Vol. 97, 1978, pp. 2235-2242.
4. R. N. Allan, R. Billinton, and S. H. Lee, "Bibliography on the Application of Probability Methods in Power System Reliability Evaluation, 1977-1982," *IEEE Trans. on PAS*, Vol. 103, 1984, pp. 275-282.
5. R. N. Allan, R. Billinton, S. M. Shahidehpour, and C. Singh, "Bibliography on the Application of Probability Methods in Power System Reliability Evaluation, 1982-1987," *IEEE Trans. on PS*, Vol. 3, No. 4, 1988, pp. 1555-1564.
6. R. Billinton and R. N. Allan, *Reliability Evaluation of Power Systems*, Plenum, New York, 1984.
7. R. Billinton and R. N. Allan, *Reliability Assessment of Large Electric Power Systems*, Kluwer, Dordrecht, 1988.
8. L. Gan, "Multi-Area Generating System Adequacy Assessment by Monte Carlo Simulation," M.Sc Thesis, University of Saskatchewan, 1991.
9. IEEE Task Group, "A Four-State Model for Estimation of Outage Risk for Units in Peaking Service," *IEEE Trans. on PAS*, Vol. 91, 1972, pp. 618-627.
10. R. N. Allan, R. Billinton, and N. M. Abdel-Gawad, "The IEEE Reliability Test System—Extension to and Evaluation of the Generating System," *IEEE Trans. on PWR*, Vol. 1, No. 4, 1986, pp. 1-7.
11. M. S. Aldenderfer and R. K. Blashfield, *Cluster Analysis*, Sage, Newbury Park, 1984.
12. H. Späth, *Cluster Analysis Algorithms for Data Reduction and Classification of Objects*, Halsted, New York, 1980.
13. R. Billinton and L. Gan, "A Monte Carlo Simulation Model for Adequacy Assessment of Multi-Area Generating Systems," Proceedings of the Third International Conference on Probabilistic Methods Applied to Electric Power Systems, IEE, London, 3-5 July, 1991.
14. R. Billinton and L. Gan, "Use of Monte Carlo Simulation in Teaching Generating Capacity Adequacy Assessment," *IEEE Trans. on PS*, Vol. 6, No. 4, 1991, pp. 1571-1577.
15. R. Billinton and W. Li, "A Monte Carlo Method for Multi-Area Generation System Reliability Assessment," *IEEE Trans. on PS*, Vol. 7, No. 4, 1992, pp. 1487-1492.
16. Wan Zikun, *Elements of Probability Theory and Its Application*, Science Publishing House, Beijing, 1979.
17. W. Li and R. Billinton, "Incorporation and Effects of Different Supporting Policies in Multi-Area Generation System Reliability Assessment," *IEEE Trans. on PS*, Vol. 8, No. 3, 1993, pp. 1061-1067.

# 5

# Composite System Adequacy Assessment

## 5.1. INTRODUCTION

The basic objective of composite generation and transmission system adequacy assessment (HL2) is to evaluate the ability of the system to satisfy the load and energy requirements at the major load points. This evaluation domain involves the joint reliability problem of generating sources and transmission facilities and is sometimes called bulk system analysis. Although this activity came much later than comparably significant developments in HL1 evaluation, considerable effort has been devoted to this area over the last 25 years.<sup>(1-7)</sup>

As in HL1 evaluation, there are two fundamental approaches to composite system adequacy assessment: analytical enumeration and Monte Carlo simulation. The analytical enumeration techniques have been developed mainly in North America.<sup>(8-15)</sup> Monte Carlo simulation techniques were first advanced in Europe by EDF (France) and ENEL (Italy) and then were further developed by work in Brazil and in North America.<sup>(16-30)</sup> A Monte Carlo based computer program named MECORE has been developed at the University of Saskatchewan and enhanced at BC Hydro. This chapter illustrates applications of Monte Carlo methods in composite system adequacy assessment. The MECORE program utilizes the techniques presented in this chapter and has been applied to reliability assessment of practical composite systems.

Adequacy assessment at HL2 is a complex task which involves the two aspects of system analysis and practical considerations in selecting a system state. The required system analyses are load flow calculations, contingency

analysis and ranking, rescheduling of generation, overload alleviation, and load shedding philosophies, etc. These requirements are the same for both analytical enumeration and Monte Carlo simulation. Selection of a system state involves many practical considerations, such as derated states of generating units, common-cause outages of transmission lines, regional weather effects, bus load uncertainty and correlation, reservoir operating rules, dependent failures, and even complex operational considerations, etc. Obviously, these considerations are different for analytical enumeration and Monte Carlo simulation. Generally, Monte Carlo methods are more flexible when complex operating conditions and system considerations need to be incorporated. It should be noted, however, that many issues associated with system considerations have not yet been fully resolved. The important aspect, therefore, is for a particular electric power utility to decide which factors and effects are important in their case and then to use the most suitable technique.

A system state sampling method for composite system adequacy evaluation and basic system analysis techniques are presented in Section 5.2. Several practical considerations in selecting system states and their effects on composite system adequacy are discussed in Sections 5.3 to 5.7. The system state sampling method cannot be used to directly calculate the frequency index and only provides the Expected Number of Load Curtailments, which is an approximation of the frequency index. Application of the system state transition sampling technique to calculate the frequency index is described in Section 5.8.

Two special issues are described in Sections 5.9 and 5.10. The first issue is that of security considerations in composite system adequacy assessment. The term “security” in this case is associated with steady state analysis and introduces the concept of security constrained adequacy assessment. It is therefore different from “security evaluation” as discussed in Section 2.1, which is associated with system dynamic disturbances. The second issue is noncoherence in composite system reliability evaluation.

## 5.2. SYSTEM STATE SAMPLING METHOD AND SYSTEM ANALYSIS TECHNIQUES

The three basic simulation methods in reliability evaluation are described in Section 3.6. In this section, the system state sampling method is applied to composite system adequacy assessment. The most important advantage of this sampling method is reduced computing time and memory requirements. The number of components in composite system assessment

is much larger than that in generation system adequacy assessment. Moreover, the system analysis associated with load flow calculation, contingency analysis, generation rescheduling, and overload alleviation requires a considerable amount of calculation.

### 5.2.1. Basic Methodology

The basic sampling procedure can be conducted by assuming that the behavior of each component can be categorized by a uniform distribution under  $[0, 1]$ . In the case of a two-state component representation, the probability of outage is the component forced unavailability. It is also assumed that component outages are independent events.

Let  $S_i$  denote the state of the  $i$ th component and  $FU_i$  be its forced unavailability. A random number generation method, such as the improved prime number multiplicative congruential method, is used to draw a random number  $U_i$  distributed uniformly under  $[0, 1]$ :

$$S_i = \begin{cases} 0 & \text{(up state)} & \text{if } U_i \geq FU_i \\ 1 & \text{(down state)} & \text{if } 0 \leq U_i < FU_i \end{cases} \quad (5.1)$$

The state of the system containing  $t$  components including generating units, transmission lines/transformers, etc., is expressed by the vector  $S$ :

$$S = (S_1, S_2, \dots, S_i, \dots, S_t)$$

When  $S$  equals zero, the system is in the normal state. When  $S$  is not equal to zero, the system is in a contingency state due to component outage(s). Assuming that each system state has the probability  $P(S)$  and the index function  $F(S)$ , the mathematical expectation of the index function of all system states is given by

$$E(F) = \sum_{s \in G} F(s)P(s) \quad (5.2)$$

where  $G$  is the set of system states.

Substituting the frequency of the state  $S$  in sampling for its probability  $P(S)$  yields

$$E(F) = \sum_{s \in G} F(s) \frac{n(s)}{N} \quad (5.3)$$

where  $N$  is the number of samples and  $n(s)$  is the number of occurrences of state  $S$ .

Load curtailment occurs in relatively few system states and therefore it is necessary to calculate  $E(F)$  only for these states. The set of system states  $G$  can be divided into four subsets  $G1$ ,  $G2$ ,  $G3$ , and  $G4$  and displayed as follows:

$$G \left\{ \begin{array}{l} G1 \\ \overline{G1} \left\{ \begin{array}{l} G2 \\ \overline{G2} \left\{ \begin{array}{l} G3 \\ G4 \end{array} \right. \end{array} \right. \end{array} \right.$$

where  $G1$  is the normal state subset (no load curtailment),  $\overline{G1}$  is the contingency state subset,  $G2$  is the subset composed of the contingency states which definitely have no load curtailment,  $\overline{G2}$  is the subset composed of the contingency states which may have load curtailment,  $G3$  is the subset composed of the contingency states which have no load curtailment after rescheduling the generation, and  $G4$  is the subset composed of the contingency states which still have load curtailment after rescheduling the generation.

After a system state is obtained by Monte Carlo sampling, it is first necessary to judge whether or not this state belongs to  $G1$ . If the state belongs to  $\overline{G1}$ , it is necessary to determine by means of contingency analysis whether or not it belongs to  $G2$ . If the state belongs to  $\overline{G2}$ , it is necessary to reschedule the generation and determine the curtailed load using the minimization model of load curtailment. If the resulting curtailed load is zero, the state belongs to  $G3$ , and if the resulting curtailed load is not zero, then the state belongs to  $G4$ . Only those system states belonging to subset  $G4$  contribute to the unreliability indices.

### 5.2.2. Contingency Analysis For Composite Systems

There are many contingency analysis techniques for composite systems. A linearized load flow based contingency analysis approach is introduced in the following. It matches the minimization model of load curtailment described in the next subsection in computational accuracy. A more accurate AC load flow based contingency analysis method is given in Appendix C.4.

Sampling all the system component states results in a specified system state. If this is a normal state, then no load curtailment exists. If this is a contingency state, load curtailment may be required. In an actual power system, however, the possibility of load curtailment due to low-level contingencies and the likelihood of high-level contingencies are relatively rare,

therefore most of the drawn contingency states belong to  $G2$  with only a few belonging to  $\overline{G2}$ . It is possible to judge whether or not a system state belongs to  $G2$  by means of a simple calculation instead of solving the load flow equations. Once it has been determined that a state belongs to  $G2$ , it makes no contribution to the unreliability indices and it is possible to proceed immediately to the next sampling. It is necessary to reschedule generation only for those states belonging to  $\overline{G2}$  and, if unavoidable, to shed loads by solving the minimization model of load curtailment.

A load flow solution of the normal system state can be obtained which includes generation outputs and line power flows. The direct analysis of possible load curtailment for any drawn contingency state can be conducted as follows:

**(a) Generating Unit Contingencies.** In general, it can be assumed that a generator bus  $i$  has several generators denoted by set  $N_i$ , with the upper limit of each generator output being  $P'_{ik}$  ( $k \in N_i$ ) and its actual power output in the normal state being  $P_{ik}$ . When a generating unit is in a contingency state, the corresponding  $P'_{ik}$  becomes  $P''_{ik}$  where  $P''_{ik}$  is the derated output limit for a generator in a derated state and zero for a generator in the full forced outage state. (Sampling and effects of generating unit derated states are discussed in Section 5.4.) If the spare generation capacity at each generator bus can compensate for the unavailable capacity at this bus, i.e., for all generator buses,

$$\sum_{k \in N_i} (P''_{ik} - P_{ik}) \geq 0 \quad (5.4)$$

then the generating unit contingencies lead to no load curtailment. In this case, it is necessary to examine whether or not transmission component outages bring about line overloads. If equation (5.4) is not satisfied for at least one generator bus, then the system contingency state belongs to  $\overline{G2}$  and it is necessary to solve the minimization model to determine if the state is in subset  $G3$  or  $G4$ .

**(b) Transmission Component Outages.** If the redistribution of load flow due to the removal of lines creates no overload in other lines under the condition that equation (5.4) for all generator buses is satisfied, then the contingency state belongs to  $G2$ . If this is not the case, then it belongs to  $\overline{G2}$ . In order to make this discrimination, it is therefore necessary to calculate line flows following the removal of transmission components.

The following relationship can be obtained using the linearized load flow formulation :

$$T(S^j) = A(S^j)(PG - PD) \quad (5.5)$$

Here, PG and PD are the generation output vector and the load power vector, respectively;  $S^j$  is the system state vector where, when  $j=0$ ,  $S^0$  denotes the normal state and, when  $j=1, 2, \dots, S^1, S^2, \dots$ , denote the contingency states due to single, double,  $\dots$ , transmission component outages;  $T(S^j)$  are the line flow vectors under state  $S^j$ ;  $A(S^j)$  is the relation matrix between line flows and power injections under state  $S^j$ . The  $m$ th row of  $A(S^j)$  can be calculated as follows:

$$A_m(S^j) = \frac{Z_r(S^j) - Z_q(S^j)}{X_m} \quad (5.6)$$

where  $r$  and  $q$  denote the two bus numbers of the  $m$ th line;  $X_m$  is the reactance of the  $m$ th line;  $Z(S^j)$  is the bus impedance matrix of the system under state  $S^j$  in which the resistances of all lines are neglected;  $Z_r(S^j)$  and  $Z_q(S^j)$  are the  $r$ th and  $q$ th rows of  $Z(S^j)$ , respectively.

The bus impedance matrices after the removal of specified lines can be calculated directly from the bus impedance matrix of the normal state:

$$Z(S^j) = Z(S^0) + Z(S^0)MQM^T Z(S^0) \quad (j \neq 0) \quad (5.7)$$

where

$$Q = [X - M^T Z(S^0) M]^{-1} \quad (5.8)$$

Here,  $X$  is a diagonal matrix whose dimension is the same as the number of the outaged lines and whose diagonal elements are the reactances of the outage circuits;  $M$  is a submatrix composed of the columns corresponding to the outage lines of the bus-line incidence matrix.

The line flows of any contingency state involving single or multiple line outage events can be calculated from  $Z(S^0)$  of the normal state and bus power injections using equations (5.5)–(5.8). When equation (5.4) is satisfied, the power injections at all buses remain constant and the following simple formulas can be derived to calculate the line flows for single line outage states<sup>(31)</sup>:

$$T_m(S^1) = T_m(S^0) + f_{mk} T_k(S^0) \quad (5.9)$$

$$f_{mk} = \frac{-B_m D_{mk} \Delta b_k}{(1 + \Delta b_k D_{kk}) B_k} \quad (m \neq k) \quad (5.10)$$

$$f_{kk} = \frac{(1 - B_k D_{kk}) \Delta b_k}{(1 + \Delta b_k D_{kk}) B_k} \quad (5.11)$$

$$D_{mk} = (M^m)^T Z(S^0) M^k \quad (5.12)$$

$$D_{kk} = (M^k)^T Z(S^0) M^k \quad (5.13)$$

Here,  $k$  denotes any outage line and  $m$  any line in the system;  $T_m(S^0)$ ,  $T_k(S^0)$ , and  $T_m(S^1)$  are the power flows in lines  $m$  and  $k$  under the normal and the single transmission component outage states, respectively;  $B_m$  and  $B_k$  are the mutual admittances of line  $m$  and line  $k$ , respectively;  $\Delta b_k$  is the change value of  $B_k$  after removal of one or several circuits in line  $k$ ;  $M^m$  and  $M^k$  are the column vectors of  $M$  corresponding to, respectively, line  $m$  and line  $k$ .

The line power flows under single transmission component outage states can be calculated directly using equations (5.9)–(5.13) from the matrix  $Z(S^0)$  and the line power flows  $T(S^0)$  of the normal state. The likelihood of single transmission component outages is much greater than those of multiple transmission component outages. This set of formulas therefore create a considerable decrease in the computational requirements. It should be noted that equations (5.9)–(5.13) are obtained under the condition that the bus loads remain unchanged. If the method of sampling load states is used, the load level under a contingency state is determined randomly and therefore these equations do not apply.

### 5.2.3. Linear Programming Optimization Model

A considerable number of contingency states in which no load curtailment exists will have been excluded after the contingency analysis of all the drawn contingency states. For those contingency states belonging to  $\overline{G2}$ , in which generation outputs at some buses cannot be maintained due to generating unit contingencies (outage or derated) and/or there exist some line overloads due to transmission component outages, generation outputs should be rescheduled to maintain generation-demand balance and alleviate line overloads and, at the same time, to avoid load curtailment if possible or to minimize total load curtailment if unavoidable. The following minimization model of load curtailment can be used for this purpose:

$$\min \sum_{i \in NC} C_i \quad (5.14)$$

subject to

$$T(S^j) = A(S^j)(PG + C - PD) \quad (5.15)$$

$$\sum_{i \in NG} PG_i + \sum_{i \in NC} C_i = \sum_{i \in NC} PD_i \quad (5.16)$$

$$PG^{\min} \leq PG \leq PG^{\max} \quad (5.17)$$

$$0 \leq C \leq PD \quad (5.18)$$

$$|T(S^j)| \leq T^{\max} \quad (5.19)$$

where  $T(S^j)$ ,  $A(S^j)$ , PG, PD are as defined in the previous subsection;  $PG^{\min}$ ,  $PG^{\max}$ , and  $T^{\max}$  are the limit vectors, respectively, of PG and  $T(S^j)$ ; C is the load curtailment vector; NC and NG are the sets of all load buses and all generator buses, respectively. The objective of this model is to minimize the total load curtailment while satisfying the power balance, the linearized load flow relationships, and the limits of line power flows and generation outputs.

Linear programming theory and computational experience indicates that the above model has multisolutions and therefore cannot be used to calculate realistic bus indices. An acceptable load curtailment philosophy should be incorporated in the minimization model. There is a wide range of possible philosophies which can be utilized. The following are two basic philosophies:

1. Loads are curtailed at buses which are as close to the elements on outage(s) as possible.
2. Loads are classified according to their importance. The least important load should be curtailed first, then the next least important, and at the last the most important load.

These two load curtailment philosophies can be incorporated by modifying the above minimization model to create the following model:

$$\min \sum_{i \in NC} \left( W_i \sum_{j=1}^{MS} \beta_j C_{ij} \right) \quad (5.20)$$

subject to

$$T_i(S^j) = \sum_{k=1}^{NS} A_{ik}(S^j) \left( PG_k + \sum_{j=1}^{MS} C_{kj} - PD_k \right) \quad (i=1, \dots, L) \quad (5.21)$$

$$\sum_{i \in NG} PG_i + \sum_{i \in NC} \sum_{j=1}^{MS} C_{ij} = \sum_{i \in NC} PD_i \quad (5.22)$$

$$PG^{\min} \leq PG \leq PG^{\max} \quad (5.23)$$

$$0 \leq C_{ij} \leq \alpha_j PD_i \quad (i \in NC; j=1, \dots, MS) \quad (5.24)$$

$$|T(S^j)| \leq T^{\max} \quad (5.25)$$

where  $L$  and  $NS$  are the numbers of the lines and buses, respectively, and other notations are as defined earlier. In the modified model, the load curtailment variable at each bus is divided into  $MS$  subvariables (in general,

$MS = 2$  or  $3$ ), while  $\alpha_j$  are the load percentages associated with each subvariable and  $\beta_j$  are the weighting factors. The least important load corresponds to the smallest  $\beta_j$  and the most important load to the largest  $\beta_j$ . Introduction of subvariables and their weighting factors allows load curtailment philosophy 2 to be realized automatically in the resolution of the model.

Quantities  $W_i$  are the weighting factors associated with each bus load. The buses closest to the elements on outage(s) have relatively small  $W_i$  and those far from outage(s) have relatively large  $W_i$ . The values of  $W_i$  for each bus load are variable and depend on outage location(s) in the particular contingency system state. Introduction of  $W_i$  allows load curtailment philosophy 1 to be realized automatically in the resolution of the model.

It should be noted that the values of  $\beta_j$  or  $W_i$  need only to be specified in terms of their relative magnitudes and therefore it is easy to select these values. The selection of one or both will depend on the actual philosophy used by the system. The model is solved by combining the linear programming relaxation technique with the dual simplex method.<sup>(32)</sup> These two approaches are given in Appendix D.1. Only the active line power constraints are introduced into equations (5.21) and (5.25), creating a small-scale linear programming problem which can be solved quite quickly.

## 5.2.4. Basic Case Studies

In this subsection, the IEEE RTS<sup>(33)</sup> is used to conduct basic case studies. The single line diagram of the system and the line and generator data are given in Appendix A.1. Annualized system and bus indices are first illustrated. Annualized indices are those calculated at the annual system peak load level and expressed on a base of one year. Annual indices considering the annual load curve and results associated with this and other factors are discussed in Sections 5.3 to 5.7. All the studies in this chapter were conducted on a VAX-6330 computer except for the cases indicated. The following adequacy indices are calculated. A comprehensive interpretation of these indices is provided in Section 2.6.2.

ENLC	Expected Number of Load Curtailments (occ./yr)
EDLC	Expected Duration of Load Curtailments (hr/yr)
PLC	Probability of Load Curtailments
EDNS	Expected Demand Not Supplied (MW)
EENS	Expected Energy Not Supplied (MWh/yr)
BPII	Bulk Power Interruption Index (MW/MW-yr)
BPECI	Bulk Power/Energy Curtailment Index (MWh/MW-yr)

BPACI	Bulk Power-supply Average MW Curtailment Index (MW/disturbance)
MBPCI	Modified Bulk Power Curtailment Index (MW/MW)
SI	Severity Index (system minutes/yr)

### (a) Comparison Between the Monte Carlo and Enumeration Methods.

The annualized system indices of the IEEE RTS considering two-state models for all generating units using Monte Carlo simulation and state enumeration are given in Table 5.1. In the case of the enumeration method, line outages and combined generating unit and line outages have been considered up to the 3rd level while generating unit outages have been considered up to the 4th and 5th levels, respectively.

The results in Table 5.1 indicate that in the case of the Monte Carlo simulation method, 10,000 samples are sufficient for this system. The results obtained from 10,000 samples have only about 6% differences compared to those obtained from 100,000 samples and approach those obtained from the enumeration method when line outages are considered up to the 3rd level and generating unit outages up to the 5th level. The coefficient of variation for the EDNS is 0.04 in the case of 10,000 samples. The CPU times listed indicate that in order to obtain basically similar results, the Monte Carlo simulation method requires much less computing time when compared to the state enumeration method for the IEEE RTS. The state enumeration approach used in this comparison was a relatively unsophisticated technique which did not involve sorting generating unit outages.<sup>(34)</sup> It was included to provide a direct comparison with the Monte Carlo approach.

**Table 5.1. Annualized System Indices for the IEEE RTS Using Monte Carlo and Enumeration Methods**

Name of index	Monte Carlo simulation		State enumeration	
	Number of samples		Generator outage level	
	10,000	100,000	Up to 4th	Up to 5th
ENLC	54.75342	57.92681	47.96653	54.21938
EDLC	698.88000	737.23102	657.78259	711.28967
PLC	0.08000	0.08439	0.07530	0.08142
EDNS	13.97045	14.87208	11.99383	13.76009
EENS	122045.88281	129922.46875	104778.14063	120208.11719
BPII	3.33652	3.64042	2.61351	3.21786
BPECI	42.82311	45.58683	36.76426	42.17828
PBACI	173.67123	179.10896	155.28572	169.14433
MBPCI	0.00490	0.00522	0.00421	0.00483
SI	2569.38672	2735.20947	2205.85522	2530.69702
CPU time(min)	0.623	6.55	18.3	53.3

**Table 5.2. Annualized Bus Indices for the IEEE RTS**

Bus No.	PLC	ENLC	EDNS	EENS
1	0.00200	1.46178	0.04144	361.98926
2	0.00220	1.57351	0.03966	346.47028
3	0.00240	1.88695	0.08150	711.98462
4	0.00280	2.04188	0.03983	347.95593
5	0.00390	2.66570	0.04306	376.17392
6	0.00530	3.75610	0.11766	1027.87903
7	0.00530	3.75610	0.02000	174.72641
8	0.00850	5.81365	0.23704	2070.79102
9	0.01140	7.98625	0.33950	2965.88159
10	0.01300	9.24670	0.47850	4180.18311
13	0.01980	13.91388	0.85216	7444.49316
14	0.02990	20.12966	0.96918	8466.77441
15	0.04090	26.91882	2.35796	20599.17383
16	0.04340	28.79770	0.85570	7475.41650
18	0.05480	37.99242	3.19185	27884.02734
19	0.07100	48.06261	2.30390	20126.89258
20	0.07980	54.56686	2.00151	17485.18555

**(b) Annualized Bus Indices.** The annualized bus indices of the IEEE RTS using the two-state model for all generating units are given in Table 5.2. Each load bus experiences load curtailments. This set of bus indices is based on the following load curtailment philosophy: The bus loads are divided into three groups. The first group corresponds to the top 20% of the bus loads, the second group to the next 20%, and the third group to the remaining 60%. When load curtailments are unavoidable, the loads in the first group are curtailed first, then those in the second group, and at the last those in the third group. This is conducted automatically by specifying different weighting factors  $\beta_j$  in the objective function (5.20). The IEEE RTS has been also evaluated using the model without a specific load curtailment philosophy [equations (5.14) to (5.19)]. Several different solutions were obtained by changing the order of the nonbasic variables entering the base. This means that under the condition that all constraints are satisfied, there is only one set of system indices but there are several sets of different bus indices. Two sets of different bus indices obtained using the model without a specific load curtailment philosophy are given in Tables 5.3 and 5.4. The indices for the buses not listed in Tables 5.3 and 5.4 are zero. The system indices associated with these two solutions are the same as those obtained using the model with the specific load curtailment philosophy. It can be seen that the bus inadequacies indicated by these two sets of bus indices are contradictory. Therefore, the model without a specific load curtailment philosophy cannot be used to calculate realistic bus indices.

**Table 5.3. The First Solution for Annualized Bus Indices in the IEEE RTS Using the Model without a Specific Load Curtailment Philosophy**

Bus No.	PLC	ENLC	EDNS	EENS
3	0.00010	0.15839	0.00431	37.64702
10	0.00010	0.02817	0.01255	109.65305
15	0.00020	0.12536	0.00580	50.66939
16	0.00040	0.31162	0.02100	183.45644
18	0.01290	9.21853	1.44220	12599.09668
19	0.04340	28.79770	5.10252	44575.58984
20	0.07980	54.56686	7.37742	64449.15234

**Table 5.4. The Second Solution for Annualized Bus Indices in the IEEE RTS Using the Model without a Specific Load Curtailment Philosophy**

Bus No.	PLC	ENLC	EDNS	EENS
3	0.00010	0.15839	0.00431	37.64702
9	0.00020	0.12536	0.02340	204.42296
10	0.00280	2.04188	0.30535	2667.56055
13	0.03760	23.91431	3.59061	31367.58008
14	0.07960	54.26879	10.01209	87465.61719
15	0.00020	0.29807	0.03000	262.08063

## 5.3. INCORPORATION OF THE ANNUAL LOAD CURVE

There are many practical factors to be considered in composite system adequacy assessment. This section discusses the incorporation and resulting effects of the annual load curve model. Generating unit derated states, regional weather effects, common cause outages of transmission lines, and bus load uncertainty and correlation are discussed in subsequent sections.

### 5.3.1. Multistep Model of the Annual Load Curve

Both annualized and annual indices can be used to assess the adequacy of a composite system. Annualized indices are calculated at a single load level (normally at the system peak load level) and expressed on a base of one year. Annual indices are calculated considering the variable load levels throughout the year. Annualized indices can be employed in a wide range

of studies, such as comparing the relative adequacies of different systems or changes in system configuration or composition. Annual indices, however, can be utilized for more comprehensive purposes, for instance, when reliability worth is considered in power system planning. Calculation of annual indices requires recognition of the various load levels that can occur during a year. This can be done by a simple sampling of the chronological load states or by utilizing a load model which eliminates the chronology and aggregates the load states. Three possible methods for modeling an annual load curve are described in Section 4.3.2. The cluster technique for a multistep load model is also given in Section 4.3.3. The utilization of a multistep model of the annual load duration curve in a Monte Carlo simulation of composite system adequacy evaluation is more effective from a computational point of view than individual sampling of the chronological load states. This is mainly due to the following:

1. As noted in Section 4.3.2, combining Monte Carlo simulation of system component states with enumeration of load level steps is a variance reduction technique similar to stratified sampling. Many of the load points in the flat segments of a load duration curve make almost the same contribution to the total indices. This is particularly true of the low load points, which have relatively high probabilities of occurrence.
2. For a specific load level, the direct contingency analysis approach described in Section 5.2.2 can be used to reduce the required computation time.
3. The same system contingency state may be drawn many times in a Monte Carlo simulation for system component outages. In these situations, the system contingency state needs to be evaluated only once for a particular load level but many times when sampling chronological load states.

### **5.3.2. Ratios of Generation–Transmission Adequacy Indices**

The accuracy of the load representation increases with the utilization of more steps in the annual load duration curve. The computation time also increases with the number of steps in the load model. The adequacy indices for different composite systems, however, can have quite different sensitivities to the number of load level steps. If the adequacy indices of a composite system are very sensitive to the load levels, then the number of load level steps can have considerable impact on the annual indices. A set of ratios of generation–transmission adequacy indices can be used to quantitatively recognize the sensitivity of composite system adequacy indices to the number of steps in the multistep load model.

The adequacy indices of a composite generation and transmission system depend on two basic aspects: the strength or weakness of the generation system (reserve generation and forced unavailability of the generating units) and the strength or weakness of the transmission system (transmission capacity limits, forced unavailability of the transmission components, and the system topology or configuration). The ratios of the contribution to the composite system adequacy indices due to the generation system and the contribution due to the transmission system can provide a general indication of which segment is significant in regard to system adequacy. A set of Ratios of Generation–Transmission Adequacy Indices (RGTAI) are defined as follows. In these definitions, the quantities without superscript \* are the annualized indices of a composite system at the peak load level while those with \* are the annualized contribution due to the generation system. The generation system contribution is determined at HL1, i.e., on a total generation–total load basis.

(1) Ratio of Load Curtailment Probability (RLCP)

$$\text{RLCP} = \frac{\text{PLC}^*}{\text{PLC} - \text{PLC}^*}$$

(2) Ratio of the Number of Load Curtailment (RNLC)

$$\text{RNLC} = \frac{\text{ENLC}^*}{\text{ENLC} - \text{ENLC}^*}$$

(3) Ratio of Energy Not Supplied (RENS)

$$\text{RENS} = \frac{\text{EENS}^*}{\text{EENS} - \text{EENS}^*}$$

(4) Ratio of Power-Interruption Index (RPII)

$$\text{RPII} = \frac{\text{BPII}^*}{\text{BPII} - \text{BPII}^*}$$

The definitions of indices PLC, ENLC, EENS, and BPII can be found in Section 2.6.2. When the RGTAI values are greater than 1.0, the inadequacy of a composite system is largely caused by the generation system. When the RGTAI values are smaller than 1.0, the inadequacy of the composite system is largely due to the transmission system. A basic requirement in a composite system reliability study is to know if a composite system should be reinforced and also to indicate which segment of it should be reinforced. The RGTAI ratios provide useful indicators regarding both the need and

the general functional areas of generation and transmission requiring reinforcement.

The RGTAI values also quantitatively reflect the sensitivity of the calculated adequacy indices of a composite system to the load curve. The greater the ratio values, the more sensitive to the load curve are the composite system adequacy indices. This is due to the fact that load level variations have a direct impact on the calculated adequacy indices of the installed generating capacity but only a secondary effect on the transmission system contribution to the composite system adequacy indices. This means that the load level variations have much greater influence on the numerator values of the ratios than the denominator values. In addition, load levels near the annual peak load have relatively short durations while other lower load levels have longer durations. It should be noted that the correlation between the RGTAI values and the sensitivity of the composite system adequacy indices to the load curve is not linear. The composite system adequacy indices are quite sensitive to the load curve only when the RGTAI values are much greater than 1.0.

### 5.3.3. Effect of the Number of Steps in a Load Model

If the load duration curve is divided into a large number of steps, then the calculated annual indices are closely representative of the actual load model. This, however, can result in excessive computing time. It is only necessary to use many steps in the load model to obtain accurate annual indices in the case of a composite system which is sensitive to the load curve. Fewer steps can be used in the case of a nonsensitive composite system with an attendant decrease in required computing time.

In order to illustrate the difference between sensitive and nonsensitive composite systems, two systems are considered. One is the IEEE RTS and another is a model of the Saskatchewan Power Corporation System (SPCS). The IEEE RTS has 24 buses (10 generator buses and 17 load buses), 38 lines/transformers, and 32 generating units. The annual system peak load is 2850 MW and the total installed generating capacity is 3405 MW. The SPCS has 45 buses (8 generator buses and 27 load buses), 71 lines/transformers, and 29 generating units. The annual system peak load is 1802.5 MW and the total installed generating capacity is 2530 MW. The single line diagram of the SPCS and the line and generator data can be found in Reference 34. The two systems were assumed to have the same load profile. The individual hourly load data are those of the IEEE RTS given in Appendix A.1.

**Table 5.5. Ratios of Generation–Transmission Adequacy Indices for the Two Test Systems**

RGTAI	IEEE RTS	SPCS
RLCP	265.67	0.31
RNLC	20.91	0.27
RENS	448.39	0.75
RPII	24.12	0.69

A load duration curve containing 8736 points can be created using these data. The mean load of the 8736 load points is 61.44% of the annual system peak load.

The RGTAI values for the IEEE RTS and the SPCS are shown in Table 5.5. It can be concluded from these values that the IEEE RTS is very sensitive to the number of steps in the load curve to which the SPCS model is not sensitive. The annual indices for the two test systems have been calculated using three load models. In Model 1, the load curve is divided into 70 steps with a step load increment of 1%. In Models 2 and 3, the load curve is divided into 15 steps and 8 steps, respectively. The load increment of each step is 5% and 10%, respectively. In each case, the final step includes all load points lower than the load level of this step. The calculated annual system indices are presented in Tables 5.6 and 5.7. The percentage values in the brackets are the differences between the results for the 15-step and the 8-step model of the load duration curve compared with the results obtained

**Table 5.6. Annual Indices Using the Three Load Models and Annualized Indices at the Mean Load for the IEEE RTS**

Index	Annual indices			Annualized indices (mean load)
	70-step model	15-step model	8-step model	
ENLC	0.80854	1.23661 (53%)	2.19343 (171%)	0.0
EDLC	10.23695	15.54475 (52%)	27.27785 (166%)	0.0
PLC	0.00117	0.00178 (52%)	0.00312 (167%)	0.0
EDNS	0.13137	0.21761 (66%)	0.42125 (221%)	0.0
EENS	1147.61108	1901.03833 (66%)	3680.02637 (221%)	0.0
BPII	0.03196	0.05286 (65%)	0.10255 (221%)	0.0
BPECI	0.40267	0.66703 (66%)	1.29124 (221%)	0.0
BPACI	112.64307	121.81555 (8%)	133.25201 (18%)	0.0
MBPCI	0.00005	0.00008 (60%)	0.00015 (200%)	0.0
SI	24.16023	40.02186 (66%)	77.47424 (221%)	0.0
CPU (min)	15.97	4.48	2.78	0.29

**Table 5.7. Annual Indices Using the Three Load Models and Annualized Indices at the Mean Load for the SPCS**

Index	Annual indices			Annualized indices (mean load)
	70-step model	15-step model	8-step model	
ENLC	1.17838	1.21734 (3%)	1.27841 (8%)	1.09548 (-7%)
EDLC	2.68576	2.84312 (6%)	2.98546 (11%)	2.27136 (-15%)
PLC	0.00031	0.00033 (6%)	0.00034 (10%)	0.00026 (-16%)
EDNS	0.01016	0.01077 (6%)	0.01173 (15%)	0.00920 (-9%)
EENS	88.72541	94.10423 (6%)	102.49805 (16%)	80.40615 (-9%)
BPII	0.02285	0.02400 (5%)	0.02570 (12%)	.02151 (-6%)
BPECI	0.04922	0.05221 (6%)	0.05686 (16%)	0.04461 (-9%)
BPACI	34.95942	35.54316 (2%)	36.23811 (4%)	35.40000 (1%)
MBPCI	0.00001	0.0000 (0%)	0.00001 (0%)	0.00001 (0%)
SI	2.95344	3.13246 (6%)	3.41186 (16%)	2.67649 (-9%)
CPU (min)	117.67	24.82	13.76	1.70

using the 70-step load model. The values in the last column are the annualized indices calculated at the mean load level and the percentage differences relative to the annual indices using the 70-step load model. The last row in Tables 5.6 and 5.7 shows the CPU solution times.

It can be seen from Tables 5.6 and 5.7 that the number of steps in the load duration curve has considerable influence on the calculated annual indices for the IEEE RTS, which has very high RGTAI values. If the load curve is divided into too few steps, the calculated annual indices can be quite inaccurate for sensitive composite systems such as the IEEE RTS. This system is so sensitive to the load level that the annualized indices at the mean load level are effectively zero. The Saskatchewan Power Corporation System which has low RGTAI values is not very sensitive to the number of steps in the load duration curve. The 15-step approximate load model provides sufficiently accurate annual indices and even the 8-step approximate load model provides relatively satisfactory results.

It is interesting to note that the annualized indices at the mean load level for the SPCS, though optimistic, are reasonably close to the calculated annual indices obtained using the 70-step load model while the computing times are much less. If computing time is limited or a problem, then it may be acceptable in some system studies to replace annual indices by calculating annualized indices at the mean load level. It can be seen from Tables 5.6 and 5.7 that this approach could be used in the SPCS but not in the IEEE RTS. This approximation should be used with caution.

Tables 5.8 and 5.9 show the contributions of each load level step to the total annual indices using the 15-step load model for the two test systems. These results further verify the previous analysis. In the case of the IEEE RTS, the four load level steps higher than 80% of the annual peak load

**Table 5.8. Contribution of Each Load Level Step to the Annual Indices (in %) Using the 15-Step Load Model for the IEEE RTS**

Load level (%)	Load duration (%)	ENLC (%)	PLC EDLC (%)	EENS EDNS (%)	BPII (%)
100.00	0.22	9.63	9.78	13.96	12.50
95.00	1.10	24.81	26.00	31.20	29.28
90.00	3.59	33.30	32.32	32.05	33.06
85.00	7.51	22.81	22.37	17.03	18.61
80.00	8.33	7.71	7.96	4.67	5.05
75.00	8.21	0.83	0.92	0.68	0.74
70.00	11.02	0.43	0.31	0.38	0.69
65.00	12.18	0.48	0.34	0.04	0.07
60.00	9.67	0.00	0.00	0.00	0.00
55.00	11.88	0.00	0.00	0.00	0.00
50.00	12.84	0.00	0.00	0.00	0.00
45.00	9.79	0.00	0.00	0.00	0.00
40.00	3.50	0.00	0.00	0.00	0.00
35.00	0.15	0.00	0.00	0.00	0.00
30.00	0.00	0.00	0.00	0.00	0.00

**Table 5.9. Contribution of Each Load Level Step to the Annual Indices (in %) Using the 15-Step Load Model for the SPCS**

Load level (%)	Load duration (%)	ENLC (%)	PLC EDLC (%)	EENS EDNS (%)	PBII (%)
100.00	0.22	0.49	0.61	0.87	0.45
95.00	1.10	2.02	2.30	2.89	1.69
90.00	3.59	6.12	6.85	7.51	4.77
85.00	7.51	8.73	10.61	12.73	8.87
80.00	8.33	9.68	11.78	11.00	8.59
75.00	8.21	9.03	11.10	8.76	7.87
70.00	11.02	9.92	8.81	10.78	10.51
65.00	12.18	10.96	9.73	11.06	11.62
60.00	9.67	8.70	7.73	8.11	9.22
55.00	11.88	10.69	9.49	9.13	11.33
50.00	12.84	11.56	10.26	8.97	12.25
45.00	9.79	8.81	7.82	6.15	9.33
40.00	3.50	3.15	2.80	1.96	3.34
35.00	0.15	0.13	0.12	0.07	0.14
30.00	0.00	0.00	0.00	0.00	0.00

contribute more than 90% of the annual indices. The duration of these four steps is only 12.42% of the year. The load level steps lower than 65% of the annual peak load make virtually no contribution to the calculated annual indices. The duration covered by these steps is 47.83% of the year. In the case of the SPCS, the contributions of each load level step to the total calculated annual indices are generally related to the durations of each load level step and do not directly depend on the load levels. All load level steps higher than 30% of the annual peak load contribute to the total calculated annual indices.

### 5.3.4. Effect of a Nonuniform Load Increment Step Model

The effect of the high load levels in the IEEE RTS suggests that if the multistep model of the load duration curve has relatively small load increments at the high load levels and relatively large load increments at the low load levels, then the accuracy of the calculated annual indices will be increased. The load curve was divided into 15 steps with a load increment for each step of 2% for the first 10 steps and 5% for the following 4 steps. The last step includes all load points lower than the load level of this step. The annual indices of the two test systems were recalculated and are shown in Table 5.10. The percentage values in brackets give the differences in the results when using the 15-step nonuniform load increment model compared with those obtained using the 70-step load model. It can be seen, by compar-

**Table 5.10. Annual Indices of the Two Test Systems Using the 15-Step Non-uniform Load Increment Model of the Load Curve**

Index	IEEE RTS annual indices	SPCS annual indices
ENLC	0.92368 (14%)	1.18735 (1%)
EDLC	11.70195 (14%)	2.73774 (2%)
PLC	0.00134 (15%)	0.00031 (0%)
EDNS	0.15568 (19%)	0.01104 (1%)
EENS	1360.02258 (19%)	96.47681 (9%)
BPII	0.03785 (18%)	0.02475 (8%)
BPECI	0.47720 (19%)	0.05352 (9%)
BPACI	116.79818 (4%)	37.56713 (7%)
MBPCI	0.00005 (0%)	0.00001 (0%)
SI	28.63250 (19%)	3.21143 (9%)

ing the results in Table 5.10 with those given in Tables 5.6 and 5.7 obtained using the 15-step uniform load increment model, that using the nonuniform load increment model considerably improves the accuracy of the calculated annual indices for the IEEE RTS. It does not result in significant differences in the SPCS study. The use of a nonuniform load model should therefore be considered when analyzing a system with high RGTAI values.

## 5.4. GENERATING UNIT DERATED STATES

### 5.4.1. Sampling Multiderated States

Large-size generating units can operate in one or more derated states and many electric power utilities are now using multistate models. In the enumeration method, the recognition of derated states in the modeling of large generating units can create a considerable increase in the number of generation contingency states and therefore result in a significant increase in overall solution time. The conventional approach in both generating capacity and composite generation and transmission system reliability studies is to use a two-state model for generating units and to replace the forced unavailability by a derating-adjusted forced unavailability. It has been shown in Chapter 4, however, that the use of a two-state equivalent can result in a pessimistic appraisal of generating capacity adequacy. This is also the case in composite system reliability assessment. One of the advantages of the system state sampling method is that multistates of generating units can be incorporated in the analysis without a significant increase in computing time.

The state sampling technique including one derated state is given in equation (4.12). This technique can be extended to the case of multiderated states. Let  $S_i$  denote the state of the  $i$ th generating unit and  $FU_i$  be its forced unavailability. The probabilities of two derated states are expressed by  $PD1_i$  and  $PD2_i$ . A uniformly distributed random number  $U_i$  is drawn in  $[0, 1]$  for the  $i$ th generating unit,

$$S_i = \begin{cases} 0 & (\text{up state}) & \text{if } U_i \geq PD1_i + PD2_i + FU_i \\ 1 & (\text{down state}) & \text{if } PD1_i + PD2_i \leq U_i < PD1_i + PD2_i + FU_i \\ 2 & (\text{derated state 2}) & \text{if } PD1_i \leq U_i < PD1_i + PD2_i \\ 3 & (\text{derated state 1}) & \text{if } 0 \leq U_i < PD1_i \end{cases} \quad (5.26)$$

More derated states can be simulated similarly.

## 5.4.2. Case Studies

In order to illustrate the effect of multiderated-state generating unit representations, two test systems (IEEE RTS and RBTS) are examined. The RBTS is a small educational test system developed at the University of Saskatchewan.<sup>(35)</sup> The complete data for the two systems are given in Appendix A. In the case of the IEEE RTS, the two 400-MW and the 350-MW generating units have been given a derated state at 50% capacity. The derating data are the same as those given in Tables 4.2 and 4.10. In the case of the RBTS, the two 40-MW thermal units have been given a more detailed state representation. Figure 5.1a shows a four-state representation, while Figure 5.1b, c, and d provide three quasi-equivalent models. It has been assumed that there are no transitions between the derated states and the down state. In both systems, the state probabilities of the derated models are such that the derating-adjusted two-state model data are identical to the original two-state model data given in Appendix A.

The annualized system indices of the IEEE RTS considering the three-state and the derating-adjusted two-state model for the 400-MW and 350-MW generating units are given in Table 5.11. The percentage values in parentheses are the differences in the indices using the derating-adjusted two-state model as compared to those obtained using the three-state model. It can be seen that the derating-adjusted two-state model leads to a pessimistic evaluation of system adequacy.

The annualized system indices and bus indices of the RBTS considering the two-state, the two three-state, and the four-state models for the 40-MW thermal generating units are given in Tables 5.12 and 5.13, respectively. The percentage values are the differences in the indices using the two-state and the two three-state models compared to those obtained using the four-state model. The results in Tables 5.12 and 5.13 indicate that if the four-state model for the 40-MW generating units is replaced by the three-state model (b) in which the lower-capacity derated state is eliminated, then the results are more optimistic (except for the average index BPACI). If the three-state model (c), in which the larger-capacity derated state is eliminated, is used, then the results are more pessimistic (except for BPACI). These replacements, however, are unnecessary in the presented method because the computing time using the four-state model is almost the same as that using the three-state models. If the derating-adjusted two-state model for the 40-MW generating units is used to replace the four-state model or the three-state models, the results are considerably more pessimistic (except for BPACI), although less computing time is needed. The quasi-equivalent models generally result in greater differences in bus indices than those obtained on a system basis. The impact is quite different, however, at different buses.

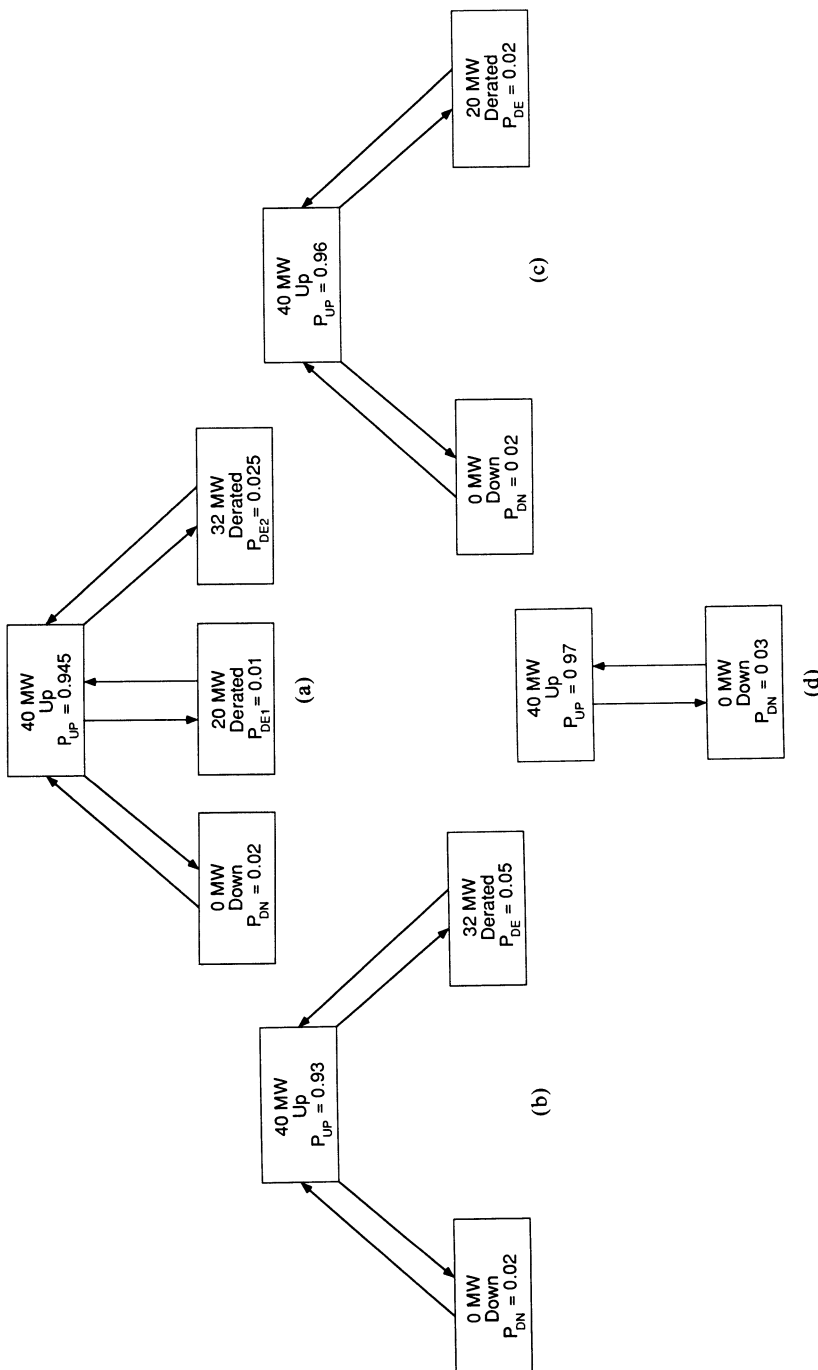


**Figure 5.1.** Two-, three-, and four-state models for a 40-MW thermal generating unit in the RBTS.

**Table 5.11. Annualized System Indices for the IEEE RTS**

Index	Three-state model	Two-state model
ENLC	47.38287	54.75342 (16%)
EDLC	630.73920	698.88000 (11%)
PLC	0.07220	0.08000 (11%)
EDNS	10.32736	13.97045 (35%)
EENS	90219.83594	122045.88281 (35%)
BPII	2.49359	3.33652 (34%)
BPECI	31.65608	42.82311 (35%)
BPACI	149.98528	173.67123 (16%)
MBPCI	0.00362	0.00490 (35%)
SI	1899.36487	2569.38672 (35%)
CPU (min)	0.740	0.623

**Table 5.12. Annualized System Indices for the RBTS**

Index	Four-state model (a)	Three-state model (b)	Three-state model (c)	Two-state model (d)
ENLC	4.33496	4.11613 (-5%)	4.59188 (6%)	5.27252 (22%)
EDLC	76.87680	69.01440 (-10%)	85.43808 (11%)	91.20384 (19%)
PLC	0.00880	0.00790 (-10%)	0.00978 (11%)	0.01044 (19%)
EDNS	0.09605	0.09015 (-6%)	0.10189 (6%)	0.12429 (29%)
EENS	839.11414	787.57202 (-6%)	890.13239 (6%)	1085.81873 (29%)
BPII	0.30090	0.29236 (-3%)	0.31019 (3%)	0.38169 (27%)
BPECI	4.53575	4.25715 (-6%)	4.81153 (6%)	5.86929 (29%)
BPACI	12.84121	13.13995 (+2%)	12.49707 (-3%)	13.39275 (4%)
MBPCI	0.00052	0.00049 (-6%)	0.00055 (6%)	0.00067 (29%)
SI	272.14511	255.42876 (-6%)	288.69156 (6%)	352.15738 (29%)
CPU (min)	0.326	0.352	0.307	0.187

## 5.5. REGIONAL WEATHER EFFECTS

### 5.5.1. General Concepts

The failure rate of an outdoor component such as a transmission line is a function of the weather environment to which the line is exposed. The failure rate of a transmission line can be much higher in adverse weather than in normal weather, and if related transmission components

**Table 5.13. Annualized Bus Indices for the RBTS**

Index	Bus No.	Four-state model (a)	Three-state model (b)	Three-state model (c)	Two-state model (d)
PLC	2	0.00012	0.00012 (0%)	0.00016 (33%)	0.00024 (100%)
	3	0.00152	0.00142 (-7%)	0.00152 (0%)	0.00246 (62%)
	4	0.00162	0.00162 (0%)	0.00166 (3%)	0.00242 (49%)
	5	0.00716	0.00614 (-14%)	0.00832 (16%)	0.00898 (25%)
	6	0.00870	0.00780 (-10%)	0.00968 (11%)	0.01034 (19%)
ENLC	2	0.06915	0.06915 (0%)	0.08805 (27%)	0.14550 (110%)
	3	0.82640	0.78659 (-5%)	0.82422 (0%)	1.26890 (54%)
	4	0.71569	0.72192 (1%)	0.74030 (3%)	1.11126 (55%)
	5	2.82644	2.56493 (-9%)	3.15742 (12%)	3.82090 (35%)
	6	4.22666	4.00783 (-5%)	4.48357 (6%)	5.16381 (22%)
EDNS	2	0.00048	0.00048 (0%)	0.00064 (33%)	0.00080 (66%)
	3	0.01656	0.01582 (-5%)	0.01640 (-1%)	0.02618 (58%)
	4	0.01242	0.01208 (-3%)	0.01252 (1%)	0.01940 (56%)
	5	0.01250	0.01148 (-8%)	0.01394 (12%)	0.01688 (35%)
	6	0.05409	0.05029 (-7%)	0.05839 (8%)	0.06103 (13%)
EENS	2	4.19328	4.19328 (0%)	5.59104 (33%)	6.98879 (67%)
	3	144.66393	138.19930 (-5%)	143.26617 (-1%)	228.70407 (58%)
	4	108.50108	105.53084 (-3%)	109.37469 (1%)	169.47839 (56%)
	5	109.19910	100.28857 (-8%)	121.77868 (12%)	147.46265 (35%)
	6	472.55692	439.36014 (-7%)	510.12170 (8%)	533.18488 (13%)

are exposed to the same adverse weather condition, then the phenomenon known as adverse weather failure bunching can occur.<sup>(3)</sup> It is therefore necessary to recognize these effects in order to incorporate weather considerations in the transmission system model for composite system adequacy evaluation. Markov state weather models,<sup>(36,37)</sup> have been developed, which basically assume that the entire transmission system is exposed to the same weather conditions. This obviously may not be valid for an actual transmission system and particularly one spread out over a large geographical area. The exponential distribution assumptions required to create a stationary Markov process also may not be valid in connection with adverse weather modeling and can become unduly restrictive. The Monte Carlo based method presented here can recognize regional weather aspects including those situations in which transmission lines traverse several geographical regions encompassing different weather conditions. Exponential distribution assumptions of weather durations are not required in the proposed method. This therefore relaxes the traditional assumption associated with a Markov process. The method can be used to analyze practical large-scale power systems.

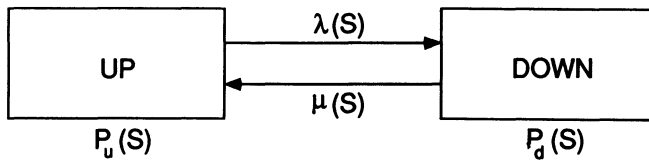


**Figure 5.2.** Transmission line model considering weather conditions.

### 5.5.2. Basic Transmission Line Model Recognizing Weather Conditions

This transmission line model is shown in Figure 5.2. This is not the conventional two-state model because the failure rate, repair rate, and probabilities of residing in the up state and down state are functions of weather states expressed by  $S$  in Figure 5.2. It is convenient in terms of data collection to divide weather into two conditions: normal and adverse. It is, however, possible that one segment of a transmission line is exposed to normal weather while its other part is exposed to adverse weather. Therefore, a specific transmission line can reside in multiple and quite different weather environments. The model shown in Figure 5.2 is a multiple-state model discriminated by weather states  $S$ . In this model, transitions between weather conditions are not specifically shown. Failure bunching of multiple facilities depends on the probability of adverse weather and the failure rates and repair rates of those transmission lines in adverse weather, but not specifically on the transitions between weather conditions.

It should be appreciated that the weather and therefore the stress levels that transmission facilities can encounter are in fact associated with a continuous distribution. The difficulties of collecting the required data are enormous and therefore, it is reasonable in the first instance to recognize only two steps, i.e., normal and adverse. In terms of the model, however, there are no practical difficulties associated with incorporating as many steps or stress levels as the data are capable of supporting. In regard to the state representation, assume that  $S=0$  indicates the normal weather condition and  $S=1$  indicates the adverse weather condition. A transmission line therefore is associated with two failure rates  $\lambda(0)$  and  $\lambda(1)$  and two repair rates  $\mu(0)$  and  $\mu(1)$ . At the present time, most data collection schemes do not recognize  $\lambda(0)$  and  $\lambda(1)$  but are only responsive to the average value  $\lambda$  of the failure rate expressed in failures per calendar year. Using the concept of expectation,

$$\lambda = (1 - U)\lambda(0) + U\lambda(1) \quad (5.27)$$

where  $U$  is the fraction of time that a line spends in adverse weather.

The proportion of failures  $F$  occurring in adverse weather reflects the degree of potential failure bunching. If quantities  $U$  and  $F$  are known,  $\lambda(0)$  and  $\lambda(1)$  can be evaluated from:

$$\lambda(0) = \lambda(1 - F)/(1 - U) \quad (5.28)$$

and

$$\lambda(1) = \lambda F/U \quad (5.29)$$

In the following case studies,  $U$  and  $F$  are specified rather than  $\lambda(0)$  and  $\lambda(1)$ . The effects of different degrees of failure bunching on the system behavior can be illustrated by considering different values of  $F$  between 0 and 1.

### 5.5.3. Sampling Regional Weather States

The physical area of a given transmission system can be divided into several regions according to their geographical and meteorological characteristics. Figure 5.3 shows a representative geographical five-region division. Region-divided weather states can be recognized in the following ways: a single region encounters adverse weather; two adjacent regions exist in adverse weather; three adjacent regions encounter adverse weather; etc. In the case of a five-region division, the possible maximum number of region-divided weather states is  ${}_5C_0 + {}_5C_1 + {}_5C_2 + {}_5C_3 + {}_5C_4 + {}_5C_5 = 32$ . The possible maximum number of region-divided weather states increases considerably as the number of regions increases. The geographical range covered by the same weather environment is generally relatively large compared to the area

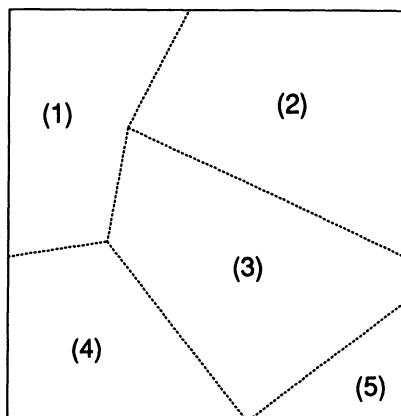


**Figure 5.3.** A geographic five-region division.

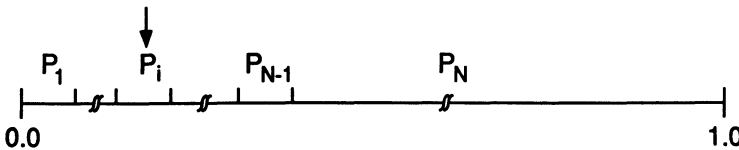


**Figure 5.4.** Sampling of region-divided weather states.

of the total transmission system, and therefore it is unnecessary to divide a system into a great number of regions. In those cases in which the number of regions is relatively large, many region-divided weather states do not exist in practice. For example, in Figure 5.3, the probability that Regions (1) and (5) are simultaneously exposed to adverse weather and Regions (2), (3), and (4) to normal weather may be effectively zero.

Given the criteria for discriminating between normal and adverse weather, the probabilities of each region-divided weather state can be obtained from the available meteorological records. The number of regions used may depend more on the existence of adequate data than on the actual transmission systems. Sensitivity analysis of the system adequacy may assist in deciding whether to pursue the collection of additional data. Assume that there are  $N$  region-divided weather states whose probabilities are not zero and that their probabilities are expressed by  $P_1, P_2, \dots, P_N$ . Let  $P_1, \dots, P_{N-1}$  correspond to the states in which at least one region undergoes adverse weather and  $P_N$  to the state of all regions in normal weather. Obviously,  $P_N$  is much larger than the summation of all  $P_i$  ( $i = 1, \dots, N-1$ ). The values of  $P_1, \dots, P_N$  are set sequentially in interval  $[0, 1]$  as shown in Figure 5.4. A uniformly distributed random number between  $[0, 1]$  can be drawn. If the random number falls in the  $i$ th region-divided weather state corresponding to  $P_i$ , the transmission system is in the  $i$ th region-divided weather state for this sample. It can be seen that the sampling efficiency is the same regardless of the number of region-divided weather states, i.e., a large number of region-divided weather states does not materially affect the computational requirements.

#### 5.5.4. Determination of Transmission Line Forced Unavailability and Repair Time with Regional Weather Effects

After obtaining a sample of the region-divided weather states, the forced unavailabilities  $FU$  and repair times  $r$  of transmission lines in this weather state can be determined. If the entire transmission line is in the region

exposed to adverse weather, its transition rates are  $\lambda(1)$  and  $\mu(1)$  and thus  $FU = \lambda(1)/[\lambda(1) + \mu(1)]$  and  $r = 1/\mu(1)$ . If the entire transmission line is in the region exposed to normal weather, its transition rates are  $\lambda(0)$  and  $\mu(0)$  and thus  $FU = \lambda(0)/[\lambda(0) + \mu(0)]$  and  $r = 1/\mu(0)$ . If the transmission line traverses several regions undergoing different weather conditions, the following method can be used to calculate its FU and  $r$ .

Assume that a transmission line traverses Regions (1) and (2), where Region (1) is in adverse weather and Region (2) in normal weather, and that  $R$  is the percentage of the line length in Region (1). Considering that the failure frequency of a line is approximately equal to its failure rate and the two sections of the line in Regions (1) and (2) are in series, the FU of the line is given by

$$FU = FU_1 + FU_2 - FU_1 FU_2 \quad (5.30)$$

where

$$FU_1 = \lambda(1)R/[\lambda(1)R + \mu(1)] \quad \text{and} \quad FU_2 = \lambda(0)(1-R)/[(\lambda(0)(1-R) + \mu(0))]$$

The contribution due to the  $FU_1 FU_2$  term is quite small and, in practice, it can be neglected in equation (5.30). The equivalent repair time of the line is given by

$$r = \frac{r(1)\lambda(1)R + r(0)\lambda(0)(1-R)}{\lambda(1)R + \lambda(0)(1-R)} \quad (5.31)$$

where  $r(0) = 1/\mu(0)$  and  $r(1) = 1/\mu(1)$ .

The calculation is similar in those cases in which a transmission line traverses more than two regions. After the FU and  $r$  of each line associated with a weather state sample are determined, the basic evaluation method can be utilized to assess the adequacy of the composite system.

### 5.5.5. Test System and Data

In order to illustrate the basic procedure, case studies were conducted using the educational test system (RBTS). In addition to the basic system data given in Appendix A.2, the data required to incorporate weather effects using the regional division shown in Figure 5.5 are as follows.

The overall area encompassed by the transmission system is divided into the three regions shown in Figure 5.5. Lines 2 and 3 are in Region (1) and Lines 6, 7, 8, and 9 are in Region (3). 30% of Line 1 is in Region (1)

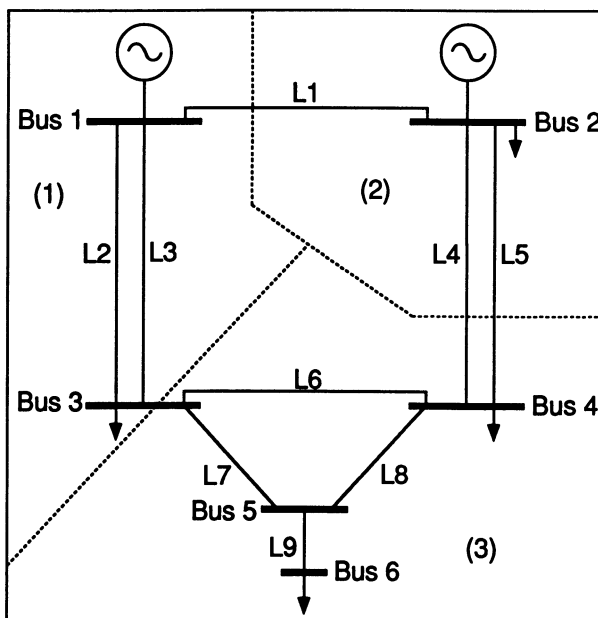


**Figure 5.5.** Geographic three-region division for the RBTS.

and 70% in Region (2). 20% of Lines 4 and 5 are in Region (3) and 80% in Region (2). The number of region-divided weather states is 8. The weather-related probabilities associated with these regions are given in Table 5.14 in which (0) denotes the state of three regions in normal weather, (1) or (2) or (3) the state of only one region in adverse weather, (1)+(2) or (1)+(3)

**Table 5.14. Region-Divided Weather-State Probabilities**

Weather state	Probabilities
(0)	0.968
(1)	0.004
(2)	0.004
(3)	0.004
(1)+(2)	0.006
(1)+(3)	0.006
(2)+(3)	0.006
(1)+(2)+(3)	0.002
Total	1.000

or (2) + (3) the state of two regions in adverse weather, and (1) + (2) + (3) the state of all three regions in adverse weather.

The percentage  $U$  of the adverse weather duration for each line can be calculated from the probabilities of region-divided weather states and the regions traversed by transmission lines. Generally, the values of  $U$  for different lines may differ. In the case of the data given above, however, all lines have the same  $U$  value, i.e., 0.018. Repair is generally more difficult during adverse weather than during normal weather and, in many cases, repair cannot proceed or commence until an adverse weather period ends. It has therefore been arbitrarily assumed that the expected repair time of a line in adverse weather is 1.5 times that in normal weather.

### 5.5.6. Case Studies

**(a) Comparison between Different Weather-Related Representations.** The effect on the adequacy indices of different weather-related representations can clearly be seen in the following analysis. In these studies, the proportion of failures in adverse weather,  $F$ , is assumed to be 0.4. Given the values of  $F$  and  $U$ , values of  $\lambda(0)$  and  $\lambda(1)$  can be calculated from the values of  $\lambda$  given in the basic data in term of equations (5.28) and (5.29). A comparison between the results obtained considering weather effects and those obtained without considering weather effects clearly illustrates their contributions. Two distinct weather models were considered: in Case 1, regional weather differences are recognized using the data of Table 5.14 and, in Case 2, it is assumed that the entire transmission system is exposed to common weather conditions. In both cases, the probabilities of the entire transmission system being in the normal weather environment are the same. The annualized and annual system and bus indices for the RBTS in the three cases are given in Tables 5.15 to 5.18. The percentage values in parentheses are the differences in the indices considering weather effects compared to those without weather effects.

It can be seen that the basic two-state model which does not recognize weather effects can lead to underestimation of the inadequacy indices, especially for the annual indices of some buses. The assumption that the entire transmission system is exposed to a common weather condition can lead to overestimation of the failure bunching effect. Weather effects are generally larger for the annual indices than for the annualized values. This is basically due to the fact that generation outages have a relatively large impact on the system adequacy at higher load levels than at lower load periods and are not affected by weather conditions. The impact of transmission components is not quite as variable and responds to the adverse weather

**Table 5.15. Annualized System Indices with and without Weather Effects for the RBTS**

Index	Without weather effects	Recognition of regional weather	Entire system in common weather
ENLC	5.27252	6.20917 (18%)	8.40546 (59%)
EDLC	91.20384	96.44544 (6%)	106.40448 (17%)
PLC	0.01044	0.01104 (6%)	0.01218 (17%)
EDNS	0.12429	0.13624 (10%)	0.16476 (33%)
EENS	1085.81873	1190.15723 (10%)	1439.33862 (33%)
BPII	0.38169	0.48665 (28%)	0.78044 (104%)
BPECI	5.86929	6.43328 (10%)	7.78021 (33%)
MBPCI	0.00067	0.00074 (10%)	0.00089 (33%)
SI	352.15738	385.99692 (10%)	466.81250 (33%)
CPU (min)	0.187	0.294	0.303

**Table 5.16. Annualized Bus Indices with and without Weather Effects for the RBTS**

Index	Bus No.	Without weather effects	Recognition of regional weather	Entire system in common weather
PLC	2	0.00024	0.00024 (0%)	0.00024 (0%)
	3	0.00246	0.00280 (14%)	0.00346 (41%)
	4	0.00242	0.00246 (2%)	0.00270 (12%)
	5	0.00898	0.00922 (3%)	0.00964 (8%)
	6	0.01034	0.01086 (5%)	0.01196 (16%)
	7	0.01034	0.01086 (5%)	0.01196 (16%)
ENLC	2	0.14550	0.14823 (2%)	0.15264 (5%)
	3	1.26890	1.82331 (44%)	3.06077 (141%)
	4	1.11126	1.18205 (6%)	1.67099 (50%)
	5	3.82090	4.21072 (10%)	5.13438 (34%)
	6	5.16381	5.98878 (16%)	8.06009 (56%)
	7	5.16381	5.98878 (16%)	8.06009 (56%)
EDNS	2	0.00080	0.00080 (0%)	0.00080 (0%)
	3	0.02618	0.03105 (19%)	0.04248 (62%)
	4	0.01940	0.02004 (3%)	0.02323 (20%)
	5	0.01688	0.01860 (10%)	0.02128 (26%)
	6	0.06103	0.06575 (8%)	0.07698 (26%)
	7	0.06103	0.06575 (8%)	0.07698 (26%)
EENS	2	6.98879	6.98879 (0%)	6.98879 (0%)
	3	228.70407	271.23013 (19%)	371.06458 (62%)
	4	169.47839	175.06944 (3%)	202.89746 (20%)
	5	147.46265	162.48865 (10%)	185.90128 (26%)
	6	533.18488	574.37982 (8%)	672.48651 (26%)
	7	533.18488	574.37982 (8%)	672.48651 (26%)

**Table 5.17. Annual System Indices with and without Weather Effects for the RBTS**

Index	Without weather effects	Recognition of regional weather	Entire system in common weather
ENLC	1.27622	1.61910 (27%)	2.62248 (105%)
EDLC	12.35270	14.34242 (16%)	19.09538 (55%)
PLC	0.00141	0.00164 (16%)	0.00219 (55%)
EDNS	0.01786	0.02128 (19%)	0.02953 (65%)
EENS	155.99113	185.91623 (19%)	257.94995 (65%)
BPII	0.08771	0.11599 (32%)	0.20105 (129%)
BPECI	0.84320	1.00495 (19%)	1.39432 (65%)
MBECI	0.00010	0.00012 (20%)	0.00016 (60%)
SI	50.59172	60.29716 (19%)	83.65944 (65%)
CPU(min)	2.75	4.39	4.42

**Table 5.18. Annual Bus Indices with and without Weather Effects for the RBTS**

Index	Bus No.	Without weather effects	Recognition of regional weather	Entire system in common weather
PLC	2	0.00002	0.00002 (0%)	0.00002 (0%)
	3	0.00007	0.00009 (29%)	0.00018 (157%)
	4	0.00009	0.00010 (11%)	0.00017 (89%)
	5	0.00017	0.00023 (35%)	0.00033 (94%)
	6	0.00141	0.00163 (16%)	0.00213 (51%)
ENLC	2	0.01101	0.01093 (0%)	0.01098 (0%)
	3	0.04219	0.08496 (101%)	0.26133 (519%)
	4	0.04827	0.07341 (52%)	0.23894 (395%)
	5	0.08410	0.18155 (116%)	0.38903 (363%)
	6	1.26807	1.59510 (26%)	2.50759 (98%)
EDNS	2	0.00005	0.00005 (0%)	0.00005 (0%)
	3	0.00046	0.00061 (33%)	0.00162 (252%)
	4	0.00053	0.00062 (17%)	0.00153 (189%)
	5	0.00055	0.00112 (104%)	0.00170 (209%)
	6	0.01627	0.01889 (16%)	0.02462 (51%)
EENS	2	0.43561	0.43561 (0%)	0.43561 (0%)
	3	4.01239	5.31128 (32%)	14.16684 (253%)
	4	4.66888	5.38681 (15%)	13.39328 (187%)
	5	4.78188	9.79080 (105%)	14.87348 (211%)
	6	142.09238	164.99171 (16%)	215.08070 (51%)

failure bunching phenomenon. Weather impacts on the bus indices are not the same at different load buses. At Bus 2, which is connected directly to generators, the bus indices are not generally affected by transmission line failures and therefore not by weather conditions. (The relatively insignificant difference in ENLC is due to the fact that the repair time in adverse weather is assumed to be larger than that in normal weather.) At those load buses connected to generators through transmission lines, the bus indices are sensitive to weather conditions but the degree of sensitivity varies from bus to bus. At a very sensitive bus such as Bus 3, the bus indices obtained assuming that the entire system is exposed to common weather conditions can be quite pessimistic, particularly in the case of the annual bus indices.

**(b) Effects of the Proportion of Failures in Adverse Weather.** The proportion of failures in adverse weather is not the same in different geographical areas. The proportion reflects the degree of failure bunching and therefore a large proportion value indicates that weather has large effects on composite system inadequacy indices. The variations in annualized and annual EENS system indices with the proportion of failures in adverse weather  $F$  are shown in Figures 5.6 and 5.7, respectively. The variations in other system indices are similar. The EENS values in the figures are

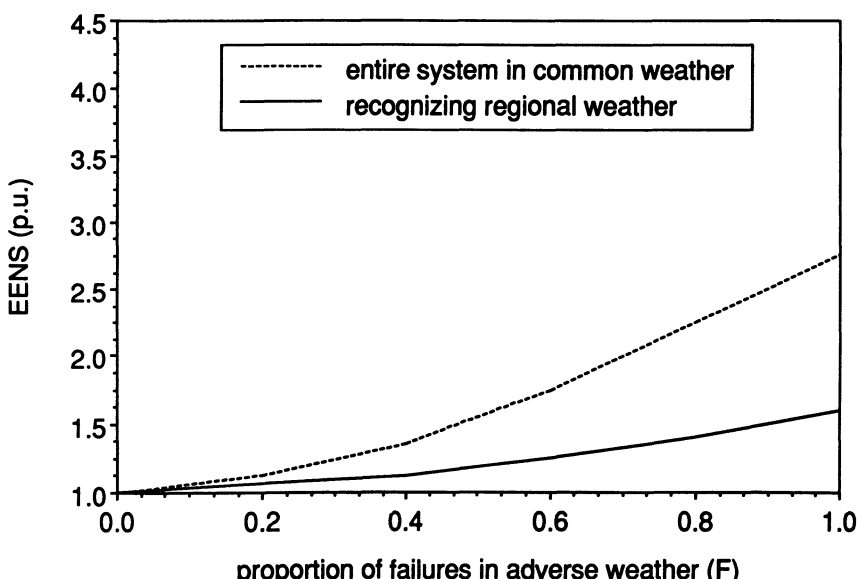


**Figure 5.6.** Variations in the annualized EENS system index with the proportion of failures in adverse weather.

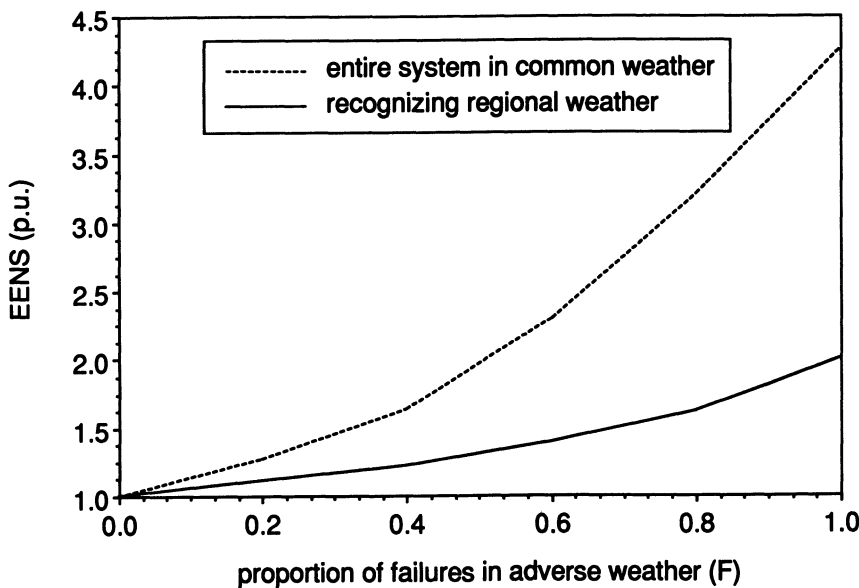


**Figure 5.7.** Variations in the annual EENS system index with the proportion of failures in adverse weather.

expressed in per unit of the annualized or annual EENS obtained without considering weather effects. The upper curve corresponds to the cases of the entire system in common weather conditions and the lower one to the cases of recognizing regional weather aspects. It can be seen that the proportion of failures in adverse weather has larger effects on annual system indices than on annualized system indices and a large value of  $F$  can result in increased overestimation of inadequacy with the assumption that the entire system is in a common weather condition.

## 5.6. TRANSMISSION LINE COMMON CAUSE OUTAGES

### 5.6.1. General Concepts

A common cause outage is an event having an external cause with multiple failure effects where the effects are not consequences of each other. The most obvious example of a common cause outage is the failure of a transmission tower supporting two or more transmission circuits. The

probability of a common cause outage can be many times larger than that of a similar event due to two or more simultaneous independent outages. The effect of the common cause outage on bus reliability indices can therefore be significant compared with the effect of second- and higher-order independent outages.

It should be noted that a common cause outage and a common environment outage are completely different concepts. The weather effects discussed in the previous section are associated with a common environment outage but not a common cause outage. Although a common weather condition affects the failure rates of the components, the actual failure process of overlapping outages still assumes the component failures to be independent with the independent failure rates enhanced because of the common environment.

Two of the most useful models for representing a second-order overlapping failure event including common cause failures are shown in Figure 5.8 in which  $\lambda_c$  represents the common cause failure rate. The difference between these two models is that one has a single down state (Figure 5.8a) and the other has two separate down states: one associated with independent failures, the other associated with common cause failures (Figure 5.8b).

In the system state sampling method, transmission line states are modeled using two-state (up and down) random variables. Transmission line common outages can be considered in such a way that a fictitious or physically existing third component, not included in the system, can outage both of these components if it should fail. Transmission line common outages

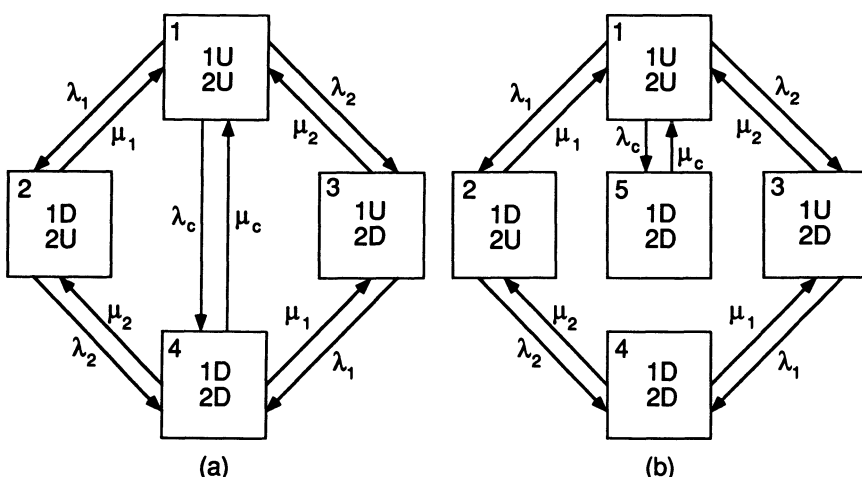


Figure 5.8. Common cause failure models.

therefore can be simulated by a separate two-state random variable using one of the two models shown in Figure 5.8. When this separate random number falls into the segment in the interval [0, 1] corresponding to the failure probability of the third component, the common outage event is considered to occur in that sampling.

## 5.6.2. Case Studies

The likelihood of multiple transmission line failures can be enhanced by common cause failures. A common cause failure, as noted earlier, is a fundamentally different event from that associated with weather-related failure bunching. It should be clearly appreciated, however, that the common cause event may itself be weather related. If this is the case, suitable data can be inserted in the modeling process to recognize the variable nature of the common cause failure phenomenon. In order to illustrate the effects of common cause failures and compare these effects with those of weather, the RBTS was used to conduct the following studies. Line pair (2,3) and Line pair (4,5) in Figure 5.5 are assumed to be susceptible to common cause failures using the data given in Appendix A.2. The calculated results obtained considering only common cause failures and considering both common cause failures and weather effects are given in Tables 5.19 to 5.22. The percentage values in parentheses are the differences in the indices compared to those obtained without considering any specified effect (see “without weather effects” columns in Tables 5.15 to 5.18).

**Table 5.19. Annualized System Indices Considering Common Cause Failures and Weather Effects for the RBTS**

Index	Only common cause failures	Common cause failures and recognizing regional weather	Common cause failures and entire system in common weather
ENLC	5.73303 (9%)	6.63230 (26%)	8.82859 (67%)
EDLC	93.30048 (2%)	98.36736 (8%)	108.32640 (19%)
PLC	0.01068 (2%)	0.01126 (8%)	0.01240 (19%)
EDNS	0.12989 (5%)	0.14138 (14%)	0.16990 (37%)
EENS	1134.74438 (5%)	1235.06079 (14%)	1484.24219 (37%)
BPII	0.43915 (15%)	0.53981 (41%)	0.83360 (118%)
BPECI	6.13375 (5%)	6.67600 (14%)	8.02293 (37%)
MBPCI	0.00070 (5%)	0.00076 (13%)	0.00092 (37%)
SI	368.02518 (5%)	400.56024 (14%)	481.37582 (37%)
CPU (min)	0.205	0.320	0.339

**Table 5.20. Annualized Bus Indices Considering Common Cause Failures and Weather Effects for the RBTS**

Index	Bus No.	Only common cause failures	Common cause failures and recognizing regional weather	Common cause failures and entire system in common weather
PLC	2	0.00024 (0%)	0.00024 (0%)	0.00024 (0%)
	3	0.00270 (10%)	0.00302 (23%)	0.00368 (50%)
	4	0.00242 (0%)	0.00246 (2%)	0.00270 (12%)
	5	0.00922 (3%)	0.00944 (5%)	0.00986 (10%)
	6	0.01058 (2%)	0.01108 (7%)	0.01218 (18%)
ENLC	2	0.14886 (2%)	0.15159 (4%)	0.15600 (7%)
	3	1.71941 (36%)	2.23644 (76%)	3.47390 (174%)
	4	1.12462 (1%)	1.19541 (8%)	1.68435 (52%)
	5	4.28141 (12%)	4.63384 (21%)	5.55750 (45%)
	6	5.62432 (9%)	6.41191 (24%)	8.48322 (64%)
EDNS	2	0.00080 (0%)	0.00080 (0%)	0.00080 (0%)
	3	0.03026 (16%)	0.03479 (33%)	0.04622 (77%)
	4	0.01940 (0%)	0.02004 (3%)	0.02323 (20%)
	5	0.01752 (4%)	0.01920 (14%)	0.02188 (30%)
	6	0.06191 (1%)	0.06655 (9%)	0.07778 (27%)
EENS	2	6.98879 (0%)	6.98879 (0%)	6.98879 (0%)
	3	264.34692 (16%)	303.90277 (33%)	403.73721 (77%)
	4	169.47839 (0%)	175.06944 (3%)	202.89746 (20%)
	5	153.05426 (4%)	167.73074 (14%)	191.14337 (30%)
	6	540.87604 (1%)	581.36859 (9%)	679.47522 (27%)

**Table 5.21. Annual System Indices Considering Common Cause Failures and Weather Effects for the RBTS**

Index	Only common cause failures	Common cause failures and recognizing regional weather	Common cause failures and entire system in common weather
ENLC	1.29873 (2%)	1.63977 (28%)	2.64315 (107%)
EDLC	12.45566 (1%)	14.43680 (17%)	19.18976 (55%)
PLC	0.00143 (1%)	0.00165 (17%)	0.00220 (56%)
EDNS	0.01797 (1%)	0.02138 (20%)	0.02963 (66%)
EENS	156.96021 (1%)	186.80725 (20%)	258.84094 (66%)
BPII	0.08886 (1%)	0.11705 (33%)	0.20211 (130%)
BPECI	0.84843 (1%)	1.00977 (20%)	1.39914 (66%)
MBPCI	0.00010 (0%)	0.00012 (20%)	0.00016 (60%)
SI	50.90601 (1%)	60.58614 (20%)	83.94841 (66%)
CPU (min)	3.02	4.59	4.64

**Table 5.22. Annual Bus Indices Considering Common Cause Failures and Weather Effects for the RBTS**

Index	Bus No.	Only common cause failures	Common cause failures and recognizing regional weather	Common cause failures and entire system in common weather
PLC	2	0.00002 (0%)	0.00002 (0%)	0.00002 (0%)
	3	0.00008 (14%)	0.00010 (43%)	0.00020 (186%)
	4	0.00009 (0%)	0.00010 (11%)	0.00017 (89%)
	5	0.00018 (6%)	0.00023 (35%)	0.00033 (94%)
	6	0.00142 (1%)	0.00163 (16%)	0.00214 (52%)
ENLC	2	0.01102 (0%)	0.01093 (0%)	0.01099 (0%)
	3	0.06431 (52%)	0.10524 (149%)	0.28162 (568%)
	4	0.04871 (1%)	0.07385 (53%)	0.23938 (396%)
	5	0.09303 (11%)	0.19038 (126%)	0.39787 (373%)
	6	1.28313 (1%)	1.60834 (27%)	2.52083 (99%)
EDNS	2	0.00005 (0%)	0.00005 (0%)	0.00005 (0%)
	3	0.00053 (15%)	0.00067 (46%)	0.00168 (265%)
	4	0.00053 (0%)	0.00062 (17%)	0.00153 (188%)
	5	0.00056 (2%)	0.00114 (107%)	0.00172 (213%)
	6	0.01629 (0%)	0.01891 (16%)	0.02465 (52%)
EENS	2	0.43561 (0%)	0.43561 (0%)	0.43561 (0%)
	3	4.59373 (14%)	5.84676 (46%)	14.70232 (266%)
	4	4.66888 (0%)	5.38681 (15%)	13.39328 (187%)
	5	4.91365 (3%)	9.92182 (107%)	15.00449 (214%)
	6	142.34833 (0%)	165.21625 (16%)	215.30522 (52%)

It can be seen that the effects on the system adequacy indices of common cause failures are smaller than those of weather in the analysis given. A single common cause failure event involves the two specified lines while an adverse weather condition can involve at least one region or several regions which multiple lines traverse. At the peak load, the common cause failure of Line pair (2,3) creates the load curtailment of 0.23 p.u. and the common cause failure of Line pair (4,5) does not create any load curtailment. The load curtailment due to the common cause failure of Line pair (2,3) also decreases as the load level decreases. When the load level is equal to or less than 86% of the peak load, the common cause failure of Line pair (2,3) no longer creates any load curtailment and therefore the common cause failures have hardly any effect on the annual system indices of this system. The differences are quite large in the case of bus indices. The load curtailment indices at Bus 2 are not affected by common cause failures as this bus is directly connected to a generator bus. The bus indices at Bus 4 are not affected by common cause failures because this bus is connected to the generator bus through Line pair (4,5) and the common cause failure of line pair (4,5) provides no load curtailment. Common cause failures have only

a little impact on Buses 5 and 6 and a quite large impact on Bus 3 which is connected directly with the Line pair (2,3). The specific effect of common cause failures depend mainly on the transmission system configuration while weather effects mainly depend on geographical distribution situations and probabilities of adverse weather conditions.

It can be also seen from the results in Tables 5.15 to 5.22 that the percentage differences between the inadequacy indices obtained considering both common cause failures and weather-related but independent line outages and those without considering these effects basically equals the sum of the percentage differences due to only weather effects and those due to only common cause failures. This indicates that these two kinds of effects can be considered to be independent.

## 5.7. BUS LOAD UNCERTAINTY AND CORRELATION

Bus load uncertainty and correlation always exist in an actual power system and it has been shown in Chapter 4 that total system load uncertainty can have a very great impact in an appraisal of generating capacity adequacy. It is therefore important to illustrate the effects of bus load uncertainty and correlation in composite system adequacy assessment. Load uncertainty can be modeled using a normally distributed random variable. In the conventional method, when a state enumeration technique is used, the total system load is usually simulated using a discrete interval normal distribution<sup>(3)</sup> and bus loads determined according to their proportion in the total system load. This implies that all bus loads are completely dependent. In an actual power system, however, bus loads are not completely dependent nor independent but are correlated to some degree. Correlation between bus loads can be expressed by a covariance matrix or a correlation coefficient matrix. In this section, a tabulating technique for normal distribution sampling is used to simulate bus load uncertainty and a correlation sampling technique is utilized to simulate bus load correlation including those situations in which bus loads are completely dependent, or independent, or correlated to some degree.

### 5.7.1. Tabulating Technique for Bus Load Normal Distribution Sampling

Bus load uncertainty can be modeled using a normal distribution and therefore it is necessary to draw normally distributed random numbers in order to simulate bus load uncertainty. The following tabulating technique

for normal distribution sampling can be used for this purpose and includes two procedures:

**(a) Tabulating.** The value interval  $[0, 1]$  of a normal cumulative probability distribution function is divided into  $M$  equal subintervals and the midpoint value of each subinterval is used to represent all values of the normal cumulative probability distribution function  $F$  in this subinterval. Therefore the value of function  $F$  at the  $i$ th subinterval is

$$F(X_i) = \frac{i - 0.5}{M} \quad (i = 1, \dots, M) \quad (5.32)$$

A normally distributed random number  $X_i$  corresponding to the value  $F(X_i)$  can be calculated by means of the inverse transform method, i.e.,

$$X_i = F^{-1}\left(\frac{i - 0.5}{M}\right) \quad (i = 1, \dots, M) \quad (5.33)$$

The random number  $X_i$  can be calculated from the value of  $F(X_i)$  using the approximate inverse function formulas of the normal cumulative probability distribution function given by equations (3.31) and (3.32) in Section 3.4.5.

When  $i = 1, \dots, M$ , the subinterval number  $i$ , the values of the normal cumulative probability distribution function  $F(X_i)$  and the values of the normally distributed random number  $X_i$  can be used to form a table.

**(b) Sampling.** The congruential method is used to generate a uniformly distributed random number  $Y$  between  $[0, 1]$ , which corresponds to a value of the normal cumulative probability distribution function. A normally distributed random number  $X_i$  can be selected directly from the formed table according to the subinterval number  $i$  in which  $Y$  is located.

The tabulating technique for normal distribution sampling is more rapid in computation compared to the direct inverse transform method in which inverse function values are calculated in each sample. Only  $M$  inverse function values are calculated in the tabulating procedure in advance regardless of the number of samples. Essentially, this is a discretization of a continuous cumulative probability distribution function and it creates two errors: a truncation error and a discretization error. A truncation error is due to the last subinterval and therefore, in order to avoid this error, the direct inverse transform method can be used only for the last subinterval instead of using the midpoint value to represent all values of the distribution function corresponding to this subinterval. When  $M$  is large enough, the discretization error is sufficiently small and negligible.

### 5.7.2. Bus Load Correlation Sampling Technique

If all bus loads are completely dependent, only one normally distributed random number is drawn for all bus loads in order to determine a load state. If all bus loads are independent of each other, it is necessary to independently draw the different normally distributed random numbers for each bus load. From a practical point of view, bus loads are not completely dependent nor independent but there is some correlation between them. In this case, it is necessary to generate a normally distributed random vector in which each component corresponds to a bus load and whose components satisfy the specified correlation.

In Section 4.5.2, a correlation sampling technique is used to incorporate area load correlation in multi-area generating system adequacy assessment. A similar technique can be applied to consider bus load correlation in composite system adequacy assessment and the details of the formulas associated with the technique are therefore not repeated. The bus load correlation sampling technique is summarized in the following steps:

1. Draw a noncorrelative, normally distributed  $N$ -dimension random vector  $G$  in which each component corresponds to a bus load. All components have a mean value of zero and a variance of unity.
2. Calculate the lower triangular matrix  $A$  according to equations (5.34) to (5.36):

$$A_{ii} = \frac{C_{ii}}{(C_{11})^{1/2}} \quad (1 \leq i \leq N) \quad (5.34)$$

$$A_{ii} = \left[ C_{ii} - \sum_{k=1}^{i-1} (A_{ik})^2 \right]^{1/2} \quad (1 < i \leq N) \quad (5.35)$$

$$A_{ij} = \left( C_{ij} - \sum_{k=1}^{j-1} A_{ik} A_{jk} \right) / A_{ii} \quad (1 < j < i \leq N) \quad (5.36)$$

where  $C$  is the covariance matrix defining bus load uncertainty and correlation.

3. Create a correlative, normal distribution  $N$ -dimension random vector  $H$  from equation (5.37):

$$H = AG + B \quad (5.37)$$

where  $B$  is the mean vector of the bus loads. Each component of  $H$  still corresponds to a bus load.

Generally, it can be assumed that all bus loads have the same forecast uncertainty. In this case, there is a simple relationship between the covariance matrix  $C$  and the correlation coefficient matrix  $\rho$  of the bus loads as follows:

$$C = \sigma^2 \rho \quad (5.38)$$

where  $\sigma$  is the standard deviation of the bus load forecast.

### 5.7.3. Case Studies

Case studies have been conducted using the RBTS and the IEEE RTS. In addition to the basic data given in Appendix A, complementary data, which are standard deviations of load normal distributions and correlation coefficients between bus loads, are provided in this subsection. Load forecast uncertainty is relatively small for short lead times but can be quite significant when looking further into the future. It is therefore necessary to consider the effects of different standard deviations. Both annualized and annual indices have been calculated. In calculating annual indices, a 15-step non-uniform increment model of the load duration curve was used. The numbers of system state samples at each load level for the RBTS and the IEEE RTS are 50,000 and 10,000, respectively. The coefficients of variation in the various simulation cases for the two systems range from 0.02 to 0.05.

**(a) Effect of Load Uncertainty.** Two load standard deviations of 4% and 10% were considered and it has been assumed that all bus loads are completely dependent. The results are shown in Tables 5.23 to 5.26. The

**Table 5.23. Annualized System Indices with and without Load Uncertainty for the RBTS**

Index	Without load uncertainty	Load normal distribution	
		SD of 4%	SD of 10%
ENLC	5.27252	5.75975 (9%)	9.89653 (88%)
EDLC	91.20384	98.19264 (8%)	230.28096 (152%)
PLC	0.01044	0.01124 (8%)	0.02636 (152%)
EDNS	0.12429	0.14208 (14%)	0.34905 (181%)
EENS	1085.81873	1241.24011 (14%)	3049.33813 (181%)
BPII	0.38169	0.43261 (13%)	0.80923 (112%)
BPECI	5.86929	6.70941 (14%)	16.48291 (181%)
MBPCI	0.00067	0.00077 (15%)	0.00189 (182%)
SI	352.15738	402.56433 (14%)	988.97449 (181%)
CPU (min)	0.187	1.01	1.08

**Table 5.24. Annualized System Indices with and without Load Uncertainty for the IEEE RTS**

Index	Without load uncertainty	Load normal distribution	
		SD of 4%	SD of 10%
ENLC	54.75342	65.23052 (19%)	96.02156 (75%)
EDLC	698.88000	887.57758 (27%)	1405.62231 (101%)
PLC	0.08000	0.10160 (27%)	0.16090 (101%)
EDNS	13.97045	17.26523 (24%)	34.12679 (144%)
EENS	122045.88281	150829.07813 (24%)	298131.62500 (144%)
BPII	3.33652	4.04968 (21%)	7.44591 (123%)
BPECI	42.82311	52.92248 (24%)	104.60758 (144%)
MBPCI	0.00490	0.00606 (24%)	0.01197 (144%)
SI	2569.38672	3175.34863 (24%)	6276.45508 (144%)
CPU (min)	0.623	1.54	1.67

**Table 5.25. Annual System Indices with and without Load Uncertainty for the RBTS**

Index	Without load uncertainty	Load normal distribution	
		SD of 4%	SD of 10%
ENLC	1.27622	1.31200 (3%)	1.44645 (13%)
EDLC	12.35270	12.99498 (5%)	15.98906 (30%)
PLC	0.00141	0.00149 (6%)	0.00183 (30%)
EDNS	0.01786	0.01813 (2%)	0.02216 (24%)
EENS	155.99113	158.40466 (2%)	193.58031 (24%)
BPII	0.08771	0.08849 (1%)	0.09818 (12%)
BPECI	0.84320	0.85624 (2%)	1.04638 (24%)
MBPCI	0.00010	0.00010 (0%)	0.00012 (20%)
SI	50.59172	51.37448 (2%)	62.78280 (24%)
CPU (min)	2.75	15.07	15.18

annualized and annual system indices obtained without considering load uncertainty are also given for comparison. The percentage values in the parentheses are the differences between the system indices obtained considering a load normal distribution and those obtained without considering load uncertainty.

The results in Tables 5.23 to 5.26 indicate that system reliability indices considering load uncertainty are larger than those obtained without considering load uncertainty and the differences between them increase as the load standard deviation increases. The effect of load uncertainty, however, is different for different systems, and for annualized and annual indices. For

**Table 5.26. Annual System Indices with and without Load Uncertainty for the IEEE RTS**

Index	Without load uncertainty	Load normal distribution	
		SD of 4%	SD of 10%
ENLC	0.92368	1.17028 (27%)	2.54645 (176%)
EDLC	11.70195	14.59255 (25%)	33.75541 (188%)
PLC	0.00134	0.00167 (25%)	0.00386 (188%)
EDNS	0.15568	0.19704 (27%)	0.60573 (289%)
EENS	1360.02258	1721.36877 (27%)	5291.66357 (289%)
BPII	0.03785	0.04831 (28%)	0.14241 (276%)
BPECI	0.47720	0.60399 (27%)	1.85672 (289%)
MBPCI	0.00005	0.00007 (40%)	0.00021 (320%)
SI	28.63205	36.23934 (27%)	111.40344 (289%)
CPU (min)	6.23	22.23	26.39

example, in the case of the relatively small load standard deviation of 4%, the differences in the annual indices between considering and not considering load uncertainty for the RBTS are quite small and may be masked by computational errors.

**(b) Effect of Bus Load Correlation.** The correlation coefficients between bus loads can be calculated according to the statistical definition of the correlation function if historical data of bus loads can be provided. When the correlation is strong, the situation approaches the completely dependent case and, when the correlation is weak, it approaches the independent case. It is therefore necessary to examine the following three cases:

1. Independence between bus loads.
2. Some correlation between bus loads.
3. Complete dependence between bus loads.

Case studies were again conducted using the RBTS and the IEEE RTS. It has been assumed that all bus loads have the same standard deviation of 10%. The correlation coefficient matrix between bus loads for the RBTS is as follows:

Bus No.	2	3	4	5	6
2	1.0	0.0	0.0	0.0	0.0
3	0.0	1.0	0.8	0.0	0.0
4	0.0	0.8	1.0	0.0	0.0
5	0.0	0.0	0.0	1.0	0.8
6	0.0	0.0	0.0	0.8	1.0

It has been assumed for the IEEE RTS that industrial customers are located mainly in the 230-kV area and commercial/residential customers in the 138-kV area. In general, commercial/residential customers are more influenced by common factors such as common weather or similar power-consuming behavior compared to industrial customers. The correlation between commercial and/or residential customers is therefore stronger than that between industrial ones. It was also assumed that there is a weak correlation between industrial and commercial/residential loads. Based on the above assumptions, the correlation coefficients between bus loads for the IEEE RTS are as follows:

- The correlation coefficients between the bus loads in the 138-kV area are 0.8.
- The correlation coefficients between the bus loads in the 230-kV area are 0.4.
- The correlation coefficients between the bus loads in the 138-kV area and those in the 230-kV area are 0.2.

The annualized and annual system indices considering bus load uncertainty and correlation for the RBTS and the IEEE RTS are given in Tables 5.27 to 5.30, respectively. The results indicate that the composite system inadequacy indices obtained considering independence and complete dependence between bus loads are lower and upper bounds of those obtained considering different degrees of correlation between bus loads.

**Table 5.27. Annualized System Indices Considering Bus Load Uncertainty and Correlation for the RBTS**

Index	Without load uncertainty	SD of 10%		
		Independent	Correlated	Completely dependent
ENLC	5.27252	6.77444	7.58001	9.89653
EDLC	91.20384	128.41920	158.12161	230.28096
PLC	0.01044	0.01470	0.01810	0.02636
EDNS	0.12429	0.16772	0.21047	0.34905
EENS	1085.81873	1465.19690	1838.62903	3049.33813
BPII	0.38169	0.47524	0.55301	0.80923
BPECI	5.86929	7.91998	9.93853	16.48291
MBPCI	0.00067	0.00091	0.00114	0.00189
SI	352.15738	475.19894	596.31207	988.97449
CPU (min)	0.187	1.17	1.25	1.08

**Table 5.28. Annualized System Indices Considering Bus Load Uncertainty and Correlation for the IEEE RTS**

Index	Without load uncertainty	SD of 10%		
		Independent	Correlated	Completely dependent
ENLC	54.75342	61.04555	77.36040	96.02156
EDLC	698.88000	804.58563	1098.11523	1405.62231
PLC	0.08000	0.09210	0.12570	0.16090
EDNS	13.97045	15.54398	22.73200	34.12697
EENS	122045.88281	135792.23438	198586.76563	298131.62500
BPII	3.33652	3.70869	5.16711	7.44591
BPECI	42.82311	47.64639	69.67956	104.60758
MBPCI	0.00490	0.00545	0.00798	0.01197
SI	2569.38672	2858.78369	4180.77344	6276.45508
CPU (min)	0.623	1.69	1.81	1.67

**Table 5.29. Annual System Indices Considering Bus Load Uncertainty and Correlation for the RBTS**

Index	Without load uncertainty	SD of 10%		
		Independent	Correlated	Completely dependent
ENLC	1.27622	1.32834	1.34947	1.44645
EDLC	12.35270	13.44740	13.94054	15.98906
PLC	0.00141	0.00154	0.00160	0.00183
EDNS	0.01786	0.01930	0.02025	0.02216
EENS	155.99113	168.62752	176.87294	193.58031
BPII	0.08771	0.09143	0.09379	0.09818
BPECI	0.84320	0.91150	0.95607	1.04638
MBPCI	0.00010	0.00010	0.00011	0.00017
SI	50.59172	54.69001	57.36420	62.78280
CPU (min)	2.75	16.18	17.72	15.18

The degrees of effects of correlation between bus loads are different for annualized and annual indices. The variations in annualized and annual EENS system indices with the bus load standard deviation for the RBTS and the IEEE RTS are shown in Figures 5.9 to 5.12, respectively. The EENS values in the figures are expressed in per unit of the annualized or annual EENS obtained without considering load uncertainty. The upper curve corresponds to complete dependence between bus loads and

**Table 5.30. Annual System Indices Considering Bus Load Uncertainty and Correlation for the IEEE RTS**

Index	Without load uncertainty	SD of 10%		
		Independent	Correlated	Completely dependent
ENLC	0.92368	1.13351	1.63481	2.54645
EDLC	11.70195	14.07685	20.44840	33.75541
PLC	0.00134	0.00161	0.00234	0.00386
EDNS	0.15568	0.18129	0.30653	0.60573
EENS	1360.02258	1583.71399	2677.87231	5291.66357
BPII	0.03785	0.04494	0.07612	0.14241
BPECI	0.47720	0.55569	0.93960	1.85672
MBPCI	0.00005	0.00006	0.00011	0.00021
SI	28.63205	33.34135	56.37626	111.40344
CPU (min)	6.23	23.16	29.25	26.36

the lower one to independence between bus loads. The range between these two curves therefore corresponds to different degrees of correlation between bus loads. It can be seen that the variation ranges are quite large with the exception of the annual system indices for the RBTS.

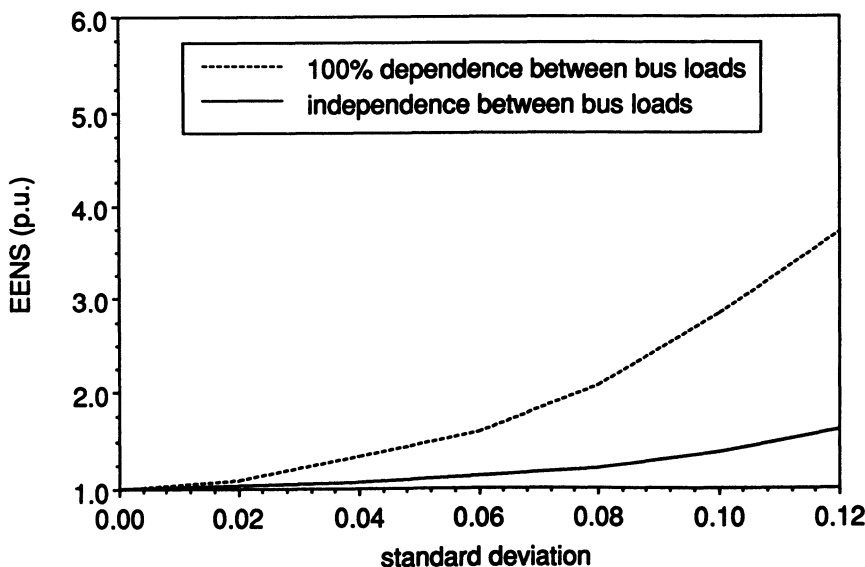


**Figure 5.9.** Variations in the annualized EENS with the bus load standard deviation for the RBTS.

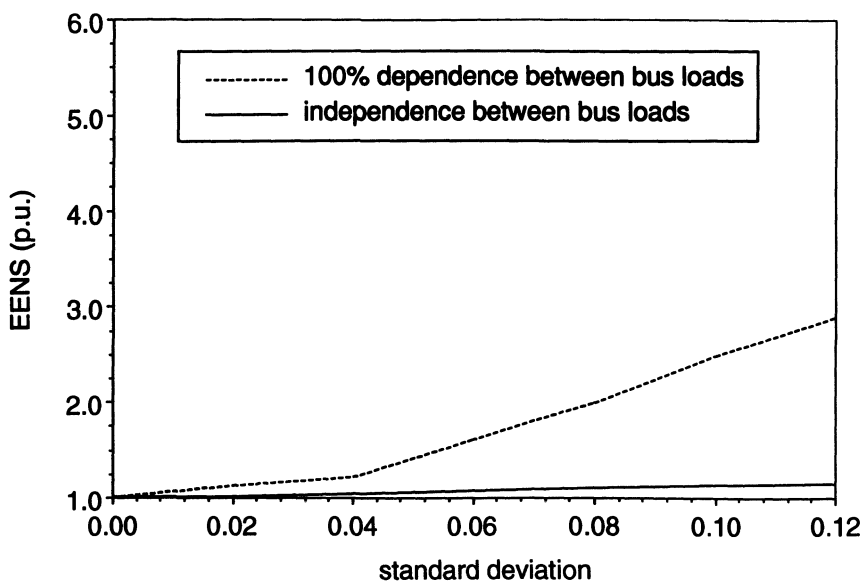


**Figure 5.10.** Variations in the annualized EENS with the bus load standard deviation for the IEEE RTS.

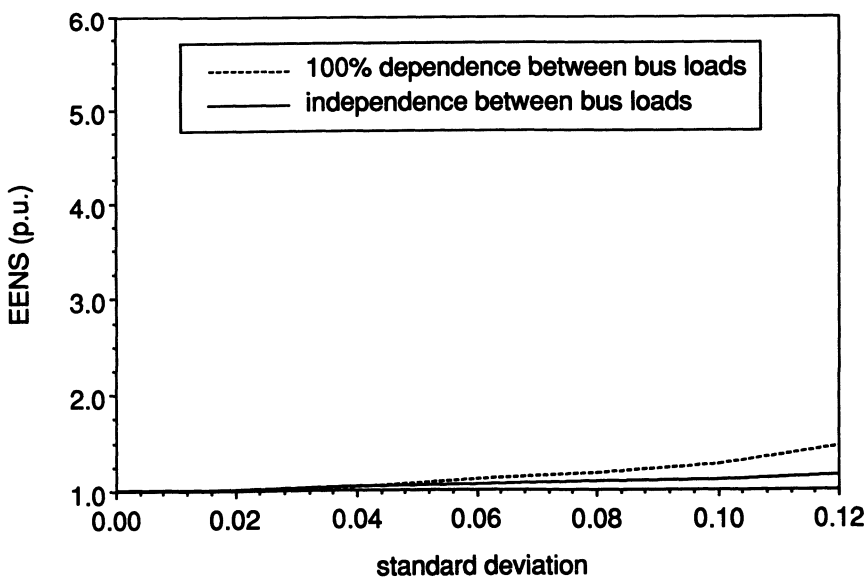


**Figure 5.11.** Variations in the annual EENS with the bus load standard deviation for the RBTS.

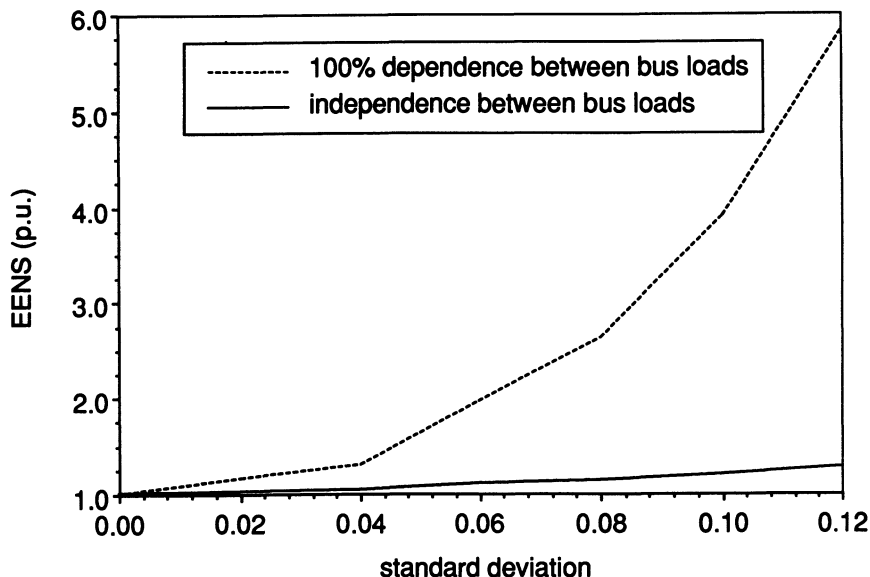


**Figure 5.12.** Variations in the annual EENS with the bus load standard deviation for the IEEE RTS.

## 5.8. FREQUENCY INDEX AND SYSTEM STATE TRANSITION SAMPLING TECHNIQUE

### 5.8.1. Discussion on the Frequency Index

The system state sampling method can provide accurate probability and energy-related indices but it cannot be used to directly calculate actual frequency-related indices. Alternatively, it calculates Expected Number of Load Curtailments, which is an approximation of the actual frequency index. The approximation results from the following two factors.

**(a) Transitions between System States are Ignored.** The frequency concept is based on transitions between system states. Consider the system state transition of the two repairable component system shown in Figure 5.13. It is assumed that component 2 down (State 3) and both components down (State 4) are load curtailment states while component 1 down (State 2) is a no-load-curtailment state. Only those transitions between States 1 and 3 and between States 2 and 4 contribute to the frequency index. The

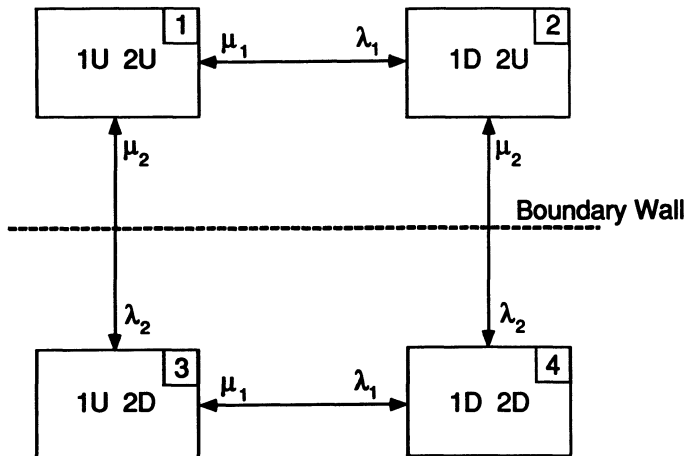


**Figure 5.13.** Transitions between system states for a two-repairable-component system.

transition between States 3 and 4 should not be included in the frequency index. This transition, however, is included in the ENLC index obtained by system state sampling. Consequently, this leads to overestimation of the frequency index. If an additional enumeration procedure is used to recognize all no-load-curtailment states which can be reached from each selected failure state in one transition, the actual frequency index can be calculated. However, this can result in a very large computational burden. If a failure state is associated with  $n$  components, each of which is modeled by two states,  $n+1$  additional adequacy evaluations including load flow calculations, corrective actions, etc. are required for this failure state to update the frequency estimate. If generating unit derated states are considered, the number of additional evaluations increases dramatically. In the case of a large composite system, this task can be computationally unfeasible.

**(b) Chronology of the Load Curve is Eliminated.** Consider the simple example shown in Figure 5.14a. It is assumed that the duration of a failure event is  $t$  and the power with which the system can provide some bus during the failure event is expressed by the horizontal line A. The load curve at this bus is expressed by B. The frequency of load curtailment at the bus should be three in the duration  $t$  in Figure 5.14a. If chronology of the load curve is eliminated, the corresponding load duration curve is expressed by C in Figure 5.14b. The frequency of load curtailment in the duration  $t$  is only one. This example indicates that elimination of chronology of the load curve may lead to underestimation of the frequency index.

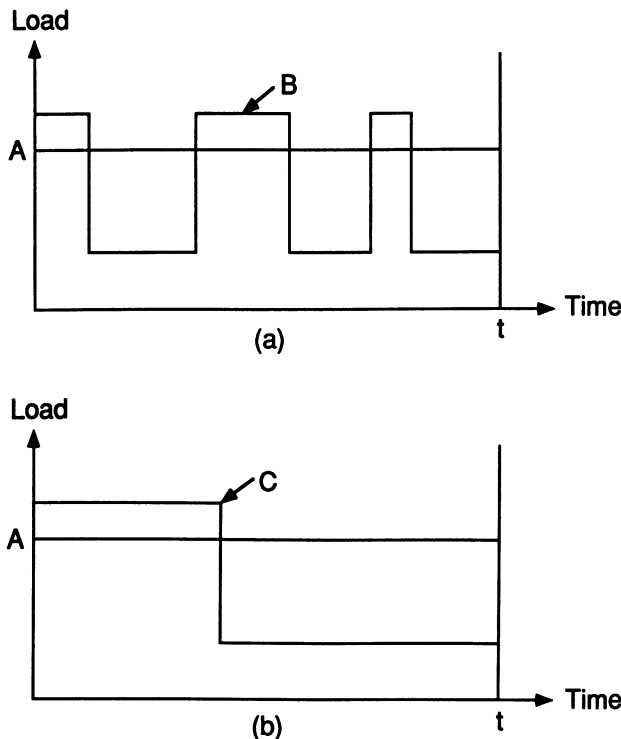


**Figure 5.14.** Effect of eliminating load curve chronology on the frequency index.

Note that total duration of load curtailment is the same and therefore the probability of load curtailment and the energy not supplied are the same in the two cases.

Annualized indices are usually calculated at the single peak load level and therefore affected only by the first aspect. As a result, the annualized ENLC index is a pessimistic estimation of the actual annualized frequency index. Annual indices considering the annual load duration curve are affected by both aspects. If the effect due to eliminating the chronology of the load curve is larger than that due to ignoring transitions between system states, the annual ENLC index can be an optimistic estimation of the actual annual frequency index. Otherwise, it is a pessimistic estimation.

Three basic simulation approaches are illustrated in Section 3.6. These techniques are designated as state sampling, state duration sampling, and system state transition sampling. The state duration sampling technique uses a chronological load curve and component state transition cycles. If this technique is applied, the actual frequency index can be obtained. This

technique has been utilized in generating system adequacy assessment in Chapter 4. Its application to composite system adequacy assessment is a much more difficult task. This is not only because one year has 8760 hourly load points but also because the chronological load curves of each bus are basically different. In composite system assessment, load curtailments occur at buses and therefore chronological bus load curves should be used if the state duration sampling method is applied. Evaluation of each system state is associated with load flow calculations, contingency analysis, overload alleviation, generation rescheduling, and other possible considerations such as those given in Sections 5.4 to 5.7. This may not be computationally feasible in the case of a practical composite system. A more difficult obstacle is that of the data problem. At the present time, most utility companies cannot provide data records of the chronological load curves for all or for even major buses.

Application of the system state transition technique to composite system adequacy assessment is presented in the following subsection. This technique is combined with the multistep load model given in Section 5.3. The approximation associated with ignoring transitions between system states is removed but the approximation due to eliminating chronology of load curves still remains. As a result, an actual annualized frequency index can be calculated and the annual frequency index is an optimistic estimation of the actual annual frequency index.

### 5.8.2. System State Transition Sampling Technique

This technique focuses on state transition of the whole system rather than on component states or component state durations. It creates a system state transition sequence without the need to sample up and down cycles of components and storing chronological information on system states. The generating unit derated states can be easily included without additional calculations. An important restriction in the method is the assumption of exponential distributions for all state residence times.

**(a) Basic Principles.** The system state transition sampling technique is described in Section 3.6.3. Two main principles associated with its application are as follows:

1. Assume that a system contains  $m$  components and that the duration of each component state follows an exponential distribution with parameter  $\lambda_i$ . The duration of the system state also follows an exponential distribution

with the parameter  $\lambda = \sum \lambda_i$ , i.e., it has the probability density function

$$f(t) = \sum_{i=1}^m \lambda_i \exp\left(-\sum_{i=1}^m \lambda_i t\right) \quad (5.39)$$

2. Starting from any system state, a system containing  $m$  components has  $m$  possible reached states. The probability that the system reaches one of these possible states is given by

$$P_j = \frac{\lambda_j}{\sum_{i=1}^m \lambda_i} \quad (5.40)$$

The probabilities of  $m$  possible reached states are successively placed in the interval  $[0, 1]$  as shown in Figure 3.11. A uniformly distributed random number  $U$  between  $[0, 1]$  is generated and if  $U$  falls into the segment corresponding to  $P_j$ , the transition of the  $j$ th component leads to the next system state. A long system state transition sequence can be obtained by drawing a number of samples and the consequences of each system state can be evaluated using the same system analysis techniques given in Section 5.2.

**(b) Evaluation Procedure.** Composite system adequacy assessment using the system state transition sampling technique can be summarized by the following steps:

1. The simulation process starts from the normal system state in which all generating units and transmission components are in the up state.

2. Let  $\lambda_i$  be the transition rate at which one component departs its present state. If the component is in the up state,  $\lambda_i$  is its failure rate, and if the component is in the down state,  $\lambda_i$  is its repair rate. If multistates of a component are considered (such as derated states of a generating unit), there are several departure rates. The duration of the system state has a probability density function shown in equation (5.39). According to the inverse transform method, the sampling value  $D_k$  of the duration of the present system state (numbered by  $k$ ) can be obtained by (see Section 3.4.4)

$$D_k = \frac{-\ln U'}{\sum_{i=1}^m \lambda_i} \quad (5.41)$$

where  $m$  is the number of departure rates corresponding to the present system state  $k$  and  $U'$  is a uniformly distributed random number between  $[0, 1]$ .

3. If the present system state is a contingency state in which at least one component is in the outage or the derated state, the system analysis techniques, including the minimization load curtailment model given in

Section 5.2, are used to evaluate the adequacy of this system state. If the present system state is the normal state in which all components are in their up states, go to Step 4 without utilizing the minimization model.

4. The adequacy indices are updated using equations (5.42) to (5.44) given later. If the coefficient of variation of the EDNS (Expected Demand Not Supplied) index is less than a given tolerance or the specified number of system state samples is reached, the simulation process ends. If not, proceed to Step 5.

5. A uniform distribution random number  $U$  is generated to determine the next system state using the system state transition sampling technique described earlier. Return to Step 2.

**(c) Calculation of Adequacy Indices.** The total load curtailment  $C_k$  for the system state  $k$  can be obtained by solving the minimization model shown by equations (5.20) to (5.25). If  $C_k$  equals zero, the system state is a no-load-curtailment state. If not, it is a failure state. The three basic system unreliability indices can be calculated using the following equations:

(1) Expected Demand Not Supplied (MW)—EDNS

$$\text{EDNS} = \sum_{k=1}^{NK} C_k D_k / \text{TD} \quad (5.42)$$

where  $C_k$  (MW) and  $D_k$  (hr) are the system load curtailment and the duration for system state  $k$ ;  $NK$  is the number of load curtailment system states; TD (hr) is the sum of the durations of all system states in a long system state transition sequence.

(2) Expected Frequency of Load Curtailments (occ./yr)—EFLC

$$\text{EFLC} = \text{NF} \cdot 8760 / \text{TD} \quad (5.43)$$

where NF is the number of occurrences of transition from a load curtailment state to a no-load-curtailment state in the system state transition sequence.

(3) Probability of Load Curtailments—PLC

$$\text{PLC} = \sum_{k=1}^{NK} D_k / \text{TD} \quad (5.44)$$

Bus indices can be obtained using similar equations since the minimization model also provides load curtailments at each bus for all drawn system states. Other unreliability indices can be calculated from these three basic indices.

### 5.8.3. Case Studies

The application of the method is illustrated using the IEEE RTS. Comparisons between the system state sampling and the system state transition sampling techniques are shown. The studies include base and generating unit derated cases. The data for both cases are the same as those given in Sections 5.2.4 and 5.4.2, respectively. In the case of annual indices, the annual load curve is considered by modeling the 8736 hourly load points by a 70-step load level model. In all study cases, the coefficient of variation for the EDNS index ranges from 0.03 to 0.05. Tables 5.31 and 5.32 show the annualized system indices in the base and the generating unit derated cases, respectively. Table 5.33 shows annual system indices for the base case. The \* flag indicates the frequency and duration indices. In the case of the system state sampling method, the Expected Number of Load Curtailments (ENLC), i.e., the sum of occurrences of load curtailment states, is calculated as a surrogate for the actual frequency index (EFLC) and therefore the corresponding ADLC (Average Duration of Load Curtailments in hr/disturbance) is also an ENLC-based index.

It can be seen that although these two methods utilize completely different sampling techniques, the unreliability indices that are not associated with the frequency index are quite close. Additional calculations indicate that when the number of samples is increased, these unreliability indices become closer. On the other hand, however, the frequency and duration indices

**Table 5.31. The Annualized System Indices for the IEEE RTS Using Two Monte Carlo Methods for the Base Case**

Index	System state transition sampling	System state sampling	Difference (in %)
PLC	0.08434	0.08000	5.1
EDLC	736.77460	698.88000	5.1
* EFLC	19.57152	54.75342 (ENLC)	179.7
* ADLC	37.64524	12.76413	194.9
EDNS	14.44465	13.97045	3.3
EENS	126188.45313	122045.88281	3.3
BPECI	44.27665	42.82311	3.3
SI	2656.59863	2569.38672	3.3
CPU (min)	1.51	0.62	

**Table 5.32. The Annualized System Indices for the IEEE RTS Using Two Monte Carlo Methods for the Generating Unit Derated Case**

Index	System-state transition sampling	System-state sampling	Difference (in %)
PLC	0.06784	0.07220	6.4
EDLC	592.67310	630.73920	6.4
* EFLC	17.73042	47.38287 (ENLC)	167.2
* ADLC	33.42691	13.31154	151.2
EDNS	10.31458	10.32736	0.2
EENS	90108.20313	90219.83594	0.2
BPECI	31.61691	31.65608	0.2
SI	1897.01465	1899.36487	0.2
CPU (min)	1.47	0.74	

**Table 5.33. The Annual System Indices for the IEEE RTS Using Two Monte Carlo Methods for the Base Case**

Index	System-state transition sampling	System-state sampling	Difference (in %)
PLC	0.00119	0.00117	1.7
EDLC	10.36991	10.23695	1.3
* EFLC	0.39417	0.80854 (ENLC)	105.1
* ADLC	26.30801	12.66103	108.2
EDNS	0.14673	0.13137	10.5
EENS	1281.79480	1147.61108	10.5
BPECI	0.44975	0.40267	10.5
SI	26.98515	24.16023	10.5
CPU (min)	39.73	15.97	

(EFLC or ENLC and ADLC) obtained using the two methods have very large differences. This indicates that the utilization of the ENLC index as a surrogate for the EFLC index can lead to a considerable overestimation. Both the annual EFLC and ENLC indices were obtained using a nonchronological multistep load model.

## 5.9. SECURITY CONSIDERATIONS IN COMPOSITE SYSTEM ADEQUACY EVALUATION

This section discusses security considerations in composite system adequacy evaluation. These considerations are designated as security constrained adequacy evaluation. The analysis is therefore within the domain of adequacy and is not “security evaluation” which is associated with dynamic conditions and the effects of cascading sequences after failures. The system operating state division used in the approach, however, does not restrict the inclusion of transient or dynamic conditions.

### 5.9.1. System Model Including Security Considerations

**(a) Classification of System Operating States.** In order to recognize security considerations in the evaluation of a composite system, the total power network can be divided into several operating states in terms of the degree to which adequacy and security considerations are satisfied. Figure 5.15 shows a possible classification of the system operating states.<sup>(38)</sup>

The definitions of the system operating states are as follows<sup>(39)</sup>:

*The Normal State:* “In the normal state, all equipment and operation constraints are within limits, including that the generation is adequate to supply

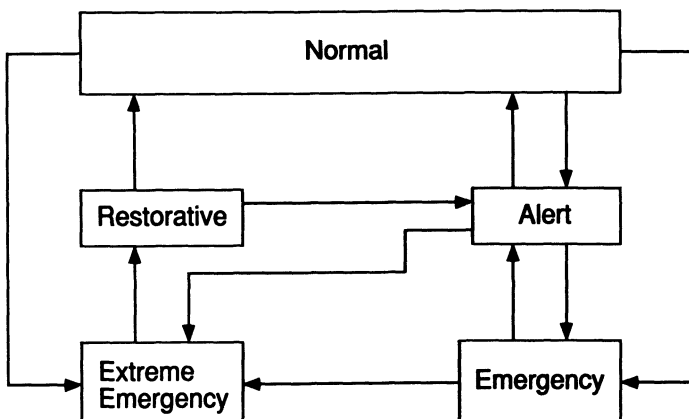


Figure 5.15. Classification of system operating states.

the load (total demand), with no equipment overloaded. In the normal state, there is sufficient margin such that the loss of any elements, specified by some criteria, will not result in a limit being violated. The particular criteria, such as all single elements, will depend on the planning and operating philosophy of a particular utility.” It is clear that the system is both adequate and secure in the normal state.

*The Alert State:* “If a system enters a condition where the loss of some element covered by the operating criteria will result in a current or voltage violation, then the system is in the alert state. The alert state is similar to the normal state in that all constraints are satisfied, but there is no longer sufficient margin to withstand an outage (disturbance). The system can enter the alert state by the outage of equipment, by a change in generation schedule, or a growth in the system load.” In the alert state the system no longer has sufficient margin to satisfy the security constraints.

*The Emergency State:* “If a contingency occurs or the generation and load changes before corrective action can be (or is) taken, the system will enter the emergency state. No load is curtailed in the emergency state, but equipment or operating constraints have been violated. If control measures are not taken in time to restore the system to the alert state, the system will transfer from the emergency state to the extreme emergency state.” In this state both adequacy and security constraints are violated. This is a temporary state which requires operator action because equipment operating constraints have been violated. The first objective will be to remove the violations without load curtailment, by such means as phase shifter adjustment, redispatch, or startup of additional generation. If successful, this could lead to the alert state, where further actions would still be necessary to achieve the normal state. Such actions could include voltage reduction. On the other hand, once the alert state is reached, it may be decided to take no further control action.

*The Extreme Emergency State:* “In the extreme emergency state, the equipment and operating constraints are violated and load is not supplied.” In this state, load has to be curtailed in a specific manner in order to return from this state to another state.

**(b) Steady State Security Constraints.** The steady state security constraints are basically the operating limits which have to be satisfied for normal operation of the power system. The basic security constraints in order to operate the system within an acceptable security domain are:

(1) Voltage magnitude constraints: Operating limits are imposed on the voltage magnitude of buses, i.e.,

$$V^{\min} \leq V \leq V^{\max} \quad (5.45)$$

(2) Branch flow constraints: These are the thermal capacity limits on transmission lines and transformers. In some cases, the steady state stability limits on transmission lines expressed by angle differences can also be transformed into branch flow constraints.

$$|T| = T^{\max} \quad (5.46)$$

where  $T$  represents the line flows on branches.

(3) Real power generation constraints: The real power generation constraints at the slack bus and generator buses are

$$P^{\min} \leq P \leq P^{\max} \quad (5.47)$$

(4) Reactive power generation constraints: The reactive power generation constraints at the slack bus and generator buses are

$$Q^{\min} \leq Q \leq Q^{\max} \quad (5.48)$$

There may be other security constraints. For example, in the operating guide of some utilities, transient stability or voltage stability limits can be expressed as power flow limits on crucial branches or generation limit curves. Therefore these stability limits can be introduced indirectly into adequacy evaluation as security constraints.

## 5.9.2. System Analysis Techniques

System analysis techniques are associated with the following two aspects:

**(a) Contingency Analysis.** In order to include bus voltage and reactive constraints, AC load flow based contingency analysis has to be utilized. The basic equations are the following fast decoupled load flow equations:

$$[\Delta P/V] = [B'][V\Delta\delta] \quad (5.49)$$

$$[\Delta Q/V] = [B''][\Delta V] \quad (5.50)$$

where

$[\Delta P]$  = Vector of bus real power injection increments

$[\Delta Q]$  = Vector of bus reactive power injection increments

$[\Delta\delta]$  = Vector of bus phase angle increments

$[\Delta V]$  = Vector of bus voltage magnitude increments

$[B']$  = Constant bus admittance matrix for real power iteration

$[B'']$  = Constant bus admittance matrix for reactive power iteration.

The contingency analysis commences with the normal decoupled load flow solution and updates the changes in bus voltage magnitudes and angles using the linearized equations, followed by the limit check for the respective constraints for a contingency without solving the load flow equations.<sup>(40)</sup> The more accurate AC load flow based contingency analysis method described in Appendix C.4 can also be used.

**(b) Corrective Actions.** Corrective actions to alleviate security constraint violations can be conducted by an Optimal Power Flow (OPF) solution. Nonlinear OPF requires a large amount of CPU time and can encounter convergency problems in some multicomponent failure situations. The ability to include a high degree of accuracy in corrective calculations will never override inherent uncertainties in the forecast data including load, failure rates, and repair times and in Monte Carlo simulation. It is therefore reasonable to use a linearized optimization model for corrective actions.

1. *Linear programming model for load curtailments and generation rescheduling.* In the event of constraint violation(s), the system could be, according to the definitions, in the emergency state or the extreme emergency state depending on whether there exist load curtailments after corrective actions have been taken. The main objective, in this regard, is to alleviate the problem using rescheduling of generation without requiring load curtailments. If it is not possible to overcome the difficulty by rescheduling the generation, then load will be curtailed from different buses. This task can be performed using the linear programming model given in equations (5.14) to (5.19). If bus indices are also required, the model expressed by equations (5.20) to (5.25) should be applied.

2. *Increment-type linear programming model for voltage adjustment and Q-load curtailment.* In the case of bus voltage violations, these violations may be alleviated by adjustments of generator bus voltages, reactive power injections of reactive sources, and transformer taps. If it is not possible to eliminate all the bus voltage violations by these adjustments, then reactive load curtailments at some buses are unavoidable. Reactive load curtailments should be minimized in this case. The following increment-type linear programming model can be used for this purpose<sup>(41)</sup>:

$$\min \sum_{i \in NG} \alpha_i |\Delta V_i| + \sum_{j \in NC} \beta_j \Delta Q_j \quad (5.51)$$

subject to

$$[B''] [\Delta V] = [\Delta Q] \quad (5.52)$$

$$\Delta V_i^{\min} \leq \Delta V_i \leq \Delta V_i^{\max} \quad (i \in \text{NG} \cup \text{NR}) \quad (5.53)$$

$$\Delta V_j \geq \Delta V_j^* \quad (j \in \text{NC}) \quad (5.54)$$

$$\Delta Q_i^{\min} \leq \Delta Q_i \leq \Delta Q_i^{\max} \quad (i \in \text{NG} \cup \text{NR}) \quad (5.55)$$

$$0 \leq \Delta Q_j \leq \Delta Q_j^{\max} \quad (j \in \text{NC}) \quad (5.56)$$

where  $\Delta V$  and  $\Delta Q$  are bus voltage and reactive power change vectors, respectively. Equation (5.52) is in the form of the voltage-reactive power equation in the decoupled load flow but the signs of the components of  $[B'']$  are treated individually. Quantities  $\Delta V_i^{\min}$ ,  $\Delta V_i^{\max}$ ,  $\Delta Q_i^{\min}$ , and  $\Delta Q_i^{\max}$  are the lower and upper limits of  $\Delta V_i$  and  $\Delta Q_i$ , respectively, while  $\Delta V_j^*$  are voltage violations at load buses; NG, NC, and NR are the sets of generator, load, and static reactive source buses, respectively. Equation (5.53) indicates that the generator and reactive source bus voltage adjustments should be within the permissible changes, which are the differences between the bus voltage limits and their actual values in the contingency state. Equation (5.54) indicates that load bus voltage changes should be larger than their violations, which are the differences between the actual load bus voltages in the contingency state and their limits. When the linear programming relaxation technique is used,<sup>(32)</sup> only load bus voltage change variables corresponding to voltage violated buses are introduced in the model at each iteration. Equation (5.55) indicates that reactive power adjustments at generator and reactive source buses should be within the permissible changes, which are the differences between the bus reactive power limits and their actual values in the contingency state. Equation (5.56) indicates that when load bus reactive power curtailments are unavoidable, these curtailments cannot exceed the reactive loads themselves. Therefore  $\Delta Q_j^{\max}$  are simply the bus reactive loads. The effects of transformer tap changes can be implicitly included in  $[B'']$ . The main objective of the optimization model is to minimize total  $Q$ -load curtailments. The weighting factors  $\beta_j$  therefore have to be larger than all  $\alpha_i$ . The first term in the objective function provides the possibility that when there is no need of  $Q$ -load curtailment, the generator bus voltage adjustments will be minimized.

### 5.9.3. Hybrid Methodology

A hybrid method consisting of the state sampling and the enumeration procedures can be used to evaluate the system operating state probabilities. The flowchart of the method is shown in Figure 5.16.

In this approach, the system state is determined using the state sampling technique described in Section 5.2.1. If the sampled situation creates a system

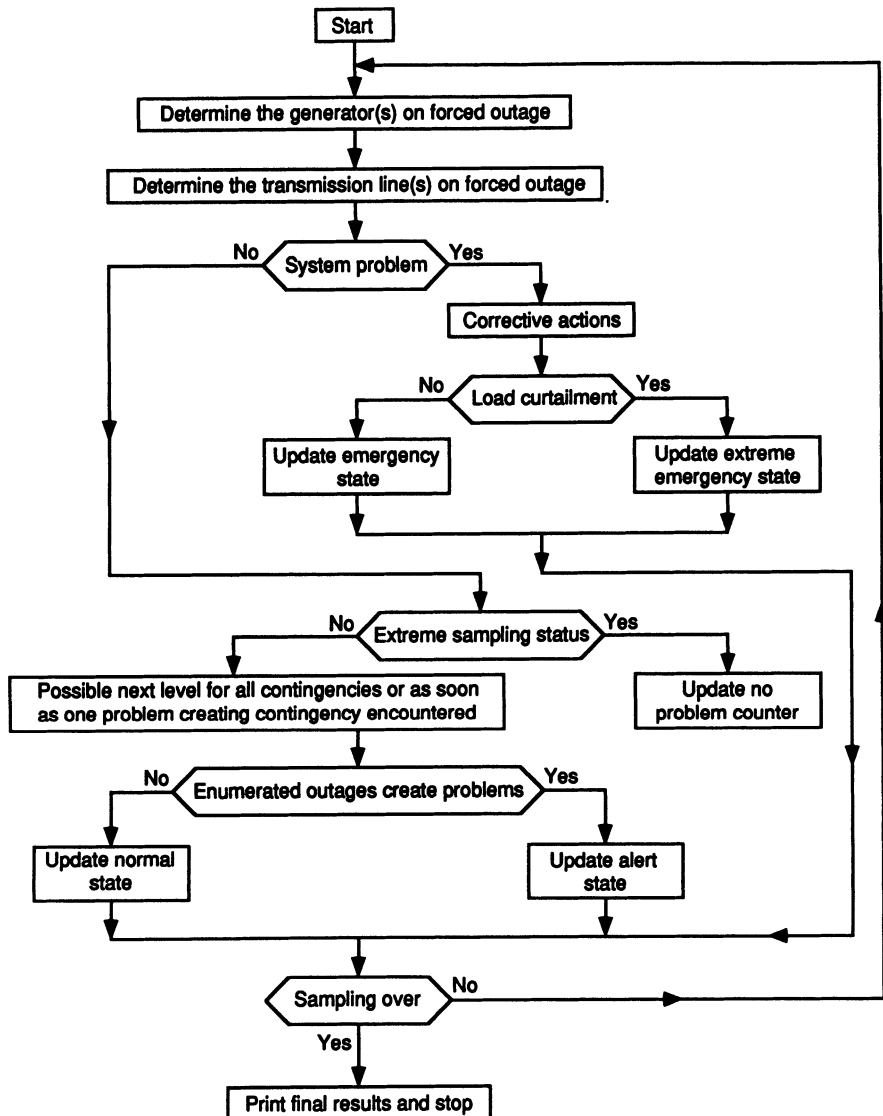


**Figure 5.16.** Flowchart for the hybrid method.

problem, the probability index of the emergency or the extreme emergency state is enhanced depending on whether or not load curtailments occur after corrective action. If the sampled situation does not create a system problem, then the enumeration method is utilized to determine whether the sampled

situation belongs to the normal or to the alert state. As soon as any system problem is encountered with the enumerated outages, no more outages using the enumeration method are considered and the index for the alert state is enhanced. If none of the enumerated states creates any system problem, the indices for the normal state are enhanced. In all the cases, the full sampling probability ( $=1.0/\text{sample number}$ ) is added to the appropriate system state. If a sampled system state is a high-level contingency state and it still does not create any system problem, this is defined as an “extreme sampling situation.” This is seldom an actual operating state. In this case, no further enumerated outages are considered. An extreme sampling situation makes a contribution to the “no problem” condition, which is a classification beyond the four operating states in Figure 5.15. The probability index of the extreme emergency state converges slower than that of other states. The coefficient of variation for the probability index of the extreme emergency state therefore should be used as a stopping rule in the Monte Carlo sampling method.

#### 5.9.4. Case Studies

The IEEE RTS and the RBTS were used to conduct case studies for composite system adequacy assessment with security considerations. The 6-bus RBTS has been modified to a 5-bus system (MRBTS) having 8 lines. This is done to remove the radial line between bus 5 and 6 as, in the original case, the probability of the normal state will be always zero because the outage of line 9 (single level contingency) will isolate bus 6 and result in the curtailment of the 20 MW load at bus 6.

The results obtained at the annual peak load level are shown in Figures 5.17 and 5.18 for the two test systems. As can be seen from the two figures, the indices converge to the corresponding analytical values as the number of samples increases. The perturbations in the probabilities of the normal and alert states for the IEEE RTS can be appreciated from the fact that on the 1256th sample, the sampled situation is a single-level outage (line 27) which creates a voltage problem. Therefore, according to the definition of the normal state, this system has no normal state since it cannot withstand all the single-level outages and thus the probability index of the normal state goes down to zero. The indices of the emergency state are zero for both the test systems for about the first 2000 samples, since the sampled situations up to this sampling number create either no system problems or only system problems which require load curtailments. The probability indices of the operating states for various coefficients of variation are presented in Table 5.34 for the MRBTS and in Table 5.35 for the IEEE RTS.

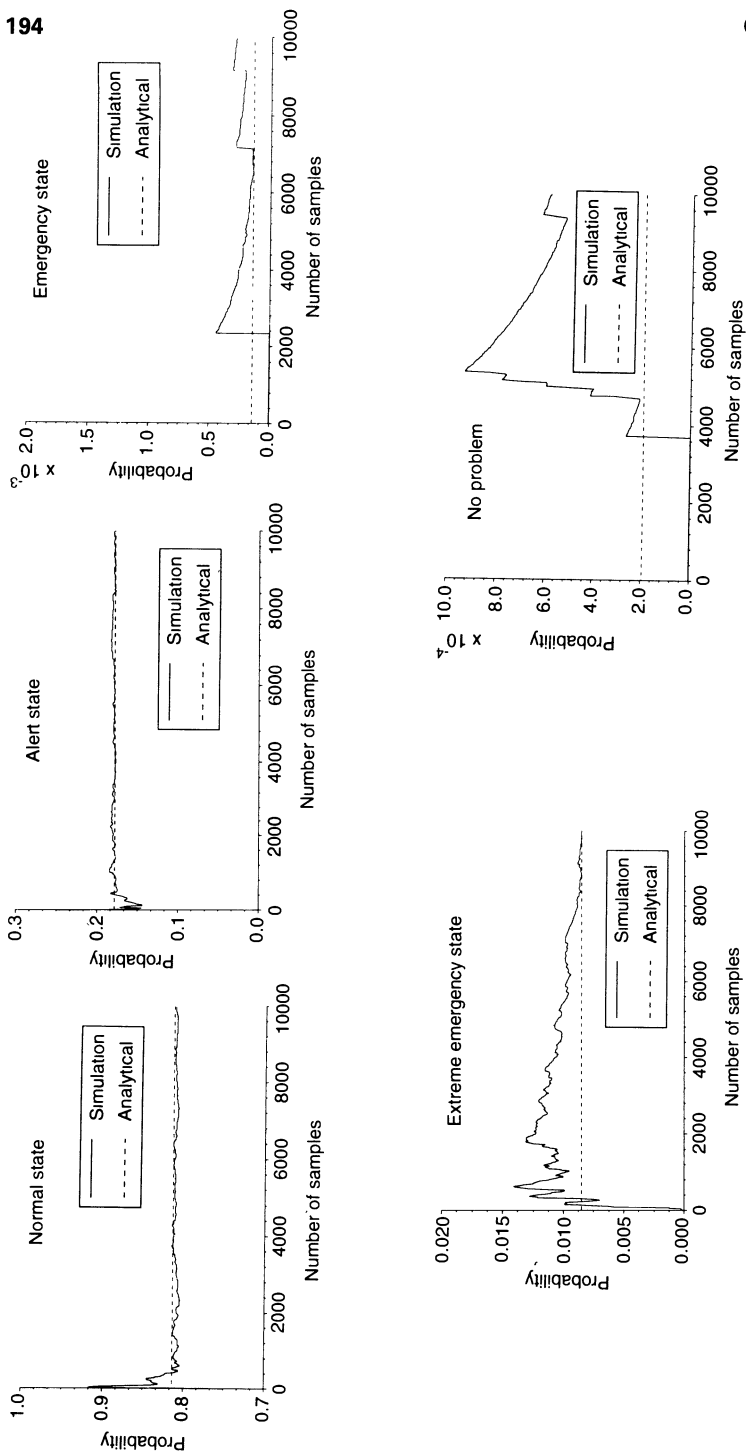


Figure 5.17. Probabilities of different operating states for the MRBTS.

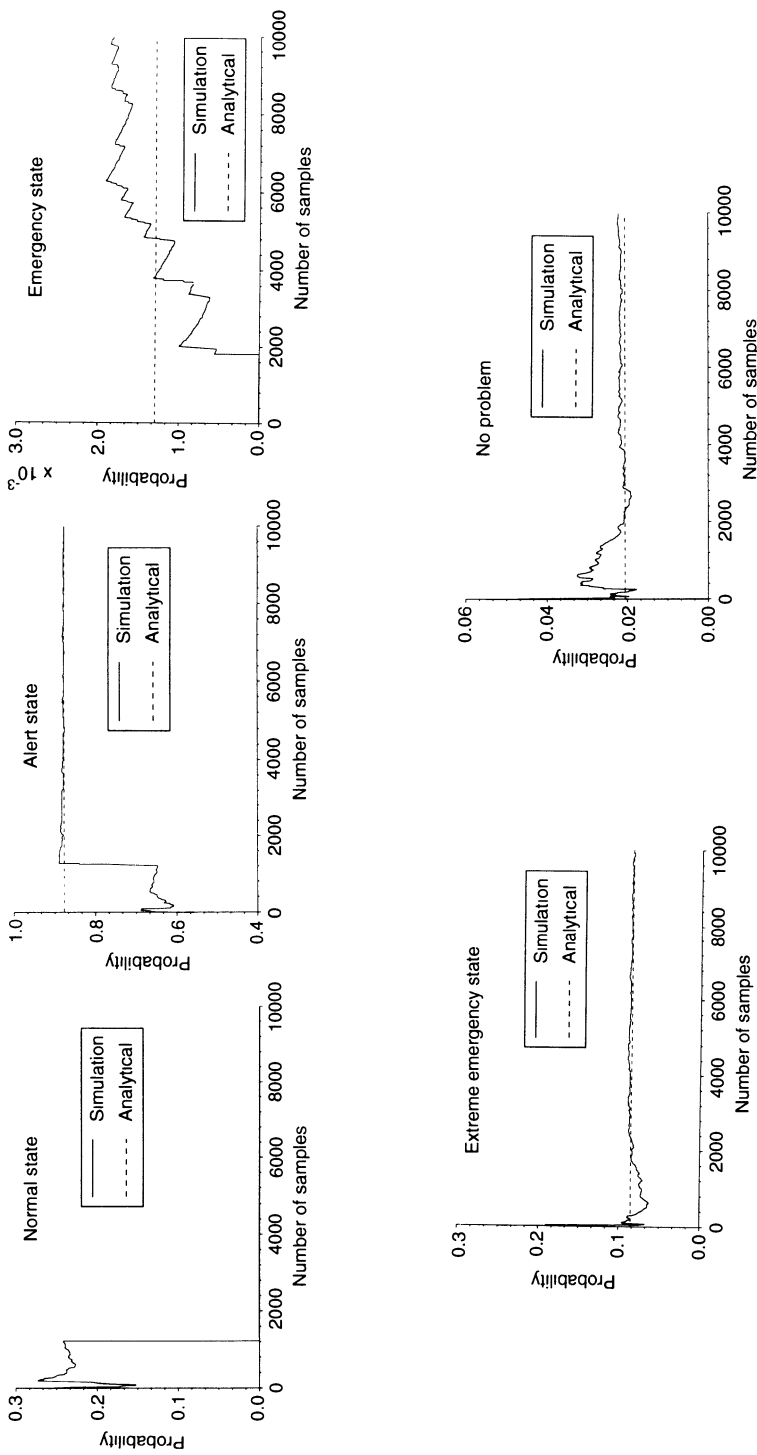


Figure 5.18. Probabilities of different operating states for the IEEE RTS.

**Table 5.34. Probability of Different States for Various Coefficients of Variation for the MRBTS**

System states	Coefficients of variation		
	0.10	0.05	0.035
Normal	0.809951	0.813126	0.813210
Alert	0.180468	0.177479	0.177860
Emergency	0.000264	0.000199	0.000170
Ext. emergency	0.008790	0.008796	0.008280
No problem	0.000527	0.000355	0.000430
Samples	11,376	45,132	100,000
CPU (sec)	9.21	36.92	83.14

**Table 5.35. Probability of Different States for Various Coefficients of Variation for the IEEE RTS**

System states	Coefficients of variation			
	0.10	0.05	0.0326	0.0102
Normal	0.000000	0.000000	0.000000	0.000000
Alert	0.887443	0.876200	0.876600	0.876990
Emergency	0.000000	0.001200	0.001800	0.001740
Ext. emergency	0.071210	0.087572	0.085800	0.087310
No problem	0.026034	0.021593	0.022200	0.019930
Samples	1306	4168	10,000	100,000
CPU (min)	0.55	1.77	4.15	41.50

### 5.9.5. Application of Variance Reduction Techniques

The variance indicates the variability of the estimator around the expected value. Therefore large variance essentially implies poor accuracy. A variance reduction technique (VRT) can be used to reduce the variance of the estimator by replacing the original sampling procedure by a new procedure that yields statistically the same expected value but with a smaller variance. With proper application, a VRT can result in a higher precision, e.g., a smaller confidence interval for the same number of samples, or alternatively, achieve a prespecified precision with a smaller number of samples. Five variance reduction techniques are described in Section 3.5. In principle, these five techniques can be used in power system reliability evaluation. Different VRTs have, however, completely different efficiencies in different cases.

**Table 5.36. Probability of Different States without and with VRT for the MRBTS**

System states	No VRT	Antithetic	Stratified after sampling
Normal	0.812880	0.811100	0.812430
Alert	0.177720	0.179840	0.178170
Emergency	0.000180	0.000180	0.000179
Extreme emergency	0.008820	0.008560	0.008813
No problem	0.000340	0.000300	0.0000325

The antithetic variates and the stratification after sampling methods were applied to study the effect of VRT on the probability indices of the operating states. The concept of the antithetic variates method is given in Section 3.5.5. The stratification after sampling method is basically the same as the stratified sampling method given in Section 3.5.4, except that in this case the number of observations in each stratum is not prefixed. It is noted in Section 5.3.1 that the utilization of a multistep model of the annual load duration curve to calculate annual indices is essentially similar to a stratified sampling method, e.g., loads are stratified in terms of their levels. The low load levels which make smaller contributions to the total indices can be allowed to have a relatively smaller number of samples or a relatively large variance. This method has been proven to be computationally efficient for that case. In the following studies, however, only the peak load level is considered. Stratification is applied to division of component outages. The five strata are:

1. No outage.
2. Only line outages.
3. Only generator outages.
4. Generator and line outages.
5. Outages beyond the level considered.

The probabilities of the above five strata (corresponding to  $d_j$  in the formulas given in Section 3.5.4) can be calculated from the failure and repair rates of the components using an analytical method.

The two test systems (the MRBTS and the IEEE RTS) were again used for this study. The total number of samples is 50,000 for the MRBTS and 10,000 for the IEEE RTS, respectively. The probability indices for the MRBTS using the two variance reduction techniques are given in Table 5.36. The number of samples belonging to each stratum for the stratification

**Table 5.37. Number of Samples in Different Operating States from Different Strata for the MRBTS**

System states	Stratum				
	1	2	3	4	Total
Normal	39,759	47	838	0	40,644
Alert	0	836	7872	178	8886
Emergency	0	5	0	4	9
Extreme emergency	0	2	422	17	441
No problem	0	0	0	17	17
Total	39,759	890	9132	216	49,997

**Table 5.38. Probability of Different States without and with VRT for the IEEE RTS**

System states	No VRT	Antithetic	Stratified
			after sampling
Normal	0.000000	0.000000	0.000000
Alert	0.876600	0.875700	0.866372
Emergency	0.001800	0.001900	0.001628
Extreme emergency	0.085800	0.084700	0.084255
No problem	0.022200	0.020700	0.020906

**Table 5.39. Number of Samples in Different Operating States from Different Strata for the IEEE RTS**

System states	Stratum				
	1	2	3	4	Total
Normal	2288	1	132	1	242
Alert	0	42	6225	77	6344
Emergency	0	5	0	13	18
Extreme Emergency	0	3	849	6	858
No problem	0	0	171	51	222
Total	2288	51	7377	148	9864

after sampling method are shown in Table 5.37. The similar results for the IEEE RTS are given in Tables 5.38 and 5.39. Table 5.40 shows the CPU times and the variances of the estimates of the extreme emergency state probability. As expressed in equation (3.11), the efficiency of the simulation method can be measured by the product of the variance and the CPU time. It can be seen from Table 5.40 that the antithetic variate technique is more efficient than the stratification after sampling method with respect to the

**Table 5.40. Variances of Estimates of Extreme Emergency State Probability and CPU Times**

Method	Variance	CPU time on Micro VAX 3600
<b>MRBTS</b>		
without VRT	1.75E-7	38.86 sec
antithetic	8.50E-8	37.74 sec
stratification	1.68E-7	38.32 sec
<b>IEEE RTS</b>		
without		
VRT	7.84E-6	4.15 min
antithetic	3.69E-6	4.13 min
stratification	7.34E-6	4.15 min

calculation of probability indices for the extreme emergency state in both test systems. In fact, the stratification after sampling method basically does not provide improvement compared to the original sampling method without VRT. It should be noted that the efficiency of the methods with respect to other system operating states may lead to different conclusions.

## 5.10. NONCOHERENCE IN COMPOSITE SYSTEM ADEQUACY ASSESSMENT

Coherence is an important concept in general engineering system reliability evaluation. This concept states that if a component fails, system reliability never improves. Conversely, if a lost component is recovered, system reliability never decreases. The coherence assumption is widely used in engineering system reliability assessment. It is valid in generating system adequacy evaluation; however, it is not always true for a transmission or a composite generation and transmission system. This is because reliability of such a system does not only depend on failure or repair of components, but also on other constraints such as load flow equations and the capacity limits of transmission components.

### 5.10.1. Definitions and Measures of Noncoherence

**(a) Definitions of Noncoherence.** A general definition of noncoherence is that the loss of a component creates a more reliable system state;

conversely, the recovery of a lost component leads to a less reliable system state. From a power system planning point of view, however, a looser definition can be used. The looser definition states that loss of a component does not create a less reliable system state and recovery of a lost component does not lead to a more reliable system state.

The noncoherence feature is a function of the system states. The effect on system performance of the loss or recovery of a component depends on not only the component itself but also the system state prior to its loss or recovery. In other words, it is possible that the loss or recovery of a component may be noncoherent for a system state but coherent for another system state. It is necessary to relate noncoherence to failure levels. The following definitions are therefore further suggested:

- If in the normal system state, loss of one or more components creates a more reliable state than that normal state, the system is zero-level noncoherent.
- If in a single-level contingency system state (a component has failed), loss of one or more components creates a more reliable state than that contingency state, the system is first-level noncoherent.

The second-level, third-level, etc., noncoherence of a system can be defined similarly. When a system is zero-level coherent, it can be first-level or higher-level noncoherent. Basically, a composite system is and should be zero-level coherent because attempts are always made to avoid noncoherence in designing it. It is possible, however, that a transmission or composite system can be first- or higher-level noncoherent. This is because detecting a first- or higher-level noncoherence event requires a very considerable number of analyses for double and higher-level contingencies, while in most cases only single-level contingency analysis is emphasized in utility system planning guidelines. This is also associated with the historical development process of a system. Some parts of a network may also become “overlooped” in some system operating states when other parts are reinforced, and such situations cannot be found easily by traditional means. This case can happen particularly in lower-voltage transmission systems (230 kV and below). Generally, second- and higher-level noncoherent events have relatively small effects on total system reliability indices due to low probabilities of occurrence. First-level noncoherence, however, can create a very significant impact in some cases.

**(b) Measure of Noncoherence.** The following noncoherence degree indices can be used to measure degree of noncoherence:

$$\text{NCDE} = (\text{EENS} - \#\text{EENS})/\text{EENS} \quad (5.57)$$

$$\text{NCDF} = (\text{EFLC} - \#\text{EFLC})/\text{EFLC} \quad (5.58)$$

$$\text{NCDP} = (\text{PLC} - \#\text{PLC})/\text{PLC} \quad (5.59)$$

where

EENS = Expected Energy Not Supplied

EFLC = Expected Frequency of Load Curtailments

PLC = Probability of Load Curtailments

NCDE = Noncoherence Degree of EENS

NCDF = Noncoherence Degree of EFLC

NCDP = Noncoherence Degree of PLC.

In equations (5.57) to (5.59), the reliability indices with prefix # are those excluding the effects of noncoherence while the reliability indices without prefix # are those including the effects of noncoherence, i.e., obtained using a reliability evaluation method without the coherence assumption. Note that the reliability indices excluding the effects of noncoherence are not the same as those obtained using a reliability evaluation method with the coherence assumption. They are completely different. In order to calculate the reliability indices excluding effects of noncoherence, the following steps should be conducted (first-level noncoherence events are taken as examples):

1. For each single component failure, open one or more transmission components intentionally (this is referred to failure-dependent disconnection) and conduct overload and/or load curtailment analysis.

2. If an intentional opening leads to less overloads or load curtailments compared to just the single component failure, this is a first-level noncoherence event. Record all such events and intentionally disconnected corresponding components.

3. Evaluate system reliability excluding the effects of noncoherence. This means that each time a single component failure associated with noncoherence is selected by state enumeration or sampled by Monte Carlo simulation, corresponding intentional disconnections are imposed. This requires that a composite system reliability evaluation program has a function to simulate dependent failures.

Calculation steps associated with higher-level noncoherence events are similar, but require much more computational effort due to analyses of very considerable contingencies. Considering that higher-level transmission failures have small probabilities of occurrence, it is generally acceptable to neglect effects of the second- and higher-level noncoherence events when computational time is limited.

Equations (5.57) to (5.59) show three noncoherence degree indices associated with the reliability indices EENS, EFLC, and PLC. Noncoherence degree indices relating to other reliability indices can also be calculated in

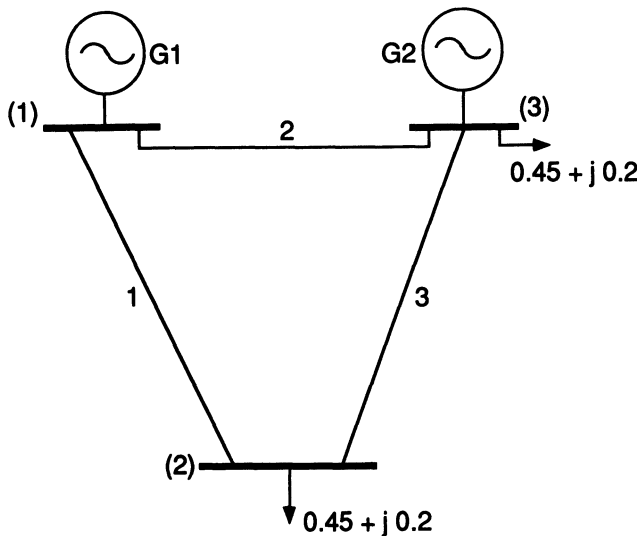


**Figure 5.19.** A three-bus system.

the same way. These indices range between 0.0 and 1.0. Essentially, they are percentages of contributions of noncoherence with respect to total system indices including effects of noncoherence. Generally, they cannot be equal to 1.0 but can be zero. Large values of the indices denote severe noncoherence. Zero is a critical value. It indicates that the system is coherent in terms of the strict noncoherence definition. It can also be said, however, that the system is noncoherent at index zero if the loosened noncoherence definition is used. Different noncoherence degree indices may give different indications. For example, it is possible that the NCDE index of a system can be close to 1.0 while the NCDF or the NCDP of the same system can be close to zero. This means that the system is quite noncoherent from the EENS index point of view but almost coherent from the EFLC or the PLC index point of view. This case can happen when intentional failure-dependent disconnections basically do not alleviate overloads or load curtailments but only reduce the extent of overloads or load curtailments. Therefore coherence or noncoherence is also a reliability-index-dependent concept.

## 5.10.2. A Simple Example

A simple example is used to illustrate the definitions and concepts given in the Section 5.10.1. Figure 5.19 shows a three-bus system. Two generating plants located in a generation center provide power to a load center at Bus

2 and local loads at Bus 3. The load center is relatively far away from the generation center while the two generating plants are quite close. Therefore, the impedance of Line 2 is much smaller than that of Line 1 or Line 3. Data are given in Tables 5.41 to 5.43. The base value is 100.0 MVA.

The contingency state enumeration technique is used to evaluate the system reliability. Contingencies are enumerated to the third level, i.e., single, double, or triple components can fail at the same time. It is unnecessary to consider the fourth- and fifth-level contingencies because of very low probabilities of occurrence. Out of the five first-level contingencies, only one (loss of G2) requires load curtailments in order to alleviate overloads on Line 2. In the case of the loss of G2, the load flow equation forces the power flow on Line 2 to be higher than its rating. Four out of the ten second-level contingencies and nine out of the ten third-level contingencies require load curtailments. The results associated with load curtailment events are listed

**Table 5.41. Bus Data of the Three-Bus System**

Bus No.	Type	Load		Specified voltage (p.u.)
		P (p.u.)	Q (p.u.)	
1	Swing	0.00	0.00	1.0
2	PQ	0.45	0.20	
3	PV	0.45	0.20	1.0

**Table 5.42. Branch Data of the Three-Bus System**

Line No.	From	To	R (p.u.)	X (p.u.)	Rating (MVA)
1	1	2	0.008	0.034	50.0
2	1	3	0.001	0.003	50.0
3	2	3	0.008	0.034	50.0

**Table 5.43. Component Failure Probabilities**

Component	Forced unavailability
G1	0.05
G2	0.05
Line 1	0.001
Line 2	0.0005
Line 3	0.001

**Table 5.44. Results Associated with Load Curtailment Events**

Event	Element out	Load curtailment (MW)	PLC	EENS (MWh/yr)
1	G2	25	0.047381345	10376.5146
2	G1 + G2	90	0.002493755	1966.0764
3	G2 + L2	45	0.000023703	9.3437
4	G2 + L1	45	0.000047429	18.6965
5	L1 + L3	45	0.000000902	0.3556
6	G1 + G2 + L1	90	0.000002496	1.9680
7	G1 + G2 + L2	90	0.000001248	0.9835
8	G1 + G2 + L3	90	0.000002496	1.9680
9	G1 + L1 + L3	45	0.000000047	0.0185
10	G1 + L2 + L3	45	0.000000024	0.0095
11	G2 + L1 + L2	90	0.000000024	0.0189
12	G2 + L1 + L3	45	0.000000047	0.0185
13	G2 + L2 + L3	45	0.000000024	0.0095
14	L1 + L2 + L3	90	4.5E - 10	0.0004

in Table 5.44. The system states without load curtailments are not listed. Among all these load curtailment contingencies, loss of G2 is a unique noncoherence event. In the case of losing G2, if Line 3 is intentionally opened, the overloads on Line 2 will disappear and consequently 25 MW of active load curtailments at Bus 3 are no longer required.

Adding event contributions to the PLC or EENS yields a total system PLC or EENS index which includes the effect of noncoherence. In order to obtain the PLC or EENS index excluding the effect of noncoherence, it is necessary to deduct the contribution due to loss of G2 (Event 1) from the total PLC or EENS index. Generally, the deduction should be the difference between the contribution due to the G2 loss event and that due to the event of loss of G2 plus intentional opening of Line 3. In this particular case, loss of G2 plus opening of Line 3 does not require any load curtailment. It can be seen from Table 5.44 that although loss of G2 is a unique noncoherence event, it is also a unique first level load curtailment event and its contribution to the total indices is dominant. It leads to a high degree of system noncoherence. Two noncoherence degree indices of the three-bus system are as follows:

$$\begin{aligned} \text{NCDE} &= 0.838 \\ \text{NCDP} &= 0.948 \end{aligned}$$

It is important to emphasize that since a noncoherence event is system state dependent, the intentional opening leading to a more reliable system state does not mean that the opened component is surplus and should be removed permanently. The intentional opening is only beneficial for this

particular system state. In the above example, for instance, opening Line 3 is only beneficial for the loss of the G2 event. It cannot be concluded that Line 3 should also be removed in other system states.

## 5.11. CONCLUSIONS

This chapter discusses the application of Monte Carlo methods in composite system adequacy assessment. The main difference between Monte Carlo simulation methods and state enumeration approaches is in the selection of the system states. Therefore, the system analysis techniques for each selected state, such as contingency analysis techniques and optimization models for corrective actions given in Sections 5.2 and 5.9, can also be applied in enumeration approaches. Monte Carlo methods can be used to consider complex practical factors associated with the selection of system states. For example, regional weather effects and bus load uncertainty and correlation described in Sections 5.5 and 5.7 may be very difficult, if not impossible, to incorporate using enumeration approaches. When generating unit derated states and transmission line common cause outages are considered, the system state sampling methods given in Sections 5.4 and 5.6 require less calculations than an enumeration technique. If the annual load curve is incorporated to calculate annual indices, however, combining the enumeration of multistep load levels with Monte Carlo simulation of component outages is more computationally efficient than sampling both load levels and component outages. This hybrid method is given in Section 5.3 and is essentially a variance reduction technique from a Monte Carlo simulation point of view.

The major advantage of the system state sampling method is reduced CPU time and memory requirements. This method can provide accurate probability and energy/power related indices. It can, however, only provide approximate frequency-related indices. This is because the transitions between system states and the chronology of the annual load curve are ignored. Theoretically, the system state duration sampling method can be used to calculate actual frequency indices. In the case of composite systems, however, there exist two obstacles. Considering chronological load curves of all buses creates a very large computational burden, which may be unfeasible at the present time for a practical composite system. Collecting chronological load data at all buses is also a very difficult task. The system state transition sampling method described in Section 5.8 provides a compromise. It creates a system state transition sequence but still uses the multistep load level model without load chronology. This method therefore can be used to calculate actual annualized frequency indices. If a multiload-level transition

model is utilized, the method can also be extended to include the effect of load state transitions on the frequency indices. However, this is still an approximation of actual annual frequency indices. There is a quite large difference between a multiload-level transition model and the actual chronological bus load curves.

Section 5.9 discusses security considerations in composite system adequacy assessment. This is not “security evaluation” involving system dynamic disturbances and a cascade collapse process. The basic idea is to incorporate steady-state security constraints in evaluation of operating state probability indices. In the operating practices of many utilities, transient and voltage stability limits are usually expressed using limit curves in generation space or power flow limits of crucial lines. If these limits are introduced in the simulation models, then transient and voltage stability are indirectly considered in the reliability evaluation. This may be a good replacement for detailed security evaluation, which reflects utility operational guidelines.

The definitions and indices of noncoherence in composite system adequacy assessment are discussed in Section 5.10. Noncoherence is system state dependent and reliability index dependent. Noncoherence of a composite system is not only theoretically meaningful, but also exists in actual power systems and has been detected in the BC Hydro South Vancouver Metro system.<sup>(42)</sup> A general composite system reliability evaluation program should not be based on the automatic assumption of coherence.

## 5.12. REFERENCES

1. IEEE Committee Report, “Bibliography on the Application of Probability Methods in Power System Reliability Evaluation,” *IEEE Trans. on PAS*, Vol. 91, 1972, pp. 649–660.
2. R. N. Allan, R. Billinton, and S. H. Lee, “Bibliography on the Application of Probability Methods in Power System Reliability Evaluation, 1977–1982,” *IEEE Trans. on PAS*, Vol. 103, 1984, pp. 275–282.
3. R. Billinton and R. N. Allan, *Reliability Evaluation of Power Systems*, Plenum, New York, 1984.
4. R. Billinton and R. N. Allan, *Reliability Assessment of Large Electric Power Systems*, Kluwer, Boston, 1988.
5. M. Th. Schilling, R. Billinton, A. M. Leite de Silva, and M. A. El-Kady, “Bibliography on Composite System Reliability (1964–1988),” *IEEE Trans. on PS*, Vol. 4, No. 3, 1989, pp. 1122–1131.
6. L. Salvadori, R. N. Allan, R. Billinton, J. Endrenyi, D. McGillis, M. Lauby, P. Manning, and R. J. Ringlee, “State of the Art of Composite System Reliability Evaluation,” 1990 CIGRE Meeting, WG38.03, Paris, Sept. 1990.
7. IEEE Tutorial Course Text, *Reliability Assessment of Composite Generation and Transmission Systems*, IEEE Publishing Services, 90EH0311-1-PWR, 1990.
8. R. Billinton, “Composite System Reliability Evaluation,” *IEEE Trans. on PAS*, Vol. 88, 1969, pp. 276–280.

9. R. Billinton, "Elements of Composite System Reliability Evaluation," *CEA Trans.*, Vol. 15, Pt. 2, 1976, Paper No. 76-SP-148.
10. P. L. Dandeno, G. E. Jorgensen, W. R. Puntel, and R. J. Ringlee, "Program for Composite Bulk Power Electric System Adequacy Assessment," *Trans. of the IEE Conference on Reliability of Power Supply Systems*, IEE Conference Publication No. 148, Feb. 1977.
11. G. E. Marks, "A Method of Combining High Speed Contingency Load Flow Analysis with Stochastic Probability Methods to Calculate a Quantitative Measure of Overall Power System Reliability," IEEE Paper A78-053-01.
12. EPRI Report, "Transmission System Reliability Methods," Project RP 1530-1, EL2526, 1982.
13. R. Billinton and T. K. P. Medicheria, "Overall Approach to the Reliability Evaluation of Composite Generation and Transmission Systems," *IEE Proc.*, Vol. 127, Pt. C, No. 2, 1980.
14. A. P. Meliopoulos, "Bulk Power Reliability Assessment with the RECS Program," Proceedings 1985 PICA Conference, pp. 38-46.
15. R. Billinton, "Composite System Adequacy Assessment—The Contingency Evaluation Approach," IEEE Tutorial Course Text, 90EH0311-1-PWR, Feb. 1990.
16. J. C. Dodu and A. Merlin, "An Application of Linear Programming to the Planning of Large Scale Power Systems: The MEXICO Model," Proceeding of the 5th PSCC, Cambridge, England, Sept. 1975.
17. P. Noferi, L. Paris, and L. Salvaderi, "Monte Carlo Methods for Power System Reliability Evaluation in Transmission and Generation Planning," Proceedings 1975 Annual Reliability & Maintainability Symposium, Washington D.C., Jan. 1975, Paper 1294, pp. 449-459.
18. P. Noferi and L. Paris, "Effect of Voltage and Reactive Power Constraints on Power System Reliability," *IEEE Trans. on PAS*, Vol. 94, 1975, pp. 482-490.
19. A. Merlin and P. H. Oger, "Application of a Variance Reducing Technique to a Monte Carlo Simulation Model of Power Transmission Systems," pp. 3-35, 3-44, Workshop Proceedings: *Power System Reliability—Research Needs and Priorities*, EPRI Report WS77-60, October, 1978.
20. R. Billinton and L. Salvaderi, "Comparison Between Two Fundamentally Different Approaches to Composite System Reliability Evaluation," *IEEE Trans. on PAS*, Vol. 104, 1985, pp. 3486-3492.
21. S. H. F. Cunha, M. V. F. Pereira, G. C. Oliveira, and L. M. V. G. Pinto, "Composite Generation and Transmission Reliability Evaluation in Large Hydroelectric Systems," *IEEE Trans. on PAS*, Vol. 104, No. 2, 1985, pp. 2657-2663.
22. EPRI Report, *Composite System Reliability Evaluation Methods*, Report EL-5178, June 1987.
23. EPRI Report, *Development of a Monte Carlo Composite System Reliability Evaluation Programming*, Report El-6926, Aug. 1990.
24. R. Billinton and W. Li, "Hybrid Approach for Reliability Evaluation of Composite Generation and Transmission Systems Using Monte Carlo Simulation and Enumeration Technique," *IEE Proc.*, Vol. 138, Pt. C, No. 3, 1991, pp. 233-241.
25. R. Billinton and W. Li, "A Novel Method for Incorporating Weather Effects in Composite System Adequacy Evaluation," *IEEE Trans. on PS*, Vol. 6, No. 3, 1991, pp. 1154-1160.
26. W. Li and R. Billinton, "Effect of Bus Load Uncertainty and Correlation in Composite System Adequacy Evaluation," *IEEE Trans. on PS*, Vol. 6, No. 4, 1991, pp. 1522-1529.
27. R. Billinton and W. Li, "Consideration of Multi-State Generating Unit Models in Composite System Adequacy Assessment Using Monte Carlo Simulation," *Canadian Journal of Electrical and Computer Engineering*, Vol. 17, No. 1, 1992.

28. R. Billinton and W. Li, "Composite System Reliability Assessment Using a Monte Carlo Approach," The Third International Conference on Probabilistic Methods Applied to Electric Power Systems, London, 3–5 July, 1991.
29. R. Billinton and W. Li, "Direct Incorporation of Load Variations in Monte Carlo Simulation of Composite System Adequacy," Inter-RAMQ Conference for the Electric Power Industry, Philadelphia, PA, Aug. 25–28, 1992.
30. R. Billinton and W. Li, "A System State Transition Sampling Method for Composite System Reliability Evaluation," *IEEE Trans. on PS*, Vol. 8, No. 3, 1993, pp. 761–770.
31. W. Li, "An On-Line Economic Power Dispatch Method with Security," *Electric Power Systems Research*, Vol. 9, 1985, pp. 173–181.
32. W. Li, "A Successive Linear Programming Model for Real-Time Economic Power Dispatch with Security," *Electric Power Systems Research*, Vol. 13, 1987, pp. 225–233.
33. IEEE Committee Report, "IEEE Reliability Test System," *IEEE Trans. on PAS*, Vol. 98, 1979, pp. 2047–2054.
34. R. Billinton and S. Kumar, "Effect of High-Level Independent Generation Outages in Composite System Adequacy Evaluation," *Proc. IEE*, Vol. 134, No. 1, 1987, pp. 17–26.
35. R. Billinton, S. Kumar, N. Chowdhury, K. Chu, K. Debnath, L. Goel, E. Khan, P. Kos, G. Nourbakhsh, and J. Oteng-Adjei, "A Reliability Test System for Educational Purpose: Basic Data," *IEEE Trans. on PS*, Vol. 4, 1989, pp. 1238–1244.
36. R. Billinton and K. E. Bollinger, "Transmission System Reliability Evaluation Using Markov Processes," *IEEE Trans. on PAS*, Vol. 87, 1968, pp. 538–547.
37. K. A. Clements, B. P. Lam, D. J. Lawrence, T. A. Mikolinna, A. D. Reppen, R. J. Ringlee, and B. F. Wollenberg, "Transmission System Reliability Methods—Mathematical Models, Computing Methods and Results," EPRI EL-2526, Power Technologie Inc., Schenectady, New York, July 1982.
38. M. E. Khan and R. Billinton, "A Hybrid Model for Quantifying Different Operating States of Composite Power Systems," *IEEE Trans. on PS*, Vol. 7, No. 1, 1992, pp. 187–193.
39. EPRI Report, "Composite System Reliability Evaluation: Phase 1—Scoping Study," Final Report, EPRI EL-5290, Dec. 1987.
40. M. E. Khan, "A Security Approach to Composite Power System Reliability Evaluation," Ph.D. Thesis, University of Saskatchewan, 1991.
41. R. Billinton and M. E. Khan, "A Security Based Approach to Composite System Reliability Evaluation," *IEEE Trans. on PS*, Vol. 7, No. 1, 1992, pp. 65–72.
42. W. Li, "Reliability Assessment of the South Metro System Planning Alternatives," BC Hydro, RSP Technical Report, File 940-R-5, Aug. 10, 1992.

# 6

# Distribution System and Station Adequacy Assessment

## 6.1. INTRODUCTION

This chapter discusses the application of Monte Carlo methods to distribution system and station adequacy assessment. The basic system analysis logic associated with distribution system and station configuration adequacy assessment is very similar. The main approach is to examine the existence of continuity between the supply point(s) and the load points. Existence of continuity is associated not only with failures of line components, but also with the switching logic of breakers and section switches, protection device actions, and operating guidelines for backup supply sources. This is obviously quite different from the system analysis principles associated with generation adequacy or composite system adequacy assessment.

Both the state sampling and state duration sampling techniques can be applied to distribution system and station configuration adequacy assessment. The state duration sampling technique, however, is preferable as this approach can be used to calculate actual frequency and duration indices using the chronological component or system state transition cycles. Frequency and duration indices are particularly important in distribution system and station adequacy assessment. Reliability evaluation of a distribution system or a voltage step-down station is usually associated directly with the customer load point performance. Most customers are very concerned about

how often outages are expected to occur and how long they are expected to last.

Distribution system and station reliability assessment can be conducted quite successfully using analytical methods.<sup>(1-13)</sup> The concepts and techniques associated with the analytical method are both useful and helpful in understanding the application of Monte Carlo methods. Some techniques are, in fact, a combination of the Monte Carlo method and the analytical approach. The basic concepts of an analytical approach to distribution system reliability assessment are first described in Section 6.2. Application of the component state duration sampling method to distribution system and station configuration adequacy assessment is illustrated in Sections 6.3 and 6.4, respectively. One advantage of the Monte Carlo method is that it can provide information related to the probability distributions of the reliability indices in addition to the mean or average values.<sup>(14,15)</sup> Simulation can also be used to recognize complex component repair or restoration time distributions. These aspects are quite difficult, if not impossible, to incorporate into an analytical method without assumptions or simplifications.

## **6.2. BASIC CONCEPTS AND ANALYTICAL TECHNIQUES FOR DISTRIBUTION SYSTEM ADEQUACY ASSESSMENT**

### **6.2.1. General Concepts**

Quantitative reliability evaluation of a distribution system can be divided into the two basic segments of measuring past performance and predicting future performance.<sup>(13)</sup> Most utilities collect data on past system performance and display the results using a range of statistics. Some of the basic indices used to assess past performance are the system average interruption frequency index (SAIFI), the system average interruption duration index (SAIDI), the customer average interruption duration index (CAIDI), the average service availability index (ASAI), the average service unavailability index (ASUI), and the energy not supplied (ENS).<sup>(2)</sup> Predictive reliability assessment of a distribution system is usually concerned with the performance at the customer load points. The basic indices normally used are load point failure rate, average outage duration, and annual unavailability. The basic indices are important with respect to a particular load point, but they do not give an overall appreciation of the area or system

**Table 6.1. Average Annual Canadian Indices**

Year	SAIFI (int./syst. cust.)	SAIDI (hr/syst. cust.)	IOR
1988	4.35	6.42	0.999267
1989	3.61	4.35	0.999503
1990	4.03	4.55	0.999480
1991	3.55	4.24	0.999516
1992	3.06	3.34	0.999619

performance. Additional indices can be calculated using these three basic indices and the number of customers/loads connected at each load point. These additional indices are weighted averages of the basic load point indices and are basically identical to those which have been used for many years to assess past system performance. The most common additional indices are SAIFI, SAIDI, CAIDI, ASAII, and ASUI. The procedure for calculating these indices is given in Section 2.6.3.

Canadian electric power utilities have been active in collecting service continuity statistics for over 30 years and produced their first national compilation in 1962. This work is now performed by the Canadian Electrical Association (CEA). The average service availability index (ASAII) is known as the index of reliability (IOR) in the CEA reporting system. Table 6.1 shows the aggregate Canadian values for SAIDI, SAIFI, and IOR for the 1988–1992 period. These data give a general indication of Canadian utility performance over the 5-yr period. Distribution engineers are acutely conscious of the contribution made by the distribution facilities toward the overall service to the customer and normally subdivide the interruptions into categories which can be used to identify causes and the need for future expenditures. This is illustrated in Tables 6.2 and 6.3, which show the average cause contributions to the overall annual SAIDI and SAIFI statistics taken from the 1988–1992 period. Values in parentheses are the percentage contributions to the annual value. It can be seen from Tables 6.2 and 6.3 that the category “loss of supply” contributes 23.5% and 17.1% to the overall average SAIFI and SAIDI values, respectively. This supports the general statement that approximately 80% of all customer interruptions occur due to failures in the distribution system. Most utilities compile service continuity statistics on individual feeders, groups of feeders, districts and areas in their systems. These data are used for a wide variety of managerial and engineering functions.<sup>(6,13)</sup>

Past performance statistics provide a valuable reliability profile of the existing system. Distribution planning, however, involves the analysis of future systems and the evaluation of system reliability when the configura-

**Table 6.2. Cause Contributions to the Annual SAIFI (int./syst. cust.)**

Cause	Average
Unknown/other	0.32 (8.5)
Scheduled interruption	0.75 (20.0)
Loss of supply	0.88 (23.5)
Tree contact	0.25 (6.7)
Lightning	0.22 (5.9)
Defective equipment	0.72 (19.2)
Adverse weather	0.21 (5.6)
Adverse environment	0.03 (0.8)
Human element	0.10 (2.7)
Foreign interference	0.27 (7.2)
Total	3.75

**Table 6.3. Cause Contributions to the Annual SAIDI (hr./syst. cust.)**

Cause	Average
Unknown/other	0.29 (6.4)
Scheduled interruption	0.69 (15.3)
Loss of supply	0.77 (17.1)
Tree contact	0.61 (13.5)
Lightning	0.32 (7.1)
Defective equipment	0.91 (20.2)
Adverse weather	0.59 (13.1)
Adverse environment	0.05 (1.1)
Human element	0.06 (1.3)
Foreign interference	0.22 (4.9)
Total	4.51

tion, or the operating conditions, or the protection scheme changes. This task is known as predictive reliability assessment, in which the distribution system reliability indices are calculated using component failure data.

## 6.2.2. Basic Distribution Systems

The distribution system is that portion of the electric power system which links the bulk power source(s) to the consumer's facilities. Sub-transmission circuits, distribution substation, primary feeders, distribution transformers, secondary circuits, and consumer's connections form different parts of what can generally be called a distribution system. Distribution system reliability evaluation therefore consists of assessing how adequately

the different parts are able to perform their intended function. The distribution system is an important part of the total electric system as it provides the link between the bulk system and the customer.

A distribution circuit normally uses primary or main feeders and lateral distributors. A main feeder originates from the substation and passes through the major load centers. The individual load points are connected to the main feeder by lateral distributors with distribution transformers at their ends. A main feeder is constructed using single, parallel, or meshed circuits. Many distribution systems used in practice have a single-circuit main feeder and are defined as radial distribution systems. There are also many systems which, although constructed using meshed circuits, are operated as radial systems using normally open switches in the meshed circuit. The main feeder, in some cases, may have branches to reach the widely distributed areas.

Radial systems are popular because of their simple design and generally low cost. These systems have a set of series components between the substation and the load points. The failure of any of these components causes outage of the load point(s). The outage duration and the number of customers affected due to a component failure are reduced by using extensive protection and sectionalizing schemes. Sectionalizing equipment provides a convenient means of isolating a faulted section. The supply can then be restored to the healthy sections, maintaining the service to some of the load points, while the faulted component is repaired. The time taken by this type of isolation and switching action is referred to as restoration time.

In some systems, there is provision for an alternate supply in the case of a failure. This alternate source is used to supply that section of the main feeder which becomes disconnected from the main supply after the faulted section has been isolated. The alternate supply, however, may not always be available and this factor should be included in the analysis. Fuses are usually provided on the lateral distributors. Faults on a lateral distributor or in a distribution transformer are normally cleared by a fuse and therefore service on the main feeder is maintained. If the fuse fails to clear the fault for some reason, the circuit breaker or the back-up fuse on the main feeder acts to clear the fault. The faulted lateral distributor is then isolated and the supply is restored to the rest of the system by switching action.

### 6.2.3. Analytical Techniques

It is useful to illustrate the basic analytical approach to distribution system assessment before discussing the proposed Monte Carlo simulation method. Analytical techniques can be readily used to calculate load point

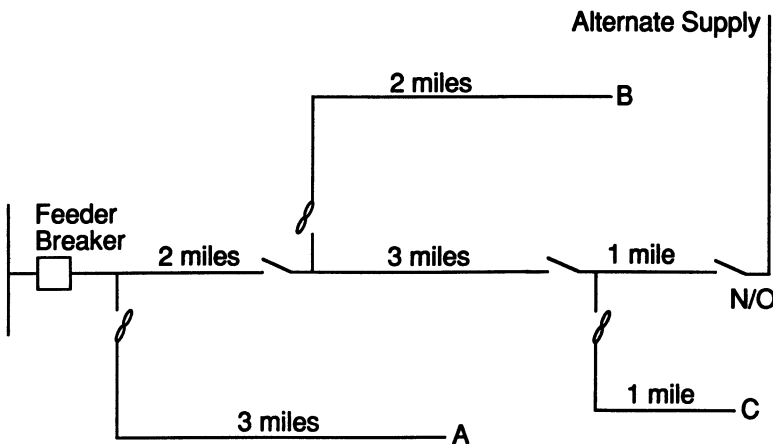


**Figure 6.1.** A simple radial configuration.

and system average performance indices.<sup>(1-3)</sup> An important benefit of the Monte Carlo method is that it can be used to provide probability distributions of these indices. The basic logic required to analyze the system failure modes is the same for both the analytical approach and the Monte Carlo method.

As noted earlier, the basic indices used to predict the reliability of a distribution system are the average load point failure rate ( $\lambda$ ), the average load point outage duration ( $r$ ), and the average annual load point outage time or unavailability ( $U$ ). The system performance indices SAIDI, SAIFI, CAIDI, etc. can be calculated from the three basic predictive indices. In order to illustrate the basic analytical technique, an example calculation is presented for the simple radial system shown in Figure 6.1. The following section presents and compares the results of Monte Carlo simulation for the same system. In this configuration, all switches except that connected to the alternate supply are normally closed, and the feeder breaker and substation supply bus are assumed to be fully reliable. In Case 1, the customer load points A, B, and C are supplied from the primary main feeder by fused laterals. The alternate supply shown in Figure 6.1 is assumed to be unavailable in Case 1. The individual component data are as follows:

**Primary main feeder**

0.1 failures/circuit mile/yr,    3.0 hr average repair time

**Primary lateral**

0.25 failures/circuit mile/yr,    1.0 hr average repair time

Manual sectionalizing time for any switching action is 0.5 hr.

**Table 6.4. Calculations for Case 1**

Component	Load point A			Load point B			Load point C		
	$\lambda$ (f/yr)	$r$ (hr/f)	$\lambda r$ (hr/yr)	$\lambda$ (f/yr)	$r$ (hr/f)	$\lambda r$ (hr/yr)	$\lambda$ (f/yr)	$r$ (hr/f)	$\lambda r$ (hr/yr)
<b>Main sections</b>									
2 miles	0.2	3.0	0.6	0.2	3.0	0.6	0.2	3.0	0.6
3 miles	0.3	0.5	0.15	0.3	3.0	0.9	0.3	3.0	0.9
1 mile	0.1	0.5	0.05	0.1	0.5	0.05	0.1	3.0	0.3
<b>Lateral sections</b>									
3 miles	0.75	1.0	0.75	—	—	—	—	—	—
2 miles	—	—	—	0.5	1.0	0.5	—	—	—
1 mile	—	—	—	—	—	—	0.25	1.0	0.25
	1.35	1.15	1.55	1.1	1.86	2.05	0.85	2.41	2.05

The basic analytical approach involves a failure mode and effect analysis utilizing the following basic equations:

$$\lambda_s = \sum \lambda_i \quad (6.1)$$

$$r_s = \frac{\sum \lambda_i r_i}{\sum \lambda_i} \quad (6.2)$$

$$U_s = \lambda_s r_s \quad (6.3)$$

This procedure for Case 1 is illustrated in Table 6.4. The results are summarized in Table 6.5.

There are many configurations, particularly in rural locations, which have a topology similar to that shown in Figure 6.1. The results shown in Table 6.5 can be used to obtain the system performance indices. The calculation formulas for these indices are given in Section 2.6.3. Assume that there are 250, 100, and 50 customers, respectively, at load points A, B, and C, giving a total of 400 customers in the system:

$$\begin{aligned} &\text{Annual Customer Interruptions} \\ &= (250)(1.35) + (100)(1.1) + (50)(0.85) = 490 \end{aligned}$$

$$\begin{aligned} &\text{Customer Interruption Duration} \\ &= (250)(1.55) + (100)(2.05) + (50)(2.05) = 695 \end{aligned}$$

**Table 6.5. Calculated Indices for Case 1**

Index	A	B	C
$\lambda$ (failures/yr)	1.35	1.10	0.85
$r$ (hr/failure)	1.15	1.86	2.41
$U$ (hr/yr)	1.55	2.05	2.05

**Table 6.6. Calculations for Case 2**

Component	Load point A			Load point B			Load point C		
	$\lambda$ (f/yr)	$r$ (hr/f)	$\lambda r$ (hr/yr)	$\lambda$ (f/yr)	$r$ (hr/f)	$\lambda r$ (hr/yr)	$\lambda$ (f/yr)	$r$ (hr/f)	$\lambda r$ (hr/yr)
<b>Main sections</b>									
2 miles	0.2	3.0	0.6	0.2	1.0	0.2	0.2	1.0	0.2
3 miles	0.3	0.5	0.15	0.3	3.0	0.9	0.3	1.0	0.3
1 mile	0.1	0.5	0.05	0.1	0.5	0.05	0.1	3.0	0.3
<b>Lateral sections</b>									
3 miles	0.75	1.0	0.75	—	—	—	—	—	—
2 miles	—	—	—	0.5	1.0	0.5	—	—	—
1 mile	—	—	—	—	—	—	0.25	1.0	0.25
	1.35	1.15	1.55	1.1	1.5	1.65	0.85	1.24	1.05

**System Average Interruption Frequency Index (SAIFI)**

$$\text{SAIFI} = 490/400 = 1.23 \text{ interruptions/system customer/yr}$$

**System Average Interruption Duration Index (SAIDI)**

$$\text{SAIDI} = 695/400 = 1.74 \text{ hr/system customer/yr}$$

**Customer Average Interruption Duration Index (CAIDI)**

$$\text{CAIDI} = 695/490 = 1.42 \text{ hr/customer interrupted}$$

**Average Service Availability Index (ASAI)**

$$\text{ASAI} = (400 \times 8760 - 695) / (400 \times 8760) = 0.999802.$$

The calculated values can be compared with measured values or, if available, with standard indices for the system to determine if the configuration is acceptable.

Similar calculations can be conducted to investigate the effect on the load point and system indices of configuration and operating changes. The calculations for two additional cases are given in Tables 6.6 and 6.8.

In Case 1, the alternate supply shown in Figure 6.1 is assumed to be unavailable. This facility is available in Case 2, with an average switching

**Table 6.7. Calculated Indices for Case 2**

Index	A	B	C
$\lambda$ (failures/yr)	1.35	1.10	0.85
$r$ (hr/failure)	1.15	1.50	1.24
$U$ (hr/yr)	1.55	1.65	1.05

System performance indices

$$\text{SAIFI} = 1.23 \text{ interruptions/system customer/yr}$$

$$\text{SAIDI} = 1.51 \text{ hr/system customer/yr}$$

$$\text{CAIDI} = 1.23 \text{ hr/customer interrupted}$$

$$\text{ASAI} = 0.999827$$

**Table 6.8. Calculations for Case 3**

Component	Load point A			Load point B			Load point C		
	$\lambda$ (f/yr)	$r$ (hr/f)	$\lambda r$ (hr/yr)	$\lambda$ (f/yr)	$r$ (hr/f)	$\lambda r$ (hr/yr)	$\lambda$ (f/yr)	$r$ (hr/f)	$\lambda r$ (hr/yr)
<b>Main sections</b>									
2 miles	0.2	3.0	0.6	0.2	3.0	0.6	0.2	3.0	0.6
3 miles	0.3	0.5	0.15	0.3	3.0	0.9	0.3	3.0	0.9
1 mile	0.1	0.5	0.05	0.1	0.5	0.05	0.1	3.0	0.3
<b>Lateral sections</b>									
3 miles	0.75	1.0	0.75	0.75	1.0	0.75	0.75	1.0	0.75
2 miles	0.5	0.5	0.25	0.5	1.0	0.5	0.5	1.0	0.5
1 mile	0.25	0.5	0.125	0.25	0.5	0.125	0.25	1.0	0.25
	2.10	0.92	1.93	2.10	1.39	2.93	2.10	1.57	3.30

time of one hour. Tables 6.6 and 6.7 illustrate the effect of this alternate supply on the calculated reliability indices. It can be seen that the load point failure rates are not affected by the ability to backfeed from an alternate configuration. This will apply in all cases in which the restoration of service is done manually. If automatic switching is used and the customer outage time is considered to be so short that the event is not classed as a failure, then the overall failure rate will be reduced to a value close to the primary lateral value. The ability to backfeed has a pronounced effect on the length of the interruption, particularly for those customers at the extremities of the primary main.

The load point failure rates are highly dependent upon the components exposed to failure and the degree of automatic isolation of a failed component in the network. Case 3 is a situation in which the alternate supply is unavailable and each lateral is solidly connected to the primary main. In this case, all load points will have the same failure rate, as any fault will result in the feeder breaker tripping. The analysis for this case is shown in Table 6.8. The load point and system results are given in Table 6.9.

**Table 6.9. Calculated Indices for Case 3**

Index	A	B	C
$\lambda$ (failures/yr)	2.10	2.10	2.10
$r$ (hr/failure)	0.92	1.39	1.57
$U$ (hr/yr)	1.93	2.93	3.30

System performance indices

SAIFI = 2.10 interruptions/system customer/yr

SAIDI = 2.35 hr/system customer/yr

CAIDI = 1.12 hr/customer interrupted

ASAI = 0.999732

## 6.3. MONTE CARLO SIMULATION APPROACH TO DISTRIBUTION SYSTEM ADEQUACY ASSESSMENT

### 6.3.1. Probability Distribution Considerations

The analytical techniques given in Section 6.2.3 can be readily used to calculate the expected or average value of the particular reliability measure. The expected values are extremely useful and are the primary indices of load point adequacy. There is, however, an increasing awareness of the need for information related to the variation of these reliability measures.<sup>(15-17)</sup> Probability distributions provide a practical means of describing this. This information can prove useful in studies involving:

1. The determination of customer costs of interruptions using nonlinear cost functions.<sup>(16)</sup>
2. The validation of reliability models and the applicability of reliability data. The index probability distributions can prove useful in estimating the errors resulting from inaccurate data.
3. Comparisons between performance indices of different years or different systems to determine the probability of their having different average values. Such a comparison can assist planners to judge whether differences in indices indicate real changes in performance or are due to statistical variations.
4. The probability of the interruptions being longer than the Critical Service Loss Duration Time or some other time of interest.<sup>(18-20)</sup> This information is especially useful in the design of distribution systems for industrial customers with critical processes or commercial customers with nonlinear cost functions.

Studies of the distributions associated with the basic reliability indices indicate that the load point failure rate is approximately Poisson-distributed.<sup>(17,21)</sup> The failure probability therefore can be readily obtained using the mean load point failure rate, since the Poisson distribution is a single-parameter function. This information can be calculated directly using the Poisson equation or from a set of published graphs.<sup>(22)</sup> It has been noted that if the restoration times of components can be assumed to be exponentially distributed, the load point outage duration is approximately gamma-distributed and the desired probability information can be readily calculated.<sup>(17,21)</sup> There are, however, many distribution systems for which

the gamma distribution does not adequately describe the load point outage duration. These systems are typically those in which the restoration times may be better described by nonexponential distributions, e.g., log-normal repair or manual sectionalizing times. When the restoration times are assumed to be nonexponential, the interruption duration cannot generally be represented by a gamma distribution.<sup>(13-15)</sup> Probability distributions for the annual load point outage time, SAIDI, SAIFI, and CAIDI indices can also not be represented by common distributions.

### 6.3.2. Component State Duration Sampling Method

In distribution system reliability assessment, the three basic load point indices are failure rate, average outage duration, and average annual outage time. As noted in Section 3.6.2, the component state duration sampling method can be used to calculate actual frequency and duration indices, recognizing component state duration distributions, and to provide reliability index probability distributions. The following two techniques based on the component state duration sampling can be applied to distribution system reliability assessment.

**(a) Individual Component Operating Cycle Technique.** A customer connected to any load point in a radial distribution system requires that all components between the load and the supply point be operating. Consequently, the principle of series systems can be applied. Equations (6.1) to (6.3) are based on this principle. The individual component operating cycle technique is a combination of the component state duration sampling and the analytical method given in Section 6.2.3. This technique includes the following steps:

1. Artificial up-down operating histories of all line sections are obtained by component state duration sampling.
2. The effects of the operating state (up or down) of each line section on a load point state are examined individually, based on the system configuration. Possible modifications associated with manual manipulations are then conducted. For example, when a load point supply can be restored by sectionalizing equipment, the down-state duration of that load point caused by a particular line section failure should be adjusted as

$$T_d = \min\{T_s, T_r\} \quad (6.4)$$

where  $T_d$  is the down-state duration after the modification,  $T_s$  is the sampled value of the down-state duration before the modification, and  $T_r$  is the manual sectionalizing time.

3. The average values of the three basic load point indices caused by each single line section (subscript  $i$ ) operating history can be calculated by

$$\lambda_i = \frac{N}{\sum T_u} \quad (6.5)$$

$$r_i = \frac{\sum T_d}{N} \quad (6.6)$$

$$U_i = \frac{\sum T_d}{\sum T_u + \sum T_d} \approx \frac{\sum T_d}{\sum T_u} = \lambda_i r_i \quad (6.7)$$

where  $\sum T_u$  and  $\sum T_d$  are summations of all up times and all down times during the total sample years, respectively;  $N$  is the number of transitions between the up and down states during the total sample years. The calculated values from these equations correspond to those in one row associated with a particular line section in Table 6.4. The total load point indices corresponding to all line sections can be obtained using the same calculation procedure shown in Table 6.4, in terms of equations (6.1) to (6.3). The analytical approach is obviously much faster than the Monte Carlo method if only mean values of the reliability indices are required. The purpose behind utilizing the Monte Carlo method is to calculate index probability distributions and possibly incorporate more complex configurations or operating logic.

4. The calculations associated with the probability distributions are similar. The average values of the three basic indices in a single year due to each single line section can be obtained by equations similar to (6.5)–(6.7). The difference is that  $\sum T_u$ ,  $\sum T_d$ , and  $N$  correspond to each year instead of the entire sampling span. Thus  $\sum T_u$ ,  $\sum T_d$ , and  $N$  should be expressed as  $(\sum T_u)_j$ ,  $(\sum T_d)_j$  and  $N_j$  where subscript  $j$  denotes year  $j$ . Corresponding  $\lambda_i$ ,  $r_i$ , and  $U_i$  also should be expressed as  $\lambda_{ij}$ ,  $r_{ij}$ , and  $U_{ij}$  (subscript  $ij$  indicates line section  $i$  and year  $j$ ). Equations (6.1) to (6.3) can be used to obtain the total load point indices caused by all line sections in each sample year. The probability distribution of a load point outage rate can be calculated using

$$P(k) = \frac{m(k)}{M} \quad (k = 0, 1, 2, \dots) \quad (6.8)$$

where  $M$  is the number of years in a whole sampling span and  $m(k)$  is the number of years in which the load point outage rate equals  $k$ . For example, when  $k = 1$ ,  $m(1)$  is the number of years in which the number of load point failures is 1. Similar calculations can be conducted to obtain the probability distributions of load point outage duration ( $r$ ) and load point unavailability ( $U$ ). Because  $r$  and  $U$  are continuous random variables, discrete class intervals must be selected.

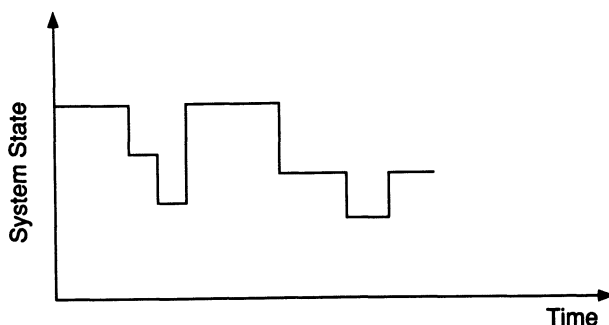


**Figure 6.2.** A simulated system operating history.

**(b) System Operating Cycle Technique.** The individual component operating cycle technique utilizes equations (6.1) to (6.3), which are based on the principle of series systems and therefore only apply to simple radial distribution systems. The system operating cycle technique can be applied in more complex situations, such as combined configurations of distribution systems and substation arrangements, or a distribution system with parallel circuits or meshed loops. It includes the following steps:

1. Artificial up-down operating histories of all line sections are obtained by the component state duration sampling.
2. A system operating history shown in Figure 6.2 can be obtained by combining up-down operating histories of all line sections. In this process, manual manipulations such as sectionalizing actions also should be incorporated. Each step shown in Figure 6.2 corresponds to a system operating state, which denotes opening due to component failure(s) or closing due to component repairs or manual switching.
3. Each system state is evaluated to obtain load point up-down operating histories. This is usually associated with checking connectivity from the source point(s) to each load point.
4. The mean values and probability distributions of the three basic load point reliability indices can be calculated using equations similar to (6.5)–(6.8). The load point up-down operating histories are obtained from evaluating whole system states but not from each single line section operating history. Consequently, utilization of equations (6.1) to (6.3) is no longer required.

### 6.3.3. Load Point Index Distributions

A Monte Carlo based computer program has been developed at the University of Saskatchewan to simulate the performance of any  $N$ -section

**Table 6.10. Load Point Indices Using the Two Methods (Case 1)**

Index	Load point		
	A	B	C
$\lambda$ (failures/yr)			
Analytical	1.35	1.10	0.85
Simulation	1.35	1.10	0.86
$r$ (hr/failure)			
Analytical	1.15	1.86	2.41
Simulation	1.17	1.87	2.42
$U$ (hr/yr)			
Analytical	1.55	2.05	2.05
Simulation	1.57	2.07	2.08

radial distribution system with loads connected to laterals or directly to the primary mains.<sup>(14,17)</sup> Any combination of exponential, normal, log-normal, and gamma distributions can be used to simulate the failure, repair, manual sectionalizing, alternate supply, and fuse times. Studies were performed using the system shown in Figure 6.1. The mean values in Case 1 (base case) obtained from the Monte Carlo simulation for a period of 5000 years and those obtained from the analytical approach are summarized in Table 6.10. In this simulation, all the failure and repair or restoration times are assumed to be exponentially distributed. It can be seen that the results using the Monte Carlo method and the analytical approach are basically the same. It should be noted that the mean load point indices are unaffected by restoration time distributions.

**(a) Distributions of Load Point Failure Rate.** The components were assumed to be in their useful operating life and therefore the failure times were exponentially distributed. The probability distribution of the load point failure rate can be calculated using the Poisson distribution:

$$P(n) = \frac{(\lambda t)^n e^{-\lambda t}}{n!} \quad (6.9)$$

where  $n$  is the number of failures in time  $t$ .

The results of Monte Carlo simulation match those obtained by theoretical analysis. Figure 6.3 presents the distributions associated with the failure rates of load points A, B, and C in Cases 1, 2, and 3 for the system shown in Figure 6.1. The distributions for Case 1 are identical to those for Case 2, due to the fact that backfeeding does not alter the probability of failure. In both cases, the distributions are noticeably different for the three

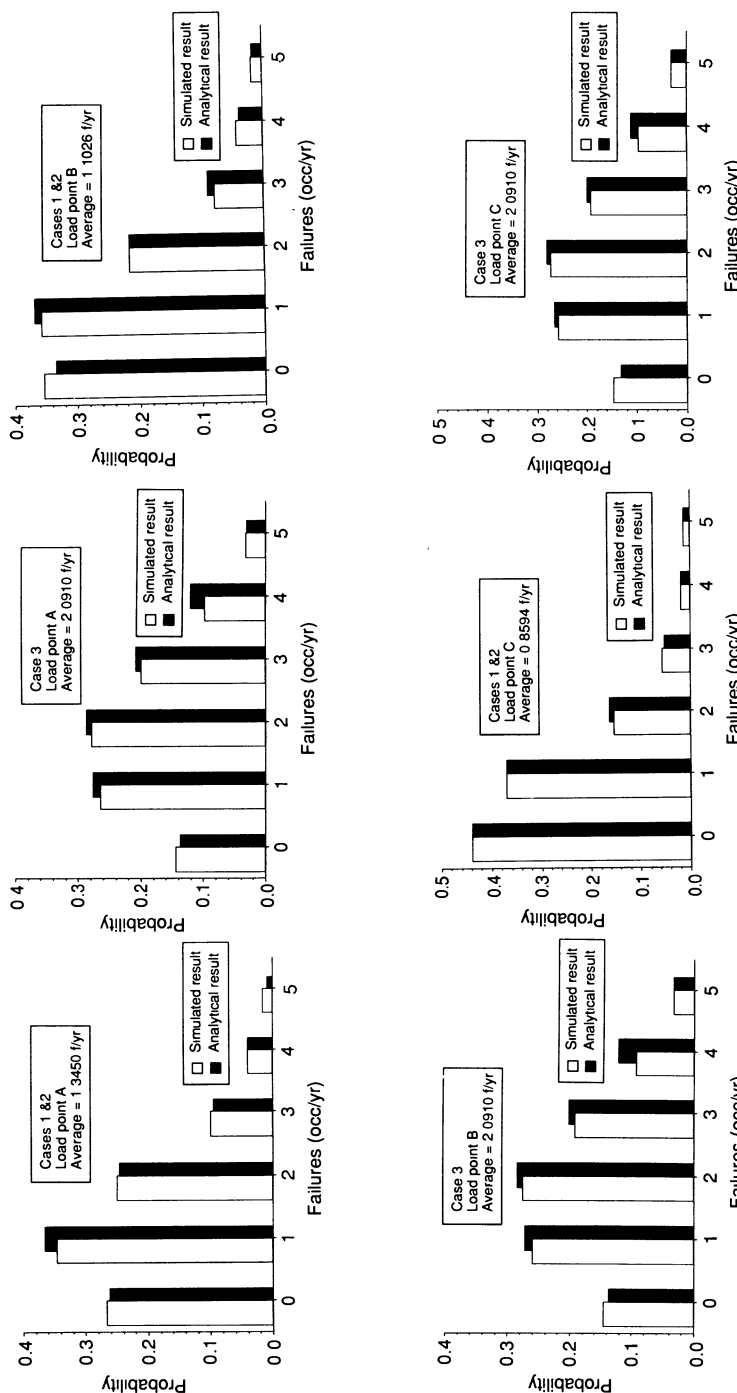


Figure 6.3. Load point failure rate distributions.

load points. At load point A, years with one failure occur most frequently while, at load point C, years with no failures occur most frequently. The distributions for Case 3 vary from those for Cases 1 and 2, but are identical for each of the three load points. This is due to the fact that each load point experiences a failure when any one of the solidly connected laterals suffers a fault.

**(b) Distributions of Load Point Outage Duration.** If the repair and other restoration times of the components can be assumed to be exponentially distributed, the load point outage duration can be approximated by a gamma distribution.<sup>(21)</sup> This is confirmed by the results of Monte Carlo simulation. Figure 6.4 shows the results for the outage durations of load points A, B, and C for Cases 1, 2, and 3 when the restoration times are exponentially distributed. These distributions can be reasonably described by the gamma distribution (chi-square test at a significance level of 0.05). As can be seen, the general shape of the distributions does not vary. Although the gamma distribution can take on many different shapes, the shape is always of this general form when it is the result of combinations of exponential distributions. The gamma distribution becomes more or less spread out, or more peaked, depending on the component average restoration durations.

In many practical systems, the restoration times are not exponentially distributed. Restoration times may be better described by nonexponential distributions, such as log-normal repair times. The studies carried out indicate that when the restoration times are assumed to be nonexponential, the load point outage duration cannot generally be represented by a gamma distribution.

It should be emphasized that the average values of the load point outage duration indices are not affected by underlying distributions. A set of averages such as those calculated for the example system can have any set of distributions associated with it.

The durations associated with repairs and other restoration activities may often be well described by the log-normal distribution. Figure 6.5 shows the simulated outage duration results, when restoration times are assumed to be log-normally distributed with a standard deviation equal to one-third of the mean. These load point outage duration distributions have a radically different shape than those assuming exponential restoration times (Figure 6.4). In Case 1, the probability of outage duration for load point A appears to be decreasing as the outage duration increases, except for a peak of two bars wide. This peak is attributable to the large number of repairs of 1-hr average duration which are made on the first primary lateral. Due to it being further down the line, load point C has a larger number of 3-hr repair

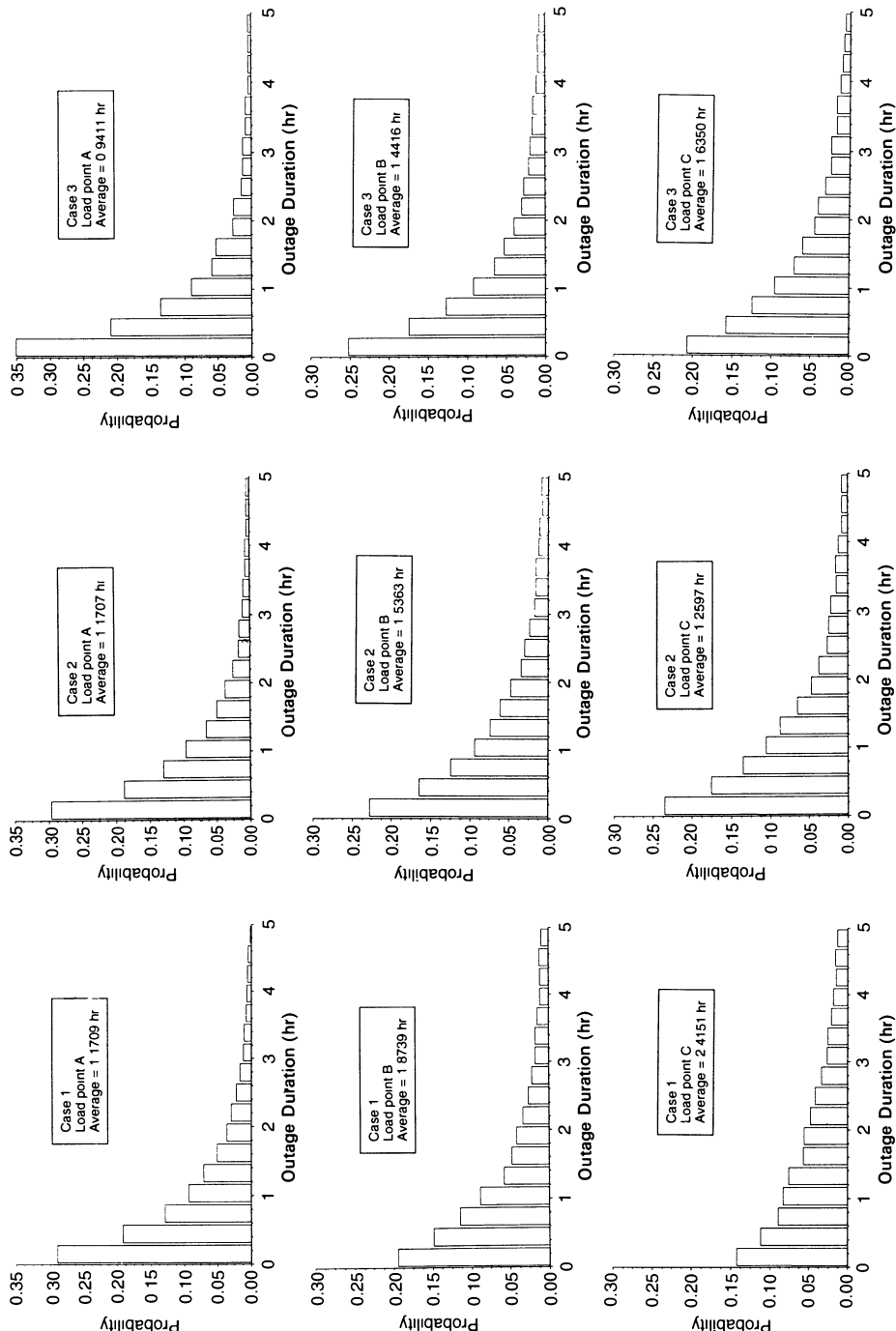


**Figure 6.4.** Load point outage duration distributions for exponentially distributed repair times.

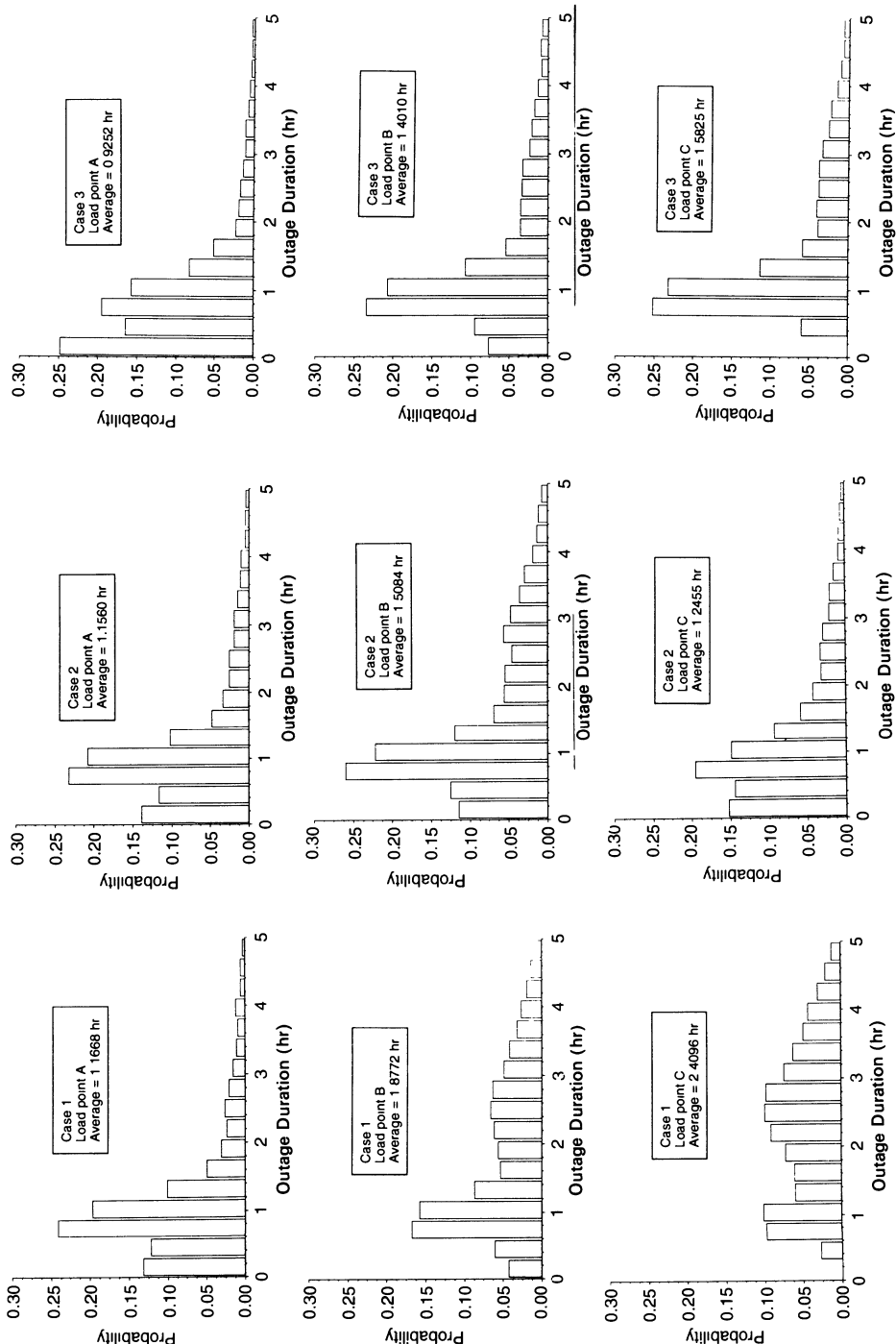


**Figure 6.5.** Load point outage duration distributions for log-normally distributed repair times ( $SD = 1/3$  mean).

average durations. The repairs to the mains in combination with repairs to the third lateral result in a bimodal distribution with two peaks at durations about 1 and 3 hr long. Load point B has a distribution that is a combination of those at A and C.

The backfeeding in Case 2 reduces the number of failures with three-hour repairs at load point C. The second mode in the distribution is eliminated. The mode resulting from the lateral repairs is now more pronounced for both load points B and C. When the laterals are connected solidly to the mains as in Case 3, the first mode is even more pronounced for all three load points. The predominant cause of outages are failures on the primary laterals resulting in 1-hr average repairs.

A visual inspection of the distributions in Figure 6.5 indicates that the distributions are quite different from those in Figure 6.4 and that attempts to predict the duration probabilities using the gamma distribution in the cases of nonexponential restoration times could lead to large errors. Similar results have been obtained from simulations in which restoration activities are assumed to be gamma and normally distributed. The study results indicate that no known distribution can universally describe the outage duration distributions.

The distributions vary with the means and the standard deviations of the component repair times. Figure 6.6 shows the outage duration distributions for load points A and C for the system in Case 1 with the assumptions that the standard deviations for the component repair times are equal to  $m$  (MTTR),  $m/2$ , and  $m/6$ . When the standard deviations are relatively large, the contributing distributions overlap, with the result that the outage duration distribution is almost a monotonically decreasing function. As the standard deviations decrease, the contributing distributions become apparent and the distribution is definitely multimodal. The sizes and the number of primary main or lateral sections affects the mean, the standard deviation, and possibly the type of the component repair time distributions. The load point outage duration distributions are then indirectly affected by these factors.

**(c) Distributions of Load Point Annual Interruption Time.** The distributions of load point annual interruption time are dependent on both the failure rate and outage duration distributions. This makes it even more difficult to describe the interruption time distributions by known functions. Figure 6.7 shows these distributions for load points A and C for the system in Case 1.

The simulations that assume exponentially distributed component repair times result in load point annual interruption time distributions that contain a sharp peak for the interval indicating the number of years with

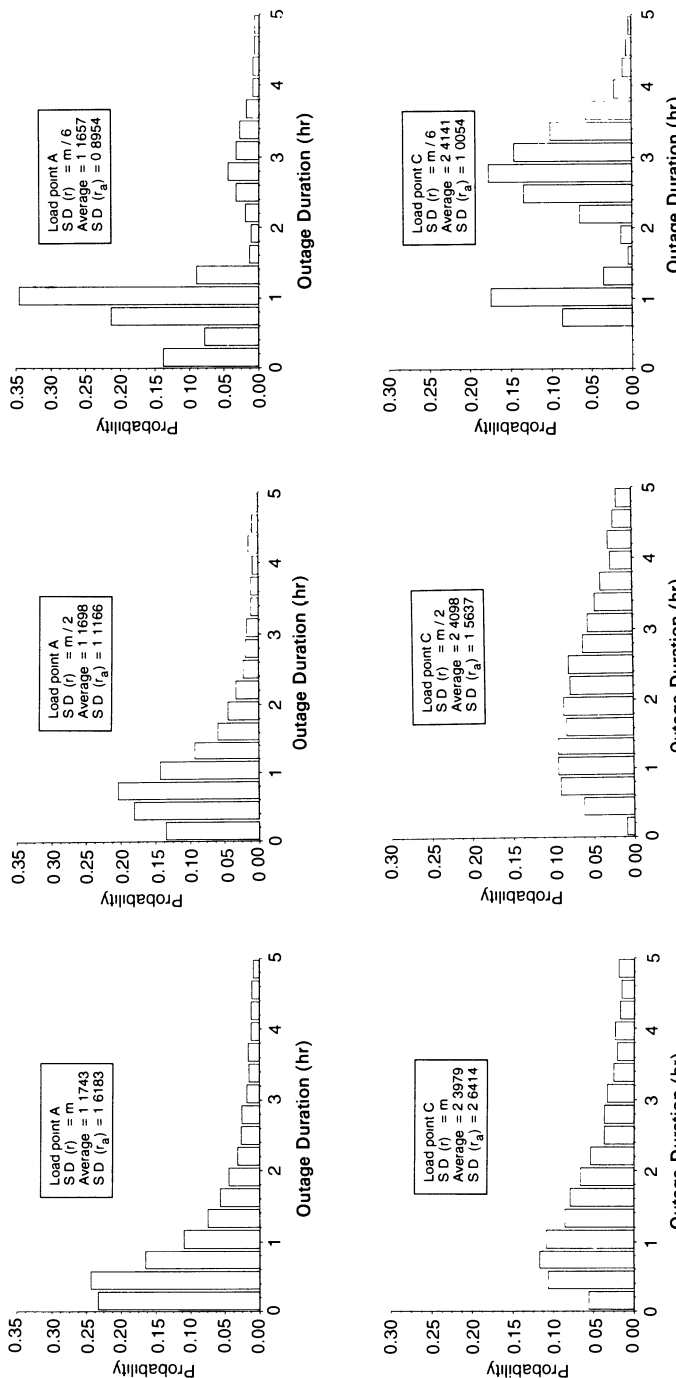


**Figure 6.6.** Load point outage duration distributions as a function of component repair time standard deviations for log-normally distributed repair times for Case 1.

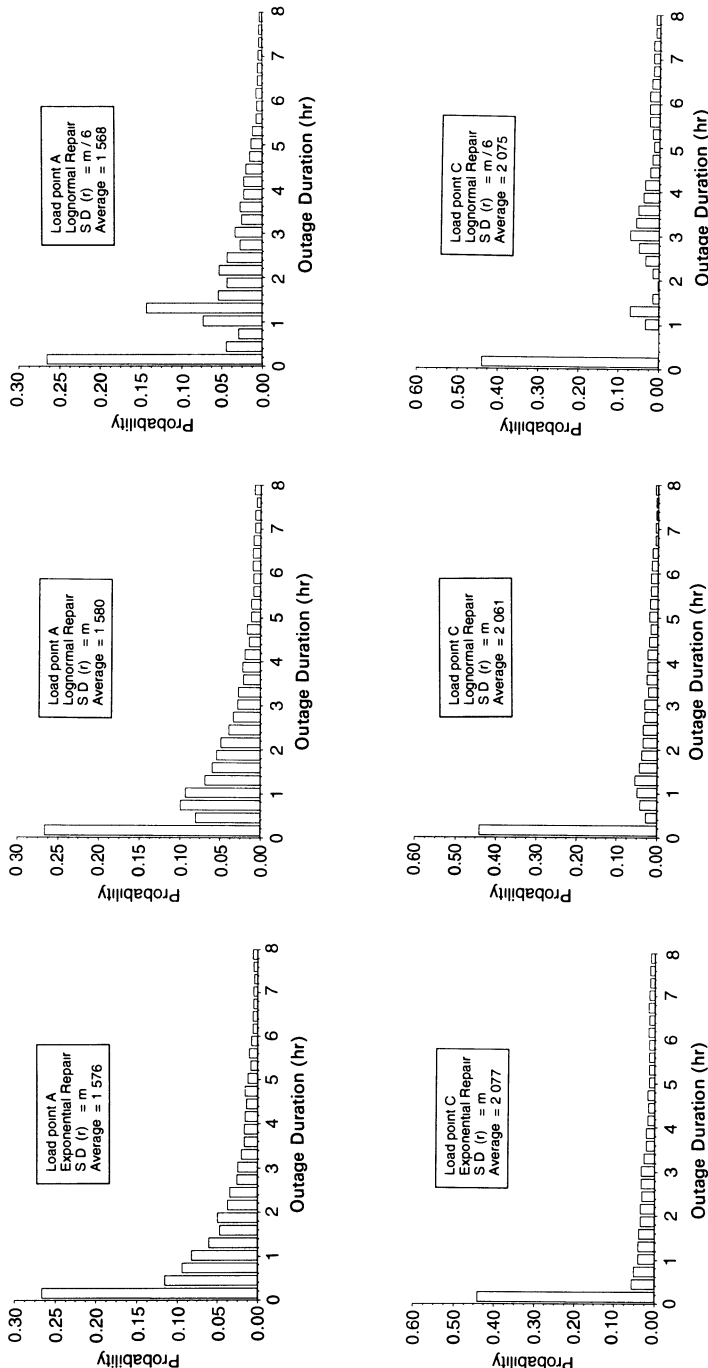


Figure 6.7. Load point annual interruption time distributions for Case 1.

no failures. The distributions are steadily decreasing with long tails. The distributions are not of exponential or gamma form. The simulations that assume log-normal distributions for the component repair times and exponential distributions for the other times also result in load point annual interruption time distributions with a sharp peak for the no-failure interval. The log-normal simulations do not result in steadily decreasing distributions but in distributions with multiple modes. The multiple modality is more prominent when the repair times are assumed to have small standard deviations. It is interesting to note that in all the three cases in Figure 6.7, the number of years with zero hours of interruption is independent of the form and the standard deviation of the component repair time distributions. This independence occurs because the number of years with zero interruption time is dominated by the failure rate distributions, which determine the number of years in which no failures occur.

### 6.3.4. System Performance Index Distributions

Section 6.2.3 notes that the system performance indices can be calculated directly from the basic load point indices. System performance indices are in fact weighted averages of the load point indices. The distributions of system performance indices therefore can also be obtained from those of the load point indices by similar calculations. Figure 6.8 shows these distributions resulting from the simulations of the system in Case 1 with the assumption that the component repair times are exponentially and log-normally distributed.

The SAIDI distribution is dependent on the repair time distributions. The number of customers at each load point and the average failure rates are weighting factors that are independent of the associated distributions. The SAIDI distributions in Figure 6.8 are more or less similar to the annual interruption time distributions in Figure 6.7. This is because SAIDI is a linear combination of annual interruption times. Additional studies indicate that in a large system, the resemblance tends to decrease because of the averaging effect of the large number of load points which are aggregated. In this small system, the number of years with a SAIDI equal to zero is relatively high (i.e.,  $P[\text{SAIDI}=0]$  is high). This might be expected in a small or moderate-size system. In the case of a large system or region it is very likely that there would be at least one interruption.

The SAIFI distributions are identical for the exponential and log-normal ( $\text{SD}=m$  and  $\text{SD}=m/6$ ) component repair times because SAIFI is only dependent on the component failure time distributions and on the

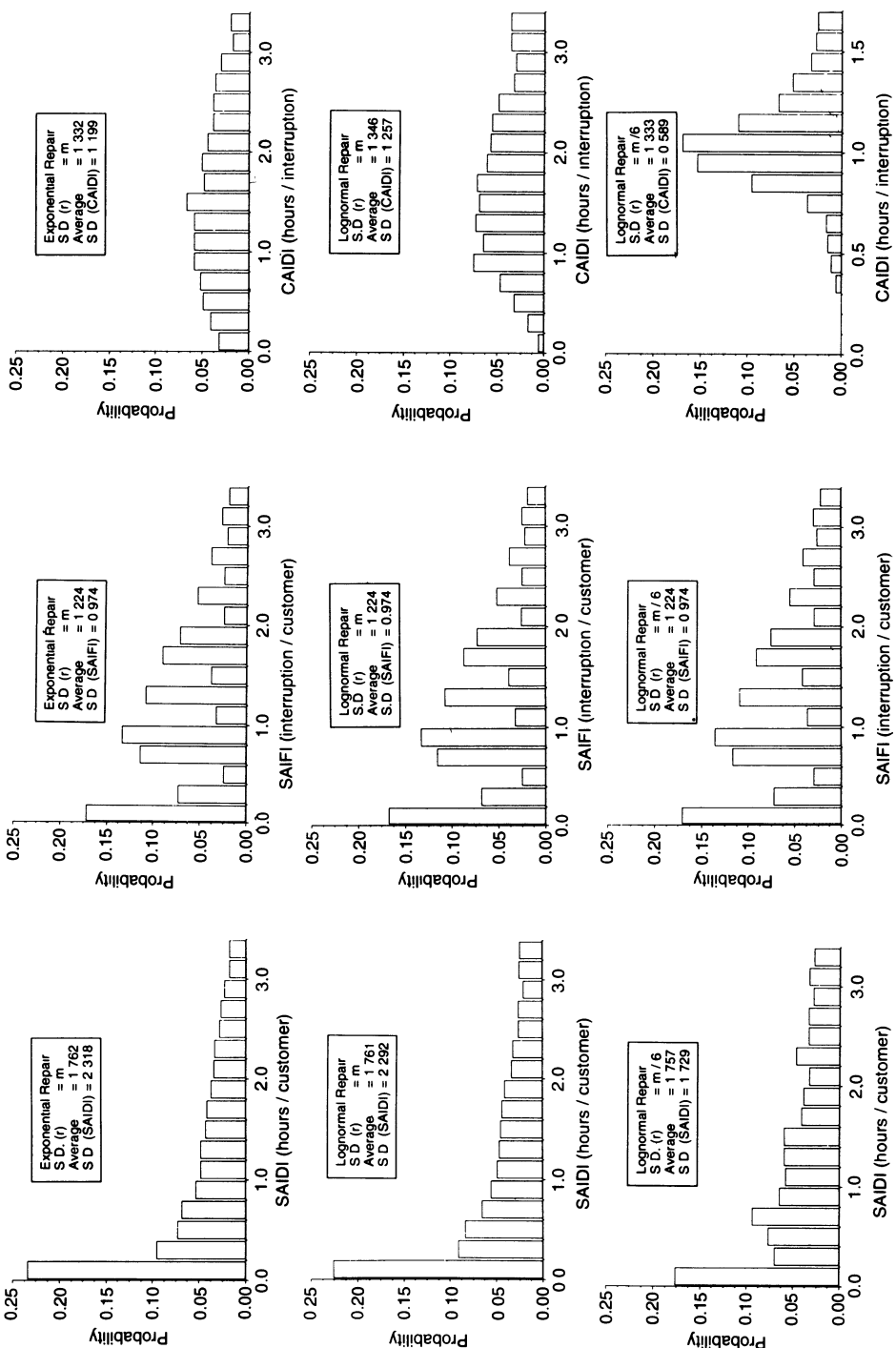


Figure 6.8. System performance index distributions for Case 1.

number of customers served at each load point. As in the case of SAIDI distributions, the probability of SAIFI equaling zero diminishes in large systems. The distribution becomes less like an exponential distribution and more like one with a mode about the average.

The CAIDI distributions are nonlinearly related to both the failure and repair times. This and other comparisons indicate that the standard deviations of the underlying component distributions can affect the shape of the CAIDI index distribution as much as or more than the form chosen for the underlying distributions. For large systems the dispersion of the CAIDI distribution also tends to decrease.

It is important to appreciate that the system performance indices of SAIDI, SAIFI, and CAIDI are associated with probability distributions. They can be expressed by their average or mean values but they are random variables. It should be expected therefore that SAIDI, SAIFI, and CAIDI statistics obtained from actual circuit or system operating behavior will vary over time as each year is simply a snapshot of a continuum in time. The ability to generate the index distribution by Monte Carlo simulation provides the opportunity to appreciate and quantify the dispersion associated with these important customer parameters.

## 6.4. STATION RELIABILITY ASSESSMENT

### 6.4.1. General Concepts

Substations and switching stations serve important functions in an electric power system. These facilities are energy transfer points between generating stations, transmission, subtransmission, and distribution systems. The structure of reliability assessment of substation and switching stations is basically similar and therefore the term station is used to describe both of them in the following sections. Stations, in a general sense, provide the connection between generating units and transmission systems (voltage step-up substations), and between transmission or distribution systems and consumer facilities (voltage step-down substations). Stations are functionally designed with considerable flexibility in the arrangement of their basic components such as circuit breakers, bus sections, and transformers. Factors considered in selecting a specific station configuration include service security and reliability, operating flexibility and simplicity, short-circuit current limitations, protective relaying, equipment maintenance, future extensions and modifications, standardization and cost, etc.

From a reliability evaluation point of view, a station divides "a point" in a bulk power network into a number of dispersed points. Some are locations where energy enters and therefore can be termed "source points." Some are locations where energy departs and can be termed "load points." The basic principle of station reliability assessment, as in radial distribution system assessment, is to evaluate connectivity from the source points to the load points. Station reliability evaluation is more complex than radial distribution system reliability evaluation, as it is associated with multiple source points, multiple breakers, and complicated switching functions.

Station reliability indices can serve two basic functions: (1) They should be in a form which can be incorporated in a composite system adequacy assessment. A complex station arrangement can be represented by a single bus with a detailed reliability model. Thus the effect of station configurations can be included in composite system evaluation. (2) Station indices should also be in a form which can be used in radial distribution system reliability assessment. A source point in a distribution system can be represented by a reliability model which permits station effects to be included in distribution system evaluation. Station reliability indices can be considered in two groups. One group contains outage probabilities and frequencies for each set of external connections. These outage sets are mutually exclusive, i.e., the remaining connections must be in service if one set of the connections is in the outage state. This group of station reliability indices can be used as input data in composite system reliability assessment. The second group contains the outage probability, outage rate, and outage duration for every point. These outage events are not mutually exclusive, i.e., the remaining points can be in service or on outage when a point is in an outage state. This group of indices contains the necessary reliability data to evaluate a particular point and therefore can be used as input data in radial distribution system reliability assessment. In order to discriminate between these two groups of indices, the terms "connection set" and "point" are utilized.

#### 6.4.2. Station Component Modeling

Station components are usually represented by Markov models in analytical station reliability evaluation.<sup>(8-12)</sup> This implies that the transition rates between different states are constant and that the duration in each state is exponentially distributed. The Markov model assumption may be invalid for many repairable components. As discussed in Section 6.3, component repair activities are generally not exponentially distributed. Log-normal<sup>(15)</sup> or Weibull distributions<sup>(24)</sup> have been suggested to represent repair or restoration times. The component representation will be non-Markovian when

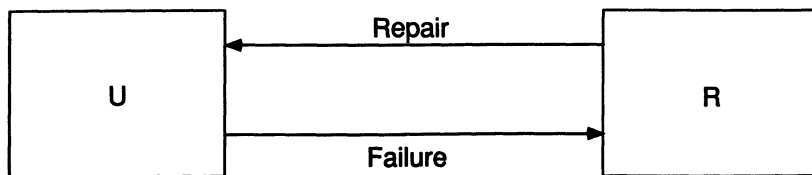


**Figure 6.9.** Two-state component model.

one or more of the transition rates are time-dependent. The model cannot be easily solved using analytical methods in the case of a non-Markovian process.<sup>(1)</sup>

A station contains three basic component types<sup>(2,12)</sup>: bus sections, transformers (or lines/cables), and breakers. Bus sections can be represented by a two-state model as shown in Figure 6.9. Transformers (or line/cable) can be represented by a three-state model as shown in Figure 6.10. This generally indicates that after the fault, a transformer (or line/cable) is first isolated by switching action and then repaired. A breaker can be represented by the more complex three-state model shown in Figure 6.11. There are two failure modes in this model, designated as passive and active failures, respectively.<sup>(2)</sup> These are defined as:

1. *Passive event*: A component failure mode that does not cause operation of protection devices and therefore does not have an impact on the remaining healthy components. Service is restored by repairing

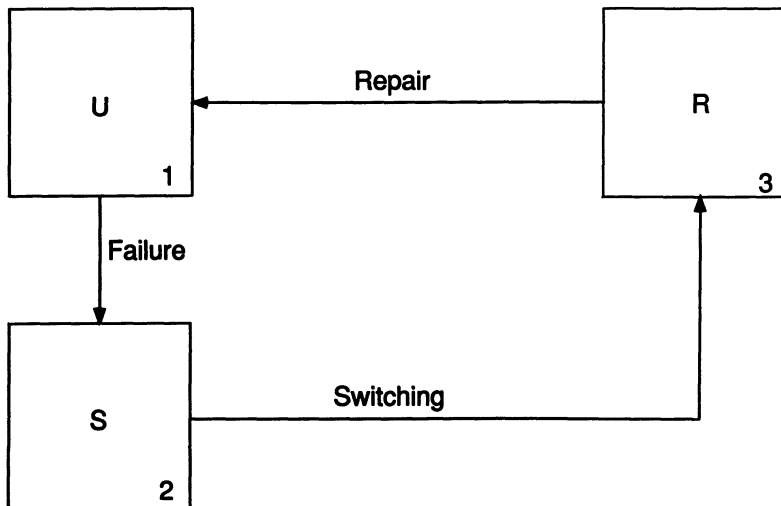


**Figure 6.10.** Three-state component model.

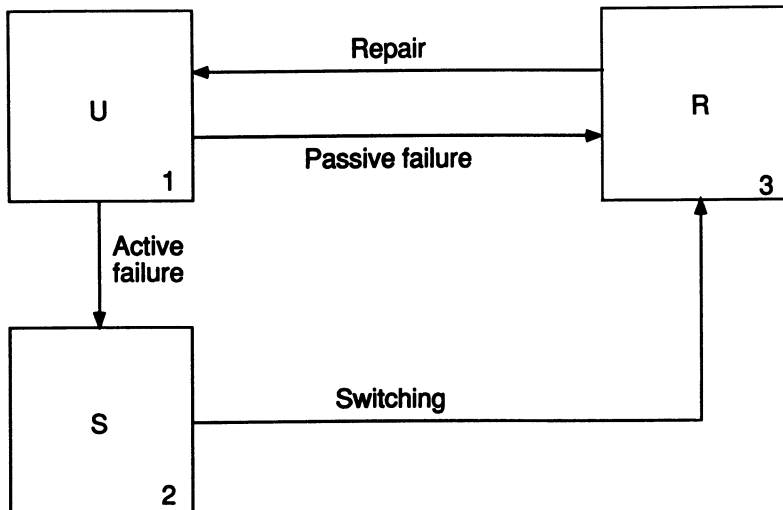


**Figure 6.11.** State space diagram for active and passive failures.

or replacing the failed component. An open-circuit failure is an example of a passive event.

2. *Active event:* A component failure mode that causes the operation of the primary protection zone around the failed component and can therefore cause the removal of other healthy components and branches from service. The actively failed component is isolated and the protective breakers are reclosed, which leads to service being restored to some or all of the load points. It should be noted, however, that the failed component itself can be restored to service only after repair or replacement.

It can be seen from the above general definitions that the passive and active events can also apply to nonbreaker-type components if it is necessary to model them using the more detailed representation. The four-state model shown in Figure 6.12 can be used when maintenance activity is considered. Two maintenance considerations should be recognized. One is to assume that both the time to the maintenance state and the time back to the up-state follow a given distribution. The parameter(s) of the distribution can be obtained from historical records of maintenance activities. This approach can be used to assess the general effects of maintenance on station reliability. The second consideration is to recognize maintenance as a series of scheduled events which occur at prespecified intervals. In this case, the scheduled outage is not a random event. Both considerations can be easily simulated using the component state duration sampling method.

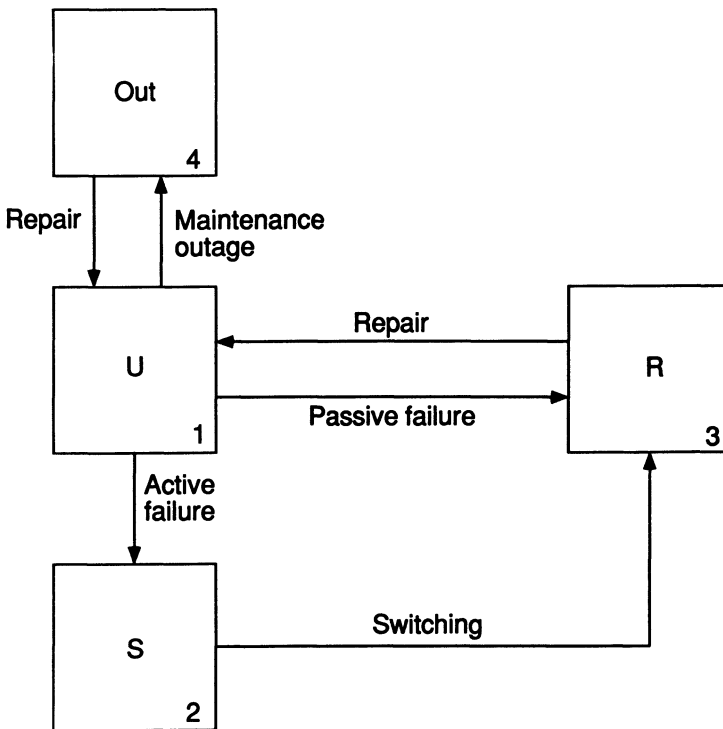


**Figure 6.12.** Four-state component model.

### 6.4.3. Component State Duration Sampling Procedure

As noted earlier, the component state duration sampling technique can be used to simulate any probability distribution. In the following analysis, for generality, repair activities are assumed to be Weibull distributed and other activities are assumed to be exponentially distributed. The cumulative probability distribution functions associated with failure, switching, and repair times are given by equations (6.10) to (6.13). If maintenance activity is expressed by a distribution, it can be included in a similar way:

$$F_a(t) = 1 - e^{-\lambda_a t} \quad (6.10)$$

$$F_p(t) = 1 - e^{-\lambda_p t} \quad (6.11)$$

$$S(t) = 1 - e^{-\mu_{sw} t} \quad (6.12)$$

$$R(t) = 1 - e^{-(t/\alpha)^\beta} \quad (6.13)$$

where  $\lambda_a$  is the active failure rate,  $\lambda_p$  the passive failure rate,  $\mu_{sw}$  the switching rate, and  $\alpha$  and  $\beta$  are the scale and shape parameters, respectively, of the Weibull distribution. The component state duration sampling procedure involves the following four basic steps:

**(a) Artificial Component Operating History.** The operating history of each component is created by random sampling. The sampling values of operating time, switching time, and repair time are designated as time to active failure ( $TTF_a$ ), time to passive failure ( $TTF_p$ ), time to switch ( $TTS$ ), and time to repair ( $TTR$ ), respectively.  $TTF_a$ ,  $TTF_p$ ,  $TTS$ , and  $TTR$  can be obtained using the inverse transform method given in Section 3.4.2, i.e.,

$$TTF_a = -\frac{1}{\lambda_a} \ln U_{fa} \quad (6.14)$$

$$TTF_p = -\frac{1}{\lambda_p} \ln U_{fp} \quad (6.15)$$

$$TTS = -\frac{1}{\mu_{sw}} \ln U_s \quad (6.16)$$

$$TTR = \alpha(-\ln U_r)^{1/\beta} \quad (6.17)$$

where  $U_{fa}$ ,  $U_{fp}$ ,  $U_s$ , and  $U_r$  are four independent, uniformly distributed random numbers between  $[0, 1]$ . If the component resides in the switching state, the sample switching time is given by equation (6.16). If the component resides in the repair state, the sample repair time is given by equation (6.17). If the component resides in the normal operating state, determination of the sample operating time is dependent on the type of the component. If the component is represented by a model without passive failure, such as a bus or a transformer, the sample operating time TTF is given by equation (6.14). If a model with passive failure is used, such as in the case of a breaker, the sample TTF is obtained by comparing  $TTF_a$  and  $TTF_p$  given in equations (6.14) and (6.15), respectively, i.e.,

$$TTF = \min\{TTF_a, TTF_p\} \quad (6.18)$$

The sample time value of the component residing in an up state is  $TTF$ , i.e.,

$$T_{up} = TTF \quad (6.19)$$

The sample time value of the component residing in a down state is dependent on how it transits from the up state. If the repair state is reached by a passive failure, the time value is TTR, i.e.,

$$T_{dn} = TTR \quad (6.20)$$

If the repair state is reached by an active failure, the time value is given by

$$T_{dn} = TTS + TTR \quad (6.21)$$

**(b) Modified Component Operating History.** The artificial component operating history obtained using the described method is a random event sequence. This operating history can be modified to include specified deterministic station operating factors. Two aspects are involved:

1. Station operation is associated with both protection and switching activities. When a component fails, protective breakers may open and the effected breakers can be reclosed when a failed component is switched out. Switching logic is prespecified in the station design and operating guidelines. The effects of the protection and switching activities can be incorporated by modifying the artificial operating history.
2. A scheduled maintenance activity cannot be modeled by a probability distribution as it is a prespecified event. The down time due to the scheduled maintenance can be easily imposed on the artificial component operating history.

**(c) Connection Set or Point Operating History.** As noted in Section 6.4.1, there are two groups of station reliability indices. One group contains the mutually exclusive connection set indices. The other contains nonmutually exclusive (source or load) point indices. The complete station operating history can be obtained by combining the individual modified component operating histories. Connection set or point operating histories can be obtained by examining the connectivity from source point(s) to load point(s) for each station system state in the complete station operating history.

**(d) Calculation of Reliability Indices and Their Distributions.** The required reliability indices can be calculated from connection set or point operating histories. The availability ( $A$ ), unavailability ( $U$ ), average failure rate ( $\lambda$ ), repair time ( $r$ ), and the outage frequency ( $f$ ) associated with a connection set or a point can be obtained using equations

(6.22) to (6.26):

$$A = \frac{\sum_{i=1}^N T_{\text{up}i}}{\sum_{i=1}^N (T_{\text{up}i} + T_{\text{dn}i})} \quad (6.22)$$

$$U = \frac{\sum_{i=1}^N T_{\text{dn}i}}{\sum_{i=1}^N (T_{\text{up}i} + T_{\text{dn}i})} \quad (6.23)$$

$$\lambda = \frac{N}{\sum_{i=1}^N T_{\text{up}i}} \quad (6.24)$$

$$r = \frac{\sum_{i=1}^N T_{\text{dn}i}}{N} \quad (6.25)$$

$$f = \frac{N}{\sum_{i=1}^N (T_{\text{up}i} + T_{\text{dn}i})} \quad (6.26)$$

where  $N$  is the number of outages associated with a connection set or a point in the simulation span,  $T_{\text{up}i}$  is the  $i$ th operating duration associated with a connection set or a point in the simulation span, and  $T_{\text{dn}i}$  is the  $i$ th outage duration associated with a connection set or a point in the simulation span.

The state duration sampling approach can be used to provide information on reliability index distributions. The probability that a specified number of outages will occur within one time unit (normally one year) is equal to the corresponding subtotal time units divided by the total simulation time units, i.e.,

$$P_f(i) = \frac{N_i}{\sum_{j=0}^n N_j} \quad (i = 0, 1, \dots, n) \quad (6.27)$$

where  $N_i$  is the number of time units in which only  $i$  outages occur within one time unit,  $n$  the maximum outages within one time unit,  $P_f(i)$  is the probability that  $i$  outages occur within one time unit.

Similarly, the outage duration probability distribution associated with a connection set or a point can be obtained using the following equation:

$$P_d(i) = \frac{N_i}{\sum_{j=0}^m N_j} \quad (i = 0, 1, \dots, m) \quad (6.28)$$

where  $N_i$  is the number of outages in which outage duration length is between  $T_i$  and  $T_{i+1}$ ,  $m$  the number of segments into which outages are divided in terms of their duration length, while  $P_d(i)$  is the probability of outages whose durations are between  $T_i$  and  $T_{i+1}$ .

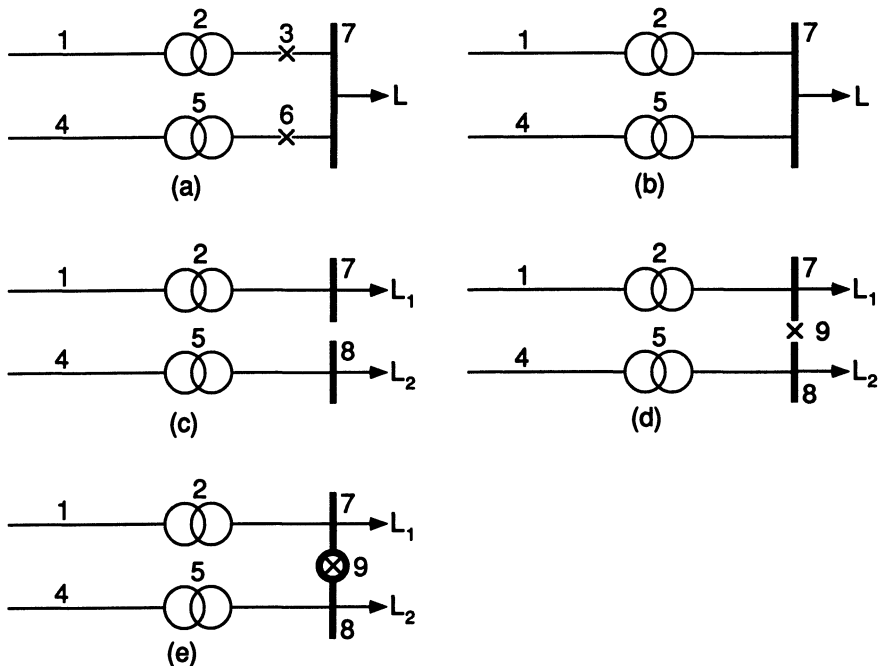


**Figure 6.13.** Five simple station configurations.

#### 6.4.4. Numerical Example 1

Figure 6.13 shows five simple station configurations.<sup>(2,25)</sup> The station component data are given in Table 6.11. A normally opened breaker was assumed to have the same data as a normally closed breaker.

- Case (a). Base case [Figure 6.13a].
- Case (b). As in Case (a) but without the breakers [Figure 6.13b].
- Case (c). The bus section is split and the load divided equally between the bus sections [Figure 6.13c].
- Case (d). As in Case (c) but with a normally closed bus section breaker between the two busbars [Figure 6.13d].
- Case (e). As in Case (d) but with a normally opened bus section breaker [Figure 6.13e].

All failure, switching, repair, and scheduled maintenance activities were modeled using exponential distributions. The five station configurations were analyzed using the Monte Carlo simulation approach<sup>(25,26)</sup> and the analytical method.<sup>(2)</sup> The results are presented in Tables 6.12 to 6.14. It can be seen

**Table 6.11. Component Reliability Data for the Simple Station Configurations<sup>a</sup>**

Component	$\lambda_a$ (f/yr)	$\lambda_p$ (f/yr)	$r$ (hr/f)	$T_{sw}$ (hr/f)	$\lambda_m$ (f/yr)	$r_m$ (hr/f)
Breaker	0.01	0.01	3.00	1.0	0.1	5.0
Bus section	0.024		2.00			
Transformer	0.10		50.00	1.0	0.2	10.0
Line	0.09		7.33	1.0		

<sup>a</sup> $\lambda_a$ , active failure rate;  $\lambda_p$ , passive failure rate;  $r$ , repair time;  $T_{sw}$ , switching time;  $\lambda_m$ , transition rate to maintenance state;  $r_m$ , maintenance time.

**Table 6.12. Load Point Outage Rates**

Case	Analytical (failures/yr)	Monte Carlo (failures/yr)	Relative error (%)
(a)	0.0449686	0.0462504	2.85
(b)	0.4046820	0.4062153	0.38
(c)	0.4140000	0.4152556	0.30
(d)	0.2248393	0.2279579	1.39
(e)	0.2240000	0.2245554	0.25

**Table 6.13. Load Point Unavailability**

Case	Analytical (hr/yr)	Monte Carlo (hr/yr)	Relative error (%)
(a)	0.0760151	0.0773285	1.73
(b)	0.4346979	0.4342171	0.11
(c)	7.8977000	7.9237038	0.33
(d)	0.2553120	0.2584898	1.24
(e)	0.2480000	0.2500889	0.84

**Table 6.14. Load Point Outage Durations**

Case	Analytical (hr/failure)	Monte Carlo (hr/failure)	Relative error (%)
(a)	1.6904025	1.6719678	1.09
(b)	1.0741716	1.0689864	0.48
(c)	19.0765700	19.0987848	0.12
(d)	1.1355310	1.1339697	0.14
(e)	1.1071429	1.1137387	0.60

that the two methods provide basically the same load point reliability indices.

The effect of nonexponential state residence distributions is illustrated by assuming that the repair times are Weibull distributed. All failure, switching, and scheduled maintenance activities are modeled using exponential distributions. The mean values of the repair times were held constant in order to compare the results. The shape parameter  $\beta$  was set at 0.5, 1.0, 2.0, and 4.0, respectively. The Weibull distribution is an exponential distribution when the shape parameter is equal to 1.0. Load point reliability indices are shown in Tables 6.15 to 6.17. It can be seen from these results that the mean reliability indices are not influenced by the change in shape parameter  $\beta$  of the Weibull distribution. The utilization of different distributions for

**Table 6.15. Load Point Outage Rates Using Weibull Repair Time Distributions**

Case	Load point outage rates (failure/yr)			
	$\beta = 0.5$	$\beta = 1.0$	$\beta = 2.0$	$\beta = 4.0$
(a)	0.0458337	0.0462504	0.0459448	0.0458337
(b)	0.4060688	0.4062153	0.4061176	0.4061663
(c)	0.4155035	0.4152556	0.4155748	0.4154948
(d)	0.2282507	0.2279579	0.2278603	0.2280067
(e)	0.2245162	0.2245554	0.2245554	0.2244770

**Table 6.16. Load Point Unavailability Using Weibull Repair Time Distributions**

Case	Load point unavailability (hr/yr)			
	$\beta = 0.5$	$\beta = 1.0$	$\beta = 2.0$	$\beta = 4.0$
(a)	0.0759160	0.0773285	0.0760292	0.0751924
(b)	0.4317163	0.4342171	0.4316121	0.4313477
(c)	8.0848246	7.9237038	7.9006220	7.9030106
(d)	0.2612150	0.2584898	0.2556588	0.2574964
(e)	0.2501599	0.2500889	0.2496769	0.2493530

**Table 6.17. Load Point Average Outage Durations Using Weibull Repair Time Distributions**

Case	Load point outage durations (hr/failure)			
	$\beta = 0.5$	$\beta = 1.0$	$\beta = 2.0$	$\beta = 4.0$
(a)	1.6563483	1.6719678	1.6548078	1.6405622
(b)	1.0632128	1.0689864	1.0628287	1.0620500
(c)	19.4758735	19.0987848	19.0284731	19.0378941
(d)	1.1444557	1.1339697	1.1220307	1.1293701
(e)	1.1142493	1.1137387	1.1119038	1.1108492

**Table 6.18. Load Point Outage Rate Probability Distributions**

Case	Probability of outage rates				
	0	1	2	3	4
(a)	0.954750	0.044250	0.001000	0.000000	0.000000
(b)	0.665415	0.271268	0.055805	0.006780	0.000683
(c)	0.645200	0.300160	0.049440	0.004960	0.000240
(d)	0.795750	0.182293	0.020537	0.001268	0.000195
(e)	0.798706	0.180078	0.019255	0.001882	0.000078

component repair durations does not affect the mean load point reliability indices but only influences the distributions of these indices.

The load point outage rate probability distributions for the five station configurations are illustrated in Table 6.18. Columns 2, 3, 4, 5, and 6. show the probabilities that there are 0, 1, 2, 3, and 4 outages within one year, respectively. The load point outage rate probability distribution for Case (b) is shown in Figure 6.14 for illustrative purposes.

Table 6.19 shows the load point outage duration probability distributions. Columns 2, 3, 4, 5, and 6. show the probabilities of outage durations between 0 to 2 hr/failure, 2 to 4, 4 to 6, 6 to 8, and 8 to 10, respectively. The probability of an outage duration longer than 10 hr is not shown in

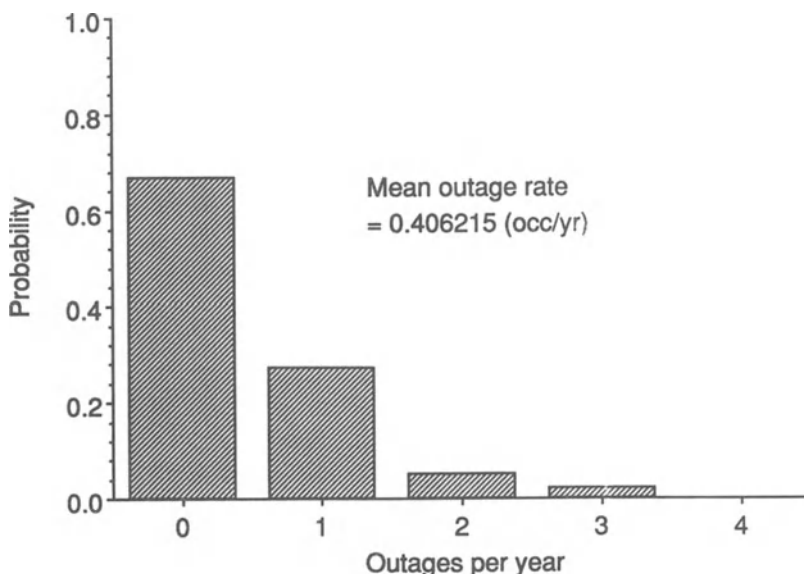


**Figure 6.14.** Load point outage rate probability distribution for Case (b).

**Table 6.19. Load Point Outage Duration Probability Distributions**

Case	Probability of outage durations				
	(0-2)	(2-4)	(4-6)	(6-8)	(8-10)
(a)	0.711111	0.184384	0.069069	0.021622	0.009610
(b)	0.852768	0.121172	0.019935	0.003483	0.002402
(c)	0.069996	0.067104	0.047243	0.036830	0.505206
(d)	0.833298	0.131393	0.024395	0.007276	0.002996
(e)	0.840203	0.126266	0.025498	0.005414	0.001921

this table. The load point outage duration probability distribution for Case (b) is given in Figure 6.15.

#### 6.4.5. Numerical Example 2

Figure 6.16 shows a station configuration taken from a Canadian Electrical Association (CEA) report.<sup>(27)</sup> This station is composed of eleven components, numbered from 1 to 11, which include five breakers, three bus sections, and three transformers. The configuration has six external connections (points) in total. This is a general configuration. As a voltage step-up station, connections (1), (2), and (3) would be connected to transmission lines, and (4), (5), and (6) to generating units. As a voltage step-down

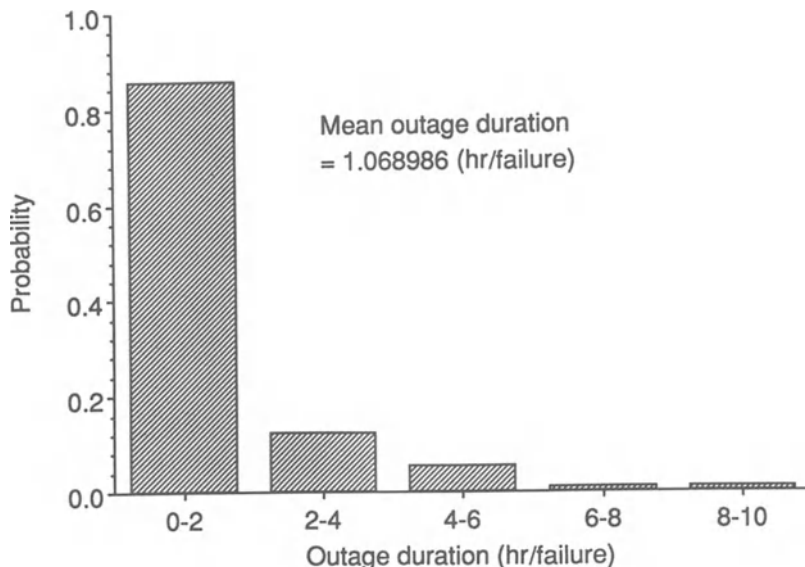


**Figure 6.15.** Load point outage duration probability distribution for Case (b).

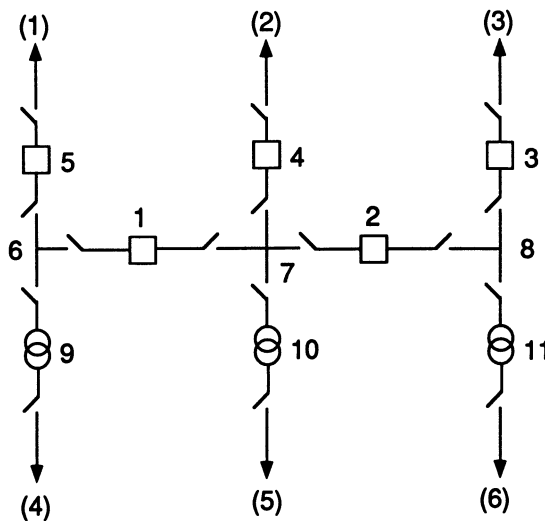


**Figure 6.16.** Station configuration with six connections.

station, connections (1), (2), and (3) would be connected to transmission lines, and (4), (5), and (6) to distribution systems or direct customers. The protection scheme associated with all of the breakers is assumed to be non-directional. A breaker can therefore be tripped out due to faults of the components which are directly or indirectly connected to it. For example, Breaker 1 can be tripped not only by a fault of component 6 or 7, but also possibly by faults of components 2, 4, 5, 9, and 10, depending on the protection coordination between these components. The component reliability data are given in Table 6.20. A breaker is represented using the three-state model shown in Figure 6.11, a transformer by the three-state model shown in Figure 6.10, and a bus section by the two-state model shown in Figure 6.9. Maintenance outages were not considered and all component state durations including failure, repair, and switching activities were assumed to be exponentially distributed. These are not necessary assumptions when using the Monte Carlo approach. As seen earlier, maintenance activities and any distribution can be incorporated with little or no extra complications.

**Table 6.20. Component Reliability Data for the Six-Connection Station**

Component	$\lambda_a$ (f/yr)	$\lambda_p$ (f/yr)	$r$ (hr/f)	$T_{sw}$ (hr/f)
Breaker	0.002	0.0001	126.0	1.0
Bus	0.025		13.0	
Transformer	0.026		43.1	1.0

**Table 6.21. Connection Set Outage Probabilities for the Station in Figure 6.16**

Connection set	Outage probability	
	Monte Carlo	Analytical
(1)	0.303784E - 04	0.301867E - 04
(2)	0.311544E - 04	0.301876E - 04
(3)	0.323512E - 04	0.301867E - 04
(4)	0.129359E - 03	0.127842E - 03
(5)	0.129863E - 03	0.127846E - 03
(6)	0.130515E - 03	0.127842E - 03
(1) + (4)	0.392641E - 04	0.402876E - 04
(2) + (5)	0.409251E - 04	0.402828E - 04
(3) + (6)	0.418704E - 04	0.402876E - 04
(1) + (2) + (4) + (5)	0.186389E - 06	0.207811E - 06
(2) + (3) + (5) + (6)	0.237587E - 06	0.207811E - 06

Both the state duration sampling approach and the analytical method were used to evaluate the station configuration connection set reliability. The outage probabilities obtained using the two methods are shown in Table 6.21. The table is not completely exhaustive as the outage probability of high-order connection sets is very small compared with the low-order set outage probabilities and therefore some high-order set outages are not listed. It can be seen from Table 6.21 that the results obtained by the two methods are basically the same.

Sensitivity analysis is an important aspect of quantitative reliability assessment and can be used to determine how the reliability indices of each connection set are affected by varying selected component parameters, such as failure rates or repair times. The effects of variation in breaker failure rates on the connection set outage probability and frequency are shown in Tables 6.22 and 6.23. In this study, Case I is the base case and the breaker failure rates are doubled and tripled in Case II and Case III, respectively.

Table 6.22 shows the effect on the outage probability of the connection sets due to varying breaker failure rates (active and passive failure rates are changed at the same percentage). It can be seen that the outage probabilities of some connection sets are greatly affected by the breaker failure rates and those of other sets are basically constant. Table 6.23 shows the effect on the outage frequency of the connection sets and leads to the same general conclusion. A general appreciation of the phenomena can be obtained by considering the configuration. For example, outages of Connection (1) are caused by failures of Breaker 5 only. Outages of Connection set (1) + (4) are caused by some combination of failures of Breaker 5, Bus 6, and Transformer 9. It should be noted that all connection set outages are by definition mutually exclusive.

**Table 6.22. Outage Probability Variation as a Function of Breaker Failure Rates**

Connection set	Outage probability		
	Case I	Case II	Case III
(1)	0.303784E-04	0.610557E-04	0.897773E-04
(2)	0.311544E-04	0.589801E-04	0.842579E-04
(3)	0.323512E-04	0.559409E-04	0.913654E-04
(4)	0.129359E-03	0.133463E-03	0.129398E-03
(5)	0.129863E-03	0.126985E-03	0.127261E-03
(6)	0.130515E-03	0.124308E-03	0.123885E-03
(1) + (4)	0.392641E-04	0.393171E-04	0.411952E-04
(2) + (5)	0.409251E-04	0.401165E-04	0.402621E-04
(3) + (6)	0.418704E-04	0.417183E-04	0.412661E-04
(1) + (2) + (4) + (5)	0.186389E-06	0.466841E-06	0.743696E-06
(2) + (3) + (5) + (6)	0.237587E-06	0.464643E-06	0.685578E-06

**Table 6.23. Outage Frequency Variation as a Function of Breaker Failure Rates**

Connection set	Outage frequency (failure/yr)		
	Case I	Case II	Case III
(1)	0.203704E-02	0.397531E-02	0.629630E-02
(2)	0.217284E-02	0.437037E-02	0.585185E-02
(3)	0.197531E-02	0.404938E-02	0.661728E-02
(4)	0.265802E-01	0.263827E-01	0.260864E-01
(5)	0.267160E-01	0.254321E-01	0.256173E-01
(6)	0.261358E-01	0.258765E-01	0.254691E-01
(1) + (4)	0.537284E-01	0.548889E-01	0.566914E-01
(2) + (5)	0.536667E-01	0.541605E-01	0.566667E-01
(3) + (6)	0.533086E-01	0.555062E-01	0.571728E-01
(1) + (2) + (4) + (5)	0.165432E-02	0.395062E-02	0.596296E-02
(2) + (3) + (5) + (6)	0.202469E-02	0.407407E-02	0.606273E-02

Similar sensitivity studies can be performed in which other parameters such as breaker repair times, bus failure and repair rates, and transformer failure and repair rates are varied.

The connection set reliability indices are important input data when incorporating the effects of station configurations in composite system reliability assessment. In other cases, such as when an external point of the station is a supply point of a radial distribution system, reliability indices at each single point which are not mutually exclusive of those of other points are required. Nonmutual exclusion means that other points may be in the operating state or outage state if one point is in the outage state.

The sensitivity studies associated with the point reliability indices are shown in Figure 6.17. Figure 6.17a shows the effect on the point outage probability (OP) of varying breaker failure rates (active and passive failure rates are changed at the same percentage). This figure includes four curves. Curve I is the simulated outage probability (SOP) at Point (1) and Curve II is the analytical outage probability (AOP) at this point. Curves III and IV are the simulated and analytical outage probabilities, respectively, of Point (4). It can be seen that the outage probability of Point (1) is greatly affected by the breaker failure rates and that the outage probability of Point (4) is almost constant. The results obtained by the two calculation techniques are basically the same. Figure 6.17b shows the effect on point outage rates (OR). Curve I is the simulated outage rate (SOR) of Point (1) and Curve II the simulated outage rate (SOR) of Point (4). The outage rates of both points increase when the breaker failure rates increase. Figure 6.17c shows the effect on average point outage durations (OD). Both curves are simulated results (SOD). Curve I shows the value of Point (1) and Curve II the value of Point (4). Curve I increases as the breaker failure rates increase, which means that the average point outage duration will be longer when the breaker failure rates increase. Conversely, the average outage duration of Point (4) will decrease as the breaker failure rates increase.

The phenomena illustrated in Figure 6.17 can be explained qualitatively as follows. Because of the symmetrical locations of Points (1) and (4) and the specified action logic of Breakers 1 and 5, the outage rates of Points (1) and (4) are basically the same. It can be determined from the component reliability data that the transformer has the largest outage probability. However, the outage of Transformer 9 creates different effects on Point (1) or (4). Breakers 1 and 5 will be reclosed after failed Transformer 9 is isolated. The outage duration of Point (1) caused by this faulted transformer is therefore only the transformer switching time. The outage duration of Point (4) due to the transformer failure is the transformer switching time plus its repair time. This leads to the fact that Point (4) has a longer outage duration and therefore higher outage probability than Point (1). When the breaker failure rates increase, contributions due to Breakers 1 and 5 increase and therefore the outage rates of Points (1) and (4) also increase. Only one breaker outage (Breaker 5) is required to cause the outage of Point (1). The outage probability of this point therefore has a relatively large increase with breaker failure rates. This leads to increase in the outage duration of Point (1) with the breaker failure rates. Simultaneous outage of the two breakers (both Breakers 1 and 5) is required to create an outage of Point (4). The outage probability of this point is affected only slightly and therefore its outage duration decreases with the breaker failure rates.

The outage rate probability distributions at the six points are illustrated in Table 6.24. Columns 2, 3, 4, 5, and 6 show the probabilities of 0, 1, 2, 3,

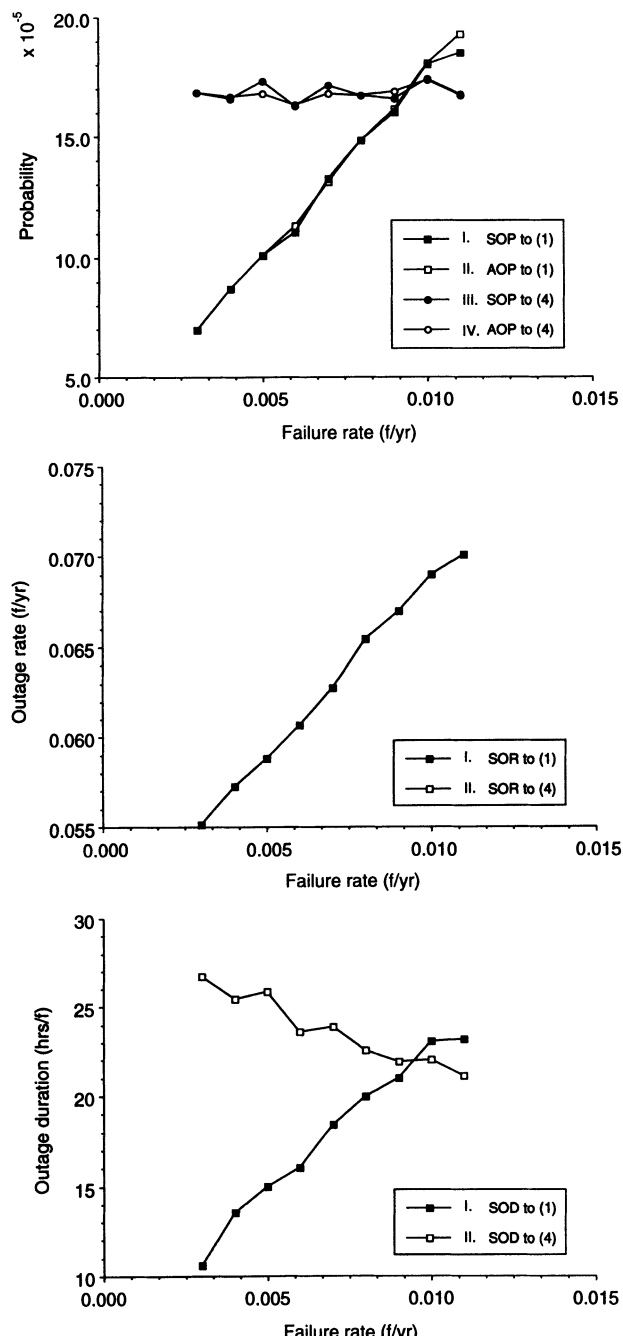


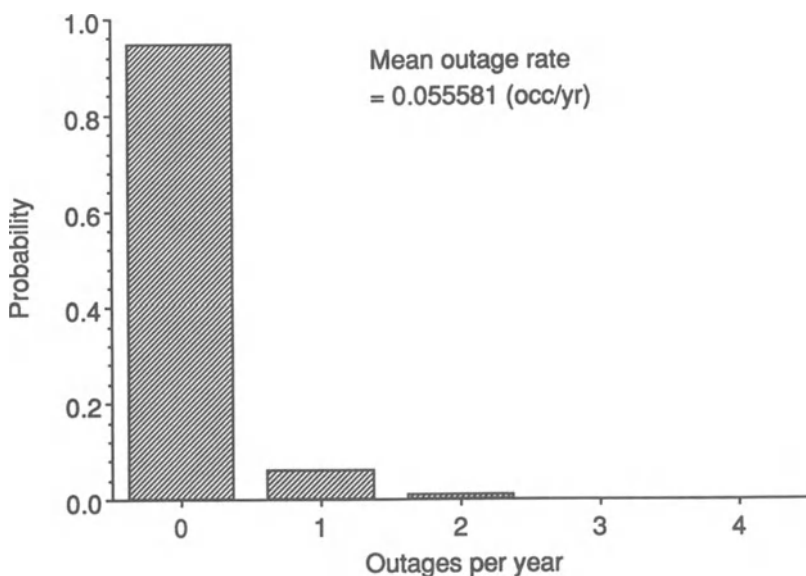
**Figure 6.17.** Reliability indices at points (1) and (4) as a function of the breaker failure rates.

**Table 6.24. Point Outage Rate Probability Distributions**

Point	Probability of outage rates				
	0	1	2	3	4
(1)	0.946160	0.052185	0.001617	0.000037	0.000000
(2)	0.944074	0.054395	0.001519	0.000012	0.000000
(3)	0.946210	0.052259	0.001506	0.000025	0.000000
(4)	0.946235	0.052123	0.001605	0.000037	0.000000
(5)	0.944185	0.054296	0.001519	0.000000	0.000000
(6)	0.946259	0.052210	0.001506	0.000025	0.000000

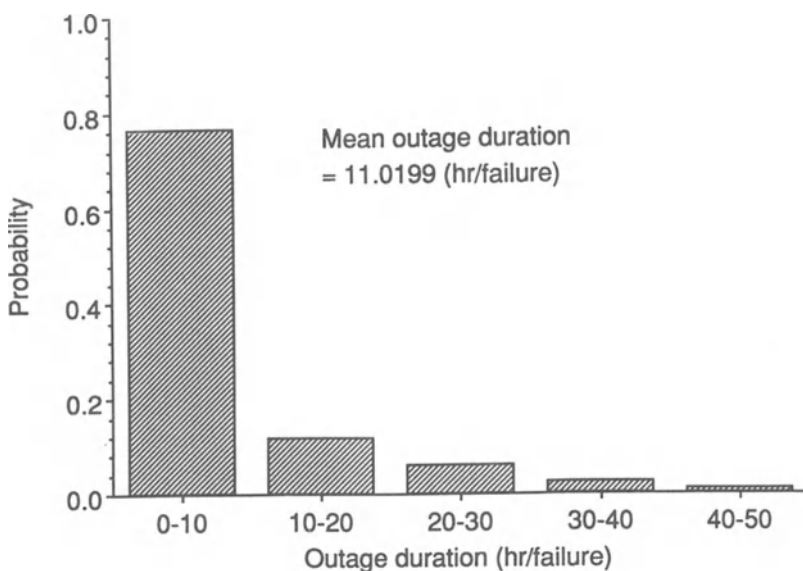
and 4 outages within 1 yr, respectively. The outage rate probability distribution at Point (1) is shown in Figure 6.18 for illustrative purpose.

Table 6.25 shows the point outage duration probability distributions. Columns 2, 3, 4, 5, and 6 show the probabilities of outage durations between 0 to 10 hr/failure, 10 to 20, 20 to 30, 30 to 40, and 40 to 50, respectively. The probability of an outage duration longer than 50 hr is not shown in this table. The outage duration probability distribution at Point (1) is shown in Figure 6.19.

**Figure 6.18.** Outage rate probability distribution at point (1).

**Table 6.25. Point Outage Duration Probability Distributions**

Point	Probability of outage durations				
	(0-10)	(10-20)	(20-30)	(30-40)	(40-50)
(1)	0.761672	0.116719	0.056247	0.021787	0.007337
(2)	0.763695	0.107197	0.052417	0.025779	0.015252
(3)	0.750613	0.111756	0.055989	0.030560	0.015838
(4)	0.410154	0.183923	0.120908	0.076375	0.046538
(5)	0.419681	0.190568	0.110680	0.074289	0.049957
(6)	0.403885	0.184193	0.119893	0.082831	0.048895

**Figure 6.19.** Outage duration probability distribution at point (1).

## 6.5. CONCLUSIONS

This chapter discusses the application of the time sequential Monte Carlo simulation method to distribution system and station reliability assessment. In each case, component operating histories are randomly simulated by the component state duration sampling technique. Practical deterministic events in the operating process, such as a prespecified switch-

ing logic or a scheduled maintenance, etc., can be imposed to obtain modified component operating histories. The system operating history can be created by combining the modified component operating histories. Reliability indices at load points (or source points) can be obtained by evaluating each system state. In the case of radial distribution systems, the modified component operating histories can also be combined with the conventional analytical method to obtain the load point reliability indices. The basic criterion in system state evaluation is connectivity from source point(s) to load point(s) and is associated with component failures, switching logic of breakers and section switches, action procedure for protection devices, and operating guidelines for backup supply sources, etc. Station reliability assessment is generally more complex than radial distribution system reliability assessment as it involves multiple source points, multiple breakers, and usually more complicated protection coordination.

Mean reliability indices can be readily calculated using the conventional analytical method.<sup>(1)</sup> The advantages of the Monte Carlo simulation method are that any component state duration probability distributions can be simulated, reliability index probability distributions can be calculated, and more complex operating procedures can be considered. The index probability distributions provide an added dimension to reliability evaluation. Maintenance times can be modeled using probability distributions similar to those used for component failure or repair times. Scheduled maintenance, however, is not a random event and it may be represented by a prespecified interval. Both cases can be readily simulated using the time sequential Monte Carlo method.

Frequency and duration parameters are major indices in distribution system and station reliability assessment. In distribution system reliability evaluation, these indices can be divided into two fundamental groups. The first group contains the three basic load point indices: failure rate, outage duration, and annual outage time. The second group contains the system performance indices, in which the most commonly used ones are SAIFI, SAIDI, CAIDI, ASAII, and ASUI. The system performance indices are weighted averages of the three basic load point indices. There are also two basic groups of indices in station reliability assessment. One group contains the outage probability and outage frequency of the external connection sets. These sets are mutually exclusive and can be used as input data in composite system adequacy assessment. The other group contains the outage probability, outage rate, and outage duration for each individual connection and are called point indices. These indices are not mutually exclusive and can be used as input data in radial distribution system reliability assessment.

## 6.6. REFERENCES

1. R. Billinton and R. N. Allan, *Reliability Evaluation of Engineering Systems: Concepts and Techniques*, Plenum, New York, 1983.
2. R. Billinton and R. N. Allan, *Reliability Evaluation of Power System*, Plenum, New York, 1984.
3. R. Billinton and R. N. Allan, *Reliability Assessment of Large Electric Power Systems*, Kluwer, Boston, 1988.
4. R. Billinton and M. S. Grover, "Distribution System Reliability Assessment," *CEA Trans.*, Vol. 13, Pt. III, 1974.
5. M. S. Grover and R. Billinton, "Quantitative Evaluation of Permanent Outages in Distribution Systems," *IEEE Trans. on PAS*, Vol. 94, 1975, pp. 733-741.
6. R. Billinton, J. E. D. Northcote-Green, T. D. Vismor, and C. L. Brooks, "Integrated Distribution System Reliability Evaluation: Part I—Current Practices," CEA Engineering and Operating Division Meeting, March 1980.
7. R. Billinton and R. Goel, "An Analytical Approach to Evaluate Probability Distributions Associated with the Reliability Indices of Electric Distribution System," *IEEE Trans. on PD*, Vol. 1, No. 3, 1986, pp. 245-251.
8. M. S. Grover and R. Billinton, "A Computerized Approach to Substation and Switching Station Reliability Evaluation," *IEEE Trans. on PAS*, Vol. 93, 1974, pp. 1488-1497.
9. M. S. Grover and R. Billinton, "Substation and Switching Station Reliability Evaluation," *CEA Trans.*, Vol. 13, Pt. III, 1974, Paper No. 74-SP-151.
10. R. Billinton and T. K. P. Medicheria, "Station Originated Multiple Outages in the Reliability Analysis of a Composite Generation and Transmission System," *IEEE Trans. on PAS*, Vol. 100, No. 8, 1981, pp. 3870-3878.
11. R. Billinton, P. K. Vohra, and S. Kumar, "Effect of Station Originated Outages in a Composite System Adequacy Evaluation of the IEEE Reliability Test System," *IEEE Trans. on PAS*, Vol. 104, No. 10, 1985, pp. 2649-2656.
12. R. Billinton and P. K. Vohra, "Station Initiated Outages in Composite System Adequacy Evaluation," *Proc. IEE*, Vol. 134, Pt. C, 1987, pp. 10-16.
13. R. Billinton, "Distribution System Reliability Performance and Evaluation," *Electrical Power and Energy Systems*, Vol. 10, No. 3, 1988, pp. 190-200.
14. R. Billinton, E. Wojczynski, and M. Godfrey, "Practical Calculations of Distribution System Reliability Indices and Their Probability Distributions," *CEA Trans.*, Vol. 20, Pt. I, 1981.
15. R. Billinton and E. Wojczynski, "Distributional Variation of Distribution System Reliability Indices," *IEEE Trans. on PAS*, Vol. 104, No. 11, 1985, pp. 3152-3160.
16. D. O. Koval and R. Billinton, "Statistical and Analytical Evaluation of the Duration and Cost of Consumer Interruptions," 1979 IEEE/PES Winter Meeting, Paper A79-057-1, Feb. 1979.
17. R. Billinton, E. Wojczynski, and V. Rodych, "Probability Distributions Associated with Distribution System Reliability Indices," 1980 Reliability Conference for the Electric Power Industry, 1980.
18. IEEE Committee Report, "Report on Reliability Survey of Industrial Plants, Part II: Cost of Power Outages, Plant Restart Time, Critical Service Loss Duration Time, and Type of Loads Lost Versus Time of Power Outages," *IEEE Trans. on Industry Applications*, Vol. IA-10, No. 2, 1974, pp. 236-241.
19. P. E. Gannon, Power Systems Reliability Subcommittee Report, "Cost of Electrical Interruptions in Commercial Buildings," IEEE 1975 I\$CPS Conference, pp. 123-129, 1975.

20. E. Wojczynski, R. Billinton, and G. Wacker, "Interruption Cost Methodology and Results—A Canadian Commercial and Small Industrial Survey," *IEEE Trans. on PAS*, Vol. 103, No. 2, 1984, pp. 437–444.
21. A. D. Patton, "Probability Distribution of Transmission and Distribution Reliability Performance Indices," 1979 Reliability Conference for the Electric Power Industry, pp. 120–123.
22. US Department of Energy, "The National Electric Reliability Study: Executive Summary," DOE/EP-003 Dist. Category UC-97C, April, 1981.
23. R. Billinton, L. Gan, L. Goel, G. Lian, and W. Li, "Applications of Monte Carlo Simulation in Power System Adequacy Assessment," *CEA Trans.*, Vol. 30, Pt. 3, 1991.
24. EPRI Final Report, "Predicting Transmission Outage for System Reliability Evaluation," Tech. Report, EPRI, El-3880, Vol. 1, May 1985.
25. R. Billinton and G. Lian, "Substation Reliability Worth Assessment Using A Monte Carlo Approach," 1992 Inter-RAMQ Conference for the Power Industry, Philadelphia, Aug. 1992.
26. R. Billinton and G. Lian, "Station Reliability Evaluation Using A Monte Carlo Approach," *IEEE Trans. on PD*, Vol. 8, No. 3, 1993, pp. 1239–1245.
27. CEA Working Group, "Report on Basic Station Single Line Diagrams in Use by Canadian Utilities and Consultants," *CEA Trans.*, Vol. 19, Pt. 5, March, 1980.

# Reliability Cost/ Worth Assessment

## 7.1. INTRODUCTION

The basic function of a modern electric power system is to provide electric power and energy to its customers at the lowest possible cost and at acceptable levels of reliability. Reliability worth assessment provides the opportunity to incorporate cost analysis and quantitative reliability assessment into a common structured framework.<sup>(1)</sup> Direct evaluation of reliability worth or benefit is very difficult and perhaps impossible and a variety of methods have evolved to provide monetary estimates.<sup>(2,3)</sup> Interruption costs are most often used to provide an indirect measure of reliability worth. It is important to realize that, while power system reliability assessment has become a well established practice over the last few decades, reliability worth assessment or unreliability cost evaluation is still relatively immature. The major reason for this is that the quantification of interruption costs is a complex and often subjective task.

Customer surveys provide a comprehensive approach to evaluate the impacts of interruptions to customer service due to failures in electric energy supply. Such surveys are normally undertaken for each user group, e.g., commercial, industrial, residential, etc., and can provide reasonably relatively definitive results.<sup>(4-12)</sup> The University of Saskatchewan has conducted several systematic customer surveys. The first series was done in 1980–1985 on behalf of the Canadian Electrical Association (CEA), and the second in 1990–1992, sponsored by the Natural Sciences and Engineering Research Council (NSERC) together with seven participating Canadian electric power utilities. The data compiled from these surveys have been used to formulate Sector Customer Damage Functions (SCDF), which depict the sector interruption cost as a function of the interruption duration. The SCDF can be

aggregated to create the Composite Customer Damage Functions (CCDF), which measure the cost associated with power interruptions as a function of the interruption duration for the customer mix at the bus, or in the area of interest, or for the whole system. Section 7.2 briefly discusses basic customer survey techniques and customer damage functions.

Interruption duration, frequency, and load curtailed are three fundamental quantities in power system reliability evaluation. Reliability worth analysis provides a value-based assessment which reflects the integrated effects of these three quantities. The CDF provides the cost/reliability link in such an evaluation. Reliability worth assessment can be performed at the different hierarchical levels and functional zones described in Chapter 2. Sections 7.3, 7.4, and 7.5 discuss generating capacity adequacy worth (HL1), composite system adequacy worth (HL2), and distribution system adequacy worth assessment, respectively. This is only one part of an overall economic analysis. However, it provides extremely important input to the overall decision-making process. In a power system planning context, an optimal alternative reinforcement or expansion scheme should achieve minimum total cost, which is the sum of the investment, operating, and customer interruption costs. Section 7.6 describes an overall economic assessment model at HL2.

## **7.2. CUSTOMER SURVEYS AND CUSTOMER DAMAGE FUNCTIONS**

### **7.2.1. Basic Customer Survey Methods**

The various approaches that have been used to evaluate the impacts of interruptions in service to electric customers can be grouped into the three categories of indirect analytical evaluations, case studies of actual blackouts, and customer surveys. Customer surveys require a large amount of effort and subsequent statistical analysis. However, they provide the best approach to interruption cost evaluation as customers are in the best position to understand how outages impact on those of their activities that depend on electricity. This approach can also include various complex factors which cannot be easily considered using other techniques.<sup>(4,5)</sup> The three basic approaches to conducting a customer survey are: (1) the contingent valuation method, (2) the direct costing method, and (3) the indirect costing method.<sup>(5)</sup> It is possible and desirable to use more than one method in a given customer survey.

**(a) Contingent Valuation Method.** The contingent valuation method establishes a monetary value of outage cost for incremental changes in levels of service. This is quantified either through the consumer's willingness to pay (WTP) to avoid having an interruption, or the willingness to accept (WTA) compensation for having had one. In theory, WTP values should be nearly equal to WTA values, but actual customer valuations reveal that WTP values are significantly less than WTA values. This is due to the fact that customers normally do not have a choice of suppliers, and therefore their responses may be governed largely by their concern for potential rate changes. They may react against providing further money for a service they consider already paid for. Valuations based on WTP and WTA are valuable measures and may serve as upper and lower bounds, respectively, in cost-of-outage assessment.

**(b) Direct Costing Method.** A direct costing method is the most obvious approach for determining customer interruption costs for given outage conditions. The respondent is given a "worksheet" and asked to identify the impacts and evaluate the costs associated with particular outage scenarios. This approach provides consistent results in those situations where most losses tend to be tangible, directly identifiable, and quantifiable. Thus it is most applicable for the industrial sector and for most large electrical users. It can also be effective in the commercial/retail markets but must be used with care.

**(c) Indirect Costing Method.** The indirect costing method is based on the economic principle of substitution in which the valuation of a replacement good is used as a measure of worth of the original good. It is extremely useful when social considerations and inconvenience effects are expected (or are known) to comprise a significant part of the overall interruption costs, such as in the residential sector. This approach attempts to provide a means to lessen the perceptions associated with rate-related antagonism and customers' lack of experience in rating the worth of reliability. The respondents are asked questions that relate to the context of their experience. These could include: the cost of hypothetical insurance policies to compensate for possible interruption effects, preparatory actions the respondent might take in the event of recurring interruptions, or ranking a set of reliability/rate alternatives. Evaluations of the financial burden that customers would be willing to bear to alleviate the effects of the interruption can be obtained through responses to these questions. The derived expenditures can be considered to be the respondents' perception of the value of avoiding the interruption consequences. As such, they represent an indirect estimate of their perception of reliability worth.

## 7.2.2. Questionnaire Content and Data Treatment

**(a) Questionnaire Content.** It is obviously desirable to investigate all possible factors which might affect interruption costs. The length of a questionnaire, however, is limited by the amount of effort that respondents are prepared to put in to fill it out. This limitation is particularly relevant in the residential sector, where a significant portion of the outage costs are related to somewhat intangible impacts. A questionnaire must therefore be developed with considerable care. In general, the following factors should be included:

*Residential questionnaire:* Interruption characteristics (duration, frequency, and season, day of week, and time of day of the occurrence); user characteristics (number and age of household members, sex and education of the respondent); type and location of the dwelling (urban or rural); electric heat usage; attitude toward utilities; undesirability as a function of activity interruption; income earning business at home; and user experience with interruption.

*Commercial and industrial questionnaires:* Customer uses of electric energy; type of standby electrical supply equipment and its purpose; past interruption frequency; cost estimates for a typical interruption time (e.g., on Friday at 10:00 am near the end of January) as a function of duration; cost variations with the month of the year, day of the week, and time of day; possibility and amount of cost saving if duration of interruption is known or if advance warning is given; power rationing preference; and demographic information on the nature and size of the company's operation (e.g., number of employees, shifts, sales volume, etc.). The industrial questionnaire also requires start-up time for various interruption durations.

**(b) Data Treatment.** Customer surveys can generate a considerable amount of data including some "bad" information, and it is necessary to conduct appropriate statistical analyses before utilizing these raw data. This includes calculations of mean values, standard deviations, and correlation coefficients, and filtering the "bad" data. Such analyses should be conducted for each customer category, for each service area, and for the regions within service areas.

## 7.2.3. Customer Damage Functions

**(a) Sector Customer Damage Function (SCDF).** The SCDF portrays the unit interruption cost as a function of the interruption duration

**Table 7.1. Sector Customer Damage Functions for the Seven Customer Categories**

Duration	Interruption cost of customer sectors (\$/kW)						
	Agri.	Large user	Resid.	Gover.	Indus.	Commer.	Office
1 min	0.060	1.005	0.001	0.044	1.625	0.381	4.778
20 min	0.343	1.508	0.093	0.369	3.868	2.969	9.878
1 hr	0.649	2.225	0.482	1.492	9.085	8.552	21.065
4 hr	2.064	3.968	4.914	6.558	25.163	31.317	68.830
8 hr	4.120	8.240	15.690	26.040	55.808	83.008	119.160

for an individual customer sector. The Standard Industrial Classification (SIC) can be used to categorize customers. The seven main sectors are: larger users, industrial, commercial, agriculture, residential, governmental, and offices. In order to obtain unit interruption cost estimates, the actual dollar values reported by customers are normalized using their annual peak or average demands (in \$/kW) and a weighted-mean unit interruption cost estimate for each category is calculated. If the interruption duration is short, the weighting factor is the percentage of the annual peak demand of each respondent with respect to the total annual peak demand of all respondents in the same category. If the interruption duration is relatively long, the weighting factor is the percentage of the annual energy consumption of each respondent with respect to the total annual energy consumption of all respondents in the same category.

Table 7.1 shows Sector Customer Damage Functions (in \$/kW) for the seven customer categories based on Canadian customer surveys. Figure 7.1 provides a graphical portrayal of the SCDF.

**(b) Composite Customer Damage Functions (CCDF).** A CCDF is the measure of the interruption cost as a function of the interruption duration for a customer mix at a bus, in a service area, or in a whole system. The customer mix in terms of energy consumption or peak demand percentages must be known so that the interruption costs for each of the various customer categories can be proportionally weighted. In the case of durations shorter than 0.5 hr, the weighting factor is the percentage of the annual peak load. In the case of durations longer than 0.5 hr, the weighting factor is the percentage of the annual energy consumption. The weighted costs are summed for each interruption duration to give the total cost for the customer mix for that duration. Table 7.2 shows a representative load mix in terms of both energy consumption and peak demand. Table 7.3 presents the Composite Customer Damage Function based on the Sector Customer Damage Functions

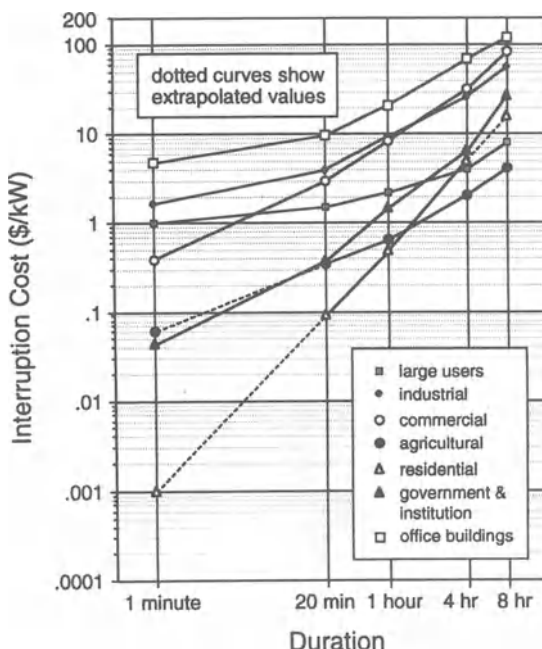


**Figure 7.1.** Sector customer damage functions.

**Table 7.2. Distribution of Customer Mix by Energy Consumption and Peak Demand**

Customer category	Energy (%)	Peak demand (%)
Agriculture	2.5	4.0
Large user	31.0	30.0
Residential	31.0	34.0
Government	5.5	6.0
Industrial	19.0	14.0
Commercial	9.0	10.0
Office	2.0	2.0

in Table 7.1 and the customer mix in Table 7.2. Figure 7.2 provides a graphical portrayal of the CCDF.

Interruption cost estimates can be used as a surrogate for electric power system reliability worth. In applying CDF, three important points should be appreciated. First, as with other reliability data, a sufficient number of

**Table 7.3. Composite Customer Damage Function for the Customer Mix**

Interruption duration	Interruption cost (\$/kW)
1 min	0.67
20 min	1.56
1 hr	3.85
4 hr	12.14
8 hr	29.41

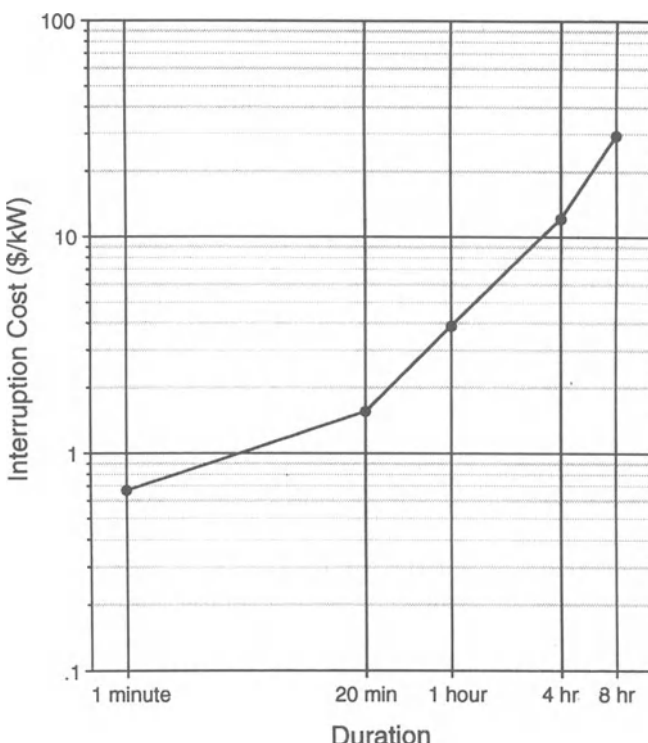


**Figure 7.2.** Composite customer damage function.

customer samples is required to ensure reasonable accuracy. Second, customer surveys should be continuously updated. Third, interruption costs are socioeconomic/demographic/geographic specific. In other words, customer damage functions are generally different for different areas, regions, and countries.

## 7.3. GENERATING SYSTEM RELIABILITY WORTH ASSESSMENT

### 7.3.1. Assessment Techniques

The most popular HL1 adequacy index at the present time is the loss of load expectation (LOLE). This index has been used by some utilities for a long time and is being considered and introduced by others. This index cannot, however, be easily linked with customer outage costs to assess HL1 adequacy worth. The most convenient index for this purpose is the loss of energy expectation (LOEE) or expected energy not supplied (EENS).

Billinton *et al.*<sup>(13)</sup> show the development of a monetary value for unserved energy using the system CCDF. Two techniques are presented. The first is an analytical approach based on the classical frequency and duration technique.<sup>(14)</sup> The second approach uses sequential Monte Carlo simulation to calculate the unserved energy cost. The results in the case studied are relatively close. The monetary value associated with unserved energy has been designated as the Interrupted Energy Assessment Rate (IEAR).<sup>(13)</sup> This monetary value can be used in a wide range of studies and developed for application at all three hierarchical levels. Equations (7.1), (7.2), and (7.3) are the basic equations used in the analytical application of this concept. Given that it is possible to calculate the frequency and duration associated with a load loss event, the EENS in MWh/yr is given by equation (7.1):

$$\text{EENS} = \sum_{i=1}^N C_i F_i D_i \quad (7.1)$$

where  $C_i$  is the load curtailment of load loss event  $i$  in MW,  $F_i$  the frequency of load loss event  $i$  in occ./yr,  $D_i$  the duration of load loss event  $i$  in hours, and  $N$  is the total number of load loss events.

The total Expected Interruption Cost (EIC) in k\$/yr is given by

$$\text{EIC} = \sum_{i=1}^N C_i F_i W(D_i) \quad (7.2)$$

where  $W(D_i)$  is the customer damage function, i.e., the unit interruption cost for the duration  $D_i$  of load loss event  $i$ .

The Interrupted Energy Assessment Rate (IEAR) in \$/kWh is defined as

$$\text{IEAR} = \frac{\sum_{i=1}^N C_i F_i W(D_i)}{\sum_{i=1}^N C_i F_i D_i} \quad (7.3)$$

The IEAR is an important concept in generating system reliability assessment and is quite stable for a given generating system, i.e., it generally does not vary significantly when the system load level and other factors change. Consequently, EIC for different load levels can be obtained by multiplying the IEAR by the EENS, which can be calculated using a wide variety of methods.

Equations (7.1)–(7.3) apply not only to the analytical approach but also to the system state sampling technique. This is due to the fact that the system state sampling technique creates load curtailments, frequencies, and durations of individual load loss events. It is important to appreciate that the analytical approach uses average duration and frequency values for  $D_i$  and  $F_i$  in equations (7.1), (7.2), and (7.3). The cost components are therefore based on average values rather than on specific random events and the load loss event duration and frequency distributions. This has little effect on the EENS index but can lead to errors in the EIC and in turn to the IEAR, particularly in the case of customer damage functions with a relatively high degree of nonlinearity. Specific random system states can be simulated if the system state sampling technique is used. This is illustrated in Section 7.4 for composite system reliability worth assessment.

In a sequential Monte Carlo simulation, individual load loss events are encountered sequentially and therefore not only the specific random system states but also the transition process between system states can be simulated. In other words, the effects of the load loss event duration and frequency distributions can be considered in the simulation. The state duration sampling technique for generating system reliability evaluation is discussed in detail in Chapter 4. The EIC and IEAR using this technique are obtained from equations (7.4) and (7.5):

$$\text{EIC} = \frac{\sum_{i=1}^N W(D_i)E_i/D_i}{M} \quad (7.4)$$

$$\text{IEAR} = \frac{\sum_{i=1}^N W(D_i)E_i/D_i}{\sum_{i=1}^N E_i} \quad (7.5)$$

where  $W(D_i)$  is the customer damage function in \$/kW,  $D_i$  the duration of interruption  $i$  in hours,  $E_i$  the energy not supplied of interruption  $i$  in MWh,  $N$  the total number of interruptions experienced in simulated years, and  $M$  is the number of simulated years.

It is noted that interruption  $i$  in a sequential system capacity margin profile can be a single load loss event or a sequence of two or more successive load loss events.

### 7.3.2. Numerical Example

Consider the IEEE RTS for which the basic data are given in Appendix A.1. The additional data associated with the generating unit derated states, peaking units, and the nonexponential distribution state durations are given in Section 4.2.4. The composite customer damage function shown in Table 7.3 was used in this study. The following results<sup>(15)</sup> were obtained using the component state duration sampling technique:

*Case 1: Base Case*—The EIC and IEAR indices in the base case are: EIC = 6255.7 k\$/yr and IEAR = 5.310 \$/kWh.

*Case 2: Peak Load Variations*—The results for different peak loads are shown in Table 7.4. It can be seen that although the value of EIC increases as the system peak load increases, the estimated IEAR does not change significantly with peak load. This is an important observation.

*Case 3: Generating Unit Derated States*—This case is the same as Case 2, except that the 350-MW and the 400-MW units were assumed to have one derated state. The results are shown in Table 7.5. Recognition of generating unit derated states has minimal effects on the IEAR.

*Case 4: Peaking Units*—This is the same as Case 1 for the annual peak load of 2850 MW, except that additional 25-MW gas turbine units are assumed to be peaking units. The results are given in Table 7.6.

*Case 5: Nonexponential Distributions*—This is the same as Case 1 for the annual peak load of 2850 MW, except that unit operating or repair durations are assumed to be nonexponentially distributed. The four distribu-

**Table 7.4. EIC and IEAR Indices for Different Peak Loads**

Index	Annual system peak load (MW)				
	2650	2750	2850	2950	3050
EIC (k\$/yr)	1343.3	2935.4	6255.7	12508.0	23909.1
IEAR (\$/kWh)	5.293	5.296	5.310	5.317	5.328

**Table 7.5. EIC and IEAR Indices for the Derating Case**

Index	Annual system peak load (MW)				
	2650	2750	2850	2950	3050
EIC (k\$/yr)	857.1	1857.9	3989.8	8401.7	16421.5
IEAR (\$/kWh)	5.270	5.281	5.264	5.290	5.306

**Table 7.6. EIC and IEAR Indices for the Peaking Unit Addition Case**

Index	Number of peaking units added		
	Zero units	One unit	Two units
EIC (k\$/yr)	6255.7	4957.0	3322.2
IEAR (\$/kWh)	5.310	5.310	5.282

**Table 7.7. EIC and IEAR Indices for the Nonexponential Distribution Case**

Index	Nonexponential distribution conditions			
	Cond. 1	Cond. 2	Cond. 3	Cond. 4
EIC (k\$/yr)	6221.8	6155.7	6055.8	6257.5
IEAR (\$/kWh)	5.302	5.310	5.303	5.301

tion conditions are identical to those given in Section 4.2.4.(d). The results are shown in Table 7.7. The effects of the different distributions on the EIC and IEAR values are minimal in this case. It should be noted that this is possibly not a general conclusion for the EIC index.

### 7.3.3. Application Of Reliability Worth Assessment in Generation Planning

HL1 adequacy depends upon many factors, such as the installed capacity, generating unit availability and size, load profile, maintenance requirements, reserve margin, etc. Additional generating capacity above the system peak load is generally maintained to protect against excessive unforeseen outages and loads in excess of forecasts and to provide opportunities for generating unit preventive maintenance. System adequacy can be significantly increased by maintaining a higher reserve level, which results in increased installation costs and reduced supply interruption costs. The selection of an optimal adequacy level, therefore, is an important engineering decision which should consider the costs of providing the specified reliability level and the corresponding benefits accruing to society due to these levels. Basic criteria, such as loss of load expectation (LOLE), cannot be used to relate system adequacy to economic parameters such as customer costs due to supply interruptions. Indices such as EENS which recognize the severity associated with generation capacity deficiencies must be used. There is a growing interest in generation system expansion planning using economic theory approaches which simultaneously optimize system costs and customer

**Table 7.8. Generating Unit Operating Costs**

Rated capacity (MW)	Type	Fixed cost (\$/kW/yr)	Variable cost (\$/MWh)
12	Oil	10.0	63.30
20	Combustion Turbine	3.0	103.60
50	Hydro	2.5	0.50
76	Coal	10.0	15.30
100	Oil	8.5	52.80
155	Coal	7.0	12.44
197	Oil	5.0	50.62
350	Coal	4.5	12.10
400	Nuclear	5.0	6.30

failure costs. Power system planners are faced with the difficult task of maintaining reasonable system reliability levels while minimizing the investment and operating costs. Judicious decisions can be made by estimating the costs and benefits associated with various levels of expansion and including the inherent uncertainties associated with system parameters.

The application of reliability worth assessment in generation planning is illustrated using the IEEE RTS. The basic data of the IEEE RTS are given in Appendix A.1. The initial analysis was done by assuming that the total system peak load is increased from 2850 MW to 3000 MW while the annual load curve shape remains unchanged, i.e., the 8736 hourly loads are increased proportionally. The total installed capacity provided by 32 generating units is 3405 MW. The associated reserve margin is 13.5% for this system peak load. Under these conditions, the expected customer interruption cost is 16,860 k\$/yr. The total fixed and variable operating cost is 126,740 k\$/yr. The system operating cost was obtained using the generating unit operating costs given in Table 7.8<sup>(16)</sup> and an economic generation loading approach. The purpose of the study is to determine the least cost reserve margin and five additional 20-MW units were considered sequentially. These units were assumed to have the same failure data as the 20-MW unit given in Appendix A.1 and a capital cost of \$17 million per unit. The annual investment cost was calculated using the present value method (see Section 7.6.2). Under the assumption of a 30-yr economic life and a 10% discount rate, the annual investment cost is 1802 k\$/yr. Table 7.9 presents the expected interruption, investment, and operating costs for the base case and with the sequential addition of five 20-MW units.

It can be seen that the expected interruption costs decrease rapidly as additional capacity is added to the system while the operating costs increase slightly. There are great differences between absolute values of the interrup-

**Table 7.9. Interruption, Investment, and Operating Costs with Sequential Capacity Additions of 20-MW units**

Number of units added	Reserve margin (%)	EIC (k\$/yr)	Investment cost (k\$/yr)	Operating cost (k\$/yr)
0	13.50	16860	0	126740
1	14.16	14606	1802	126930
2	14.83	12651	3604	127010
3	15.50	11170	5406	127060
4	16.17	9960	7208	127090
5	16.83	8680	9010	127120

tion, investment, and operating costs. An incremental comparison approach can be used to highlight the effect of the added units, since the investment is associated only with the added units while the interruption and operating costs are for the whole system. The increment costs are shown in Table 7.10. The values in the second column are the interruption cost reduction caused by unit addition(s) compared to the base case, and those in the fourth column are the increase in the operating cost. The values in the last column are the annual net gains, which are presented graphically in Figure 7.3. The maximum benefit or the least cost reserve margin occurs with the addition of the two 20-MW units. The reserve margin and the LOEE at this point are 14.83% and 2386.94 MWh/yr respectively. The optimum reserve margin is obviously dependent on the data used in the system evaluation, including the perceived customer interruption costs. The optimum reserve margin is also very dependent on the size and type of the units used in the proposed expansion and will vary with different proposed configurations. It is not, however, a fixed predetermined value which can be used under all conditions and expansion scenarios.

**Table 7.10. Incremental Costs and Annual Net Gains with Sequential Capacity Additions of 20-MW Units**

Number of units added	EIC reduction (k\$/yr) (1)	Investment cost (k\$/yr) (2)	Operat. cost increase (k\$/yr) (3)	Annual net gain (k\$/yr) (1) - [(2) + (3)]
0	0	0	0	0
1	2254	1802	190	+262
2	4209	3604	270	+335
3	5690	5406	320	-36
4	6900	7208	350	-658
5	8180	9010	380	-1210

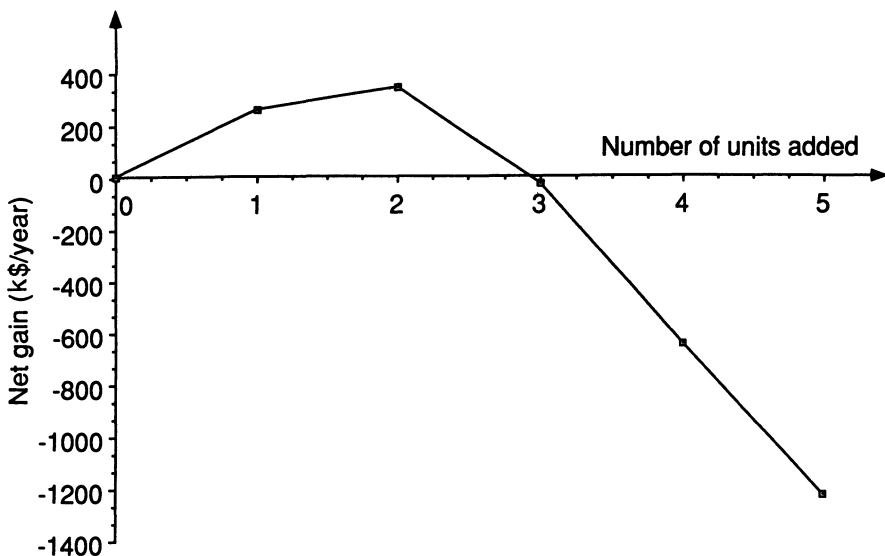


**Figure 7.3.** Annual net gains due to 20-MW unit additions for the IEEE RTS generating system.

In the explicit cost approach, the reserve margin is an outcome of the analysis, not a fixed criterion used to drive the unit addition process. It is noted that the analysis presented here is only a simple example and factors such as effects of load growth, unit size and type, and different operating conditions, etc., are not considered. These can be easily included using the procedure presented.

## 7.4. COMPOSITE SYSTEM RELIABILITY WORTH ASSESSMENT

### 7.4.1. Assessment Method

HL2 adequacy assessment involves the consideration of transmission network constraints, generation rescheduling, overload alleviation, bus load curtailment philosophies, etc., in addition to the recognition of equipment failure and repair phenomena. The basic techniques for composite system adequacy assessment are presented in Chapter 5 and can be extended to composite system reliability worth assessment by introducing certain additional considerations. The fundamental procedures, however, remain the same.

**(a) Minimum System Interruption Cost Model.** The optimization model given in Section 5.2 minimizes the total system load curtailment while satisfying the power balance, linearized load flow equations, line flow limits, and generation output limits. In order to conduct reliability worth assessment, it is necessary to introduce customer damage functions into the model. The following linear programming minimization model can be used for a particular drawn system state to calculate the possible load curtailments at different buses and the interruption costs for the system and for each load bus:

$$\min TD = \sum_{i=1}^{NC} \sum_{j=1}^{IC_i} W_{ij}(D_k) C_{ij} \quad (7.6)$$

subject to

$$T_n = \sum_{i=1}^{NS} A_{ni} \left( PG_i + \sum_{j=1}^{IC_i} C_{ij} - \sum_{j=1}^{IC_i} PD_{ij} \right) \quad (i=1, \dots, L) \quad (7.7)$$

$$\sum_{i=1}^{NG} PG_i + \sum_{i=1}^{NC} \sum_{j=1}^{IC_i} C_{ij} = \sum_{i=1}^{NC} \sum_{j=1}^{IC_i} PD_{ij} \quad (7.8)$$

$$PG_i^{\min} \leq PG_i \leq PG_i^{\max} \quad (i=1, \dots, NG) \quad (7.9)$$

$$0 \leq C_{ij} \leq PD_{ij} \quad (i=1, \dots, NC; j=1, \dots, IC_i) \quad (7.10)$$

$$|T_n| \leq T_n^{\max} \quad (n=1, \dots, L) \quad (7.11)$$

where  $PG_i$  is the generation variable at Bus  $i$ ;  $PD_{ij}$  and  $C_{ij}$  are the load and the load curtailment variables, respectively, of the  $j$ th sector customer at Bus  $i$ ;  $T_n$  is the line flow on Line  $n$ ;  $A_{ni}$  is an element of the relation matrix between line flows and power injections;  $PG_i^{\min}$ ,  $PG_i^{\max}$ , and  $T_n^{\max}$  are the limits, respectively, of  $PG_i$  and  $T_n$ ;  $W_{ij}(D_k)$  is the customer damage function (in \$/kW) of the  $j$ th sector customer at Bus  $i$ ;  $D_k$  is the duration of the system state  $k$ ;  $NS$ ,  $NG$ ,  $NC$ , and  $L$  are the numbers of system buses, generator buses, load buses, and system lines, respectively;  $IC_i$  is the number of customer sectors at Bus  $i$ .

The objective of this model is to minimize the total system interruption cost while satisfying the power balance, the linearized load flow relationships, line flow limits, and generation output limits. Customer damage functions for different customer sectors at load buses and the effect of system state durations on interruption costs have been incorporated in the model. The constraints in this model are essentially the same as those in the model given in Section 5.2. The difference between them is associated with the objective function. The objective of this model is to minimize the total system

interruption cost while that of the model in Section 5.2 is to minimize the total load curtailment. The two load curtailment philosophies described in Section 5.2 are performed, respectively, by introducing weighting factors  $W_i$  and  $\beta_j$  in equation (5.20). The load curtailment philosophy in this model is that the load with the lowest interruption cost is curtailed first, then that with the next lowest interruption cost, and at the last that with the highest interruption cost. This philosophy is followed automatically in the resolution of the model. This model also calculates all the adequacy indices for composite system evaluation defined in Section 5.2.4. The system adequacy indices obtained by the two models should be basically the same. The bus adequacy indices, however, can be different due to the different load curtailment philosophies used.

**(b) Determination of System State Duration.** In solving the above minimization model, the system state duration  $D_k$  must be known. It has been pointed out in Section 3.6.3 that if the state duration of each component follows an exponential distribution with parameter  $\lambda_i$ , where  $\lambda_i$  is the transition rate of component  $i$  at the present state, the duration of the system state also follows an exponential distribution with parameter  $\lambda = \sum \lambda_i$ . This means that the duration of the system state has the probability density function

$$f(t) = \sum_{i=1}^m \lambda_i \exp\left(-\sum_{i=1}^m \lambda_i t\right) \quad (7.12)$$

where  $m$  is the number of system components.

Two methods can be used to determine the system state duration  $D_k$  in equation (7.6). The first method is to use the mean value of the system state duration, i.e.,

$$D_k = \frac{1}{\sum_{i=1}^m \lambda_i} \quad (7.13)$$

Note that the transition rates  $\lambda_i$  of components are dependent on the system state. If the component  $i$  is in the up state for a drawn system state  $k$ ,  $\lambda_i$  is its failure rate. If it is in the down state,  $\lambda_i$  is its repair rate. Utilization of the mean value of the system state duration can lead to errors, particularly when the relevant customer damage functions have a high degree of non-linearity. However, calculations indicate that in some cases, this error is not significant and therefore can be accepted. The second method is to use the sample value of the system state duration. In terms of the inverse transform method, the sample value  $D_k$  of the system state duration having the

probability density function shown in equation (7.12) can be obtained by

$$D_k = -\frac{\ln U}{\sum_{i=1}^m \lambda_i} \quad (7.14)$$

where  $U$  is a uniformly distributed random number between  $[0, 1]$ .

Both methods given above are based on the assumption that the component state durations follow exponential distributions. When the component repair times follow nonexponential distributions, the distribution of the system state duration for composite systems is complex and there is no simple analytical expression for the distribution density function. If it is assumed that the system state duration follows a known distribution such as a Weibull or gamma distribution, the sample value of the system state duration can be obtained using the Monte Carlo sampling methods given in Section 3.4.

**(c) Index Calculations.** Load curtailments for each customer sector at each bus  $C_{ij}$  can be obtained by solving the minimization model. Consequently, both bus and system indices can be calculated. Note that  $C_{ij}$  in the model corresponds to a particular system state  $k$  whose duration is  $D_k$ . The subscript  $k$  in the variables, except  $D_k$  in the above model, has been omitted for simplicity. The annual bus and system indices are given by the following equations:

$$\text{EENS}_i = \sum_{k=1}^N \sum_{j=1}^{\text{IC}_i} C_{ijk} F_k D_k \quad (7.15)$$

$$\text{EIC}_i = \sum_{k=1}^N \sum_{j=1}^{\text{IC}_i} C_{ijk} F_k W_{ij}(D_k) \quad (7.16)$$

$$\text{EENS} = \sum_{i=1}^{\text{NC}} \text{EENS}_i \quad (7.17)$$

$$\text{EIC} = \sum_{i=1}^{\text{NC}} \text{EIC}_i \quad (7.18)$$

where  $C_{ijk}$ ,  $D_k$ ,  $W_{ij}$ , NC, and  $\text{IC}_i$  are as defined earlier;  $\text{EENS}_i$  and  $\text{EENS}$  are the Expected Energy Not Supplied at Bus  $i$  and for the system, respectively (MWh/yr);  $\text{EIC}_i$  and  $\text{EIC}$  are Expected Interruption Costs at Bus  $i$  and for the system (k\$/yr);  $N$  is the number of system states sampled;  $F_k$  is the frequency of system state  $k$  (occ./yr). The value of  $F_k$  can be obtained from the following general relationship between  $F_k$ ,  $D_k$ , and  $p_k$ :

$$p_k = F_k D_k \quad (7.19)$$

where  $p_k$  is the probability of system state  $k$ .

As in generation reliability worth evaluation, IEAR indices at HL2 can also be calculated. The IEAR indices for the system and buses are given by equations (7.20) and (7.21), respectively:

$$\text{IEAR} = \frac{\text{EIC}}{\text{EENS}} \quad (7.20)$$

$$\text{IEAR}_i = \frac{\text{EIC}_i}{\text{EENS}_i} \quad (7.21)$$

Analyses indicate that the IEAR at HL2 does not vary significantly with the system peak load. However, it may have a relatively large variation when the system topological configuration changes. This is due to the fact that changes in the system configuration lead to a change of network constraints which, in turn, may change the order of bus load curtailments when minimizing the total interruption cost. This case can happen particularly when a line addition creates a new loop from an original radial branch. Therefore, the HL2 IEAR should be utilized with caution when the system configuration changes significantly. In this case, it is advisable to evaluate EIC directly.

#### 7.4.2. Modified IEEE Reliability Test System and Additional Data

The original IEEE RTS version<sup>(17)</sup> has a relatively strong transmission network. Beroldi *et al.*<sup>(18)</sup> suggested several modifications based on an EPRI version of the IEEE RTS<sup>(19)</sup> for the purpose of conducting transmission planning studies. The Modified IEEE Reliability Test System (MRTS) was used to conduct the case studies described in this section and in Section 7.6. The basic data of the IEEE RTS are given in Appendix A.1. The modifications and additional data are as follows.

**(a) Load and Installed Capacity.** The system peak load was increased to 125% of the annual peak value given in the original version, assuming that the distribution among the load buses and the percentage values of the 8736 hourly loads remain unchanged. Eight generators are added at the selected buses shown in Table 7.11. The failure data of these eight generators are identical to those of the generators having the same capacity in the original system.

**Table 7.11. Added Generating Units Based on the Original IEEE RTS**

Bus No.	Unit size
1	76 MW × 1
2	76 MW × 1
13	197 MW × 1
22	50 MW × 4
23	350 MW × 1

**(b) Transmission Network.** Six lines and one transformer branch were removed from the original version and are shown by the dashed lines in Figure 7.4.

**(c) Additional Data.** The additional data required in order to conduct composite system reliability worth assessment are the sector customer damage functions and the customer sector allocations at load buses. The seven sector customer damage functions are the same as those given in Table 7.1. The customer sector allocations are given in Table 7.12.

### 7.4.3. Numerical Results

**(a) Base Case.** Reliability worth evaluation for the IEEE MRTS was conducted using the described method. A 15-step load model of the annual load duration curve was used to evaluate the annual bus and system EENS, EIC, and IEAR indices. The results for the base case are given in Table 7.13. There are no load curtailments and interruption costs at Buses 1, 2, 4, 5, and 8. This can be explained as follows. In addition to effects associated with the system topology and load flow constraints, customer sector allocations and specific SCDFs are the important aspects causing differences between load curtailments and interruption cost indices at the various buses. It can be seen from Table 7.1 that agriculture and large industrial users have the lowest unit interruption costs. When a minimum interruption cost principle is utilized in the resolution of the linear programming model, agriculture and large industrial users are automatically curtailed first. There are, however, no agriculture and large industrial customers at Buses 1, 2, 4, 5, and 8. In addition, these buses are either the generator buses (1 and 2) or close to the generator buses (4, 5, and 8).

**(b) Effect of Load Level Variations.** Annual system EENS and EIC indices and the corresponding IEAR for various load levels are shown

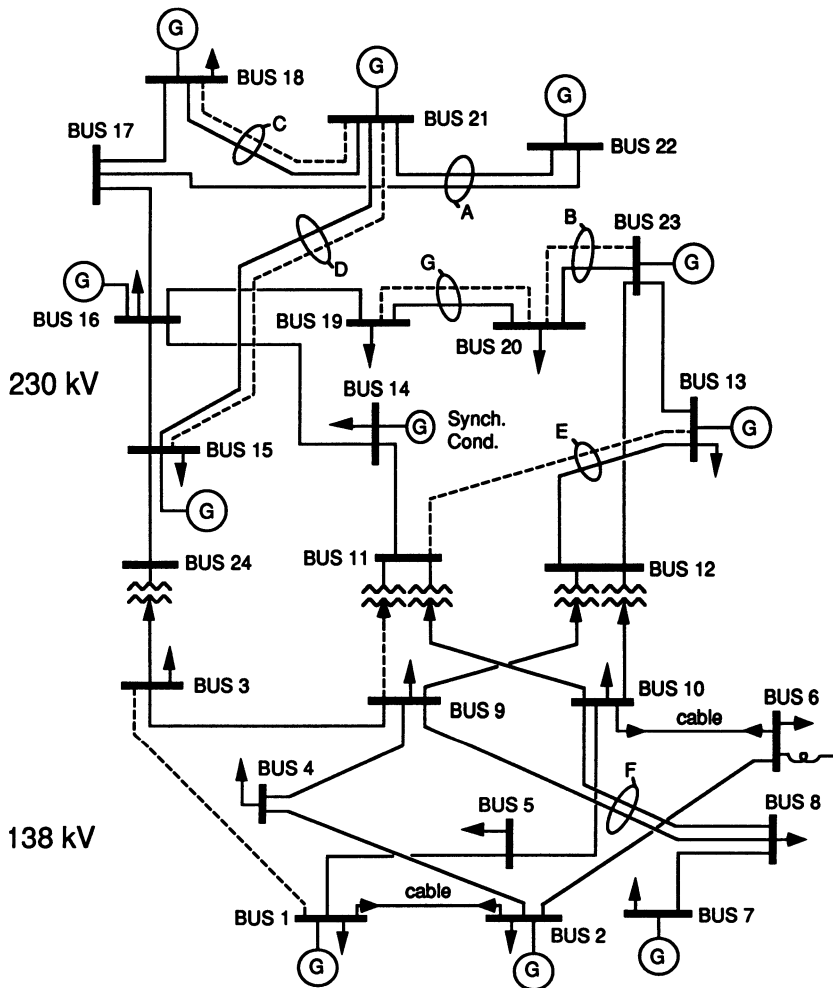


Figure 7.4. IEEE MRTS network configuration.

in Table 7.14. The EENS and EIC indices increase with load levels while the system IEAR remains virtually constant.

**(c) Effect of Composite Customer Damage Functions.** Replacing the sector customer damage functions by composite customer damage functions may lead to different conclusions. The bus CCDFs for the IEEE MRTS were calculated using the customer sector allocations shown in Table 7.12 and the SDCFs given in Table 7.1. These CCDFs are presented in Table 7.15.

**Table 7.12. Customer Sector Allocations at Load Buses**

Bus No.	Peak load (MW)	Load percentage of customer sector (in %)						
		Agri.	Large user	Resid.	Gover.	Indus.	Commer.	Office
1	135.00	0.0	0.0	34.03	15.83	36.94	13.20	0.0
2	121.25	0.0	0.0	50.05	35.26	0.0	14.69	0.0
3	225.00	6.33	0.0	52.50	0.0	33.25	7.92	0.0
4	92.50	0.0	0.0	34.52	46.22	0.0	19.26	0.0
5	88.75	0.0	0.0	51.38	0.0	28.10	20.07	0.0
6	170.00	8.38	0.0	49.70	0.0	29.34	10.48	2.10
7	156.25	18.24	0.0	38.44	0.0	31.92	11.40	0.0
8	213.75	0.0	0.0	55.00	15.00	11.67	16.66	1.67
9	218.75	19.54	48.86	23.46	0.0	0.0	40.87	3.27
10	243.75	8.77	21.92	41.54	0.0	20.46	7.31	0.0
13	331.25	6.45	16.13	30.09	9.69	22.59	10.75	4.30
14	242.50	0.0	44.07	32.42	0.0	20.57	2.94	0.0
15	396.25	0.0	67.43	17.29	0.0	0.0	10.78	4.50
16	125.00	0.0	42.75	25.90	17.10	0.0	14.25	0.0
18	416.25	0.0	56.49	18.69	0.0	11.98	6.85	5.99
19	226.25	0.0	61.41	30.72	0.0	0.0	7.87	0.0
20	160.00	0.0	33.40	42.11	13.36	0.0	11.13	0.0

**Table 7.13. Bus and System EENS, EIC, and IEAR for the IEEE MRTS for the Base Case**

Bus No. or system	EENS (MWh/yr)	EIC (k\$/yr)	IEAR (\$/kWh)
1	0.00	0.00	
2	0.00	0.00	
3	259.96	160.98	0.619
4	0.00	0.00	
5	0.00	0.00	
6	41.97	21.62	0.515
7	32.42	16.69	0.515
8	0.00	0.00	
9	61.16	32.32	0.528
10	78.87	41.47	0.525
13	32.06	16.51	0.515
14	1.13	1.15	1.018
15	2.66	2.72	1.023
16	66.10	69.57	1.052
18	76.24	78.78	1.033
19	664.96	691.84	1.040
20	574.43	597.92	1.041
System	1891.96	1731.57	0.915

**Table 7.14. System EENS, EIC, and IEAR in the IEEE MRTS at Different Load Levels**

Load increment (%)	Peak load (MW)	EENS (MWh/yr)	EIC (k\$/yr)	IEAR (\$/kWh)
0.0	3562.5	1891.96	1731.57	0.915
4.0	3705.0	4331.45	3968.66	0.916
6.0	3776.3	6254.57	5733.87	0.917
8.0	3747.5	8855.44	8103.47	0.915
10.0	3918.8	12436.87	11319.84	0.910

**Table 7.15. Bus Composite Customer Damage Functions for the IEEE MRTS (\$/kW)**

Bus No.	1 min	20 min	1 hr	4 hr	8 hr
1	0.6579	1.9108	4.8851	16.1394	41.0340
2	0.0720	0.6128	2.0236	9.3723	29.2284
3	0.5748	1.5918	3.9922	13.5575	33.6284
4	0.0941	0.7745	2.5031	10.7591	33.4392
5	0.5336	1.7310	4.5191	15.9031	40.4739
6	0.6226	1.7284	4.2981	14.7255	35.7186
7	0.5735	1.6714	4.1785	13.8676	34.0596
8	0.3401	1.2175	3.3257	12.9898	34.8674
9	0.6778	1.2933	2.4323	7.2708	16.4510
10	0.5863	1.4077	3.2288	10.5297	26.1714
13	0.7840	1.9468	4.5678	14.8979	35.4935
14	0.7887	1.5777	3.2570	9.4386	22.6382
15	0.9339	1.7975	3.4535	9.9986	22.5795
16	0.4917	1.1549	2.5498	8.5531	23.8678
18	1.0749	2.1277	4.2839	12.4426	27.0968
19	0.6475	1.1893	2.1875	6.4110	16.4129
20	0.3844	0.9226	2.0973	7.7563	22.0770

The results obtained using the bus CCDFs with other conditions being the same as those in the base case are given in Table 7.16. The buses at which load curtailments and interruption costs are zero are not listed. It can be seen that load curtailments occur only at Buses 3, 9, 10, 14, 15, 16, 19, and 20 and mainly at Buses 9 and 19. This can be explained as follows. Most system state durations are longer than one hour. It can be seen from Table 7.15 that these buses, particularly Buses 9 and 19, have relatively low unit interruption costs beyond 1-hr outage duration. In addition, Buses 9 and 19 are relatively far away from generation sources. When SCDFs are used, customer sectors with lowest unit interruption costs will be curtailed first in the minimum interruption cost model. When bus CCDFs are used, load curtailments will be performed in terms of the relative magnitudes of

**Table 7.16. Bus and System EENS, EIC, and IEAR for the IEEE MRTS Using Bus CCDF**

Bus No. or system	EENS (MWh/yr)	EIC (k\$/yr)	IEAR (\$/kWh)
3	55.23	244.38	4.425
9	169.31	355.30	2.099
10	0.35	1.07	3.057
14	4.99	13.39	2.683
15	4.34	12.37	2.850
16	0.69	1.85	2.681
19	1519.32	3296.56	2.170
20	96.01	281.20	2.905
System	1850.24	4206.12	2.273

bus CCDFs. Comparing the system indices obtained using the two approaches, it can be seen that the system EENS is basically the same in the two cases while the systems EIC and IEAR are quite different. The utilization of SCDFs or bus CCDFs reflects two completely different bus load curtailment philosophies. Utilization of CCDFs may create the much higher expected system interruption costs and IEAR values compared to using SCDFs.

#### **7.4.4. Application of Reliability Worth Assessment in Composite System Planning**

Composite system expansion planning is basically concerned with the addition of new generation and transmission facilities at a specified time in the future and at appropriate location(s). The objective is to select the most economical and reliable expansion plan(s) in order to meet the expected future load growth at minimum cost and optimum reliability subject to economic and technical constraints. Comparison analysis between the annual Expected Interruption Cost and the annual investment of different alternatives is often utilized in composite system planning. This section examines the impacts of additional generating and transmission facilities using the IEEE MRTS.

The basic data for the IEEE MRTS is given in Section 7.4.2. A 15-step load model for the annual load duration curve was used to evaluate the annual expected interruption costs of three alternatives. The first alternative (A1) is the addition of a circuit between Buses 16 and 17 (18 miles). The second alternative (A2) is the addition of a circuit between Buses 20 and 23 (15 miles). The third alternative (A3) is the addition of a generating unit at

**Table 7.17. EIC Indices of the Base System and Three Alternatives for the IEEE MRTS (k\$/yr)**

Load increment (%)	Base system	Alternative		
		A1	A2	A3
0.0	1731.57	1726.31	569.26	603.24
2.0	2636.98	2637.51	907.64	940.18
4.0	3968.66	3967.54	1427.01	1441.66
6.0	5733.87	5727.55	2178.04	2136.45
8.0	8103.47	8082.22	3251.35	3090.21
10.0	11319.84	11287.14	4813.06	4461.00

Bus 16 (155 MW). The annual expected interruption costs (EIC) of the base system and three alternatives for load increments from 0.0% to 10.0% are shown in Table 7.17. Figure 7.5 is a graphical representation of the results. It can be seen that Alternative 1 has basically the same EIC indices as the base case. This means that the addition of the circuit between Buses 16 and 17 does not improve the reliability of the system. This is an example of the noncoherence concept (the loosened definition) described in Section 5.10. A2 is the addition of a shorter circuit between Buses 20 and 23 which leads to much lower EIC than A1. This indicates that the different line addition

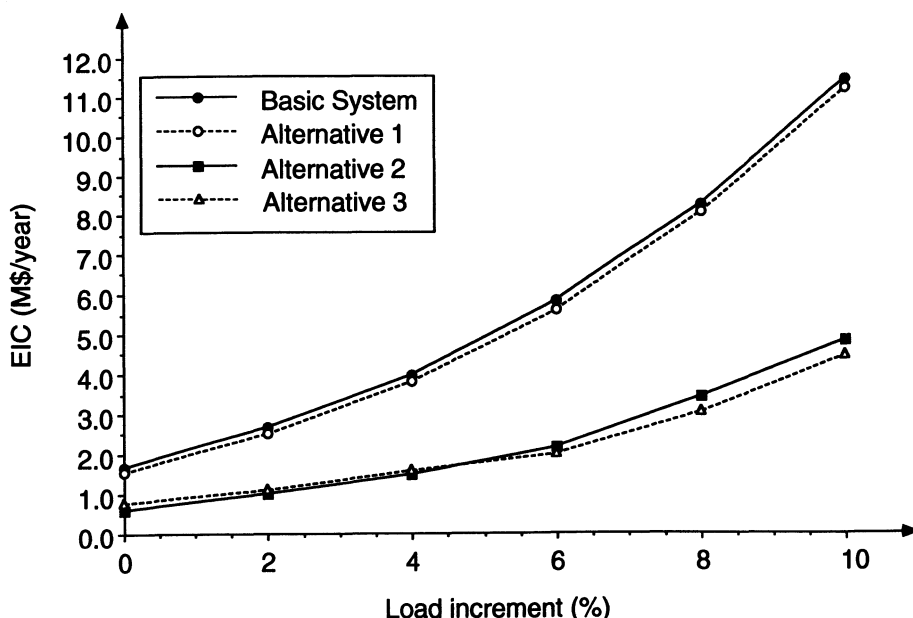


**Figure 7.5.** Variations in EIC index for the IEEE MRTS with load increments.

locations have completely different impacts on composite system reliability. It is interesting to note that A2 and A3 have basically the same EIC indices for load increases of 0.0% to 10.0%. A 155-MW generating unit requires much higher investment cost than one 15-mile 230-kV circuit. The addition of the 155-MW unit at Bus 16 should therefore be avoided or at least deferred.

Further analyses can be conducted to evaluate the total cost, which is the sum of the annual expected interruption cost and the annual investment for the alternatives. The economic life of the power system facilities was assumed to be 30 yr and the discount rate 10%. The unit capital cost of a 230-kV line is 90 k\$/mile and the capital cost of a 155-MW generating unit 100 M\$. The annual investment for the 230-kV circuit of 15 miles (A2) and the 155-MW generating unit (A3) can be calculated using the present value method (see Section 7.6.2) and the given economic data. The calculated annual investment costs of A2 and A3 are 143.21 k\$/yr and 10,607.9 k\$/yr, respectively. At the present load level (0.0% increment), Alternative 2 can reduce the expected interruption cost by 1162.29 k\$/yr (1731.55–569.26). This reduction is much larger than its annual investment of 143.21 k\$/yr and therefore Alternative 2 is a beneficial option even for the present load level. On the other hand, the reduction of the EIC due to Alternative 3 at 10.0% load increment level is 6858.84 k\$/yr (11,319.84–4461.00). This reduction is still smaller than the annual investment of A3 (10,607.9 k\$/yr). This indicates that the addition of the 155-MW unit is not a cost-effective option even when the load has 10.0% growth.

The above analysis is based on composite system reliability worth assessment. The method considers both investment and reliability worth on a unified basis. The system operating cost is not included in the analysis. This is discussed in Section 7.6.3 where it is shown that, although Alternative 1 does not improve system reliability, it improves the operating economy in the system and is a good option from an overall minimum cost viewpoint. It is therefore necessary to incorporate the system operating costs in the model to provide a more complete analysis. This is discussed in more detail in Section 7.6.

## 7.5. DISTRIBUTION SYSTEM RELIABILITY WORTH ASSESSMENT

### 7.5.1. Assessment Techniques

As previously noted, both analytical and Monte Carlo techniques can be used to provide average load point reliability indices. In order to include

the effects of load point outage duration distributions on interruption costs, however, it is usually necessary to apply a simulation approach. The system operating cycle technique given in Section 6.3.2 can be used quite effectively.

Three basic models are required for distribution system reliability worth assessment. These are the cost model, the load model, and the system model. The cost model is associated with the customer type at the load point and described by an appropriate customer damage function (CDF). The load model can be in the form of either average loads or actual time-dependent loads in a chronological load curve. The system model consists of the system configuration, relevant reliability parameters of all components such as the main feeders and lateral branches serving the individual customers, and the operating logic. The system model also involves additional factors such as inclusion or not of disconnects on the main feeders, fuses in lateral branches, alternate backup supply, replacing a failed low voltage transformer with a spare instead of repairing it, main and/or lateral branches consisting of underground cables or overhead lines, etc. The individual failure events are determined by simulation and the outage events evaluated in terms of the failure rate, average outage duration, annual outage time, and load curtailments at each load point. The basic system analysis method and evaluation technique are discussed in Chapter 6. The following formulas can be used in conjunction with the state duration sampling technique to evaluate the load point EENS, EIC, and IEAR:

$$\text{EENS}_k = \frac{\sum_{i=1}^{N_k} P_{ik} D_i}{M} \quad (7.22)$$

$$\text{EIC}_k = \frac{\sum_{i=1}^{N_k} W_k(D_i) P_{ik}}{M} \quad (7.23)$$

$$\text{IEAR}_k = \frac{\sum_{i=1}^{N_k} W_k(D_i) P_{ik}}{\sum_{i=1}^{N_k} P_{ik} D_i} \quad (7.24)$$

where  $W_k(D_i)$  is the customer damage function at load point  $k$ ,  $D_i$  the sampling value of duration for interruption  $i$ ,  $P_{ik}$  the demand at load point  $k$  (it can be either the average load or the actual load during interruption  $i$ ),  $M$  the number of simulated years, and  $N_k$  is the number of interruptions contributing to load point  $k$  in the span of the simulated years.

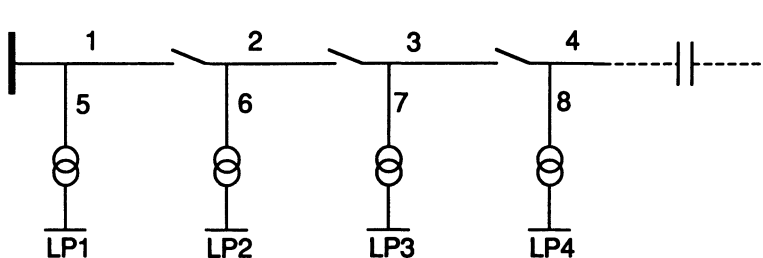


Figure 7.6. Example system feeder configuration.

### 7.5.2. Numerical Example

**(a) Example System.** Consider the distribution system shown in Figure 7.6.<sup>(20)</sup> The reliability data, i.e., failure rates and mean time to repair for all components are given in Table 7.18. All switching actions require 1 hr. It has been assumed that the alternate supply is always available and that the fuses in the laterals are fully reliable. The customer data at each of the four load points are given in Table 7.19. The sector customer damage

**Table 7.18. Example Distribution System Component Reliability Data**

Component	Failure rate (failures/yr)	Mean time to repair (hr/failure)
1	0.0520	5.00
2	0.0488	5.00
3	0.0488	5.00
4	0.0390	5.00
5	0.0638	8.53
6	0.0540	9.17
7	0.0670	8.36
8	0.0638	8.53
Transformer	0.0150	20.00

**Table 7.19. Example Distribution System Customer Data**

Load point	Average load (kW)	Peak load (kW)	Customer type
1	454.0	750.0	Commercial
2	450.0	729.1	Residential
3	566.0	916.7	Governmental
4	566.0	916.7	Governmental

functions for the commercial, residential, and governmental customer categories in the example system are the same as those given in Table 7.1. The cost in \$/kW of durations greater than 8 hr is evaluated using the assumption that the slope is the same as that between the 4 and 8 hr duration. Average loads at the load points are used in the study.

**(b) Case Studies.** The sequential Monte Carlo simulation approach was used with 10,000 replication years. In order to examine the effects of various distributions, the component state durations were assumed to be described by either a normal, log-normal (LN), gamma, or exponential (EXP) distribution. The annual average outage times and the annual expected interruption costs of all load points for the different distribution assumptions are shown in Table 7.20.

It can be seen that the different distribution assumptions provide basically the same annual average outage time indices. This is confirmed by the analysis and results given in Chapter 6. Unlike the three basic load point reliability indices, however, the interruption costs generally depend on the outage duration distributions. Different distribution assumptions, in principle, lead to different interruption cost indices. In the given example, however, Cases (c), (d), (e), and (f) provide basically the same interruption costs, which are different from those obtained assuming the repair activities to be exponentially distributed in Cases (a) and (b).

The load point interruption costs for the example distribution system using an analytical approach are shown in Table 7.21. It can be seen that the analytical load point interruption costs are quite close to those obtained in Cases (c), (d), (e), and (f) of the simulation studies. This suggests that although the average outage duration is used in the analytical method, in some cases, such as when the component restoration mode distributions are assumed to be other than exponential with a small standard deviation, the analytical method provides results which are comparable to those from simulation studies.

## 7.6. MINIMUM COST ASSESSMENT IN COMPOSITE SYSTEM EXPANSION PLANNING

### 7.6.1. Basic Concepts

The fundamental objective of an electric power utility is to plan and operate the system to satisfy the load and energy requirements of its customers

**Table 7.20. Load Point Annual Average Outage Times and Expected Interruption Costs**

Case	Description	Load point	Annual Outage time (hr/yr)	Expected interruption costs (k\$/yr)
(a)	EXP rep.; all other times are EXP	1 2 3 4	0.951 0.827 0.956 0.912	5.130 0.895 2.783 2.752
			Total	11.560
(b)	EXP rep.; all other times are LN ( $sd = m/6$ )	1 2 3 4	0.920 0.863 0.940 0.901	4.918 0.976 2.676 2.680
			Total	11.250
(c)	all times are LN ( $sd = m/6$ )	1 2 3 4	0.961 0.848 0.976 0.913	4.299 0.646 1.571 1.497
			Total	8.013
(d)	Normal rep. ( $sd = m/6$ ); other times LN ( $sd = m/6$ )	1 2 3 4	0.962 0.848 0.976 0.913	4.303 0.646 1.573 1.499
			Total	8.021
(e)	Gamma rep. ( $sd = m/6$ ); all other times EXP	1 2 3 4	0.959 0.832 0.983 0.906	4.290 0.643 1.601 1.500
			Total	8.034
(f)	LN rep. ( $sd = m/10$ ); other times EXP	1 2 3 4	0.962 0.844 0.976 0.911	4.277 0.656 1.561 1.480
			Total	7.974

**Table 7.21. Load Point Interruption Costs Using the Analytical Method**

Load point	Expected interruption costs (k\$/yr)
1	4.171
2	0.666
3	1.477
4	1.419

at as low a cost as possible and with an acceptable level of continuity and quality of supply. This involves the two aspects of economy and reliability. System reliability worth can be indirectly incorporated by interruption cost evaluation and, consequently, the system adequacy problem is converted into a cost problem. This makes it possible to assess system economy and reliability on a unified basis. System operating costs are important aspects of overall system economy. Simulation of the system operating cost therefore should be incorporated in composite system expansion planning so that an optimum decision can be made in terms of overall minimum cost.

A potential optimal generation loading schedule (POGLS) can be easily obtained when transmission network constraints and component forced outages are not considered. In practical composite system operation, however, the power allocation between generators will deviate from the POGLS due to transmission network constraints and system component forced outages. This leads to an increase in the total operating cost. The addition of generation or/and transmission facilities can move a practical operating schedule closer to the POGLS and therefore improve not only reliability but also the operating economy of a composite system.

An optimal expansion decision achieves the minimum total cost  $Q$ :

$$\min Q = I + O + D \quad (7.25)$$

where  $I$  is the investment cost,  $O$  the operating cost, and  $D$  the customer damage (interruption) cost associated with system unreliability.

The investment cost is a fixed value for a particular addition decision and can be easily calculated using the present value method. Both operating and customer damage costs depend on system states and therefore it is necessary to simulate a considerable number of system contingency states involving various load levels in order to obtain the annual expected values of these costs. The minimization linear program model described in Section 7.4.1 can be extended to include system generating cost simulation.

## 7.6.2. Minimum Cost Assessment Method

**(a) Annual Investment Cost.** The total cost of an expansion decision is the sum of investment, operating, and damage costs. This total cost can be expressed on the basis of one year. The annual investment cost ( $I$ ) can be calculated using the present value method:

$$I = A \frac{i(1+i)^n}{(1+i)^n - 1} \quad (7.26)$$

where  $A$  is the capital cost of the additional system facility in a particular expansion decision at the starting year,  $i$  is the discount rate which generally equals the interest rate plus the inflation rate, and  $n$  is the economic life of the added system facility.

### (b) Minimization Model for Operating and Damage Costs.

It is necessary to simulate a considerable number of system states involving various load levels in order to obtain the annual expected operating and damage costs. The system states can be selected using the Monte Carlo sampling technique. The following linear programming minimization model can be used to calculate the power allocation between generators, possible load curtailments at different buses, operating costs at each generator and of the system and damage (interruption) costs at each load bus and of the system, for a particular drawn system state:

$$\min \text{TOD} = \sum_{i=1}^{\text{NG}} \sum_{j=1}^{\text{IG}_i} D_k b_{ij} \text{PG}_{ij} + \sum_{i=1}^{\text{NC}} \sum_{j=1}^{\text{IC}_i} W_{ij}(D_k) C_{ij} \quad (7.27)$$

subject to

$$T_n = \sum_{i=1}^{\text{NS}} A_{ni} \left( \sum_{j=1}^{\text{IG}_i} \text{PG}_{ij} + \sum_{j=1}^{\text{IC}_i} C_{ij} - \sum_{j=1}^{\text{IC}_i} \text{PD}_{ij} \right) \quad (i=1, \dots, L) \quad (7.28)$$

$$\sum_{i=1}^{\text{NG}} \sum_{j=1}^{\text{IG}_i} \text{PG}_{ij} + \sum_{i=1}^{\text{NC}} \sum_{j=1}^{\text{IC}_i} C_{ij} = \sum_{i=1}^{\text{NC}} \sum_{j=1}^{\text{IC}_i} \text{PD}_{ij} \quad (7.29)$$

$$\text{PG}_{ij}^{\min} \leq \text{PG}_{ij} \leq \text{PG}_{ij}^{\max} \quad (i=1, \dots, \text{NG}; j=1, \dots, \text{IG}_i) \quad (7.30)$$

$$0 \leq C_{ij} \leq \text{PD}_{ij} \quad (i=1, \dots, \text{NC}; j=1, \dots, \text{IC}_i) \quad (7.31)$$

$$|T_n| \leq T_n^{\max} \quad (n=1, \dots, L) \quad (7.32)$$

where  $\text{PG}_{ij}$  is the generation variable of the  $j$ th generator at Bus  $i$ ;  $\text{PG}_{ij}^{\min}$ ,  $\text{PG}_{ij}^{\max}$  are the lower and upper bounds of  $\text{PG}_{ij}$ ;  $\text{IG}_i$  is the number of generators at Bus  $i$ ;  $b_{ij}$  is the unit generating cost (in \$/kWh) of the  $j$ th generator at Bus  $i$ , all other notations are the same as those used in the minimization model given in Section 7.4.1.

This model is an extension of that in Section 7.4.1, in which simulation of the system operating cost has been included. The objective of the model is to minimize the sum of the operating and damage costs while satisfying the power balance, the linearized load flow relationships, the line power flow limits and output limits of each generating unit. The customer damage functions for different customer sectors and effects of system state durations on the interrupted damage cost are incorporated in the model. In order to

reduce the scale of the LP problem, generators which are connected to the same bus and have the same unit generating cost ( $b_{ij}$ ) can be represented by an equivalent generation variable in the model.

The values of  $C_{ij}$  and  $\text{PG}_{ij}$  obtained by solving this model correspond to a particular system state  $k$  whose duration is  $D_k$ . As in the previous model, the subscript  $k$  in the variables except  $D_k$  in the model has been omitted for simplicity. The system state duration  $D_k$  can be calculated using the sampling method given in Section 7.4.1. The model provides the annual Expected Energy Produced by Generators (EEPG) and Expected Generation Cost (EGC) of the generation buses and the system in addition to EENS and EIC indices of the load buses and the system. The equations for calculating bus and system EENS and EIC indices are the same as those given in Section 7.4.1, i.e., equations (7.15)–(7.18). The annual bus and system EEPG and EGC indices are given by the following equations:

$$\text{EEPG}_i = \sum_{k=1}^N \sum_{j=1}^{\text{IG}_i} \text{PG}_{ijk} F_k D_k \quad (7.33)$$

$$\text{EGC}_i = \sum_{k=1}^N \sum_{j=1}^{\text{IG}_i} \text{PG}_{ijk} F_k D_k b_{ij} \quad (7.34)$$

$$\text{EEPG} = \sum_{i=1}^{\text{NG}} \text{EEPG}_i \quad (7.35)$$

$$\text{EGC} = \sum_{i=1}^{\text{NG}} \text{EGC}_i \quad (7.36)$$

where  $\text{PG}_{ijk}$ ,  $D_k$ ,  $F_k$ ,  $b_{ij}$ , and  $\text{IG}_i$  are as defined earlier;  $\text{EEPG}_i$  and  $\text{EEPG}$  are the expected energy produced by generators at Bus  $i$  and for the system, respectively (MWh/yr);  $\text{EGC}_i$  and  $\text{EGC}$  are the expected generation cost at Bus  $i$  and for the system (k\$/yr);  $N$  is the number of system states. The system state frequency  $F_k$  (occ./yr) is obtained using equation (7.19).

**(c) Basic Minimum Cost Assessment Procedure.** A computer program named MICOAS for minimum cost assessment in composite system expansion planning has been developed at the University of Saskatchewan based on the above minimization model and Monte Carlo simulation techniques. A brief description of the MICOAS program follows. The flowchart is shown in Figure 7.7.<sup>(21)</sup>

1. A multistep annual load model is created which eliminates the chronology and aggregates the load states using hourly load records. The number of load level steps depends on the sensitivities of the composite system adequacy indices to load variation (see Section 5.3.2). All load level steps

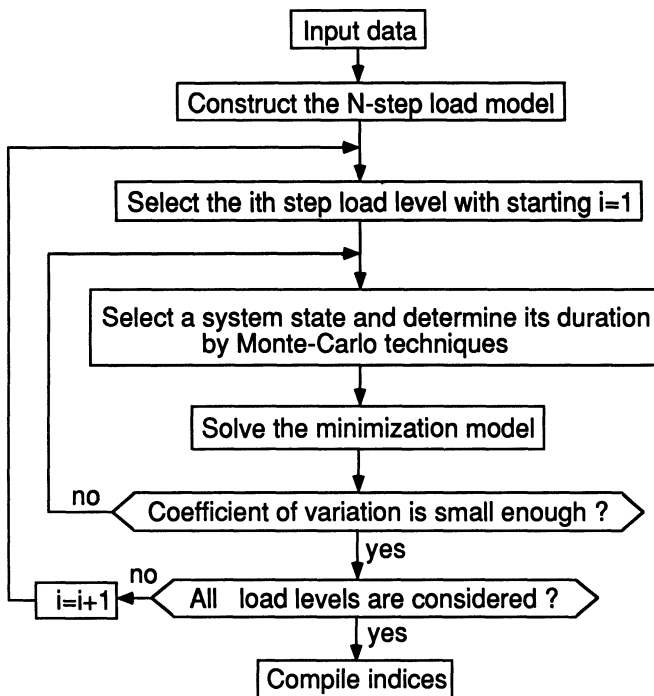


**Figure 7.7.** Flowchart of the minimum cost assessment method.

are considered successively and the results for each load level are weighted by their probabilities to obtain the annual indices.

2. The system states at a particular load level are selected using the simulation techniques discussed in Chapter 5. Generating unit and transmission line states are modeled using two-state random variables. If necessary, other system considerations, such as generating unit derated states,<sup>(22)</sup> effects of regional weather on transmission line outages,<sup>(23)</sup> and bus load uncertainty and correlation,<sup>(24)</sup> etc., can also be incorporated using the methods presented in Chapter 5.

3. System state durations are modeled using the sampling method given in Section 7.4.1. System state frequencies are calculated using equation (7.19).

4. The operating and damage cost minimization model presented earlier is solved to obtain the generation allocations, generation costs, load curtailments, and interruption costs.

5. Steps (2)–(4) are repeated until convergence for each particular load level. Annual bus and system EENS, EIC, EEPG, and EGC indices are

calculated using equations (7.15) to (7.18) and (7.33) to (7.36) by considering all load level steps.

6. The annual investment cost is calculated using equation (7.26). The total cost shown in equation (7.25) is obtained.

In addition to the load bus indices, the generator bus indices, and the system indices noted above, the MICOAS program also provides two transmission line indices. These are: (i) probability of the line power at its limit in no-load-curtailment system states; and (ii) proportion of load curtailments associated with the line power at its limit in total load curtailments. The line indices together with load bus and generator bus indices provide initial information regarding what system facilities to add and where to locate them. System indices provide quantitative evaluation of overall system economy and reliability and can be used to select the optimal expansion plan.

### 7.6.3. Case Studies

In order to demonstrate the application of the minimum cost assessment method in composite system expansion planning, case studies were conducted using the IEEE MRTS given in Section 7.4.2. The basic system data, system single line diagram, and the customer data (the customer sector allocation at load buses) are given in Section 7.4.2. The sector customer damage functions are given in Table 7.1. The additional data required to perform minimum cost assessment are generating unit operating costs given in Table 7.8<sup>(16)</sup> and investment cost related data given in Table 7.22.

**(a) Selecting the Optimal Expansion Plan at the Present Load Level.** The IEEE MRTS was considered to be the original system at the present load level. The line, load bus, and generator bus indices calculated using the MICOAS program indicate that the lines from Bus 16 to Bus 17 and from Bus 15 to Bus 21 have the largest and the next-largest probabilities of the line powers being at their limits in no-load-curtailment states, respectively [line index (i)]. The line from Bus 20 to Bus 23 has the largest proportion of load curtailments associated with the line power at its

**Table 7.22. Investment Cost Related Data**

Life of facilities	30 yr
Discount rate	10%
Capital cost of 230-kV line	90 k\$/mile
Capital cost of 155-MW generating unit	100 M\$/unit

limit in total load curtailments [line index (ii)]. The expected generation costs at generator buses 18 and 21 deviate most significantly from their bus generation costs in the ponential optimal generation loading schedule (POGLS). The largest and the next-largest expected energy not supplied (EENS<sub>i</sub>) are at Bus 19 and Bus 20, respectively. The following possible expansion plans are therefore initially selected:

- L1-1 adding a circuit from Bus 15 to Bus 21
- L1-2 adding a circuit from Bus 16 to Bus 17
- L1-3 adding a circuit from Bus 17 to Bus 18
- L1-4 adding a circuit from Bus 20 to Bus 23
- G1 adding a 155-MW generating unit at Bus 16.

The cost and adequacy of each of these five alternate plans were evaluated using the minimum cost assessment method. The basic system indices are shown in Table 7.23. The annual operating costs are much higher than

**Table 7.23. Basic System Indices of the Original System and the Alternate Plans at the Present Load Level**

Alternate plans	System index							
	AGCP	AEGC	EGC	EENS	EIC	EOIC	AEIC	AIOIC
Base system	185.53	189.56	229.55	1902.54	1.73	231.28	0.00	231.28
L1-1								
Index	185.53	185.62	226.37	1901.52	1.73	228.10	0.33	228.42
Diff.	0.00	3.94	3.18	1.02	0.00	3.18	-0.33	2.86
L1-2								
Index	185.53	185.63	226.38	1901.54	1.73	228.11	0.17	228.28
Diff.	0.00	3.93	3.17	1.00	0.00	3.17	-0.17	3.00
L1-3								
Index	185.53	190.56	230.48	1903.57	1.73	232.21	0.10	232.31
Diff.	0.00	-1.00	-0.93	-1.03	0.00	-0.93	-0.10	-1.03
L1-4								
Index	185.53	189.53	229.12	694.39	0.56	229.68	0.14	229.82
Diff.	0.00	0.03	0.43	1208.15	1.17	1.60	-0.14	1.46
G1								
Index	183.97	188.06	224.81	685.63	0.60	225.41	10.61	236.02
Diff.	1.56	1.50	4.74	1216.91	1.13	5.87	-10.61	-4.74
L2								
Index	185.53	185.63	225.96	693.04	0.56	226.52	0.32	226.84
Diff.	0.00	3.93	3.59	1209.50	1.17	4.76	-0.32	4.44
L2G1								
Index	183.97	184.45	221.87	386.56	0.31	222.18	10.92	233.10
Diff.	1.56	5.11	7.68	1515.98	1.42	9.10	-10.92	-1.82

the annual interruption costs or the annual investment costs due to the system facility additions and therefore it is necessary to show the differences between the indices for the original system and those of the alternate plans. These differences are designated by "Diff." in Table 7.23. The interpretation of the basic system indices is as follows:

AGCP	Annual Generating Cost in the Potential optimal generation loading schedule (M\$/yr). This is the system generating cost when transmission network constraints and component outages are not considered and generators are loaded according to their increasing \$/MWh (fixed operation costs are not included).
AEGC	Annual Economic Generating Cost in the normal system state (M\$/yr). This is the system economic generating cost when transmission network constraints are incorporated but generator and line outages are not considered. This cost corresponds to economic dispatch of the composite system in the normal state (the fixed operation costs are not included).
EGC	Expected Generating Cost in normal and outage states (M\$/yr). This is the annual expected system economic operating costs when transmission network constraints and system component outages are considered. This cost corresponds to the first term of the minimization model for operating and damage costs (the fixed operation costs are included).
EENS	Expected Energy Not Supplied for the composite system (MWh/yr).
EIC	Expected Interruption Cost (M\$/yr). This is the annual expected minimum damage costs when transmission network constraints and system component outages are considered. This cost corresponds to the second term of the minimization model for operating and damage costs.
EOIC	Expected Operating and Interruption Cost (M\$/yr). It equals the sum of EGC and EIC.
AEIC	Annual Expansion Investment Cost (M\$/yr).
AIOIC	Annual Investment, Operating and Interruption Cost (M\$/yr). It equals the sum of EOIC and AEIC.

It can be seen from Table 7.23 that although the L1-1 and L1-2 alternate plans do not improve the system reliability when compared to the original system (the EENS indices and the expected annual interruption costs remain unchanged), these two plans greatly improve system operating economy

(the annual expected generating cost decreases by 3.18 M\$ and 3.17 M\$, respectively). This indicates that the addition of a system facility depends on not only the improvement in system reliability but also on the improvement in system operating economy and, in some cases, system operating economy can be the dominant factor. It is interesting to note that the different additions in the L1-1 and L1-2 plans have the same effects on system reliability (no improvement) and basically make the same improvements in system operating economy. The addition of a circuit from Bus 15 to Bus 21 requires line reinforcement of 34 miles and an annual investment cost of 0.33 M\$. The total annual investment, operating, and interruption cost of the L1-1 plan decreases by 2.86 M\$ compared to the original system. The addition of a circuit from Bus 16 to Bus 17 requires only line reinforcement of 18 miles and the annual investment cost of 0.17 M\$. The total annual investment, operating, and interruption cost of the plan L1-2 decrease by 3.00 M\$. Plan L1-2 therefore is superior to Plan L1-1. The L1-3 plan does not improve system reliability (the EENS index and the expected annual interruption cost remain unchanged) nor system operating economy (the annual expected generating cost increases by 0.93 M\$). This means that the addition of the 10-mile line from Bus 17 to Bus 18 does nothing other than increase the investment cost. The L1-4 plan improves system reliability quite considerably (the EENS index decreases from 1902 MWh/yr to 694 MWh/yr and the expected annual interruption cost decreases by 1.17 M\$) but has only a small impact on system operating economy (the expected annual generating cost decreases only by 0.43 M\$). By adding the annual investment cost of the circuit from Bus 20 to Bus 23 (0.14 M\$), the total annual investment, operating, and interruption cost of the L1-4 plan decreases by 1.46 M\$. The G1 plan improves both system reliability (the EENS index decreases to 685 MWh/yr and the expected annual interruption cost decreases by 1.13 M\$) and system operating economy (the expected annual generating cost decreases by 4.74 M\$). The annual investment cost, however, increases by 10.61 M\$ due to the addition of a 155-MW generating unit at Bus 16. The total annual investment, operating, and interruption cost of the G1 plan increases 4.74 M\$ compared to the original system. In this case, the annual investment cost is the dominant factor.

The results for the initial five alternate plans suggest that the following two expansion options should be examined further:

- L2 adding a circuit from Bus 16 to Bus 17 and a circuit from Bus 20 to Bus 23
- L2G1 adding a 155-MW generating unit at Bus 16 to the L2 plan

The basic system indices for these two new alternatives are also shown in Table 7.23. The L2 plan considerably improves system reliability and

operating economy (the EENS index decreases to 693 MWh/yr and the expected annual operating and interruption cost decreases by 4.76 M\$) for only a small increase in the annual investment cost (0.32 M\$). The total annual investment, operating, and interruption cost decreases by 4.44 M\$. Although the L2G1 plan leads to a greater decrease in the expected annual operating and interruption cost (9.10 M\$) than the L2 plan, it requires much higher annual investment cost (10.92 M\$). The total annual investment, operating, and interruption cost of the L2G1 plan is higher than that of the original system.

Using the minimum cost assessment method and comparing the decreases in the total annual costs for the alternate plans, the L2 plan is the optimal expansion plan for the base system at the present load level.

**(b) Selecting an Optimal Expansion Plan to Meet Load Growth.** The objective of power system expansion analysis is the selection of the optimal (the most economical and reliable) expansion plan for the system not only at the present load level but also recognizing future load growth. The results in Section 7.4.4 indicate that when only reliability worth and investment cost are considered, the addition of a 155-MW generating unit at Bus 16 is not cost-effective even for 10.0% load growth. It can be seen from the previous expansion analysis that the addition of this unit can improve system operating economy considerably, but that the G1 and L2G1 plans in which the 155-MW generating unit is added are not economical at the present load level. It may be reasonable, however, to add such a generating unit as the demand grows if the total investment, operating, and interruption cost is considered. The L2, G1, and L2G1 plans were therefore re-examined using the minimum cost assessment method assuming load growth of 4%, 6%, 8%, and 10%, respectively. The basic system indices are shown in Tables 7.24 to 7.27. For comparison, the calculation results for the original system have been also listed. The values in the “Diff.” rows are the decreased values of the system indices for the three alternatives compared to those of the original system.

The results in Tables 7.24 to 7.27 indicate that in the 4% load growth case, the G1 plan involves higher total annual cost than for the original system. The addition of a 155-MW generating unit at Bus 16 is therefore uneconomical at this load level. When load growth is equal to or greater than 6%, however, the G1 plan becomes more economical than the original system. The L2G1 plan always has lower total annual cost at the various load growth levels than the original system and the G1 plan. This is due to the fact that additions of two circuits from Bus 16 to Bus 17 and from Bus 20 to Bus 23 decrease the operating and interruption costs considerably but only slightly increase the annual investment cost. At load levels smaller than

**Table 7.24. Basic System Indices of the Original System and the Alternate Plans for 4% Load Growth**

Alternate plans	System index							
	AGCP	AEGC	EGC	EENS	EIC	EOIC	AEIC	AIOIC
Base system	198.39	201.83	245.96	4358.47	3.97	249.93	0.00	249.93
L2								
Index	198.39	198.43	242.57	1749.28	1.43	244.00	0.32	244.32
Diff.	0.00	3.40	3.39	2609.19	2.54	5.93	-0.32	5.61
G1								
Index	195.37	198.91	238.99	1614.27	1.44	240.43	10.61	251.04
Diff.	3.02	2.92	6.97	2744.20	2.53	9.50	-10.61	-1.11
L2G1								
Index	195.37	195.84	236.32	860.74	0.71	237.03	10.92	247.95
Diff.	3.02	5.99	9.64	3497.73	3.26	12.90	-10.92	1.98

**Table 7.25. Basic System Indices of the Original System and the Alternate Plans for 6% Load Growth**

Alternate plans	System index							
	AGCP	AEGC	EGC	EENS	EIC	EOIC	AEIC	AIOIC
Base system	205.40	208.65	254.85	6285.00	5.73	260.58	0.00	260.58
L2								
Index	205.40	205.49	251.50	2680.03	2.18	253.68	0.32	254.00
Diff.	0.00	3.16	3.35	3604.97	3.55	6.90	-0.32	6.58
G1								
Index	201.46	204.74	246.62	2375.62	2.13	248.75	10.61	259.36
Diff.	3.94	3.91	8.23	3909.38	3.60	11.83	-10.61	1.22
L2G1								
Index	201.46	201.94	244.07	1259.18	1.04	245.11	10.92	256.03
Diff.	3.94	6.71	10.78	5025.82	4.69	15.47	-10.92	4.55

8% load growth, the L2 plan decreases the total annual cost more than the L2G1 plan. In the case of 8% load growth, the L2 and L2G1 plans result in basically the same decrease in the total annual cost. Considering that the L2G1 plan leads to much smaller expected energy not supplied (EENS) and much lower interruption cost (EIC) than the L2 plan, it is necessary for 8% load growth to add a 155-MW generating unit at Bus 16. When the load growth is larger than 8%, the L2G1 plan results in a larger decrease in the total annual investment, operating, and interruption cost than the L2 plan.

**Table 7.26. Basic System Indices of the Original System and the Alternate Plans for 8% Load Growth**

Alternate plans	System index							
	AGCP	AEGC	EGC	EENS	EIC	EOIC	AEIC	AIOIC
Base system	213.19	216.18	264.45	8891.05	8.10	272.55	0.00	272.55
L2								
Index	213.19	213.24	261.04	4014.22	3.25	264.29	0.32	264.61
Diff.	0.00	2.94	3.41	4876.83	4.85	8.26	-0.32	7.94
G1								
Index	207.85	210.83	254.75	3446.02	3.09	257.84	10.61	268.45
Diff.	5.34	4.35	9.70	5445.03	5.01	14.71	-10.61	4.10
L2G1								
Index	207.85	208.27	252.29	1819.48	1.50	253.79	10.92	264.71
Diff.	5.34	7.91	12.16	7071.57	6.60	18.76	-10.92	7.84

**Table 7.27. Basic System Indices of the Original System and the Alternate Plans for 10% Load Growth**

Alternate plans	System index							
	AGCP	AEGC	EGC	EENS	EIC	EOIC	AEIC	AIOIC
Base system	222.08	224.82	274.91	12480.87	11.32	286.23	0.00	286.23
L2								
Index	222.08	222.13	271.39	5963.51	4.81	276.20	0.32	276.52
Diff.	0.00	2.69	3.52	6517.36	6.51	10.03	-0.32	9.71
G1								
Index	214.58	217.37	263.34	4976.70	4.46	267.80	10.61	278.41
Diff.	7.50	7.45	11.57	7504.17	6.86	18.43	-10.61	7.82
L2G1								
Index	214.58	215.04	260.98	2644.54	2.17	263.15	10.92	274.07
Diff.	7.50	9.78	13.93	9836.33	9.15	23.08	-10.92	12.16

Based on these results, the final expansion decision should be that before load growth reaches 8%, two circuits from Bus 16 to Bus 17 and from Bus 20 to Bus 23 are required and, when load growth reaches 8%, a 155-MW generating unit should be added at Bus 16.

## 7.7. CONCLUSIONS

This chapter deals with reliability cost/worth assessment using Monte Carlo simulation. Direct evaluation of reliability worth is very difficult and perhaps impossible. The customer interruption costs due to unreliability can

be used as an indirect measure of reliability worth. The procedure illustrated to assess customer interruption costs at HL1, HL2, and in the distribution functional zone utilizes Customer Damage Functions (CDF). Interruption cost data obtained from customer surveys are specific to area, region, and country. In general, the data for a particular area, or region, or country cannot be automatically utilized for other areas, regions, and countries. As with other reliability data, such as component failure rates and repair times, interruption cost data also should be continuously monitored and updated.

Analytical techniques utilize average outage state durations and basically provide average or expected values for load points and system indices. In many reliability worth evaluations, the use of analytical techniques will provide acceptable results. In the case of customer damage functions exhibiting a high degree of nonlinearity, however, analytical methods may create relatively large errors. Monte Carlo methods which sample system outage state durations are theoretically accurate, and the effects on interruption costs of outage duration distributions are automatically evaluated.

The basic index for reliability worth assessment is the annual Expected Interruption Cost (EIC). This index is a combination of the unit interruption cost, the demand not supplied, the outage duration, and the outage frequency and therefore it contains more information than other reliability indices. The EIC is a monetary representation of reliability worth. This makes it possible to compare reliability worth with other economic indices such as investment and operating costs on a common base. In generation planning, for example, if the investment cost of a generating unit is smaller than the decrease in the system EIC, the addition of the unit is beneficial. This principle also generally applies to composite system and distribution system planning. In the case of composite systems, however, the addition of a generation or transmission facility may not only improve system reliability but also operating economy. Minimum cost assessment associated with the total investment, operating, and interruption costs is therefore a more realistic method for composite system expansion planning.

Generating system reliability worth assessment involves the calculation of the annual system EIC. The Interrupted Energy Assessment Rate (IEAR) is an important factor and concept in generating system reliability worth assessment. IEAR basically does not vary with the peak load level and therefore the system EIC can be obtained by multiplying the EENS by the IEAR. The IEAR can also be calculated at HL2 and in the distribution functional zone. In the case of composite systems, however, IEAR should be used with caution. This is due to the fact that IEAR at HL2 may not be the same for different load curtailment philosophies and for different configuration changes. Distribution system reliability assessment involves the calculation of the load point EIC indices. Composite system reliability

worth assessment involves both system and bus EIC indices. Complications in composite system evaluation lie not only in system analysis associated with load flow calculations, contingency studies, overload alleviation, generation rescheduling, and load curtailments, but they also result from incorporation of sector customer damage functions (SCDF) at the load buses. Utilization of bus composite customer damage functions (CCDF) can create different results from those obtained using the SCDF in composite system reliability worth assessment.

## 7.8. REFERENCES

1. G. Wacker, E. Wojczynski, and R. Billinton, "Cost/Benefit Considerations in Providing an Adequate Electric Energy Supply," Third International Symposium on Large Engineering Systems, July 10–11, 1980, St. John's, Newfoundland, pp. 3–8.
2. R. Billinton, G. Wacker, and E. Wojczynski, "Comprehensive Bibliography on Electrical Service Interruption Costs," *IEEE Trans. on PAS*, Vol. 102, 1983, pp. 1831–1837.
3. G. Tollefson, R. Billinton, and G. Wacker, "Comprehensive Bibliography on Reliability Worth and Electrical Service Consumer Interruption Costs: 1980–1990," *IEEE Trans. on Power Systems*, Vol. 6, No. 4, 1991, pp. 1508–1514.
4. L. V. Skof, "Ontario Hydro Surveys on Power System Reliability: Summary of Customer Viewpoints," Ontario Hydro Report, R&MR 80-12, EPRI Seminar, October 11–13, 1983.
5. R. Billinton, G. Wacker, and E. Wojczynski, "Customer Damage Resulting from Electric Service Interruptions," Canadian Electrical Association, R&D Project 907, U131 Report, 1982.
6. E. Wojczynski, R. Billinton, and G. Wacker, "Interruption Cost Methodology and Results—A Canadian Commercial and Small Industrial Survey," *IEEE Trans. on PAS*, Vol. 103, 1984, pp. 437–444.
7. G. Wacker, E. Wojczynski, and R. Billinton, "Interruption Cost Methodology and Results—A Canadian Residential Survey," *IEEE Trans. on PAS*, Vol. 102, 1983, pp. 3385–3392.
8. Ontario Hydro Survey on Power System Reliability: Viewpoint of Small Industrial Users (Under 5000 kW), OH Report No. R&U 78-3, April, 1978.
9. R. Billinton, G. Wacker, and R. K. Subramaniam, "Factors Affecting the Development of a Residential Customer Damage Function," *IEEE Trans. on PWRS*, Vol. 2, No. 1, 1987, pp. 204–209.
10. R. Billinton, G. Wacker, and R. K. Subramaniam, "Factors Affecting the Development of a Commercial Customer Damage Function," *IEEE Trans. on PWRS*, Vol. 1, No. 4, 1986, pp. 28–33.
11. R. K. Subramaniam, R. Billinton, and G. Wacker, "Factors Affecting the Development of an Industrial Customer Damage Function," *IEEE Trans. on PAS*, Vol. 104, No. 11, 1985, pp. 3209–3215.
12. G. Wacker, P. Kos, and R. Billinton, "Farm Losses Resulting Electric Service Interruptions," CEA Meeting, Toronto, March 1989.
13. R. Billinton, J. Oteng-Adjei, and R. Ghajar, "Comparison of Two Alternate Methods to Establish an Interrupted Energy Assessment Rate," *IEEE Trans. on PWRS*, Vol. 2, No. 3, 1987, pp. 751–757.

14. R. Billinton and R. N. Allan, *Reliability Evaluation of Power System*, Plenum, New York, 1984.
15. L. Gan, "Multi-Area Generation System Adequacy Assessment by Monte Carlo Simulation," M.Sc. Thesis, University of Saskatchewan, 1991.
16. J. Oteng-Adjei, "Cost/Benefit Assessment In Electric Power Systems," Ph.D. Thesis, University of Saskatchewan, Canada, January 1990.
17. IEEE Committee Report, "IEEE Reliability Test System," *IEEE Trans. on PAS*, Vol. 98, 1979, pp. 2047–2054.
18. O. Beroldi, L. Salvadori, and S. Scalcino, "Monte Carlo Approach in Planning Studies—An Application to IEEE RTS," *IEEE Trans. on PS*, Vol. 3, No. 3, 1988, pp. 1146–1154.
19. EPRI Report, "Transmission System Reliability Methods," EL-2526, Vol. 1, July 1982, Appendix Q.
20. L. Goel and R. Billinton, "Evaluation of Interrupted Energy Assessment Rates in Distribution Systems," *IEEE Trans. on PD*, Vol. 6, No. 4, 1991, pp. 1876–1882.
21. W. Li and R. Billinton, "A Minimum Cost Assessment Method for Composite Generation and Transmission System Expansion Planning," *IEEE Trans. on PS*, Vol. 8, No. 2, 1993, pp. 628–635.
22. R. Billinton and W. Li, "Consideration of Multi-State Generating Unit Models in Composite System Adequacy Assessment Using Monte Carlo Simulation," *Can. Journal of Electrical and Computer Engineering*, Vol. 17, No. 1, 1992, pp. 24–28.
23. R. Billinton and W. Li, "A Novel Method for Incorporating Weather Effects in Composite System Adequacy Evaluation," *IEEE Trans. on PS*, Vol. 6, No. 3, 1991, pp. 1154–1160.
24. W. Li and R. Billinton, "Effects of Bus Load Uncertainty and Correlation in Composite System Adequacy Evaluation," *IEEE Trans. on PS*, Vol. 6, No. 3, 1991, pp. 1522–1529.

# APPENDIX A

## Reliability Test Systems

### A.1. IEEE RELIABILITY TEST SYSTEM (IEEE RTS)

The IEEE Reliability Test System (RTS) was developed by the Subcommittee on the Application of Probability Methods in the IEEE Power Engineering Society to provide a common test system which could be used for comparing the results obtained by different methods. The details of the RTS can be found in Reference 1. Since the IEEE RTS was created, there have been many new developments in power system reliability evaluation. Additional data or modifications are therefore required to conduct extended studies.<sup>(2-8)</sup> This appendix presents the basic data and the additional data for the IEEE RTS.

#### A.1.1. Load Model

The basic annual peak load for the test system is 2850 MW. Table A.1 gives data on weekly peak loads in percentage of the annual peak load. If week 1 is taken as January, Table A.1 describes a winter peaking system. If week 1 is taken as a summer month, a summer peaking system can be described. Table A.2 gives a daily peak load cycle, in percentage of the weekly peak. The same weekly peak load cycle is assumed to apply for all seasons. The data in Tables A.1 and A.2 together with the annual peak load define a daily peak load model of  $52 \times 7 = 364$  days, with Monday as the first day of the year. Table A.3 gives weekday and weekend hourly load models for each of three seasons. Combination of Tables A.1, A.2, and A.3 with the annual peak load defines an hourly load model of  $364 \times 24 = 8736$  hr.

**Table A.1. Weekly Peak Load in Percentage of Annual Peak**

Week	Peak	Week	Peak	Week	Peak	Week	Peak
1	86.2	14	75.0	27	75.5	40	72.4
2	90.0	15	72.1	28	81.6	41	74.3
3	87.8	16	80.0	29	80.1	42	74.4
4	83.4	17	75.4	30	88.0	43	80.0
5	88.0	18	83.7	31	72.2	44	88.1
6	84.1	19	87.0	32	77.6	45	88.5
7	83.2	20	88.0	33	80.0	46	90.9
8	80.6	21	85.6	34	72.9	47	94.0
9	74.0	22	81.1	35	72.6	48	89.0
10	73.7	23	90.0	36	70.5	49	94.2
11	71.5	24	88.7	37	78.0	50	97.0
12	72.7	25	89.6	38	69.5	51	100.0
13	70.4	26	86.1	39	72.4	52	95.2

**Table A.2. Daily Peak Load in Percent of Weekly Peak**

Day	Peak load
Monday	93
Tuesday	100
Wednesday	98
Thursday	96
Friday	94
Saturday	77
Sunday	75

## A.1.2. Generating System

Table A.4 shows the generating unit ratings and reliability data. The 50-MW units are assumed to be hydro units and their capacity and energy limitations are given in Table A.5. Table A.6 gives operating cost data for the generating units. Power production data are given in terms of heat rates at selected output levels, since fuel costs are subject to considerable variation due to geographical location and other factors. The following fuel costs were suggested for general use (1979 base):

#6 oil	\$2.30/MBtu
#2 oil	\$3.00/MBtu
Coal	\$1.20/MBtu
Nuclear	\$0.60/MBtu

**Table A.3. Hourly Peak Load in Percentage of Daily Peak**

Hour	Winter week 1-8 & 44-52		Summer weeks 18-30		Spring/fall weeks 9-17 & 31-43	
	Wkdy <sup>a</sup>	Wknd <sup>a</sup>	Wkdy	Wknd	Wkdy	Wknd
12-1 am	67	78	64	74	63	75
1- 2	63	72	60	70	62	73
2- 3	60	68	58	66	60	69
3- 4	59	66	56	65	58	66
4- 5	59	64	56	64	59	65
5- 6	60	65	58	62	65	65
6- 7	74	66	64	62	72	68
7- 8	86	70	76	66	85	74
8- 9	95	80	87	81	95	83
9-10	96	88	95	86	99	89
10-11	96	90	99	91	100	92
11-Noon	95	91	100	93	99	94
Noon-1 pm	95	90	99	93	93	91
1- 2	95	88	100	92	92	90
2- 3	93	87	100	91	90	90
3- 4	94	87	97	91	88	86
4- 5	99	91	96	92	90	85
5- 6	100	100	96	94	92	88
6- 7	100	99	93	95	96	92
7- 8	96	97	92	95	98	100
8- 9	91	94	92	100	96	97
9-10	83	92	93	93	90	95
10-11	73	87	87	88	80	90
11-12	63	81	72	80	70	85

<sup>a</sup>Wkdy = weekday, Wknd = weekend.

**Table A.4. Generating Unit Reliability Data**

Unit size (MW)	Number of units	Forced outage rate	MTTF (hr)	MTTR (hr)	Scheduled maintenance (weeks/yr)
12	5	0.02	2940	60	2
20	4	0.10	450	50	2
50	6	0.01	1980	20	2
76	4	0.02	1960	40	3
100	3	0.04	1200	50	3
155	4	0.04	960	40	4
197	3	0.05	950	50	4
350	1	0.08	1150	100	5
400	2	0.12	1100	150	6

**Table A.5. Hydro Capacity and Energy**

Quarter	Capacity available <sup>a</sup> (%)	Energy distribution <sup>b</sup> (%)
1	100	35
2	100	35
3	90	10
4	90	20

<sup>a</sup>100% capacity = 50 MW,<sup>b</sup>100% energy = 200 GWh.

### A.1.3. Transmission System

The transmission network consists of 24 bus locations connected by 38 lines and transformers, as shown in Figure A.1. The transmission lines are at two voltages, 138 kV and 230 kV. The 230-kV system is the top part of Figure A.1, with 230/138 kV tie stations at Buses 11, 12, and 24. The locations of the generating units are shown in Table A.7. Table A.8 gives data on generating unit MVar capacities. The system has voltage corrective devices at Bus 14 (synchronous condenser) and Bus 6 (reactor). Table A.9 gives the MVar capacities of these devices. Bus load data at the time of system peak are shown in Table A.10. Transmission line forced outage data are given in Table A.11. Impedance and rating data for lines and transformers are given in Table A.12. The “B” values in the impedance data are the total, not the values in one leg of an equivalent circuit.

Outages on station components which are not switched as a part of a line are not included in the outage data in Table A.11. The following data are provided for bus sections:

	138 kV	230 kV
Faults per bus section/yr	0.027	0.021
Percentage of permanent faults	42	43
Outage duration for permanent faults (hr)	19	13

The following statistics are provided for circuit breakers:

Physical failures/breaker/yr	0.0066
Breaker operational failure per breaker/yr	0.0031
Outage duration (hr)	72

**Table A.6. Generating Unit Operating Cost Data**

Unit size (MW)	Type	Fuel	Output (%)	Heat rate (BTu/kWh)	O & M Cost	
					Fixed (\$/kW/yr)	Variable (\$/MWh)
12	Fossil steam	#6 oil	20	15600	10.0	0.90
			50	12900		
			80	11900		
			100	12000		
20	Combust. turbine	#2 oil	80	15000	0.3	5.00
			100	14500		
50	Hydro					
76	Fossil steam	Coal	20	13000	10.5	0.90
			50	12900		
			80	11900		
			100	12000		
100	Fossil steam	#6 oil	25	13000	8.5	0.80
			55	10600		
			80	10100		
			100	10000		
155	Fossil steam	Coal	35	11200	7.0	0.80
			60	10100		
			80	9800		
			100	9700		
197	Fossil steam	#6 oil	35	10750	5.0	0.70
			60	9850		
			80	9840		
			100	9600		
350	Fossil steam	Coal	40	10200	4.5	0.70
			65	9600		
			80	9500		
			100	9500		
400	Nuclear steam	LWR	25	12550	5.0	0.30
			50	10825		
			80	10170		
			100	10000		

A physical failure is a mandatory unscheduled removal from service for repair or replacement. An operational failure is a failure to clear a fault within the breaker's normal protection zone.

There are several lines which are assumed to be on a common right-of-way or common tower for at least a part of their length. These line pairs are indicated in Figure A.1 by circles around the line pair, and an associated letter identification. Table A.13 gives the actual length of common right-of-way or common tower facility.

**Table A.7. Generating Unit Locations**

Bus	Unit 1 (MW)	Unit 2 (MW)	Unit 3 (MW)	Unit 4 (MW)	Unit 5 (MW)	Unit 6 (MW)
1	20	20	76	76		
2	20	20	76	76		
7	100	100	100			
13	197	197	197			
15	12	12	12	12	12	155
16	155					
18	400					
21	400					
22	50	50	50	50	50	50
23	155	155	350			

**Table A.8. Generating Unit MVAr Capacities**

Size (MW)	MVAr	
	Minimum	Maximum
12	0	6
20	0	10
50	-10	16
76	-25	30
100	0	60
155	-50	80
197	0	80
350	-25	150
400	-50	200

**Table A.9. Voltage Correction Devices**

Device	Bus	MVAr capacity
Synchronous Condenser	14	50 Reactive 200 Capacitive
Reactor	6	100 Reactive

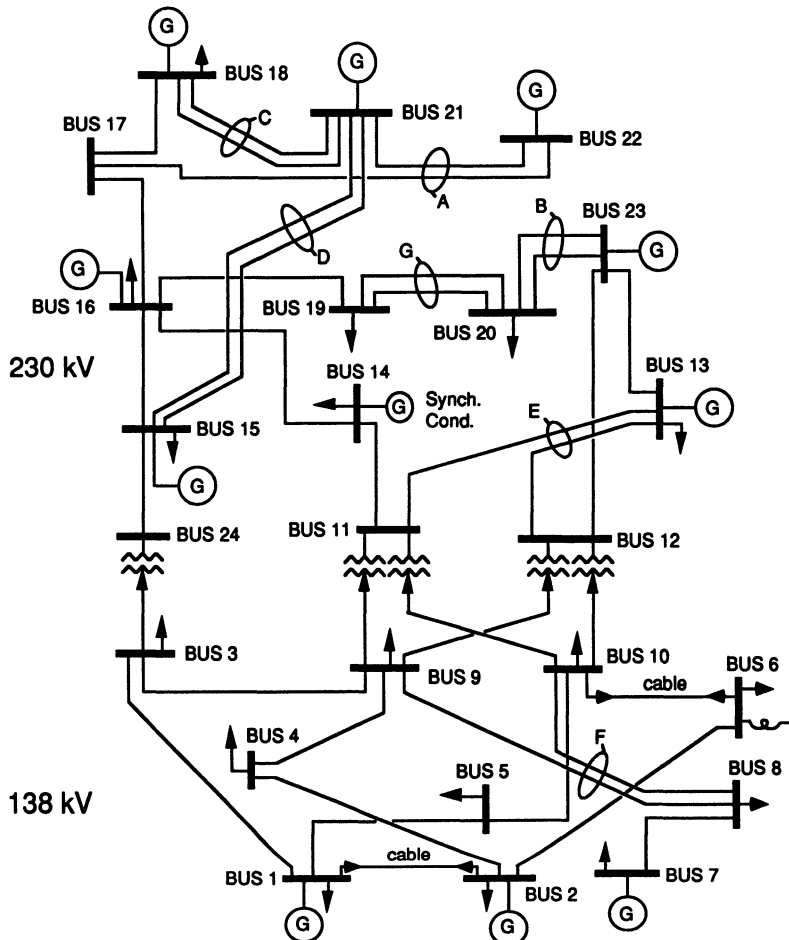


**Figure A.1.** IEEE Reliability Test System.

#### A.1.4. Additional Data

The extended studies using the IEEE RTS require additional data. The following additional data are given in the text.

1. Table 4.2 gives derated state data for the 400-MW and 350-MW generating units.
2. Table 4.4 gives data on additional 25-MW gas turbine units.
3. Data associated with nonexponential distribution repair times of generating units are shown in Section 4.2.4(d).
4. Data associated with bus load uncertainty and correlation are shown in Section 5.7.3.

**Table A.10. Bus Load Data**

Bus	Load	
	MW	MVAr
1	108	22
2	97	20
3	180	37
4	74	15
5	71	14
6	136	28
7	125	25
8	171	35
9	175	36
10	195	40
13	265	54
14	194	39
15	317	64
16	100	20
18	333	68
19	181	37
20	128	26
Total	2850	580

5. Table 7.1 gives sector customer damage functions for seven customer categories. Table 7.12 gives customer sector allocations (in %) at the load buses. The bus peak load MW values in Table 7.12 are for the Modified IEEE RTS. These values are 125% of the bus peak loads in the original RTS. The percentage loads for the customer sectors remain unchanged.
6. Table 7.8 gives modified generating unit operating cost data. Table 7.22 gives investment-cost-related data.
7. The IEEE RTS has an oversized transmission network. Several modifications have been suggested for the purpose of transmission planning studies. The Modified IEEE RTS is described in Section 7.4.2.

## A.2. ROY BILLINTON TEST SYSTEM (RBTS)

The RBTS is a six-bus composite system developed at the University of Saskatchewan for educational purpose. It is sufficiently small to permit the conduct of a large number of reliability studies with reasonable solution time but sufficiently detailed to reflect the actual complexities involved in practical reliability analysis and can be used to examine a newly developed technique or method. The details of the RBTS are given in Billinton *et al.*<sup>(9)</sup>

**Table A.11. Transmission Line Length and Forced Outage Data**

From bus	To bus	Length (miles)	Permanent		Transient outage rate (occ/yr)
			Outage rate (occ/yr)	Outage duration (hr)	
1	2	3	0.24	16	0.0
1	3	55	0.51	10	2.9
1	5	22	0.33	10	1.2
2	4	33	0.39	10	1.7
2	6	50	0.48	10	2.6
3	9	31	0.38	10	1.6
3	24	0	0.02	768	0.0
4	9	27	0.36	10	1.4
5	10	23	0.34	10	1.2
6	10	16	0.33	35	0.0
7	8	16	0.30	10	0.8
8	9	43	0.44	10	2.3
8	10	43	0.44	10	2.3
9	11	0	0.02	768	0.0
9	12	0	0.02	768	0.0
10	11	0	0.02	768	0.0
10	12	0	0.02	768	0.0
11	13	33	0.40	11	0.8
11	14	29	0.39	11	0.7
12	13	33	0.40	11	0.8
12	23	67	0.52	11	1.6
13	23	60	0.49	11	1.5
14	16	27	0.38	11	0.7
15	16	12	0.33	11	0.3
15	21	34	0.41	11	0.8
15	21	34	0.41	11	0.8
15	24	36	0.41	11	0.9
16	17	18	0.35	11	0.4
16	19	16	0.34	11	0.4
17	18	10	0.32	11	0.2
17	22	73	0.54	11	1.8
18	21	18	0.35	11	0.4
18	21	18	0.35	11	0.4
19	20	27.5	0.38	11	0.7
19	20	27.5	0.38	11	0.7
20	23	15	0.34	11	0.4
20	23	15	0.34	11	0.4
21	22	47	0.45	11	1.2

**Table A.12. Impedance and Rating Data**

From bus	To bus	Impedance p.u. (100 MVA base)			Rating (MVA)			Equipment
		R	X	B	Normal	Short term	Long term	
1	2	0.0026	0.0139	0.4611	175	200	193	138-kV cable
1	3	0.0546	0.2112	0.0572	175	220	208	138-kV line
1	5	0.0218	0.0845	0.0229	175	220	208	138-kV line
2	4	0.0328	0.1267	0.0343	175	220	208	138-kV line
2	6	0.0497	0.1920	0.0520	175	220	208	138-kV line
3	9	0.0308	0.1190	0.0322	175	220	208	138-kV line
3	24	0.0023	0.0839		400	600	510	Transformer
4	9	0.0268	0.1037	0.0281	175	220	208	138-kV line
5	10	0.0228	0.0883	0.0239	175	220	208	138-kV line
6	10	0.0139	0.0605	2.4590	175	200	193	138-kV cable
7	8	0.0159	0.0614	0.0166	175	220	208	138-kV line
8	9	0.0427	0.1651	0.0447	175	220	208	138-kV line
8	10	0.0427	0.1651	0.0447	175	220	208	138-kV line
9	11	0.0023	0.0839		400	600	510	Transformer
9	12	0.0023	0.0839		400	600	510	Transformer
10	11	0.0023	0.0839		400	600	510	Transformer
10	12	0.0023	0.0839		400	600	510	Transformer
11	13	0.0061	0.0476	0.0999	500	625	600	230-kV line
11	14	0.0054	0.0418	0.0879	500	625	600	230-kV line
12	13	0.0061	0.0476	0.0999	500	525	600	230-kV line
12	23	0.0124	0.0966	0.2030	500	525	600	230-kV line
13	23	0.0111	0.0865	0.1818	500	525	600	230-kV line
14	26	0.0050	0.0389	0.0818	500	625	600	230-kV line
15	16	0.0022	0.0173	0.0364	500	625	600	230-kV line
15	21	0.0063	0.0490	0.1030	500	525	600	230-kV line
15	21	0.0063	0.0490	0.1030	500	525	600	230-kV line
15	24	0.0067	0.0519	0.1091	500	525	600	230-kV line
16	17	0.0033	0.0259	0.0545	500	525	600	230-kV line
16	19	0.0030	0.0231	0.0485	500	525	600	230-kV line
17	18	0.0018	0.0144	0.0303	500	525	600	230-kV line
17	22	0.0135	0.1053	0.2212	500	625	600	230-kV line
18	21	0.0033	0.0259	0.0545	500	625	600	230-kV line
18	21	0.0033	0.0259	0.0545	500	625	600	230-kV line
19	20	0.0051	0.0396	0.0833	500	525	600	230-kV line
19	20	0.0051	0.0396	0.0833	500	525	600	230-kV line
20	23	0.0028	0.0216	0.0455	500	525	600	230-kV line
20	23	0.0028	0.0216	0.0455	500	525	600	230-kV line
21	22	0.0087	0.0678	0.1424	500	525	600	230-kV line

**Table A.13. Circuits on Common Right-of-Way or Common Structure**

Right-of-way identification	From bus	To bus	Common ROW (miles)	Common structure (miles)
A	22	21	45.0	
	22	17	45.0	
B	23	20		15.0
	23	20		15.0
C	21	18		18.0
	21	18		18.0
D	15	21	34.0	
	15	21	34.0	
E	13	11		33.0
	13	12		33.0
F	8	10		43.0
	8	9		43.0
G	20	19	27.5	
	20	19	27.5	

### A.2.1. Brief Description of the RBTS

The single line diagram of the test system is shown in Figure A.2. The system has two generator buses, four load buses, nine transmission lines, and eleven generating units. The system voltage level is 230 kV and the voltage limits for system buses are assumed to be between 1.05 p.u. and 0.97 p.u. The system peak load is 185 MW and the total installed generating capacity is 240 MW. The transmission network shown in Figure A.2 has been drawn to give a geographical representation. The line lengths are shown in proportion to their actual lengths. Customer sectors at the load buses are given in Figure A.2.

### A.2.2. Load Model

The annual peak load for the system is 185 MW. The data on weekly peak loads in percentage of the annual peak load, daily peak load in percentage of the weekly peak, and hourly peak load in percentage of the daily peak are the same as those given in Tables A.1, A.2, and A.3.

### A.2.3. Generating System

The generating unit ratings and reliability data for the RBTS are shown in Table A.14. The two 40-MW thermal units have been given an optional three-state representation. The derated model is shown in Figure A.3. It

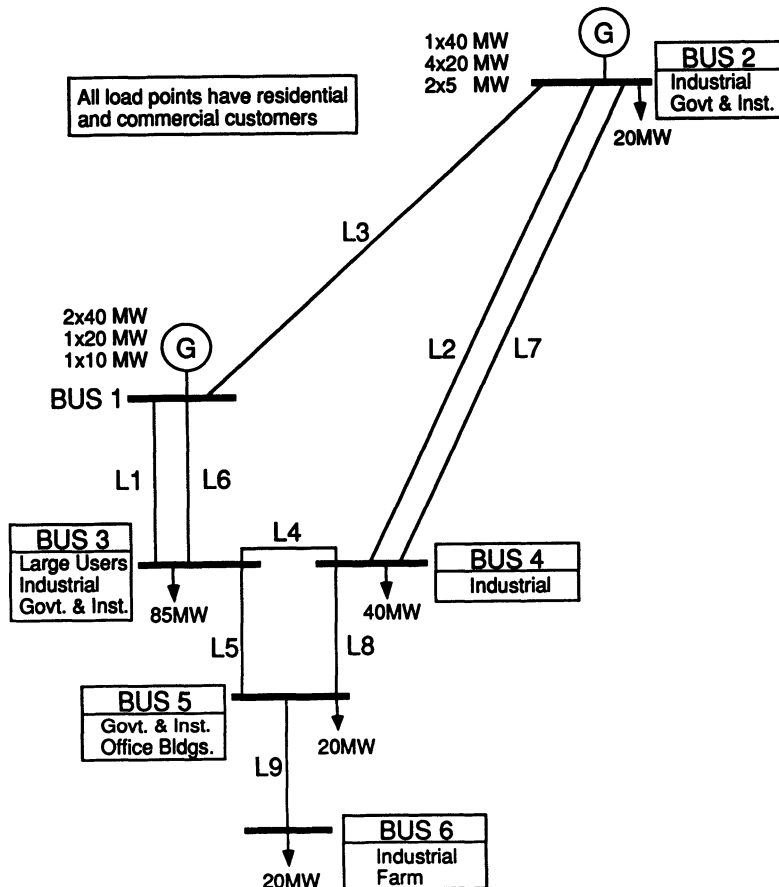


Figure A.2. Single line diagram of the RBTS.

has been assumed that there are no transitions between the derated state and the down state. The state probabilities and transition rates of the derated model are such that the derating-adjusted two-state model data are identical to those given in Table A.14. The two-state model is also shown in Figure A.3.

The generating unit cost data are shown in Table A.15. The operating costs include materials, supplies, manpower, etc. The fuel costs are those directly associated with energy production. The fuel cost for a hydro unit includes water rental charges. The fixed costs include the annual charges which continue as long as capital is tied up in the enterprise and whether or not the equipment is operating. The capital cost is the total cost to install

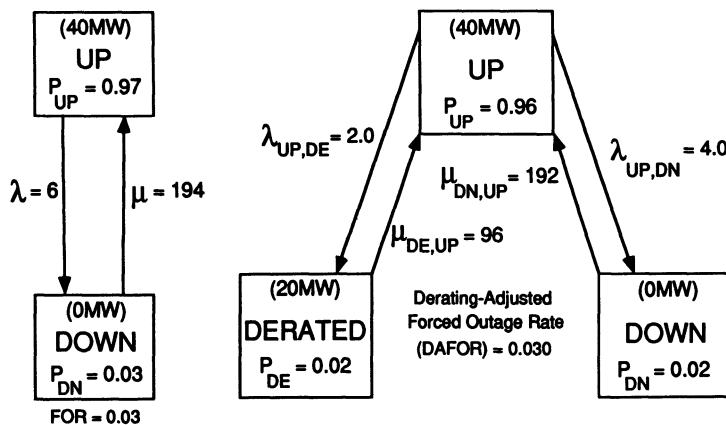


Figure A.3. Two- and three-state models for a 40-MW thermal generating unit.

Table A.14. Generating Unit Rating and Reliability Data

Unit size (MW)	Type	No. of units	Forced outage rate	Failure rate (1/yr)	Repair rate (1/yr)	Scheduled maintenance (weeks/yr)
5	Hydro	2	0.010	2.0	198.0	2
10	Thermal	1	0.020	4.0	196.0	2
20	Hydro	4	0.015	2.4	157.6	2
20	Thermal	1	0.025	5.0	195.0	2
40	Hydro	1	0.020	3.0	147.0	2
40	Thermal	2	0.030	6.0	194.0	2

Table A.15. Generating Unit Cost Data

Unit size (MW)	Type	No. of units	Loading order		Variable cost (\$/MWh)			Fixed cost (k\$/yr)	Capital cost (M\$)
			1st	2nd	Fuel	Operat.	Total		
40	(Hydro)	1	1	1	0.45	0.05	0.50	100.0	160.0
20	(Hydro)	2	2-3	2-3	0.45	0.05	0.50	50.0	80.0
40	(Thermal)	2	8-9	4-5	9.50	2.50	12.00	790.0	80.0
20	(Thermal)	1	10	6	9.75	2.50	12.25	680.0	60.0
10	(Thermal)	1	11	7	10.00	2.50	12.50	600.0	40.0
20	(Hydro)	2	4-5	8-9	0.45	0.05	0.50	50.0	80.0
5	(Hydro)	2	6-7	10-11	0.45	0.05	0.50	12.5	40.0

**Table A.16. Generation, Outage, and Cost Data for Additional Gas Turbines**

Capacity (MW)	FOR	MTTF (hr)	MTTR (hr)	Fuel cost (\$/MWh)	Operating cost (\$/MWh)	Fixed cost (k\$/yr)	Capital cost (M\$)
10	0.12	550	75	52.0	4.5	40.0	5.0

a generating unit. Two loading orders are given in Table A.15. The first loading order is on a purely economic basis. The second loading order allocates some hydro units as peaking units which could reflect limited energy considerations. Either of the loading orders can be selected depending upon the operating philosophy in conducting reliability studies. Additional gas turbine units can be added to the RBTS. The generation, outage, and cost data for these units are given in Table A.16.

#### A.2.4. Transmission System

The transmission network consists of six buses and nine transmission lines. The locations of the generating units are shown in Table A.17. Table A.18 gives data on generating unit MVAr capacity. Bus load data at the time of system peak in MW and in percentage of the total system load are shown in Table A.19. At 0.98 power factor, the reactive load MVAr

**Table A.17. Generating Unit Locations**

Bus No.	Unit 1 (MW)	Unit 2 (MW)	Unit 3 (MW)	Unit 4 (MW)	Unit 5 (MW)	Unit 6 (MW)	Unit 7 (MW)
1 (Thermal plant)	40	40	10	20			
2 (Hydro plant)	5	5	40	20	20	20	20

**Table A.18. Generating Unit MVAr Capacities**

Unit size (MW)	MVAr	
	Minimum	Maximum
5	0	5
10	0	7
20	-7	12
40	-15	17

**Table A.19. Bus Load Data**

Bus	Load (MW)	Bus load in % of system load
2	20.0	10.81
3	85.0	45.95
4	40.0	21.62
5	20.0	10.81
6	20.0	10.81
Total	185.0	100.00

requirements at each bus is 20% of the corresponding MW load. The load forecast uncertainty can be assumed to follow a normal distribution having a standard deviation from 2.5% to 10%.

Table A.20 shows the transmission line lengths and outage data. The permanent outage rate of a given line is obtained using a value of 0.02 outages/yr/km. Line transient outage rates are calculated using a value of 0.05 outages/yr/km. The outage duration of a transient outage is assumed to be less than 1 min and is, therefore, not included in Table A.20. Outages of substation components which are not switched as a part of a line are not included in the outage data given in Table A.20. Two pairs of transmission lines are assumed to be on a common right-of-way or common tower for their entire length. The common mode data for these two line pairs are given in Table A.21. The line impedance and rating data are given in Tables A.22.

## A.2.5. Station Data

The station configurations for the load and generator buses are given in the extended single line diagram shown in Figure A.4.

**Table A.20. Transmission Line Length and Outage Data**

Line	From	To	Length (kM)	Permanent		Transient outage rate (occ/yr)
				Outage rate (occ/yr)	Duration (hr)	
1	1	3	75	1.5	10.0	3.75
2	2	4	250	5.0	10.0	12.50
3	1	2	200	4.0	10.0	10.00
4	3	4	50	1.0	10.0	2.50
5	3	5	50	1.0	10.0	2.50
6	1	3	75	1.5	10.0	3.75
7	2	4	250	5.0	10.0	12.50
8	4	5	50	1.0	10.0	2.50
9	5	6	50	1.0	10.0	2.50

**Table A.21. Common Mode Data for the Circuits on a Common Right-of-Way or a Common Tower**

Line pair	Buses		Line No.	Common length (kM)	Outage rate (occ/yr)	Outage duration (hr)
	From	To				
A	1	3	1 & 6	75	0.15	16.0
B	2	4	2 & 7	250	0.50	16.0

**Table A.22. Line Impedance and Rating Data (100-MVA Base and 230-kV Base)**

Line	Buses		Impedance (p.u.)			Current rating (p.u.)
	From	To	R	X	B/2	
1, 6	1	3	0.0342	0.180	0.0106	0.85
2, 7	2	4	0.1140	0.600	0.0352	0.71
3	1	2	0.0912	0.480	0.0282	0.71
4	3	4	0.0228	0.120	0.0071	0.71
5	3	5	0.0028	0.120	0.0071	0.71
8	4	5	0.0228	0.120	0.0071	0.71
9	5	6	0.0028	0.120	0.0071	0.71

The station equipment data are as follows:

#### *Circuit Breaker*

Active failure rate = 0.0066 failure/yr

Passive failure rate = 0.0005 failure/yr

Average outage duration = 72 hr

Maintenance outage rate = 0.2 outages/yr

Maintenance time = 108 hr

Switching time = 1 hr

#### *Bus Section*

Failure rate = 0.22 failures/yr

Outage duration = 10 hr

#### *Station Transformer*

Failure rate = 0.02 failures/yr

Outage duration = 768 hr

Maintenance outage rate = 0.2 outages/yr

Maintenance time = 72 hr

Switching time = 1 hr

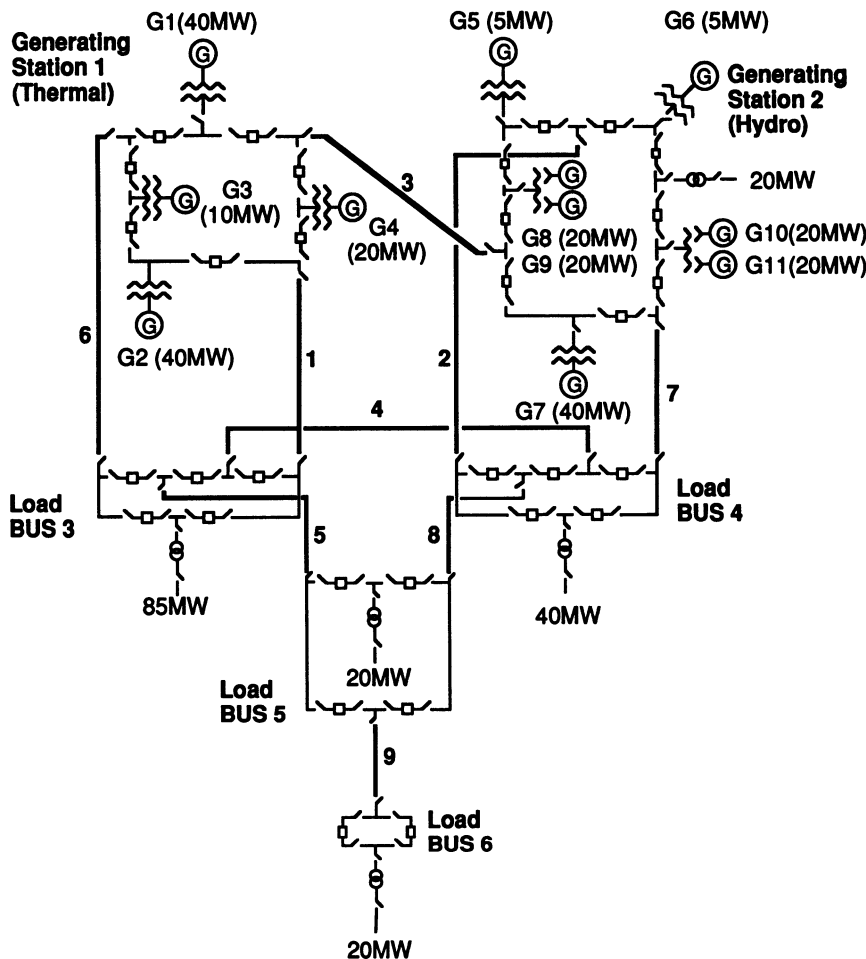


Figure A.4. Extended single line diagram of the RBTS.

### A.2.6. Reliability Worth Assessment Data

The sector customer damage function data are the same as those given in Table 7.1. Customer sector allocations at buses are shown in Table A.23. The system customer mix by energy consumption and peak demand and system composite customer damage function for the customer mix are the same as those given in Tables 7.2 and 7.3, respectively. Bus composite customer damage functions can be calculated using the data given in Tables 7.1 and A.23.

**Table A.23. Customer Sector Allocations at Load Buses**

Bus No.	Peak load (MW)	Load percentage of customer sector (in %)					
		Agri.	Large user	Resid.	Gover.	Indus.	Commer.
2	20	0.0	0.0	50.95	22.20	12.95	13.90
3	85	0.0	65.29	23.16	0.0	4.58	4.35
4	40	0.0	0.0	37.12	0.0	42.08	20.80
5	20	0.0	0.0	50.05	33.30	0.0	9.25
6	20	37.0	0.0	40.8	0.0	12.95	9.25

### A.3. REFERENCES

- IEEE Committee Report, "IEEE Reliability Test System," *IEEE Trans. on PAS*, Vol. 98, 1979, pp. 2047-2054.
- R. N. Allan, R. Billinton, and N. M. Abdel-Gaead, "The IEEE Reliability Test System—Extension to and Evaluation of the Generating System," *IEEE Trans. on PWR*, Vol. 1, No. 4, 1986, pp. 1-7.
- R. Billinton, P. K. Vohra, and S. Kumar, "Effects of Station Originated Outages in a Composite System Adequacy Evaluation of the IEEE Reliability Test System," *IEEE Trans. on PAS*, Vol. 104, No. 10, 1985, pp. 2649-2656.
- W. Li and R. Billinton, "Effects of Bus Load Uncertainty and Correlation in Composite System Adequacy Evaluation," *IEEE Trans. on PS*, Vol. 6, No. 3, 1991, pp. 1522-1529.
- J. Oteng-Adjei, "Cost/Benefit Assessment in Electric Power Systems," Ph.D. Thesis, University of Saskatchewan, Canada, January 1990.
- W. Li and R. Billinton, "A Minimum Cost Assessment Method for Composite Generation and Transmission System Expansion Planning," *IEEE Trans. on PS*, Vol. 8, No. 2, 1993, pp. 628-635.
- O. Bertoldi, L. Salvaderi, and S. Scalcino, "Monte Carlo Approach in Planning Studies—An Application to IEEE RTS," *IEEE Trans. on PS*, Vol. 3, No. 3, 1988, pp. 1146-1154.
- EPRI Report, "Transmission System Reliability Methods," EL-2526, Vol. 1, July 1982, Appendix Q.
- R. Billinton, S. Kumar, N. Chowdhury, K. Chu, K. Debnath, L. Goel, E. Khan, P. Kos, G. Nourbakhsh, and J. Oteng-Adjei, "A Reliability Test System for Educational Purposes: Basic Data," *IEEE Trans. on PS*, Vol. 4, No. 3, 1989, pp. 1238-1244.

# Elements of Probability and Statistics

## B.1. PROBABILITY CONCEPT AND CALCULATION RULES

### B.1.1. Probability Concept

A random event can be considered as a phenomenon which may or may not occur in a given trial, time, or space. Assume that an experiment is repeated  $N$  times under the same conditions and that the number of occurrences of event A is  $M$ . The ratio  $M/N$  approaches a determined value when  $N$  becomes very large. This value is defined as the probability of event A occurring, i.e.,

$$P(A) = \lim_{N \rightarrow \infty} \frac{M}{N} \quad (\text{B.1})$$

Probability is a numerical measure of likelihood of a random event occurring and its value lies between 0.0 and 1.0.

### B.1.2. Probability Calculation Rules

Some important and basic rules of probability theory are as follows:

$$P(A \cup B) = P(A) + P(B) - P(A \cap B) \quad (\text{B.2})$$

$$P(A \cap B) = P(A)P(B/A) \quad (\text{B.3})$$

where  $P(A \cup B)$  is the probability of the occurrence of either A or B or both,  $P(A \cap B)$  is the probability of the simultaneous occurrence of events A and B, and  $P(B/A)$  is the conditional probability of B occurring given that A has occurred. If events A and B are mutually exclusive,  $P(A \cap B) = 0$ . This can be generalized to  $N$  events. If  $N$  events are mutually exclusive, the following probability equation applies:

$$P(A_1 \cup A_2 \cup \dots \cup A_N) = P(A_1) + P(A_2) + \dots + P(A_N) \quad (\text{B.4})$$

If events A and B are independent,  $P(A \cap B) = P(A)P(B/A) = P(A)P(B)$ . This can also be generalized to  $N$  events. If  $N$  events are independent of each other, the following probability equation holds:

$$P(A_1 \cap A_2 \cap \dots \cap A_N) = P(A_1)P(A_2) \dots P(A_N) \quad (\text{B.5})$$

If the events  $\{B_1, B_2, \dots, B_N\}$  represent a full and mutually exclusive set, i.e.,  $P(B_1) + P(B_2) + \dots + P(B_N) = 1.0$  and  $P(B_i \cap B_j) = 0.0$  ( $i \neq j; i, j = 1, 2, \dots, N$ ), then for any event A,

$$P(A) = \sum_{i=1}^N P(B_i)P(A/B_i) \quad (\text{B.6})$$

## B.2. PROBABILITY DISTRIBUTIONS OF RANDOM VARIABLES

### B.2.1. Probability Distribution Function and Density Function

A random event or phenomenon can be represented by a random variable. Given a continuous random variable  $X$ , the probability of  $X$  being not larger than a real number  $x$  is a function of  $x$ . This function is defined as the cumulative distribution function  $F(x)$  of random variable  $X$ , i.e.,

$$F(x) = P(X \leq x) \quad (-\infty < x < \infty) \quad (\text{B.7})$$

The cumulative distribution function indicates the probabilities of all possible values of  $X$ . Function  $F(x)$  can be expressed in the following form:

$$F(x) = \int_{-\infty}^x f(x) dx \quad (\text{B.8})$$

where  $f(x)$  is the probability density function, and

$$f(x) = \frac{dF(x)}{dx} \quad (\text{B.9})$$

The probability of  $X$  lying between  $a$  and  $b$  can be calculated by

$$P(a \leq X \leq b) = \int_a^b f(x) dx \quad (\text{B.10})$$

When  $a=b$ , the integration value given by equation (B.10) is zero. This indicates that the probability of a continuous random variable being equal to a single point value is zero.

Assume that the random variable  $Y$  is a function of a random variable  $X$ , i.e.,  $y=y(x)$ . The following relationship exists between the probability density functions of  $Y$  and  $X$ :

$$f(y) = f(x) \left| \frac{dx}{dy} \right| \quad (\text{B.11})$$

The concepts and the relationship shown in equation (B.11) can be generalized to the case of multiple random variables (random vector). Consider a two-dimensional random vector and assume that the random vector  $\xi=(X, Y)$  has a density function  $f(x, y)$  and the random vector  $\eta=(Z_1, Z_2)$  is a function of  $\xi$ , i.e.,  $z_1=z_1(x, y)$  and  $z_2=z_2(x, y)$ . The inverse functions can be expressed as  $x=x(z_1, z_2)$  and  $y=y(z_1, z_2)$ . The density function of the random vector  $\eta$  is given by

$$f(z_1, z_2) = f[x(z_1, z_2), y(z_1, z_2)] |J| \quad (\text{B.12})$$

where  $J$  is the Jacobian determinant of the inverse functions:

$$J = \begin{vmatrix} \frac{\partial x}{\partial z_1} & \frac{\partial x}{\partial z_2} \\ \frac{\partial y}{\partial z_1} & \frac{\partial y}{\partial z_2} \end{vmatrix} \quad (\text{B.13})$$

When a random variable is discrete, its probability density function can be expressed as

$$p_k = P(X=x_k) \quad (k=1, 2, \dots) \quad (\text{B.14})$$

and its cumulative probability distribution function as

$$F(x_k) = P(X \leq x_k) \quad (\text{B.15})$$

The relationship between the density function and the cumulative distribution function of a discrete random variable is described by

$$F(x_k) = \sum_{i \leq k} p_i \quad (\text{B.16})$$

and

$$p_k = F(x_k) - F(x_{k-1}) \quad (\text{B.17})$$

## B.2.2. Important Distributions in Reliability Evaluation

The following five distributions are used in the text:

### 1. Exponential Distribution

The density function:

$$f(t) = \lambda \exp(-\lambda t) \quad (t \geq 0) \quad (\text{B.18})$$

The cumulative distribution function:

$$F(t) = 1 - \exp(-\lambda t) \quad (\text{B.19})$$

The mean and variance of the exponential distribution are  $1/\lambda$  and  $1/\lambda^2$ , respectively.

### 2. Normal Distribution

The density function:

$$f(t) = \frac{1}{\sigma\sqrt{2\pi}} \exp\left[-\frac{(t-\mu)^2}{2\sigma^2}\right] \quad (-\infty \leq t \leq \infty) \quad (\text{B.20})$$

where  $\mu$  and  $\sigma^2$  are the mean and variance of the normal distribution.

### 3. Log-Normal Distribution

The density function:

$$f(t) = \frac{1}{t\sigma\sqrt{2\pi}} \exp\left[-\frac{(\ln t - \mu)^2}{2\sigma^2}\right] \quad (t > 0) \quad (\text{B.21})$$

It should be noted that  $\mu$  and  $\sigma^2$  in equation (B.21) are not the mean and variance of the log-normal distribution. The mean and variance of the log-normal distribution are given, respectively, by

$$E(t) = \exp\left(\mu + \frac{\sigma^2}{2}\right) \quad (\text{B.22})$$

and

$$V(t) = \exp(2\mu + \sigma^2)[\exp(\sigma^2) - 1] \quad (\text{B.23})$$

If the mean and variance of the log-normal distribution (i.e.,  $E$  and  $V$ ) are specified, the parameters  $\mu$  and  $\sigma^2$  in equation (B.21) are given by

$$\mu = \ln \left[ \frac{E^2}{(V+E^2)^{1/2}} \right] \quad (\text{B.24})$$

and

$$\sigma^2 = \ln \left[ \frac{V+E^2}{E^2} \right] \quad (\text{B.25})$$

#### 4. Gamma Distribution

The density function:

$$f(t) = \frac{t^{\beta-1}}{\alpha^\beta \Gamma(\beta)} \exp \left[ -\frac{t}{\alpha} \right] \quad (t \geq 0, \beta > 0, \alpha > 0) \quad (\text{B.26})$$

where  $\alpha$  and  $\beta$  are the scale and shape parameters of the gamma distribution.

There are no explicit analytical expressions for the cumulative distribution functions for normal, log-normal, and gamma distributions.

#### 5. Weibull Distribution

The density function:

$$f(t) = \frac{\beta t^{\beta-1}}{\alpha^\beta} \exp \left[ -\left( \frac{t}{\alpha} \right)^\beta \right] \quad (\infty > t \geq 0, \beta > 0, \alpha > 0) \quad (\text{B.27})$$

The cumulative distribution function:

$$F(t) = 1 - \exp \left[ -\left( \frac{t}{\alpha} \right)^\beta \right] \quad (\text{B.28})$$

where  $\alpha$  and  $\beta$  are the scale and shape parameters of the Weibull distribution.

### B.3. NUMERICAL CHARACTERISTICS OF RANDOM VARIABLES

Random variables can be generally described by one or more parameters rather than as a specific distribution. These parameters are known as numerical characteristics. The most useful numerical characteristics are mathematical expectation (mean), variance, covariance, and correlation functions.

### B.3.1. Expectation and Variance

If a random variable  $X$  has a probability density function  $f(x)$  and the random variable  $Y$  is a function of  $X$ , i.e.,  $y = y(x)$ , then

$$E(Y) = \int_{-\infty}^{\infty} y(x)f(x) dx \quad (\text{B.29})$$

where  $E(Y)$  is called the expected or mean value of the random variable  $Y$ . The expected value of the random variable  $X$  is

$$E(X) = \int_{-\infty}^{\infty} xf(x) dx \quad (\text{B.30})$$

where  $E(X)$  indicates the mean of all possible values of  $X$ .

The variance of  $X$  is the expected value of the function  $[x - E(X)]^2$ , i.e.,

$$E([X - E(X)]^2) = \int_{-\infty}^{\infty} [x - E(X)]^2 f(x) dx \quad (\text{B.31})$$

The variance indicates the degree of dispersion of the possible values of  $X$  from its mean. The variance is often expressed by the notation  $V(X)$  or  $\sigma^2(X)$ . The square root of the variance,  $\sigma(X)$ , is known as the standard deviation.

In the case of a discrete random variable, equations (B.29), (B.30), and (B.31) become equations (B.32), (B.33), and (B.34):

$$E(Y) = \sum_{i=1}^n y(x_i)p_i \quad (\text{B.32})$$

$$E(X) = \sum_{i=1}^n x_i p_i \quad (\text{B.33})$$

$$V(X) = \sum_{i=1}^n [x_i - E(X)]^2 p_i \quad (\text{B.34})$$

### B.3.2. Covariance and Correlation Function

Given an  $N$ -dimension random vector  $\mathbf{y} = (X_1, X_2, \dots, X_N)$ , the covariance between any two elements  $X_i$  and  $X_j$  is defined as

$$\begin{aligned} c_{ij} &= E\{[X_i - E(X_i)][X_j - E(X_j)]\} \\ &= E(X_i X_j) - E(X_i)E(X_j) \end{aligned} \quad (\text{B.35})$$

The covariance is often expressed by the notation  $\text{cov}(X_i, X_j)$ . The covariance between an element and itself is its variance, i.e.,

$$\text{cov}(X_i, X_i) = V(X_i) \quad (\text{B.36})$$

The covariances of all elements of random vector  $\eta$  form the covariance matrix:

$$(c_{ij}) = \begin{bmatrix} c_{11} & c_{12} & \dots & c_{1N} \\ c_{21} & c_{22} & \dots & c_{2N} \\ \cdot & \cdot & \ddots & \cdot \\ \cdot & \cdot & & \cdot \\ c_{N1} & c_{N2} & \dots & c_{NN} \end{bmatrix} \quad (\text{B.37})$$

This is a symmetrical matrix whose diagonal components are variances of each element of  $\eta$ .

The correlation function (coefficient) of  $X_i$  and  $X_j$  is defined as

$$\rho_{ij} = \frac{\text{cov}(X_i, X_j)}{\sqrt{V(X_i)} \sqrt{V(X_j)}} \quad (\text{B.38})$$

The correlation functions of all elements of random vector  $\eta$  form the correlation matrix:

$$(\rho_{ij}) = \begin{bmatrix} \rho_{11} & \rho_{12} & \dots & \rho_{1N} \\ \rho_{21} & \rho_{22} & \dots & \rho_{2N} \\ \cdot & \cdot & \ddots & \cdot \\ \cdot & \cdot & & \cdot \\ \rho_{N1} & \rho_{N2} & \dots & \rho_{NN} \end{bmatrix} \quad (\text{B.39})$$

The absolute value of  $\rho_{ij}$  is smaller or equal to 1.0. When  $\rho_{ij}=0$ ,  $X_i$  and  $X_j$  are not correlated; when  $\rho_{ij}>0$ ,  $X_i$  and  $X_j$  are positively correlated; when  $\rho_{ij}<0$ ,  $X_i$  and  $X_j$  are negatively correlated.

## B.4. LIMIT THEOREMS

The limit theorems are the theoretical bases of Monte Carlo simulation.

### B.4.1. Law of Large Numbers

The following is one of several different representations of the law of large numbers:

If  $N$  independent random variables  $X_1, X_2, \dots, X_N$  follow the same distribution and  $E(X_i) = \mu$ , then for a sufficiently small positive number  $\varepsilon$

$$\lim_{N \rightarrow \infty} P\left[\left|\frac{1}{N} \sum_{i=1}^N X_i - \mu\right| < \varepsilon\right] = 1.0 \quad (\text{B.40})$$

The law of large numbers indicates that when  $N$  is very large, the arithmetic mean of a group of random variables approaches its expectation with a very large probability.

## B.4.2. Central Limit Theorem

If  $N$  independent random variables  $X_1, X_2, \dots, X_N$  follow the same distribution and  $E(X_i) = \mu$ ,  $V(X_i) = \sigma^2$ , then

$$\lim_{N \rightarrow \infty} P\left[\frac{|1/N \sum_{i=1}^N X_i - \mu|}{\sigma/\sqrt{N}} \leq x\right] = \frac{1}{\sqrt{2\pi}} \int_{-\infty}^x e^{-t^2/2} dt \quad (\text{B.41})$$

This theorem indicates that when  $N$  is sufficiently large, the arithmetic mean approximately follows a normal distribution. If the effect of each variable  $X_i$  is “uniformly small,” the central limit theorem still holds even if these random variables do not follow the same distribution.

## B.5. PARAMETER ESTIMATION

Mathematically, the calculation of a reliability index using the Monte Carlo method is a parameter estimation problem.

### B.5.1. Basic Definitions

1. Population ( $X$ ): set of all possible observed outcomes.
2. Samples ( $X_1, X_2, \dots, X_N$ ): a subset of the population.
3. Sample size ( $N$ ): the number of samples in the subset.
4. Statistic: a function of the sample not containing any unknown parameter.
5. Sampling distribution: distribution of a statistic.

6. Estimate: Assume that a population has density function  $f(x, \theta_1, \dots, \theta_M)$  where  $\theta_1, \dots, \theta_M$  are unknown parameters, and that the statistic of the samples  $\theta_i = \theta_i(X_1, \dots, X_N)$  can be used to estimate the parameter  $\theta_i$  of the population;  $\theta_i$  is called the estimate of the parameter  $\theta_i$ .

### B.5.2. Sample Mean and Sample Variance

Quantities  $X_1, X_2, \dots, X_N$  are samples of a population  $X$ . The sample mean is defined as

$$\bar{X} = \frac{1}{N} \sum_{i=1}^N X_i \quad (\text{B.42})$$

where  $\bar{X}$  is an unbiased estimate of the population mean. The sample mean is a random variable and its variance is  $1/N$  of the population variance, i.e.,

$$V(\bar{X}) = \frac{1}{N} V(X) \quad (\text{B.43})$$

If the population follows a distribution with mean  $\mu$  and variance  $\sigma^2$ , then the sample mean approximately follows a normal distribution with mean  $\mu$  and variance  $\sigma^2/N$  when the sample size is sufficiently large.

The sample variance is defined as

$$s^2 = \frac{1}{N-1} \sum_{i=1}^N (X_i - \bar{X})^2 \quad (\text{B.44})$$

where  $s^2$  is an unbiased estimate of the population variance. The sample variance is also a random variable and its variance is given by

$$V(s^2) = \frac{1}{N} \left[ v_4 - \frac{N-3}{N-1} V^2(X) \right] \quad (\text{B.45})$$

where  $v_4$  is the fourth-order central moment of the population  $X$ .

In Monte Carlo simulation, the sample mean and the sample variance are calculated repeatedly as the number of samples increases. The recursive equations for the sample mean and the sample variance are as follows:

$$\bar{X}_N = \frac{1}{N} [(N-1)\bar{X}_{N-1} + X_N] \quad (\text{B.46})$$

and

$$s_N^2 = \frac{1}{N-1} [(N-2)s_{N-1}^2 + (N-1)\bar{X}_{N-1}^2 - N\bar{X}_N^2 + X_N^2] \quad (\text{B.47})$$

## B.6. REFERENCES

1. A. Papoulis, *Probability, Random Variables and Stochastic Processes*, McGraw-Hill, New York, 1965.
2. P. L. Meyer, *Introductory Probability and Statistical Applications*, Addison-Wesley, Reading, Massachusetts, 1972.
3. A. W. Drake, *Fundamentals of Applied Probability Theory*, McGraw-Hill, New York, 1967.
4. R. Billinton and R. N. Allan, *Reliability Evaluation of Engineering Systems: Concepts and Techniques*, Plenum, New York, 1983.
5. R. Y. Rubinstein, *Simulation and the Monte Carlo Method*, Wiley, New York, 1981.
6. Z. Fang, *Computer Simulation and Monte Carlo Method*, Publishing House of Beijing Industrial Institute, 1988.

# APPENDIX C

# Power System Analysis Techniques

## C.1. AC LOAD FLOW MODELS

### C.1.1. Load Flow Equations

The basic load flow equations in polar coordinate form are as follows:

$$P_i = V_i \sum_{j=1}^n V_j (G_{ij} \cos \delta_{ij} + B_{ij} \sin \delta_{ij}) \quad (i = 1, \dots, n) \quad (\text{C.1})$$

$$Q_i = V_i \sum_{j=1}^n V_j (G_{ij} \sin \delta_{ij} - B_{ij} \cos \delta_{ij}) \quad (i = 1, \dots, n) \quad (\text{C.2})$$

where  $P_i$  and  $Q_i$  are bus real and reactive power injections at Bus  $i$ ;  $V_i$  and  $\delta_i$  are the magnitude and angle of the voltage at Bus  $i$ ;  $\delta_{ij} = \delta_i - \delta_j$ ;  $G_{ij}$  and  $B_{ij}$  are the real and imaginary parts of the element of the bus admittance matrix;  $n$  is the number of system buses.

Each bus has four variables ( $V_i$ ,  $\delta_i$ ,  $P_i$ , and  $Q_i$ ) and therefore  $n$  buses have  $4n$  variables in total. (C.1) and (C.2) consists of  $2n$  equations. In order to solve the load flow equations, two of the four variables for each bus have to be prespecified. In general,  $P_i$  and  $Q_i$  of the load buses are known and they are called PQ buses;  $P_i$  and  $V_i$  of generator buses are specified and they are called PV buses;  $V_i$  and  $\delta_i$  of one bus in the system must be specified to adjust the power balance of whole system, and this bus is called the swing bus.

## C.1.2. Newton–Raphson Model

The load flow equations can be solved by the successive linearization method. This is the well-known Newton–Raphson model. Equations (C.1) and (C.2) are linearized to yield the following matrix equation:

$$\begin{pmatrix} \Delta P \\ \Delta Q \end{pmatrix} = \begin{pmatrix} H & N \\ J & L \end{pmatrix} \begin{pmatrix} \Delta \delta \\ \Delta V/V \end{pmatrix} \quad (\text{C.3})$$

The Jacobian coefficient matrix is a  $(n+m-1)$ -dimensional square matrix where  $n$  and  $m$  are the numbers of all buses and load buses, respectively;  $\Delta V/V$  implies that its elements are  $\Delta V_i/V_i$ . The elements of the Jacobian matrix are calculated by

$$H_{ij} = \frac{\partial P_i}{\partial \delta_j} = V_i V_j (G_{ij} \sin \delta_{ij} - B_{ij} \cos \delta_{ij}) \quad (\text{C.4})$$

$$H_{ii} = \frac{\partial P_i}{\partial \delta_i} = -Q_i - B_{ii} V_i^2$$

$$N_{ij} = \frac{\partial P_i}{\partial V_j} V_j = V_i V_j (G_{ij} \cos \delta_{ij} + B_{ij} \sin \delta_{ij}) \quad (\text{C.5})$$

$$N_{ii} = \frac{\partial P_i}{\partial V_i} V_i = P_i + G_{ii} V_i^2$$

$$J_{ij} = \frac{\partial Q_i}{\partial \delta_j} = -N_{ij} \quad (\text{C.6})$$

$$J_{ii} = \frac{\partial Q_i}{\partial \delta_i} = P_i - G_{ii} V_i^2$$

$$L_{ij} = \frac{\partial Q_i}{\partial V_j} V_j = H_{ij} \quad (\text{C.7})$$

$$L_{ii} = \frac{\partial Q_i}{\partial V_i} V_i = Q_i - B_{ii} V_i^2$$

## C.1.3. Fast Decoupled Model

Branch reactances are normally much larger than branch resistances and angle differences between two buses are very small in power systems. This results in strong dominance of the diagonal matrix block, i.e., the values

of matrix blocks  $N$  and  $J$  are much smaller than those of  $H$  and  $L$ . Equation (C.3) can be decoupled by assuming  $N=0$  and  $J=0$ . Considering  $|G_{ij} \sin \delta_{ij}| \ll |B_{ij} \cos \delta_{ij}|$  and  $|Q_i| \ll |B_{ii} V_i^2|$ , the decoupled equation can be further simplified to

$$\begin{aligned} [\Delta P/V] &= [B'][V\Delta\delta] \\ [\Delta Q/V] &= [B''][\Delta V] \end{aligned} \quad (\text{C.8})$$

where  $[\Delta P/V]$  and  $[\Delta Q/V]$  are vectors whose elements are  $\Delta P_i/V_i$  and  $\Delta Q_i/V_i$ , respectively;  $[V\Delta\delta]$  is a vector whose elements are  $V_i\Delta\delta_i$ . The elements of the constant matrices  $[B']$  and  $[B'']$  are obtained using

$$B'_{ij} = \frac{-1}{x_{ij}} \quad (\text{C.9})$$

$$B'_{ii} = - \sum_{j \in R_i} B'_{ij}$$

$$B''_{ij} = - \frac{x_{ij}}{r_{ij}^2 + x_{ij}^2} \quad (\text{C.10})$$

$$B''_{ii} = -2b_{i0} - \sum_{j \in R_i} B''_{ij}$$

where  $r_{ij}$  and  $x_{ij}$  are the branch resistances and reactances, respectively;  $b_{i0}$  is the branch susceptance between Bus  $i$  and the ground;  $R_i$  is the set of buses directly connected to Bus  $i$ .

## C.2. DC LOAD FLOW MODELS

### C.2.1. Basic Equations

DC load flow equations relate the real power to bus voltage angles. DC load flow based models are widely used in composite system adequacy evaluation because: (a) Many of the important reliability indices are associated with real power load curtailments and calculating these indices only requires real power related information. (b) Load flow calculations in practical application indicate that in many systems there are relatively small (3%–10%) differences between AC and DC load flows. These are small compared to possible errors due to uncertainties in basic reliability data such as component failure rates and outage times. (c) A large number of system states have to be evaluated to guarantee accuracy of probability

indices. DC load flow based models including optimal power flow type can be rapidly calculated.

It should be clearly appreciated that if voltage and reactive power considerations are important requirements in a particular system study, then DC load flow is not an acceptable approach.

DC load flow is based on the following four assumptions:

1. Branch resistances are much smaller than branch reactances. Branch susceptances can be approximated by

$$b_{ij} \approx -\frac{1}{x_{ij}} \quad (\text{C.11})$$

2. Voltage angle difference between two buses of a line is small and therefore

$$\begin{aligned} \sin \delta_{ij} &\approx \delta_i - \delta_j \\ \cos \delta_{ij} &\approx 1.0 \end{aligned} \quad (\text{C.12})$$

3. Susceptances between the buses and the ground can be neglected, i.e.,

$$b_{i0} = b_{j0} = 0 \quad (\text{C.13})$$

4. All bus voltage magnitudes are assumed to be 1.0 p.u.

Based on the above assumptions, the real line flow in a branch can be calculated by

$$P_{ij} = \frac{\delta_i - \delta_j}{x_{ij}} \quad (\text{C.14})$$

and therefore bus real power injections are

$$P_i = \sum_{j \in R_i} P_{ij} = B'_{ii} \delta_i + \sum_{j \in R_i} B'_{ij} \delta_j \quad (i = 1, \dots, n) \quad (\text{C.15})$$

where

$$B'_{ij} = -\frac{1}{x_{ij}} \quad \text{and} \quad B'_{ii} = -\sum_{j \in R_i} B'_{ij} \quad (\text{C.16})$$

Equation (C.15) can be expressed in a matrix form:

$$P = [B'][\delta] \quad (\text{C.17})$$

If Bus  $n$  is selected as the swing bus and we let  $\delta_n = 0$ ,  $[B']$  is a  $(n-1)$  dimensional square matrix. It is exactly the same as  $[B']$  in equation (C.8).

## C.2.2. Relationship between Power Injections and Line Flows

Based on the DC load flow equation (C.17), a linear relationship between power injections and line flows can be obtained. Combining equations (C.14) and (C.17) yields

$$[T_P] = [A][P] \quad (\text{C.18})$$

where  $T_P$  is the line flow vector and its elements are line flows  $\{P_{ij}\}$ . Matrix  $[A]$  is the relationship matrix between power injections and line flows and its dimension is  $L \times (n - 1)$ , where  $L$  is the number of lines and  $n$  the number of buses;  $[A]$  can be calculated directly from  $[B']$ . Assume that two buses of line  $k$  are  $i$  and  $j$ . For  $k = 1, \dots, L$ , the  $k$ th row of matrix  $[A]$  is the solution of the following linear equations:

$$[B'][X] = [b] \quad (\text{C.19})$$

where

$$b = \left[ 0, \dots, 0, \frac{1}{x_{ij}}, 0, \dots, 0, -\frac{1}{x_{ij}}, 0, \dots, 0 \right]^T \quad (\text{C.20})$$

$\uparrow \quad \uparrow$   
 $i\text{th element} \quad j\text{th element}$

## C.3. OPTIMAL POWER FLOW

Optimal power flow (OPF) can be defined as finding a solution of the power system operating state including control variables and state variables to optimize a given objective and satisfy load flow equations (equality constraints) and all given feasibility and security requirements (inequality constraints).

There are a number of possible types or forms of OPF depending on different objectives and constraints. Generally, OPF is a nonlinear optimization problem. Many linearized OPF models, however, are used for different purposes, particularly in composite system reliability evaluation. The minimization models given in Chapters 5 and 7 are essentially linearized OPF. This section provides a general representation of OPF.

OPF is an optimization problem and can be mathematically described as follows:

$$\min F = f(P, Q, V, \delta) \quad (\text{C.21})$$

subject to

$$P_i(V, \delta) = \text{PD}_i \quad (i \in \text{ND}) \quad (\text{C.22})$$

$$Q_i(V, \delta) = \text{QD}_i \quad (i \in \text{ND}) \quad (\text{C.23})$$

$$\text{PG}_i^{\min} \leq P_i(V, \delta) \leq \text{PG}_i^{\max} \quad (i \in \text{NG}) \quad (\text{C.24})$$

$$\text{QG}_i^{\min} \leq Q_i(V, \delta) \leq \text{QG}_i^{\max} \quad (i \in \text{NG}) \quad (\text{C.25})$$

$$|T_k(V, \delta)| \leq T_k^{\max} \quad (k \in L) \quad (\text{C.26})$$

$$V_i^{\min} \leq V_i \leq V_i^{\max} \quad (i \in N) \quad (\text{C.27})$$

where  $P$  and  $Q$  are bus real and reactive power injection vectors, respectively;  $P_i$  and  $Q_i$  are their elements;  $V$  and  $\delta$  are bus voltage magnitude and angle vectors;  $V_i$  is an element of  $V$ ;  $\text{PD}_i$  and  $\text{QD}_i$  are real and reactive loads at Bus  $i$ ;  $\text{PG}_i^{\min}$ ,  $\text{PG}_i^{\max}$ ,  $\text{QG}_i^{\min}$ , and  $\text{QG}_i^{\max}$  are lower and upper limits of real and reactive generations at Bus  $i$ , respectively;  $T_k$  is the line power flow on line  $k$  and  $T_k^{\max}$  is its capacity limit;  $V_i^{\min}$  and  $V_i^{\max}$  are lower and upper limits of bus voltage magnitude at Bus  $i$ ;  $\text{ND}$ ,  $\text{NG}$ ,  $N$ , and  $L$  are sets of load buses, generator buses, all buses, and all lines in the system, respectively. The  $P$ ,  $Q$ ,  $V$ , and  $\delta$  in the objective function  $F$  may be different subsets of these variables, depending on the selection of control and state variables.

In composite system reliability evaluation, it is necessary to introduce bus load curtailment variables into the OPF model. This has been done in the linearized OPF models given in Chapters 5 and 7. It is possible to consider more constraints in an OPF model which can reflect system security, such as operating limits on voltage and transient stability.

## C.4. CONTINGENCY ANALYSIS

The purpose of contingency analysis in composite system adequacy evaluation is to calculate line flows following one or more line outages and judge if there are overloads in other lines. The most accurate method is to rebuild the bus admittance matrix and resolve the load flow equations for each line outage state. This is not practical when tens of thousands or even hundreds of thousands of outage states need to be evaluated in a composite system adequacy assessment. Outage state line flows can be approximately obtained from information from the normal state using contingency analysis techniques without resolving the load flow equations. A linearized load-flow-based contingency analysis method is described in Section 5.2.2. This section presents a supplementary AC load-flow-based sensitivity method for contingency analysis.

Figures C.1a and C.1b show the preoutage and the postoutage states for the line  $i-j$  outage. Figure C.1c shows the case in which additional power  $\Delta P_i + j\Delta Q_i$  and  $\Delta P_j + j\Delta Q_j$  are injected at Buses  $i$  and  $j$ , respectively, in the preoutage state. If the additional power injections can produce power flow increments so that power flows on the rest of the system are the same as those in the postoutage state, the effect of the additional power injections is equivalent to the outage of line  $i-j$ . In the postoutage state,

$$\begin{aligned} P_i + jQ_i &= P'_{ia} + jQ'_{ia} \\ P_j + jQ_j &= P'_{jb} + jQ'_{jb} \end{aligned} \quad (\text{C.28})$$

In the equivalent power injection case,

$$\begin{aligned} (P_i + \Delta P_i) + j(Q_i + \Delta Q_i) &= (P'_{ia} + P_{ij} + \Delta P_{ij}) + j(Q'_{ia} + Q_{ij} + \Delta Q_{ij}) \\ (P_j + \Delta P_j) + j(Q_j + \Delta Q_j) &= (P'_{jb} + P_{ji} + \Delta P_{ji}) + j(Q'_{jb} + Q_{ji} + \Delta Q_{ji}) \end{aligned} \quad (\text{C.29})$$

where  $P_{ij} + jQ_{ij}$  and  $P_{ji} + jQ_{ji}$  are the power flows on line  $i-j$  in the preoutage state and  $\Delta P_{ij} + j\Delta Q_{ij}$  and  $\Delta P_{ji} + j\Delta Q_{ji}$  are power increments on line  $i-j$  due to additional power injections to the preoutage state.

Subtracting equation (C.28) from equation (C.29) yields

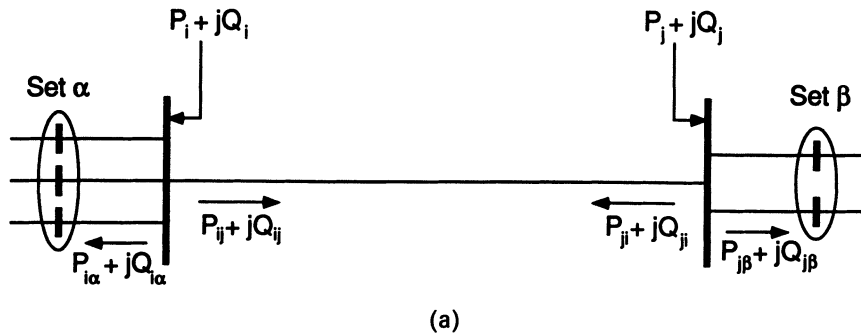
$$\begin{aligned} \Delta P_i + j\Delta Q_i &= (P_{ij} + \Delta P_{ij}) + j(Q_{ij} + \Delta Q_{ij}) \\ \Delta P_j + j\Delta Q_j &= (P_{ji} + \Delta P_{ji}) + j(Q_{ji} + \Delta Q_{ji}) \end{aligned} \quad (\text{C.30})$$

Equation (C.30) can be rewritten in matrix form:

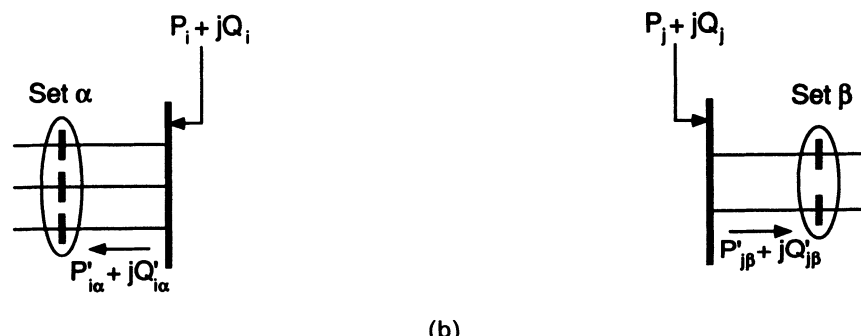
$$\begin{bmatrix} P_{ij} \\ Q_{ij} \\ P_{ji} \\ Q_{ji} \end{bmatrix} = \begin{bmatrix} \Delta P_i \\ \Delta Q_i \\ \Delta P_j \\ \Delta Q_j \end{bmatrix} - \begin{bmatrix} \Delta P_{ij} \\ \Delta Q_{ij} \\ \Delta P_{ji} \\ \Delta Q_{ji} \end{bmatrix} \quad (\text{C.31})$$

By introducing the sensitivity relationship between the power injection increments and power flow increments on line  $i-j$ , equation (C.32) can be obtained from equation (C.31):

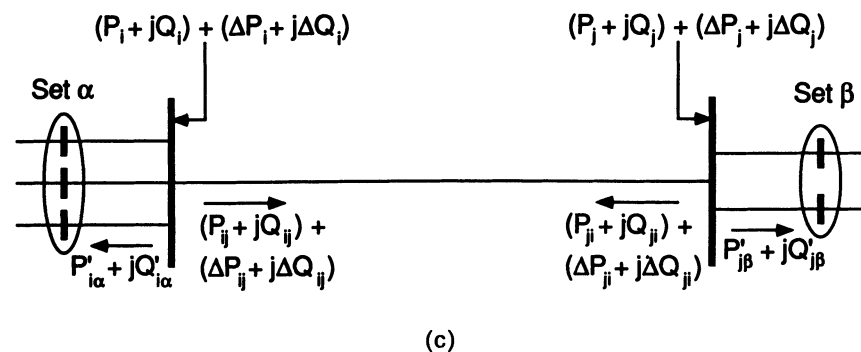
$$\begin{bmatrix} P_{ij} \\ Q_{ij} \\ P_{ji} \\ Q_{ji} \end{bmatrix} = \left[ \begin{bmatrix} 1 & 0 & 0 & 0 \\ 0 & 1 & 0 & 0 \\ 0 & 0 & 1 & 0 \\ 0 & 0 & 0 & 1 \end{bmatrix} - \begin{bmatrix} \frac{\partial P_{ij}}{\partial P_i} & \frac{\partial P_{ij}}{\partial Q_i} & \frac{\partial P_{ij}}{\partial P_j} & \frac{\partial P_{ij}}{\partial Q_j} \\ \frac{\partial Q_{ij}}{\partial P_i} & \frac{\partial Q_{ij}}{\partial Q_i} & \frac{\partial Q_{ij}}{\partial P_j} & \frac{\partial Q_{ij}}{\partial Q_j} \\ \frac{\partial P_{ji}}{\partial P_i} & \frac{\partial P_{ji}}{\partial Q_i} & \frac{\partial P_{ji}}{\partial P_j} & \frac{\partial P_{ji}}{\partial Q_j} \\ \frac{\partial Q_{ji}}{\partial P_i} & \frac{\partial Q_{ji}}{\partial Q_i} & \frac{\partial Q_{ji}}{\partial P_j} & \frac{\partial Q_{ji}}{\partial Q_j} \end{bmatrix} \right] \begin{bmatrix} \Delta P_i \\ \Delta Q_i \\ \Delta P_j \\ \Delta Q_j \end{bmatrix} \quad (\text{C.32})$$



(a)



(b)



(c)

**Figure C.1.** Equivalent power injections for a line outage.

The sensitivity matrix  $S$  can be calculated by decomposition into two factors:

$$S = \begin{bmatrix} \frac{\partial P_{ij}}{\partial \delta_i} & \frac{\partial P_{ij}}{\partial \delta_j} & \frac{\partial P_{ij}}{\partial V_i} & \frac{\partial P_{ij}}{\partial V_j} \\ \frac{\partial Q_{ij}}{\partial \delta_i} & \frac{\partial Q_{ij}}{\partial \delta_j} & \frac{\partial Q_{ij}}{\partial V_i} & \frac{\partial Q_{ij}}{\partial V_j} \\ \frac{\partial P_{ji}}{\partial \delta_i} & \frac{\partial P_{ji}}{\partial \delta_j} & \frac{\partial P_{ji}}{\partial V_i} & \frac{\partial P_{ji}}{\partial V_j} \\ \frac{\partial Q_{ji}}{\partial \delta_i} & \frac{\partial Q_{ji}}{\partial \delta_j} & \frac{\partial Q_{ji}}{\partial V_i} & \frac{\partial Q_{ji}}{\partial V_j} \end{bmatrix} \begin{bmatrix} \frac{\partial \delta_i}{\partial P_i} & \frac{\partial \delta_i}{\partial Q_i} & \frac{\partial \delta_i}{\partial P_j} & \frac{\partial \delta_i}{\partial Q_j} \\ \frac{\partial \delta_j}{\partial P_i} & \frac{\partial \delta_j}{\partial Q_i} & \frac{\partial \delta_j}{\partial P_j} & \frac{\partial \delta_j}{\partial Q_j} \\ \frac{\partial V_i}{\partial P_i} & \frac{\partial V_i}{\partial Q_i} & \frac{\partial V_i}{\partial P_j} & \frac{\partial V_i}{\partial Q_j} \\ \frac{\partial V_j}{\partial P_i} & \frac{\partial V_j}{\partial Q_i} & \frac{\partial V_j}{\partial P_j} & \frac{\partial V_j}{\partial Q_j} \end{bmatrix} \quad (C.33)$$

The first matrix is obtained from the explicit expression of the line power as a function of the two terminal bus voltages. The elements of the second matrix are included in the inverse matrix of the Newton–Raphson load flow Jacobian matrix and can be obtained by solving the linear equations. For example, the elements of the first row in the second matrix are included in the solution of the following linear equation:

$$[J][X] = [b] \quad (C.34)$$

where

$$\begin{aligned} [J] &= \text{Jacobian matrix prior to the outage} \\ [b] &= [0, \dots, 0, 1, 0, \dots, 0]^T \\ &\quad \uparrow \\ &\quad (\text{corresponding to } \delta_i) \end{aligned}$$

Having obtained the equivalent power injection increments from solving equation (C.32), the increments of bus voltage magnitudes and angles due to the line outage can be obtained by resolution of the equation

$$J \begin{bmatrix} \Delta \delta \\ \Delta V/V \end{bmatrix} = [\Delta I] \quad (C.35)$$

where

$$[\Delta I] = [0, \dots, 0, \Delta P_i, 0, \dots, 0, \Delta P_j, 0, \dots, 0, \Delta Q_i, 0, \dots, 0, \Delta Q_j, 0, \dots, 0]^T$$

The line power flows following the line outage can be calculated using bus voltages.

The concept and the procedure given above can also be applied to multiple line outages. The procedure is similar for the fast decoupled load flow model. The equivalent real and reactive power injections can be calculated separately in this case.

## C.5. REFERENCES

1. W. F. Tinney and C. E. Hart, "Power Flow Solution by Newton's Method," *IEEE Trans. on PAS*, Vol. 86, No. 11, 1967.
2. B. Stott and O. Alsac, "Fast Decoupled Load Flow," *IEEE Trans. on PAS*, Vol. 93, No. 3, 1974.
3. W. Li, "Optimal Power Flow Solution by Combination of Penalty Method and BFS Technique," *Journal of Chongqing University*, No. 1, 1982, pp. 95–107.
4. K. R. C. Mamandur and G. J. Berg, "Efficient Simulation of Line and Transformer Outages in Power Systems," *IEEE Trans. on PAS*, Vol. 101, No. 10, 1982.
5. A. J. Wood and B. F. Wollenberg, *Power Generation, Operation and Control*, Wiley, New York, 1984.
6. W. Li, *Secure and Economic Operation of Power Systems—Models and Methods*, Chongqing University Publishing House, 1989.

# APPENDIX D

# Optimization Techniques

## D.1. LINEAR PROGRAMMING

The following is a brief summary of the optimization techniques used in this book.

### D.1.1. Basic Concepts

The basic linear programming problem is to minimize (or maximize) a linear function while satisfying a set of linear equality and inequality constraints and has the following standard form:

$$\min cx \tag{D.1}$$

subject to

$$Ax = b \tag{D.2}$$

$$x \geq 0 \tag{D.3}$$

where  $c$  is an  $n$ -dimensional row vector,  $x$  an  $n$ -dimensional column vector,  $b$  an  $m$ -dimensional column vector,  $b \geq 0$ , and  $A$  is an  $m \times n$  dimensional matrix.

A linear programming problem in nonstandard form can be converted into the standard form by equivalent transformation. In the following two LP problems, for example, the left one can be converted into the right one

in the standard form by adding relaxation variable vector  $y$ :

$$\begin{array}{ll}
 \min cx & \min cx \\
 \text{subject to} & \text{subject to} \\
 Ax \leq 0 & Ax + y = 0 \\
 x \geq 0 & x \geq 0 \\
 & y \geq 0
 \end{array}$$

Basic definitions associated with linear programming are as follows:

1. Feasible solution: A solution  $x$  satisfying (D.2) and (D.3). The set of all feasible solutions is called a feasible zone.
2. Optimal and feasible solution: A feasible solution satisfying (D.1).
3. Base: If the rank of Matrix  $A$  is  $m$ , a nonsingular  $m \times m$  dimensional matrix block  $B$  in Matrix  $A$  is known as a base. The columns of  $B$  are known as basic vectors. The elements of  $x$  corresponding to the basic vectors are basic variables and the remaining elements of  $x$  are nonbasic variables.
4. Basic solution: A solution of (D.2) with all nonbasic variables being zero.
5. Basic feasible solution: A basic solution satisfying (D.2) and (D.3). The base corresponding to the basic feasible solution is called the feasible base.
6. Optimal basic solution: A basic feasible solution satisfying (D.1). The base corresponding to the optimal basic solution is called the optimal base.

### D.1.2. Generalized Simplex Method

When variable  $x$  has both lower and upper bounds, the constraints of  $x$  can be converted into a form  $0 \leq x \leq h$ . A more general LP problem therefore is

$$\begin{array}{l}
 \min cx \\
 \text{subject to} \\
 Ax = b \\
 0 \leq x \leq h
 \end{array}$$

The approach to solving such a general LP problem is called the generalized simplex method. Its basic steps are as follows.

*Step 1:* Determine an initial basic feasible solution using the artificial variable technique and create an initial simplex tableau:

	$x_1$	.	.	.	$x_m$	$x_{m+1}$	.	$x_n$	$b$
	$c_1$	.	.	.	$c_m$	$c_{m+1}$	.	$c_n$	
$x_1$	1	0	.	.	0	$y_{1,m+1}$	.	$y_{1,n}$	$y_{10}$
$x_2$	0	1	.	.	0				
.	.	.	.	.	.	.	.	.	.
.	.	.	.	.	.	.	.	.	.
.	.	.	.	.	.	.	.	.	.
$x_i$	0	0	.	1	.	$y_{i,m+1}$	.	$y_{i,n}$	$y_{i0}$
.	.	.	.	.	.	.	.	.	.
.	.	.	.	.	.	.	.	.	.
.	.	.	.	.	.	.	.	.	.
$x_m$	0	0	.	.	1	$y_{m,m+1}$	.	$y_{m,n}$	$y_{m0}$
	0	0	.	.	0	$r_{m+1}$	.	$r_n$	$-z_0$
$e_1$	$e_2$	.	.	.	$e_m$	$e_{m+1}$	.	$e_n$	

In the tableau,  $y_{ij}$  and  $y_{i0}$  are coefficients corresponding to Matrix  $A$  and Vector  $b$ , respectively, following each Gaussian elimination step;  $r_j = c_j - z_j$  ( $j = m+1, \dots, n$ ), where  $c_j$  are the coefficients in the objective function of the original problem which are known as direct cost coefficients;  $z_j = \sum c_i y_{ij}$  are known as composite cost coefficients and  $r_j$  are known as relative cost coefficients;  $z_0 = \sum c_i y_{i0}$  is the value of the objective function at the present step;  $e_j = +$  or  $-$  ( $j = 1, \dots, n$ ) which is called the sign row. For the initial basic feasible solution

$$x_i = \begin{cases} y_{i0} & \text{(if } x_i \text{ is a basic variable)} \\ 0 & \text{(if } x_i \text{ is a nonbasic variable)} \end{cases}$$

the  $e_j$  take + signs.

*Step 2:* Select  $r_k = \min\{r_j < 0, j = m+1, \dots, n\}$ . The  $k$ th column is called the pivotal column. If there is no negative  $r_j$ , the present solution is already an optimal and feasible solution and the simplex process ends. The values of the variables are determined according to the signs of  $e_j$ . If  $e_j = +$ ,  $x_j = x_j$ , and if  $e_j = -$ ,  $x_j = h_j - x_j$ .

*Step 3:* Calculate the following three values for the selected pivotal column:

- $h_k$
- $\theta_1 = \min\{y_{ik}/y_{ik} \mid y_{ik} > 0\}$  for all  $y_{ik} > 0$  (if there is no positive  $y_{ik}$ ,  $\theta_1 = \infty$ )
- $\theta_2 = \min\{(y_{i0} - h_i)/y_{ik} \mid y_{ik} < 0\}$  for all  $y_{ik} < 0$  (if there is no negative  $y_{ik}$ ,  $\theta_2 = \infty$ )

*Step 4:* Modify the simplex tableau according to the magnitude of the three values in Step 3:

- If  $h_k$  is minimum, the last column is subtracted by a column which is obtained from the  $k$ th column multiplying  $h_k$  and then the  $k$ th column is multiplied by  $-1$  (including the change of the sign for  $e_k$ ). The base remains unchanged.
- If  $\theta_1$  is minimum and  $\theta_1$  appears in the  $q$ th row, then  $y_{qk}$  is selected as a pivot.
- If  $\theta_2$  is minimum and  $\theta_2$  appears in the  $q$ th row, then  $y_{q0(\text{new})} = y_{q0(\text{old})} - h_q$ ,  $y_{qq}$  is multiplied by  $-1$ , and the sign of  $e_q$  is changed;  $y_{qk}$  is selected as a pivot.

*Step 5:* With the selected pivot element  $y_{qk}$ , conduct Gaussian elimination in the simplex tableau so that the pivot becomes 1; the other elements in the pivotal column become 0. An updated simplex tableau is obtained and go to Step 2.

### D.1.3. Duality Principle

For each minimum-value linear programming problem, there is a corresponding dual maximum-value linear programming problem. The coefficients of the objective functions and the right-side terms of the constraints in the two LP problems exchange and they have an equal optimal objective function value. This is known as the duality of linear programming.

Two pairs of dual LP problems are given in the following. The first pair is called the symmetrical form of the dual LP and the second pair the nonsymmetrical form.

	Primary problem	Dual problem
Symmetrical form		
	$\min cx$ subject to $Ax \geq b$ $x \geq 0$	$\min \lambda b$ subject to $\lambda A \leq c$ $\lambda \geq 0$
Nonsymmetrical form		
	$\min cx$ subject to $Ax = b$ $x \geq 0$	$\min \lambda b$ subject to $\lambda A \leq c$

where  $x$  and  $\lambda$  are variable vectors for the primary and dual problems, respectively.

The optimal basic solution of the dual problem can be obtained from the final simplex tableau of the primary problem. This solution is

$$\lambda = c_B B^{-1} \quad (D.4)$$

where  $B$  is the optimal base and  $c_B$  a subvector of  $c$  coefficient row in the final simplex tableau, which corresponds to the basic variables. At optimal solution, the nonbasic variables are zero and therefore the optimal value of the objective function is

$$F = c_B x_B = c_B B^{-1} b \quad (D.5)$$

where  $x_B$  is the basic variable vector. Differentiating equation (D.5) yields

$$\Delta F = c_B B^{-1} \Delta b \quad (D.6)$$

Combining equations (D.4) and (D.6) yields

$$\Delta F = \lambda \Delta b \quad (D.7)$$

This equation indicates that the optimal dual variable  $\lambda_i$  is a partial differential of the objective function with respect to the right-side value  $b_i$  of the constraints. This is the fundamental to calculate sensitivity indices in reliability assessment.

#### D.1.4. Dual Simplex Method

The simplex method given in Section D.1.2 is known as the primal simplex algorithm. Starting from an initial feasible solution, an optimal solution is gradually obtained while retaining feasibility in the primal algorithm. The dual simplex method starts with an initial basic solution satisfying optimality of the objective function but not satisfying feasibility. Feasibility is gradually obtained under the condition that optimality is retained. Which method is used depends upon the features of the problems to be solved. If an initial feasible solution can be easily obtained, the primal algorithm is used. If an initial optimal but nonfeasible solution can be obtained, the dual algorithm is used. The primal simplex method is used in the LP models for multi-area reliability evaluation in Chapter 4 and the increment-type LP model for voltage adjustment in Section 5.9.2, while all other LP models in Chapters 5 and 7 utilize the dual simplex method. It should be noted that the dual algorithm is used to perform dual treatment on the simplex tableau of the primal problem but not to solve a dual problem of the primal problem. The basic steps of the dual simplex method can be summarized as follows:

*Step 1:* Create the initial simplex tableau of the primal problem.

*Step 2:* Find a dual basic feasible solution  $X_B$ , i.e., in the simplex tableau corresponding to this solution,  $r_j \geq 0$  for  $j = m+1, \dots, n$ . If  $x_B \geq 0$ , i.e., there is no negative element in the column  $b$  of the simplex tableau, then an optimal and feasible solution is already obtained. If there are any negative elements in the column  $b$ , go to Step 3.

*Step 3:* Select the smallest value in the negative elements of  $x_B$ , i.e.,

$$\min_i \{(x_B)_i | (x_B)_i < 0\} = x_q$$

The  $x_q$  is the leaving base variable. This means that the  $q$ th row is the pivotal row.

*Step 4:* Check all elements of the pivotal row  $y_{qj}$  ( $j = 1, \dots, n$ ). If all  $y_{qj} \geq 0$ , there is no feasible solution. If there are negative elements in the pivotal row, then

$$\theta = \min_j \{(z_j - c_j) / y_{qj} | y_{qj} \leq 0\} = (z_k - c_k) / y_{qk}$$

where  $z_j$ ,  $c_j$ , and  $y_{qj}$  are as defined in Section D.1.2;  $x_k$  is the entering base variable, which means that the  $k$ th column is the pivotal column.

*Step 5:* With the pivot element  $y_{qk}$ , conduct Gaussian elimination to update the simplex tableau. An updated base is obtained and then a new dual basic feasible solution is calculated:  $x_B = B^{-1}b$ . Go back to Step 2.

## D.1.5. Linear Programming Relaxation Technique

In composite system adequacy assessment, the number of constraints in linear programming OPF models are very large, particularly when preventive outage constraints are considered. Active constraints at an optimal solution or in the process of resolution, however, are relatively few. If the active constraints are satisfied, all constraints will be satisfied. The basic characteristic of the linear programming relaxation technique is that a large-scale LP problem is decomposed into a sequence of small-scale linear programming problems and only a few active constraints are considered in each small LP problem.

Consider the linear programming problem:

$$\text{LP1} \left\{ \begin{array}{l} \text{subject to} \\ \min cx \\ A_1x = b \\ \underline{y} \leq A_2x \leq \bar{y} \\ \underline{x} \leq x \leq \bar{x} \end{array} \right.$$

where  $A_1$  is a  $J \times S$  dimensional matrix;  $A_2$  is an  $M \times S$  dimensional matrix;  $x$  is an  $S$  dimensional column vector;  $b$  is a  $J$  dimensional column vector;  $c$  is an  $S$  dimensional row vector.

Let

$$A_2x = y \quad \text{and} \quad h = [0, c]$$

$$z = \begin{bmatrix} y \\ x \end{bmatrix}, \quad \underline{z} = \begin{bmatrix} \underline{y} \\ \underline{x} \end{bmatrix}, \quad \bar{z} = \begin{bmatrix} \bar{y} \\ \bar{x} \end{bmatrix}$$

the linear programming problem LP1 can be rewritten as LP2:

$$\text{LP2} \left\{ \begin{array}{l} \text{subject to} \\ \min hz \\ Az = d \\ \underline{z} \leq z \leq \bar{z} \end{array} \right.$$

where

$$A = \begin{bmatrix} -I & A_2 \\ 0 & A_1 \end{bmatrix} \quad \text{and} \quad d = \begin{bmatrix} 0 \\ b \end{bmatrix}$$

Let  $K \subset M$ , i.e.,  $K$  is a subset of  $M$ . The following linear programming problem is constructed:

$$\text{LP2}(K) \left\{ \begin{array}{l} \text{subject to} \\ \min h_H z_H \\ A_G^H z_H = d_G \\ \underline{z}_H \leq z_H \leq \bar{z}_H \end{array} \right.$$

where  $h_H$  denotes a subvector of  $h$  and the subscript set of its elements is  $H$ . The definitions of  $z_H$  and  $d_G$  are similar;  $A_G^H$  denotes a submatrix of  $A$ . The subscript set of its columns is  $H$  and the subscript set of its rows is  $G$ ;  $G = K \cup J$  and  $H = K \cup S$ .

The LP2( $K$ ) is a small-scale linear programming problem which contains the partial inequalities and all equalities in the original problem LP1.

Subset  $K$  can be quite small and even an empty set initially. Consequently, LP2( $K$ ) can be a very small problem despite the scale of the original problem. A solution of LP2( $K$ ) satisfies optimality of the original problem but does not necessarily satisfy its feasibility (not all inequality constraints are necessarily satisfied). The LP2( $K$ ) is solved using the dual simplex method.

Let

$$z_H(K) = \begin{bmatrix} y_K(K) \\ x(K) \end{bmatrix}$$

denote the optimal basic solution of LP2( $K$ ) and  $I(K)$  is the subscript set of the basic variable components of the solution. Assume that

$$R = M - K, \quad y(K) = \begin{bmatrix} y_K(K) \\ y_R(K) \end{bmatrix}, \quad z(K) = \begin{bmatrix} y(K) \\ x(K) \end{bmatrix}$$

There are two cases:

(a) If

$$\underline{y} \leq y(K) \leq \bar{y}$$

is satisfied, then  $z(K)$  is an optimal basic solution of the original problem LP1.

(b) If subset

$$F(K) = \{i \in R \mid y_i(K) > \bar{y}_i, \text{ or } y_i(K) < \underline{y}_i\}$$

is not empty, let

$$E(K) = K \cap I(K)$$

and

$$K^* = K - E(K) + F(K)$$

and  $K^*$  is used to replace  $K$  to construct a new small-scale linear programming LP2( $K^*$ ). This LP2( $K^*$ ) is solved using the dual simplex method. The initial basic solution of LP2( $K^*$ ) is  $z_{H^*}$  where  $H^* = K^* \cup S$ . The subscript set of the basic variable components of  $z_{H^*}$  is  $I^* = I(K) - E(K) + F(K)$ .

The above process is repeated (the old  $K^*$  is replaced by a new  $K^*$ ) until Case (a) is achieved.

## D.2. MAXIMUM FLOW METHOD

The maximum flow method is applied to multi-area generating system adequacy evaluation in Chapter 4. This section presents its basic concepts and procedure.

## D.2.1. Basic Concepts

### (a) Definitions

Network (oriented graph):	A set composed of node subset $P$ and oriented branch subset $B$ , denoted by $G(P, B)$
Arc:	An oriented branch between two nodes $i$ and $j$ , denoted by $a_{ij}$ .
Arc parameters:	Arc length $w_{ij}$ , arc flow $f_{ij}$ , and arc capacity $c_{ij}$ .
Source:	A node producing flow, denoted by $s$ .
Sink:	A node collecting flow, denoted by $t$ .
Path:	An oriented sequence of nodes and arcs.
	An arc having the same direction as the path is called a forward arc and an arc having the opposite direction to the path is called a backward arc.
Augmented path:	If all arc flows on a path satisfy the following conditions, this path is called an augmented path: $\begin{aligned} 0 \leq f_{ij} < c_{ij} && \text{if } a_{ij} \in \mu^+ \\ 0 < f_{ij} \leq c_{ij} && \text{if } a_{ij} \in \mu^- \end{aligned}$ where $\mu^+$ and $\mu^-$ denote forward and backward arc sets, respectively.
Cut set:	A set of arcs connecting two mutually complementary node subsets in a network, denoted by $\{a_{ij}   i \in P_i, j \in P_j\}$ . The sum of all arc capacities in a cut set is called the cut capacity. The one having minimum cut capacity in all possible cut sets is called the minimum cut set.

### (b) Two Basic Theorems

Theorem 1: A feasible flow  $f = \{f_{ij}\}$  is the maximum flow if and only if there is no augmented path between the source and the sink.

Theorem 2 (Ford–Fulkerson theorem): The flow capacity of a maximum flow from the source to the sink equals the cut capacity of the minimum cut set separating the source and the sink.

## D.2.2. Maximum Flow Problem

The maximum flow problem is to find a feasible flow  $f = \{f_{ij}\}$  which has maximum flow capacity. It is described mathematically as follows:

$$\max F(f_{ij})$$

subject to

$$0 \leq f_{ij} \leq c_{ij} \quad (\text{for all } a_{ij})$$

$$\sum_j f_{sj} = F$$

$$\sum_j f_{jt} = F$$

$$\sum_j f_{ij} - \sum_j f_{ji} = 0 \quad (i \neq s, t)$$

where  $s$  and  $t$  indicate the source and the sink, respectively;  $F$  is the flow capacity.

There are different methods for solving the maximum flow problem. The most commonly used method is the labeling algorithm. This algorithm starts from a feasible flow and includes the two processes of labeling and adjusting.

**(a) Labeling.** In this process, nodes are classified into the labeled and the unlabeled. The labeled nodes are further divided into the checked and the unchecked. Each label includes two numbers: The first number indicates from which node the label is obtained. The second number gives the possible maximum flow increment from the prior node to the present node.

*Step 1:* Label the source with  $(0, +\infty)$  so that the source is a labeled but unchecked node and other nodes are unlabeled.

*Step 2:* Consider any labeled but unchecked node  $i$ . There are three cases for all nodes  $j$  which are connected to  $i$  but unlabeled:

- If  $f_{ij} = c_{ij}$  for arc  $a_{ij}$ , node  $j$  is ignored.
- If  $f_{ij} < c_{ij}$  for arc  $a_{ij}$ , node  $j$  is labeled with  $(+i, \delta(j))$ , where  $\delta(j) = \min[\delta(i), c_{ij} - f_{ij}]$ .  $+i$  indicates that the flow can be increased from  $i$  to  $j$  and  $\delta(j)$  is the possible magnitude to be increased.
- If  $f_{ji} > 0$  for arc  $a_{ji}$ , node  $j$  is labeled with  $(-i, \delta(j))$ , where  $\delta(j) = \min[\delta(i), f_{ji}]$ .  $-i$  indicates that the flow can be decreased from  $j$  to  $i$  and  $\delta(j)$  is the possible magnitude to be decreased.

After all possible  $j$  are labeled,  $i$  becomes a labeled and checked node and all  $j$  become the labeled but unchecked nodes.

*Step 3:* Repeat the above process until the sink is labeled and then go to the adjusting process. If all possible nodes are checked and the labeling process cannot proceed further to label the sink, the algorithm ends. The present flow is a maximum flow.

### (b) Adjusting

*Step 1:* Find an augmented path  $\mu$  from the source to the sink in terms of the first number in the labels. Assume that the first number in the label for the sink  $t$  is  $+k$  (or  $-k$ ). Arc  $a_{kt}$  (or  $a_{tk}$ ) is an arc on the augmented path. Then the first number in the label for node  $k$  is checked. If it is  $+i$  (or  $-i$ ),  $a_{ik}$  (or  $a_{ki}$ ) is an arc on the augmented path. The pursuit is conducted until the source is checked.

*Step 2:* Adjust the flow capacities of the arcs on the augmented path:

$$f'_{ij} = \begin{cases} f_{ij} & \text{if } a_{ij} \in \mu \\ f_{ij} + \delta(t) & \text{if } a_{ij} \in \mu^+ \\ f_{ij} - \delta(t) & \text{if } a_{ij} \in \mu^- \end{cases}$$

where  $\delta(t)$  is the second number in the label for the sink.

*Step 3:* Erase all labels and return to the labeling process with the new feasible flow  $\{f'_{ij}\}$ .

A minimum cut is also obtained using the presented labeling method. When labeling ends, the cut set between labeled and unlabeled node subsets is the minimum cut set. It locates the “bottle neck” from the source to the sink.

## D.3. REFERENCES

1. D. G. Luenberger, *Introduction to Linear and Nonlinear Programming*, Addison-Wesley, Reading, Massachusetts, 1973.
2. L. S. Lasdon, *Optimization Theory for Large Systems*, Macmillan, New York, 1970.
3. W. Li, *Secure and Economic Operation of Power Systems—Models and Methods*, Chongqing University Publishing House, 1989.
4. W. Li, “A Penalty Linear Programming Model for Real-Time Economic Power Dispatch with  $N-1$  Security, International Symposium on Engineering Mathematics and Application, Beijing, July, 1988.

5. J. C. Dodu and A. Merlin, "Une Application de la Programmation Linéaire à l'Étude des Réseaux Électriques de Grande Taille," *Bulletin de la DER, EDF*, Série C, No. 1, 1974, pp. 29–56.
6. P. A. Jensen and J. W. Barnes, *Network Flow Programming*, Wiley, New York, 1980.
7. L. R. Ford and D. R. Fulkerson, *Flows in Networks*, Princeton University Press, 1962.

# Index

- ACCI, 28
- Active event, 235
- Adequacy, 9
- Adequacy indices, 22
- ADLC, 25
- AEIC, 290
- AEGC, 290
- AENS, 28
- AGCP, 290
- AIOIC, 290
- Alert state, 188
- Annual index, 27
- Annual load curve, 93
- Annualized index, 27
- Antithetic variates, 58
- Arc, 345
- ASAI, 28
- ASUI, 28
- Augmented path, 345
- Base, 338
- Basic solution, 338
- Basic variable, 338
- BES, 21
- BPACI, 26
- BPECI, 26
- BPII, 26
- Bus load correlation, 171
- CAIDI, 28
- CAIFI, 27
- CCDF, 259
- Central limit theorem, 324
- Chronology, 180
- Cluster technique, 95
- Coefficient of variation, 36
- Coherence, 199
- Common cause outage, 164
- Component operating cycle, 219
- Composite system, 131
- Composite system adequacy, 131
- Congruential generator, 39
- Connection set, 233
- Contingency analysis, 332
- Control variates, 53
- Corrective actions, 190
- Correlation function, 322
- Covariance, 322
- Customer damage function, 258
- Customer survey, 256
- Cut set, 345
- Dagger sampling, 58
- DC load flow, 329
- Delivery point, 21
- Density function, 318
- Derated state model, 79
- Distribution function, 318
- Distribution of index, 84
- Distribution system adequacy, 209
- Dual problem, 340
- Dual simplex, 341
- Duality, 340
- EDLC, 25
- EDNS, 26
- EENS, 26
- EEPQ, 286
- EFLC, 25
- EGC, 286

- EIC, 29  
 ELC, 25  
 Emergency state, 188  
 ENLC, 25  
 ENS, 28  
 EOIC, 290  
 EPSRA, 20  
 ERIS, 19  
 Estimate, 325  
 Expectation, 322  
 Exponential distribution, 320  
 Extreme emergency state, 188
- Fast decoupled model, 328  
 Feasible solution, 338  
 Forced unavailability, 91  
 Ford–Fulkerson theorem, 345  
 Frequency index, 179  
 Functional zone, 10
- Gamma distribution, 321  
 Generalized simplex, 338  
 Generating system adequacy, 75  
 Generating unit contingency, 135  
 Generating unit modeling, 78
- Hierarchical level, 11  
 Hybrid method, 191
- IEAR, 29  
 IEEE RTS, 299  
 Independence, 39  
 Importance sampling, 53  
 Interruption cost model, 269  
 Inverse transform, 43  
 IOR, 211
- K-mean algorithm, 95
- Labeling, 346  
 Law of large numbers, 323  
 Limit theorem, 323  
 Linear programming, 337  
 Linear programming relaxation, 342  
 Load curtailment, 137  
 Load flow, 327  
 Load point failure rate, 214  
 Load point outage duration, 214
- Load point unavailability, 214  
 Load uncertainty, 110  
 LOEE, 23  
 Log-normal distribution, 320  
 LOLD, 24  
 LOLE, 23  
 LOLF, 24
- Multistep model, 93  
 Maximum flow method, 344  
 MBPCI, 26  
 Minimization model, 137  
 Minimum cost assessment, 284  
 Modulus, 39  
 Monte Carlo, 33
- NCDE, 200  
 NCDF, 200  
 NCDP, 201  
 Network, 345  
 Newton–Raphson model, 328  
 Noncoherence, 199  
 Normal distribution, 320  
 Normal state, 187  
 Numerical characteristic, 321
- Optimal and feasible solution, 338  
 Optimal load flow, 331  
 Optimization techniques, 337
- Parameter estimation, 324  
 Passive event, 234  
 Path, 346  
 Peaking unit model, 81  
 PLC, 24  
 Point, 233  
 Population, 324  
 Present value, 284  
 Primary problem, 340  
 Probabilistic analysis, 1  
 Probability, 317  
 Probability distribution, 318
- Q*-load curtailment, 190

- Random number, 39  
Random variate, 42  
RBTS, 306  
Regional weather states, 153  
Reliability evaluation, 3  
Reliability worth, 16  
RENS, 144  
RGTAI, 144  
RLCP, 144  
RNLC, 144  
RPII, 144
- SAIDI, 27  
SAIFI, 27  
Sample mean, 325  
Sample variance, 325  
Samples, 324  
Sampling distribution, 324  
SCDF, 258  
Security, 9  
Security constraints, 188  
Sensitivity index, 114  
Service continuity, 22  
SI, 26  
SIC, 259  
Sink, 345  
Source, 345  
Standard deviation, 322  
State duration sampling, 62
- State sampling, 60  
State transition sampling, 64  
Station component modeling, 233  
Station reliability, 232  
Stopping rules, 83, 96  
Stratification, 197  
Stratified sampling, 56  
Supporting policy, 120  
System operating cycle, 221  
System operating states, 187  
System performance index, 230
- Tabulating technique, 45  
Transmission component outage, 135  
TTF, 79  
TTR, 79
- Unavailability, 35  
Uniformity, 39
- Variance, 322  
Variance reduction technique, 52
- Weibull distribution, 321  
WTA, 257  
WTP, 257